SECURITY CONSTRAINED UNIT COMMITMENT PROBLEM INTEGRATED WITH PLUG-IN ELECTRIC VEHICLES AND RENEWABLE ENERGY SOURCES

Thesis Submitted for the Award of the Degree of

DOCTOR OF PHILOSOPHY
in
Electrical Engineering

By

Pravin Gajananrao Dhawale
Registration Number: 41900675

Supervised By
Dr. Vikram Kumar Kamboj
Professor
School of Electronics and Electrical Engineering
Lovely Professional University
Phagwara, Punjab-144402

Co-Supervised by
Dr. S. K. Bath
Professor
Department of Electrical Engineering
GZSCCET, MRS Punjab Technical University
Bathinda, Punjab-151005

LOVELY PROFESSIONAL UNIVERSITY, PUNJAB
2024

Dedicated

To

My Brother, Supervisors

& My Parents

DECLARATION

I, hereby declared that the presented work in the thesis entitled "***Security Constrained Unit Commitment Problem Integrated With Plug-In Electric Vehicles and Renewable Energy Sources"*** in fulfilment of the degree of **Doctor of Philosophy (Ph. D.)** is the outcome of research work carried out by me under the supervision Dr. Vikram Kumar Kamboj working as Professor in the School of Electronics and Electrical Engineering, of Lovely Professional University, Punjab, India and co-supervision of Dr. S.K. Bath, Professor and Head of the Electrical Department, Maharaja Ranjit Singh Punjab Technical University, India. In keeping with the general practice of reporting scientific observations, due acknowledgments have been made whenever the work described here has been based on the findings of other investigators. This work has not been submitted in part or full to any other University or Institute for the award of any degree.

Name of the scholar: Pravin Gajananrao Dhawale

Registration No.:41900675

School of Electronics and Electrical Engineering

Lovely Professional University, Phagwara

Punjab, India

CERTIFICATE

This is to certify that the work reported in the Ph. D. thesis entitled **"*Security Constrained Unit Commitment Problem Integrated With Plug-In Electric Vehicles and Renewable Energy Sources*"** submitted in fulfillment of the requirement for the reward of the degree of **Doctor of Philosophy (Ph.D.)** in the School of Electronics and Electrical, is a research work carried out by PRAVIN GAJANANRAO DHAWALE, 41900675, is bonafide record of his/her original work carried out under my supervision and that no part of the thesis has been submitted for any other degree, diploma or equivalent course.

Dr. Vikram Kumar Kamboj
Professor
School of Electronics and Electrical Engineering
Lovely Professional University
Phagwara, Punjab-144402

Dr. S. K. Bath
Professor
Department of Electrical Engineering
GZSCCET, MRS Punjab Technical University
Bathinda, Punjab-151005

ACKNOWLEDGMENTS

It is with a deep sense of gratitude and reverence that I express my sincere thanks to my supervisors Dr. Vikram Kumar Kamboj, Professor, School of Electronics & Electrical Engineering, Lovely Professional University, Phagwara, Punjab, and Dr. S.K. Bath, Professor, Power System Domain, Department of Electrical Engineering, Maharaja Ranjit Singh Punjab Technical University, Bhatinda, Punjab for their guidance, encouragement and valuable suggestions throughout my research work. Their untiring and painstaking efforts, methodical approach, and individual help made it possible for me to complete this research work in time.

Dr. Vikram Kumar Kamboj has an optimistic and helpful personality; he has always made himself ready to clarify my doubts and it was a great opportunity to work under his supervision. He always shed light whenever I felt stuck in my research ambitions path. I would like to thank my co-supervisor, Dr. S.K. Bath, for her worthy guidance, support, and suggestions, in every step of this research project during my Ph.D. journey. She always shed light whenever I was feeling stuck in my path of research ambitions.

I would like to express my gratitude toward the entire Lovely Professional University family for providing a suitable infrastructure and environment for completing my research work in a time-bound manner. Also, thank the Division of Research & Development and the School of Electrical and Electronics Engineering for their help and encouragement in my Ph.D. journey. Finally, I like to thank the almighty God who helped me to achieve such a big milestone.

Date: 09/02/2024 Pravin G. Dhawale

ABSTRACT

The economy and development of every country are significantly influenced by electric power. For the economy to grow sustainably, appropriate infrastructure must be created and in place. The major contributors to the development of a country are the power sectors, as electricity is essential to modern societies. Electricity can be produced from a variety of sources. Conventional energy sources, such as thermal plants, nuclear plants, hydroelectric plants, and oil and natural gas-based plants, are the main sources of electricity. The modern power system utilizes both conventional and non-conventional energy sources like solar, tidal, geothermal, wind, and so on. India's load demand is rapidly shifting. The gigantic power age limit is expected to fulfill the rising power need, and this limit can be filled.

In the design and management of power systems, the security constraint unit commitment (SCUC) problem is a significant optimization challenge. In order to satisfy the demand for energy at the lowest possible cost while still adhering to a number of operational and security requirements, it must determine the optimum method to commit and dispatch power-generating units. The SCUC problem gets increasingly challenging as plug-in electric vehicles (PEVs) and renewable energy sources grow more common in power networks because of the intermittent and unpredictable nature of renewable energy and the existence of PEVs as an extra-demand source.

Examining innovative solutions to the SCUC problem is the aim of the current study. The impacts of PEVs and the unpredictability of renewable energy sources (RES) are also taken into consideration for both summer and winter days. The innovative methodologies were created by fusing optimization algorithms. These hybrid optimization algorithms combine local and global search optimizers as their foundation. As a result, the new algorithms are better at exploring and exploiting the entire search space. The introduction to SCUC problem and its importance in contemporary power sectors are covered in the first section of the dissertation.

In addition, the fundamental concepts of optimization methods, renewable energy sources, and electric vehicles have been examined in the subsections. The blend of a meta-heuristic

and classical optimization algorithm including hybrid methods has been suggested to solve the Security Constraint Unit Commitment Problem.

Another section of this research deals with the proper justifications and explanations of the various optimization methodologies used in optimization research. Review of various testing standards, including the PEVs' charging and discharging properties, which are utilized to solve the SCUC problem. The nature of PEVs, the uncertainty of RES, and a literature review of several optimization approaches are covered in great length in this chapter as well. The literature review revealed that several optimizers still have some shortcomings. Numerous researchers have also made the argument that no optimizer is appropriate for all types of optimization problems. Therefore, it is imperative to investigate additional metaheuristic search algorithm variations. The development of new metaheuristic optimizers for numerical, engineering, and security constraint-based unit commitment problems is the sole focus of this entire chapter.

The following chapter illustrates novel hybrid metaheuristic optimization methods that draw inspiration from arithmetic operations like division, multiplication, addition, subtraction, and various chaotic maps. Levy flight and random walk strategies are also used to enhance the exploitation search capability of the current optimizers. The chaotic map strategy has been applied to the arithmetic optimizer. Furthermore, these optimizers, namely CAOA, LAOA, and RWAOA, have better exploitation capabilities by combining these chaotic, levy flight, and random walk strategies. To evaluate the efficacy of such hybrid optimizers, hypothesis tests are taken into account. The hybrid chaotic arithmetic optimization algorithm, hybrid Levy flight arithmetic optimization algorithm, and random walk arithmetic optimization algorithm have been developed to enhance the ability to exploit and explore the entire search space.

The next chapter is an overview of the exploitation and exploration of the current AOA. The chaotic tent function was used to successfully update the optimizer. The AOA optimizer additionally updated the exploitation and exploration phase using Levy flight and random walk methods. The CAOA, LFAOA, and RWAOA optimizers have been

successfully tested for unimodal, multimodal, fixed dimension standard benchmark issues, and interdisciplinary engineering design challenges. For unimodal, multimodal, fixed dimension standard benchmark problems and multidisciplinary engineering design challenges, the CAOA, LFAOA, and RWAOA optimizers have been tested effectively. The proposed CAOA, LFAOA, and RWAOA optimization techniques are used to solve SCUC problem in the following chapter. The performance of these algorithms is evaluated using the standard test system, which consists of thermal generating units for the small, medium, and large power sectors. For frameworks with 10, 20, and 40 generators, the proposed calculation's viability was assessed. After a successful experiment, it was determined that the security constraint unit commitment problem efficiency of these algorithms was superior to that of competing algorithms. The proposed CAOA, LFAOA, and RWAOA optimizer outperforms the existing alternatives, as shown by the comparison results.

The SCUC problem has been solved using hybrid CAOA with consideration for the effects of PEVs and renewable energy sources, including solar and wind, on summer and winter days in the following chapter. For maximum profit and the lowest fuel costs, the test systems with 10, 20, and 40 units have been tested successfully. The simulated results analysis reveals that the CAOA optimizer outperforms both established and recently created heuristics, meta-heuristics, and evolutionary search optimizers. A powerful optimizer like this can be used to find a solution for modern power sector security constraint unit commitment. The proposed algorithms were subjected to statistical analysis using the standard deviation, median value, best fitness, average fitness, and worst fitness metrics. The hypothesis testing was supported by the t-test and the Wilcoxon rank sum technique. Also, the computation time has been tracked to verify the computations' level of computational complexity.

The significant contribution of the proposed research study is summarized in the final chapter. To further improve the security constraint, suggestions are made for several generating utilities. In order to get a better result, the usage and contributions of the

suggested optimizers CAOA, LFAOA, and RWAOA to the solution of the SCUC problem with PEVs and RES have been compared to those of other competitive algorithms. In addition, new researchers are given directions for future research activities.

TABLE OF CONTENTS

LIST OF FIGURES

LIST OF TABLES

LIST OF SYMBOLS

MDT_k = Minimum down time for the k unit

MUT_k = Minimum up-time for k unit

SUC_{kt} = Start up cost of k th unit for time t hour

NG = Number of generator

NH = Number of hours

HSC_k = Hot start up for k unit

CSC_k = Cold Start up cost for k unit

P_{mn} = Active Power flow between nodes m and n

T_k^{OFF} = Duration of time off for k unit

P_D^k = Power demand for k unit

P_{EV}^k = Power of electric vehicle for k unit

P_G^k = Power of generation for k unit

P_{RES}^k = Re*newable* power generation for k unit

EV = Electric Vehicle

PEV = Plug electric vehicle

P_{D_t} = Power demand for time t

SR_t = Spinning Reserve for time t hour

$P_{Thermal,t}$ = Power generated form thermal power generation for t hour

α = safety factor

$MOA(C_{Iter})$ = function value for the t^{th} iteration

C_{Iter} = the current iteration

M_{Iter} = maximum iteration

LB_k = Represent lower bound value of the k^{th} position

UB_k = Upper bound value of the position k^{th} position

MOP = Math optimizer probability

$MOP(C_{Iter})$ = Function value at the t^{th} iteration.

a_k, b_k, c_k = Fuel coefficient constraints

INS_k = Initial status of the system

$F_{k,t}$ = *R*epresent the cost associated with the k^{th} generating unit at the t^{th} hour

$U_{k,t}$ = *t*he committed status of the k^{th} unit at t^{th} hour

$P_{Renewable_k}$ = Renewable power generation

LIST OF ABBREAVIATION

Acronym	Definition
AOA	Arithmetic Optimization Algorithm
ACO	Ant colony optimizer
ALO	Ant Lion Optimizer
BBO	Biogeography Based Optimization
CAOA	Chaotic Arithmetic Optimization Algorithm
CE	Constrained Engineering
DER	Distributed Energy Resources
DP	Dynamic Programming
DPS	Distributed power systems
DR	Demand Response
DT	Dynamic Technique
EA	Evolutionary Algorithm
EFO	Electromagnetic Field Optimization
EHO	Elephant Herding Optimization
ELD	Economic Load Dispatch
EMA	Exchange Market Algorithm
EOA	Equilibrium Optimization Algorithm
EPPSO	Evolutionary Parallel Particle Swarm Optimizer
EPSO	Evolutionary Particle Swarm Optimizer
ESF	Energy storage facilities
FCR	Frequency Containment Reserves
FPA	Flower Pollination Algorithm
GBO	Gradient Based Optimizer
HGSO	Henry gas solubility optimizer
HS	Harmony Search
LFAOA	Levy flight arithmetic optimization algorithm
MAPE	Mean Absolute Percentage Error
MBA	Mine Blast Algorithm
MBO	Monarch Butterfly Optimization
MDE	Modified Differential Evolution
MDP-PSO	Modified Dynamic Programming with Particle Swarm Optimization

MFO	Moth Flame Optimizer
MFO-HHO	Moth Flame Optimizer - Harris Hawks Optimizer
MFO-SVM	Moth Flame Optimizer with Support Vector Machine
MGSCA	Memory Guided Sine Cosine Algorithm
MGWO	Modified Grey Wolf Optimizer
MILP	Mixed Integer Linear Programming
MM	Muller Method
MO	Multi-objective Optimization
MOGA	Multi-Objective Genetic Algorithm
MOMBO	Multi-Objective Migrating Bird Optimization
MSESCA	Multi-Strategy Enhanced Sine Cosine Algorithm
MVO	Multi Verse Optimizer
NSGA	Non-Dominated Sorting Genetic Algorithm
NWOA	Novel Whale Optimization Algorithm
PBUCP	Profit Based Unit Commitment Problem
PEM	Point Estimate Method
PEVs	Plug Electric Vehicles
PNACO	Parallel Nodal Ant Colony Optimization
PSA	Photon Search Algorithm
PSO	Particle Swarm Optimization
RES	Renewable Energy Sources
RWAOA	Random walk arithmetic optimization algorithm
SCA	Sine-Cosine algorithm
SCUC	Security Constrained Unit Commitment
TLBO	Teaching Learning Based Optimization
TS	Tabu Search
TSA	Tree Seed Algorithm
UCP	Unit commitment problem
V2G	Vehicle to Grid
WOA	Whale Optimization Algorithm
WSA	Wind Stride Algorithm

LIST OF PUBLICATION

Journal Publication

1. Pravin G. Dhawale, Vikram Kumar Kamboj, S.K. Bath, "A Levy flight-based strategy to improve the exploitation capability of arithmetic optimization algorithm for engineering global optimization problems". Transaction on Emerging Telecommunication Technology (2023), (SCIE), Impact Factor: 3.6, (Q2), https://doi.org/10.1002/ett.4739

2. Pravin Dhawale, Vikram Kumar, S.K. Bath, "Integrating Renewable Energy and PEVs into Security Constrained Unit Commitment for Hybrid Power Systems", Energy Report Journal. [Accepted], Elsevier, (SCIE), Impact Factor: 5.2, (Q1).

Conference Publication

1. Pravin G. Dhawale, Vikram Kumar Kamboj, S.K. Bath, O.P Malik, "Chaotic Arithmetic Optimization Algorithm for Optimal Sizing of Security Constrained Unit Commitment Problem in Integrated Power System", 11th Humanitarian Technology Conference, organized by IEEE Gujarat section at Marwadi University, on 16-18 October 2023, Rajkot, Gujarat (IEEE Conference)

2. Pravin G. Dhawale, Vikram Kumar Kamboj, S.K. Bath, Chaman Verma, Maria Simona Raboaca, Constantin Filote, Deepak Kumar, "Optimal Sizing of Security Constrained Unit Commitment Problem integrated with Renewable Energy Sources and PEVs", 15th International Conference on Electronics, Computers & Artificial Intelligence, ECAI, 29-30 June 2023, Bucharest (IEEE Conference)

3. Pravin G. Dhawale, Vikram Kumar Kamboj, S.K. Bath, "Arithmetic Optimizer Algorithm: A Comprehensive Survey of its Results, Variants, and Application", International Conference on Materials for Emerging Technologies (ICMET-21), LPU, Phagwara. (2022) (AIP Conference proceedings).

4. Pravin G. Dhawale, Vikram Kumar Kamboj, S.K. Bath, "Security Constraints Unit Commitment Problems Incorporated with Renewable Energy Sources and Plug-in Electric Vehicle", International Conference on Materials for Emerging Technologies (ICMET-21), LPU, Phagwara. (2022), (AIP Conference proceedings)

5. Pravin G. Dhawale, Vikram Kumar Kamboj, S.K. Bath, “A Comprehensive Review of Real-Time Monitoring and Controlling Challenges for Smart Grid Application and Its Probable Solution”, International Conference on Materials for Emerging Technologies (ICMET-21), LPU, Phagwara. (2022), (AIP Conference proceedings).

Communicated Publication

1. Pravin Dhawale, Vikram Kumar, S.K. Bath, “Optimizing Hybrid Power Systems with Renewable Energy Sources and Plug-in Electric Vehicles for the Security-Constrained Unit Commitment Problem” submitted to Computers and Electrical Engineering Journal. [Under Review], *(SCIE), Impact Factor:4.3, Paper ID: COMPELECENG-S-23-05946*

2. Pravin Dhawale, Vikram Kumar, S.K. Bath, “Integration of a Renewable Hybrid Power System for Security Constrained Unit Commitment Problem with a Novel Levy-Flight Arithmetic Optimizer” submitted to Energy Technology Journal [Under Review] *(SCIE), Impact Factor: 4.149, Paper ID: ente.20301484*

CHAPTER-1

INTRODUCTION

1.1 INTRODUCTION

The extensive network of connections and extremely non-linear operation of the contemporary power system have led to a major expansion of the power system. The ever-increasing demand for power in various sectors, such as residential, commercial, agricultural, and industrial, has caused overloading issues in electrical grids. This has been further aggravated by the trend toward privatization and deregulation. The expansion of the electrical grid must keep pace with demand, while also accounting for time-varying power demands, environmental constraints, and optimal utilization of available resources. India has set ambitious targets for expanding its renewable energy capacity. By 2030, it aims to achieve 450 GW of renewable energy capacity, with a specific target of 175 GW by 2022. To achieve this, the government has launched various initiatives, including the National Solar Mission, National Wind Mission, and National Bioenergy Mission. 100 GW of solar energy, 60 GW of wind energy, 10 GW of bioenergy, and 5 GW of small hydro energy will be added to the national grid as a result of these efforts [1].

Restructured power systems represent a significant shift in the organization and operation of electricity markets. Traditionally, power systems were vertically integrated, meaning a single utility managed the entire process of electricity generation, transmission, and distribution. However, in the latter part of the 20^{th} century, many countries began adopting restructuring policies to introduce competition and enhance efficiency in the power sector.

1.1.1 Key Components of Restructured Power Systems

Generation: In restructured power systems, the generation sector is often unbundled from transmission and distribution. Independent power producers (IPPs) or generators operate in a competitive market, where various entities can participate in electricity generation, fostering competition and driving innovation.

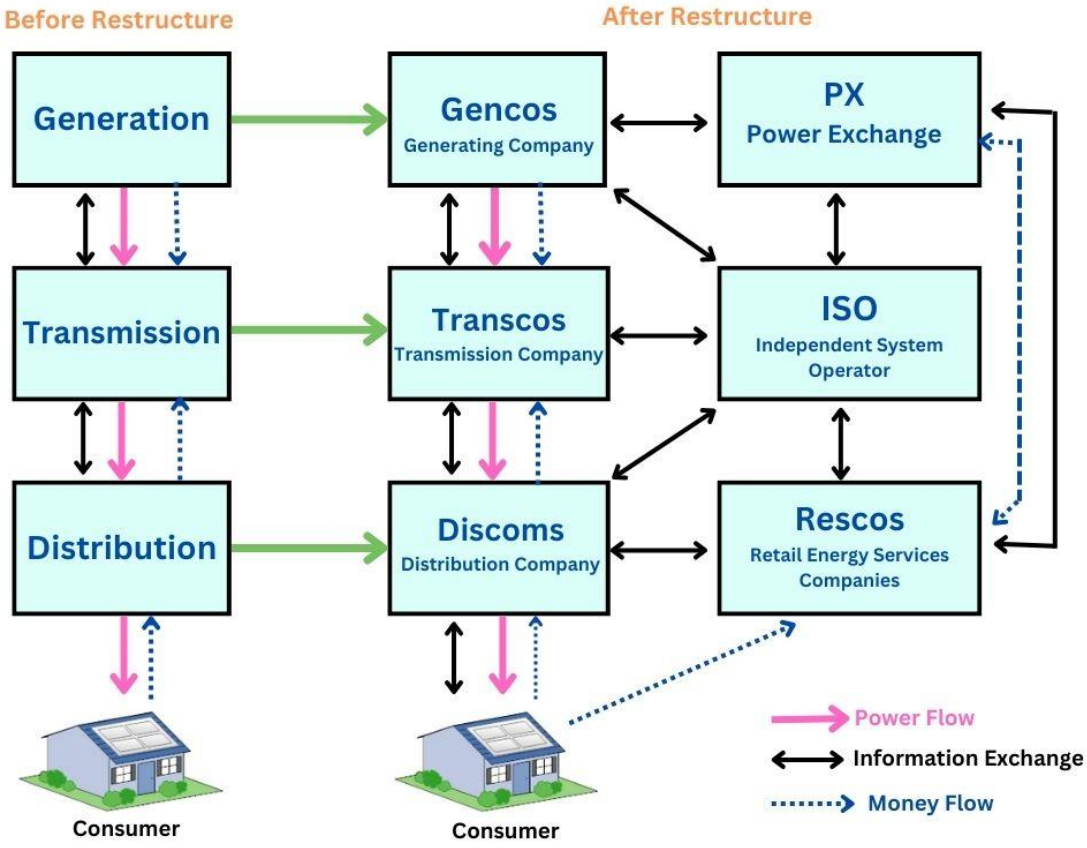

Figure 1.1 Block Diagram of Restructured Power System

Transmission: Transmission networks, responsible for transporting electricity over long distances from power plants to distribution networks, are typically managed independently. The goal is to ensure fair access to the transmission grid for multiple generators, promoting efficiency and reliability.

Distribution: Distribution networks, responsible for delivering electricity to end-users, are also subject to restructuring. Multiple entities, including competitive retailers, may operate in the distribution sector, providing consumers with options and promoting service quality.

Retail: Restructuring introduces competition at the retail level, allowing consumers to choose their electricity supplier. This competition aims to improve service quality, encourage innovation, and offer consumers a variety of pricing plans and energy sources.

Market Mechanisms: Restructured power systems often incorporate market mechanisms such as wholesale electricity markets. These markets enable the buying and selling of electricity among generators, traders, and other market participants, establishing transparent pricing based on supply and demand dynamics.

The motivation behind the research with the title "Security Constrained Unit Commitment Problem integrated with Renewable Energy Sources and Plug-in Electric Vehicles" is rooted in addressing critical challenges in power system operation and planning. This research endeavour is driven by several key motivations:

Grid Resilience and Reliability: Enhancing System Security: With the increasing penetration of renewable energy sources, power systems face greater variability and uncertainty. Integrating RES and PEVs into the SCUC problem is motivated by the need to enhance the resilience and reliability of the grid under varying conditions.

Transition to Clean Energy: Reducing Carbon Emissions: The integration of RES and PEVs is a crucial component of the global effort to transition towards a low-carbon energy system. By addressing the security-constrained unit commitment problem in the presence of renewables and electric vehicles, the thesis aims to contribute to the reduction of greenhouse gas emissions associated with power generation.

Optimizing Resource Utilization: Maximizing Renewable Energy Integration: The research seeks to optimize the utilization of renewable energy sources within the power system. This involves developing algorithms and models that consider the intermittency and variability of RES while ensuring system security and reliability [2].

Grid Flexibility and Adaptability: Accommodating PEV Charging Dynamics: With the growing adoption of PEVs, the thesis is motivated to explore ways to integrate their charging dynamics into the unit commitment process. This involves developing strategies to manage the impact of PEV charging on the grid and leverage the flexibility offered by these vehicles.

Technological Advancements: Innovations in Grid Management: The thesis is motivated by the opportunity to contribute to the advancement of grid management technologies. This includes exploring novel approaches to handle the complexities introduced by RES and PEVs, ensuring that the power system remains secure and efficient.

Policy Compliance and Market Dynamics: Meeting Regulatory Requirements: Power systems must adhere to stringent security and reliability standards. The thesis is motivated by the need to develop solutions that align with existing regulations and market dynamics while accommodating the increasing share of renewable energy and the integration of PEVs [3].

Economic Viability: Cost-Effective Power System Operation: By integrating security constraints with the unit commitment problem in the context of RES and PEVs, the thesis aims to contribute to cost-effective power system operation. This involves finding optimal solutions that balance the economic considerations of power generation with environmental and reliability constraints.

Contributing to Academic and Industry Knowledge: Advancing Research Frontiers: The thesis seeks to contribute to the academic knowledge base by pushing the boundaries of research in the intersection of security-constrained unit commitment, renewable energy integration, and electric vehicle charging management. The findings may offer insights for industry practitioners and policymakers.

The motivation for the thesis lies in its potential to address pressing challenges in power system operation, align with global efforts towards sustainable energy, and contribute valuable insights to both academic research and practical applications in the field of power system optimization and management.

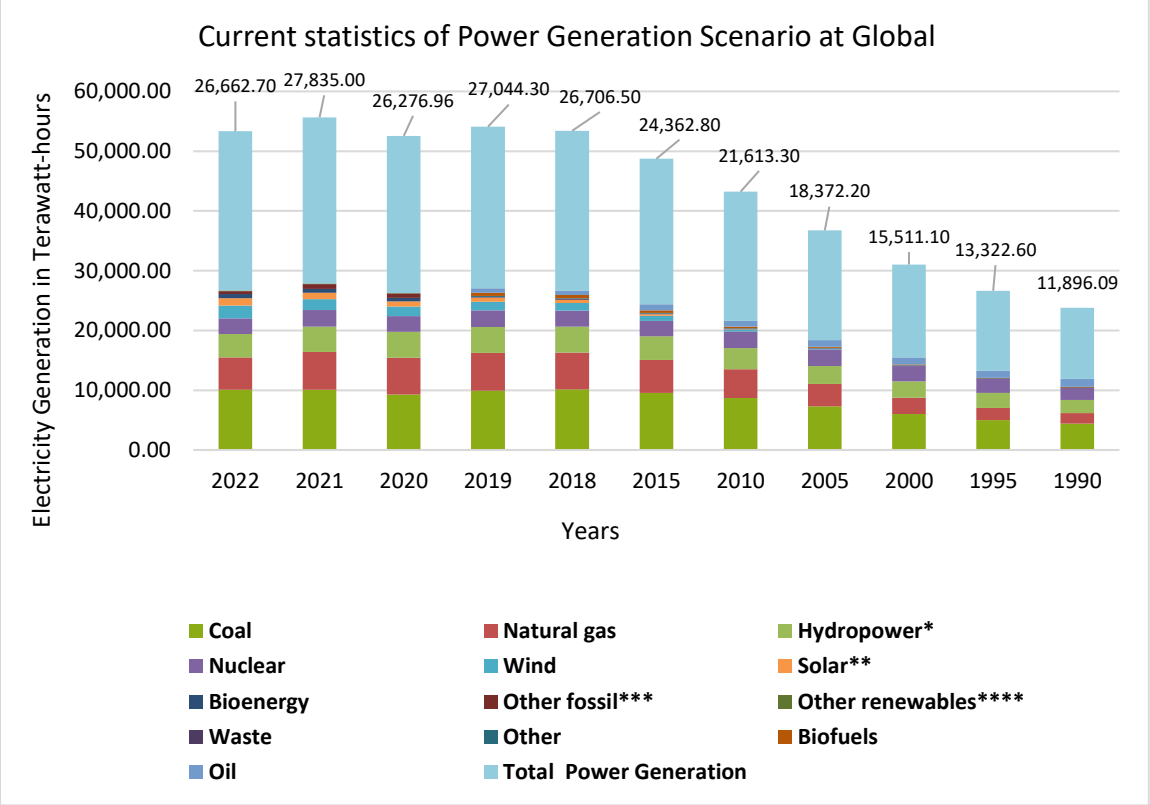

Figure 1.2 Current statistics of Power Generation Scenario at Global level [4]

Nuclear, thermal, hydroelectric, and other power-generating units make up the modern power system. Additionally, power demand varies throughout the day. Therefore, to achieve optimal generation cost, it is necessary to choose which generating unit should be turned on for a specific hour and which should be turned off to meet time-varying power demand. SCUC refers to the entire process of making this intelligent decision, and a committed unit is a unit that has been programmed to connect to the power system network [5].

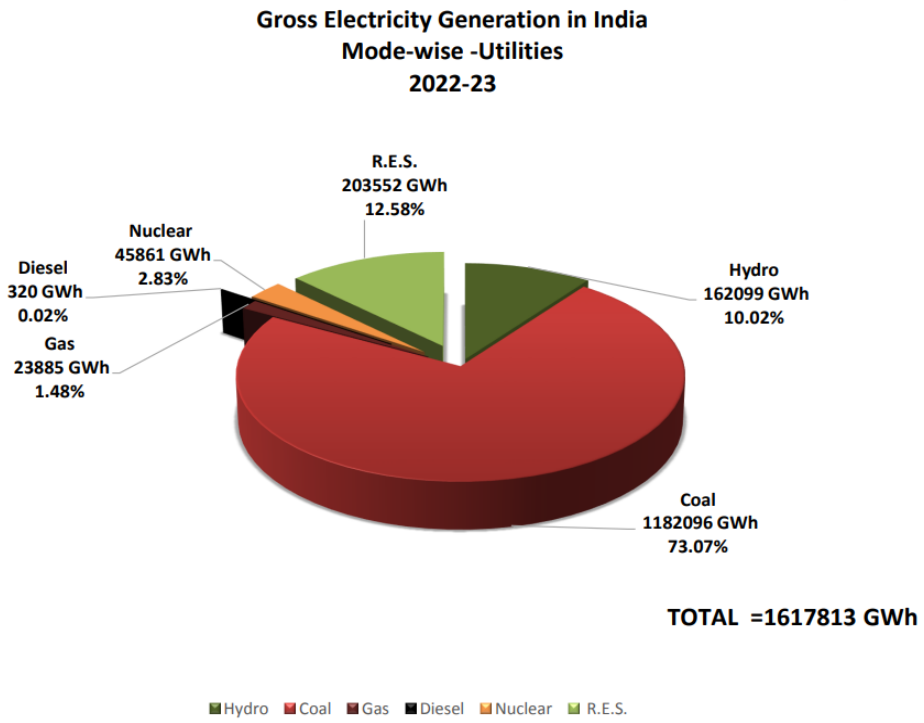

Figure 1.3 Power Generation Scenario at National level [4]

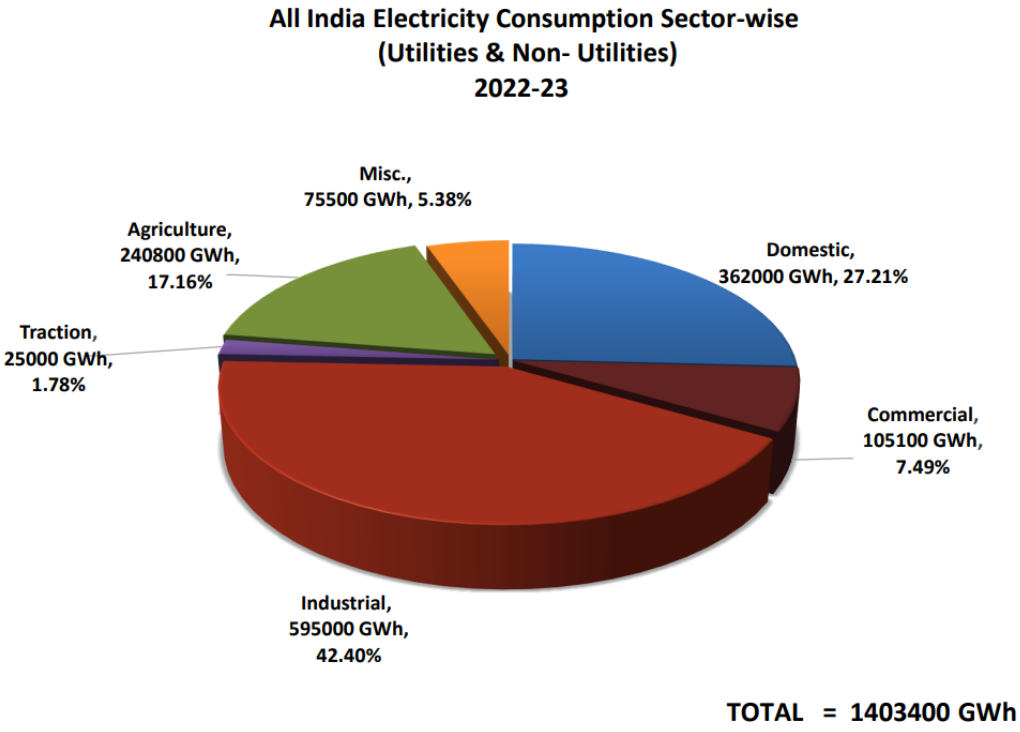

Figure 1.4 All India Electricity Consumption Sector-wise 2022-23 [4]

A mathematical optimization problem called the SCUC issue is employed in the design and management of power systems. The Unit Commitment issue, which is a subset of the SCUC problem, is concerned with planning the operation of producing units over a certain time horizon while satisfying the system's load requirement. By taking into account the constraints and contingencies of the transmission network, the SCUC problem elevates the UC problem to a higher level of complexity. To put it another way, the safety and dependability of the power system are guaranteed by SCUC's consideration of the security aspects of its operation. SCUC takes into account the power grid's available transmission capacity and ensures that scheduled power flows do not exceed transmission limits [6].

SCUC takes into account the possibility of power system failures or outages involving transmission lines, generating units, or other parts. It guarantees that the power system can continue to function safely and reliably even in such circumstances. SCUC makes sure that the power system works within the limits of voltage stability, which is important for keeping the power system’s reliability. The SCUC problem's objective is to meet security constraints while reducing electricity generation and transmission costs. The SCUC problem solution provides the optimal schedule for power generation units, transmission lines, and other parts of the power system over a given time horizon. To guarantee the power system's safe and dependable operation, planners and operators need access to the SCUC problem. It aids in maximizing the utilization of transmission infrastructure and resources for power generation while preserving the power system's safety and dependability [7].

1.2 SECURITY CONSTRAINT UNIT COMMITMENT

SCUC issue is a mathematical optimization problem used in power systems to determine the optimum method to schedule power generators while keeping the power system secure and dependable. The availability and capacity of generators, transmission line capacities, voltage limits, and other technical constraints are all taken into consideration in the SCUC problem. It also takes into account unforeseen contingencies like transmission line outages or generator failures that could affect the power system's stability and dependability. The

SCUC challenge seeks to make the power system safe and reliable under a variety of operating scenarios while lowering total power generating and distribution costs.

The SCUC problem is challenging and calls for complex mathematical methods and optimization techniques. Several tactics have been developed throughout time, including MILP and MIQP. Modern power systems, which are becoming increasingly interconnected, depend heavily on the SCUC problem to function safely and reliably. The SCUC problem helps to reduce the likelihood of blackouts, voltage collapses, and other critical events that could affect the stability and dependability of the power system by optimizing the scheduling of generators and taking into account a variety of operational and security constraints [8].

1.3 SECURITY CONSTRAINT UNIT COMMITMENT PROBLEM WITH ELECTRIC VEHICLES

The introduction of PEVs into the system has presented additional challenges to the SCUC problem in power systems. The increasing ambiguity and fluctuation caused by the PEV charging demand might threaten the security and dependability of the power supply. To include PEVs in the SCUC issue, it is required to model the charging demand of PEVs as a stochastic variable that is affected by many variables such as the quantity of PEVs, their charging patterns, and the availability of charging infrastructure. The demand for PEV charging can also be influenced by outside variables including the climate, traffic, and customer behaviour.

Numerous modelling and optimization strategies, including robust optimization, and scenario-based optimization, have been proposed as solutions to these issues. By taking into account the uncertainty and variability of PEV charging demand, these methods can contribute to increasing the power system's security and reliability. Besides, the integration of PEVs into the power system can likewise give new chances to request power demand response and energy storage. By carefully planning the timing of PEV charging and discharging, it is feasible to lower the costs and environmental impacts of electricity generation while increasing the flexibility and efficiency of the power system. PEVs must

be integrated into the SCUC problem, which calls for novel approaches and enhanced practices that can handle the cyclical and unpredictable nature of PEV charging demand. The power system's security, dependability, and effectiveness can all be enhanced in this way, and the advantages of PEV integration can also be secured [9].

1.4 SECURITY CONSTRAINT UNIT COMMITMENT PROBLEM WITH RENEWABLE ENERGY

The SCUC challenge in power networks becomes very difficult when renewable energy sources are incorporated. Due to the unpredictability and inconsistency of renewable energy sources like wind and solar power, it is difficult to schedule generators optimally while still assuring the security and reliability of the power system. To address these difficulties, sophisticated modelling and optimisation techniques like resilient optimisation and scenario-based optimisation have been developed. These techniques are able to deal with the volatility and unpredictability of renewable energy sources and help to increase the security and dependability of the power system by applying a number of operational and security limitations.

The SCUC problem can be approached in a different way by incorporating energy storage systems. Energy storage systems can provide a flexible energy source that can be used to balance the power system and help to smooth out the variability and uncertainty of renewable energy sources. By maximising the scheduling of energy storage devices, the SCUC issue has the potential to help increase the dependability and efficiency of the power system while also reducing electricity generating costs and environmental effects. Renewable energy sources must be included into the SCUC issue using sophisticated modelling and optimisation techniques that can handle their fluctuation and uncertainty. It is possible to take advantage of the advantages of the generation of renewable energy while simultaneously increasing the power system's security and reliability [10].

1.5 OUTLINES OF THE DISSERTATION

The SCUC problem in the modern power system is the main focus of the current study. The present research focuses on optimizing and overcoming the security constraint unit commitment problem in the modern power system. The effect of PEVs is taken into consideration by a metaheuristics optimizer when solving the SCUC problem using the hybrid algorithm. Also take into account the RES uncertainty in the summer and winter. The primary objective is to achieve maximum profit and reliability while meeting time-varying, technical, electricity demand-response, and other physical constraints. To find the best SCUC problem solution, three hybrid algorithms have been tested, and various scenarios have been taken into consideration. The potential of the proposed work has been examined by testing a variety of small, medium, and large test systems. In this thesis, the work of the current study has been organized as follows:

Chapter 1 is an introduction to the SCUC problem and its significance in the current power sectors discussed. The integration of the SCUC problem with PEVs and RES is discussed. In addition, various types of metaheuristic search algorithm optimisation techniques are presented in this chapter. For the SCUC problem, the hybrid method, as well as the stochastic search algorithm and conventional algorithm, have been proposed.

Chapter 2 discusses the explanations of various optimization techniques' methodologies. The chapter discusses the various optimizers utilized to resolve SCUC problem related issues. the examination of some of the testing benchmarks used to solve the SCUC problem, including PEVs' charging and discharging capabilities. This chapter also provides an in-depth discussion of the RES literature.

Chapter 3 identifies some brand-new metaheuristic optimization methods that are inspired by arithmetic mathematical operations like division, multiplication, addition, subtraction, a number of chaotic map numbers, and adaptive search methods. The effectiveness of these hybrid optimizers is evaluated using hypothesis tests. In order to enhance diversification and intensification, in other words, we can say that exploration and exploitation over the whole search space, CAOA, RWAOA, and LAOA have been developed. These developed

hybrid algorithms are tested successfully for different benchmark functions, including multidisciplinary engineering design problems.

Chapter 4 shows that the proposed optimization techniques, CAOA and LFAOA, are effective and valid for solving the SCUC problem. Also, a conventional test system with thermal generating units for the different power sectors is used to assess how effectively the recommended hybrid optimization technique works. The effectiveness of the suggested method was assessed with 10, 20, and 40 generators. After a successful experiment, it was found that the proposed optimizer outperforms another existing optimizer in solving continuous, discrete, and non-linear optimization issues. The novel CAOA and LFAOA optimizers outperform all other methods in terms of different constraints, including profit comparison.

Chapter 5 The reliable solution for the SCUC problem, taking into account the influence of PEVs, solar RES during summer and winter, and wind power, is provided through the utilization of hybrid optimizers such as CAOA and LFAOA. These optimizers have been applied to systems comprising 10, 20, and 40 generating units, which have undergone successful scheduling, resulting in minimum cost. Through simulation results, it has been established that the performance of the CAOA and LFAOA optimizers is superior to that of previously established heuristics, metaheuristics, and evolutionary search optimizers, as well as those currently in use, in terms of profit. The simulation results indicate that the proposed optimizer can determine a satisfactory generating cost value within a reasonable computational time frame while incorporating commitment scheduling. Such a powerful tool can be employed to obtain solutions for the crucial issue of unit commitment in modern power systems. The variation in cost values, including the best, average, and worst values, along with their standard deviation and median values, is taken into consideration. Several hypothesis tests, including the Wilcoxon rank-sum test and t-test, are utilized to analyze the results, although p-values and h-values are subject to uncertainty. Furthermore, the computational times for the best, average, and worst simulation times are evaluated. A

comprehensive representation and summary of the applications and contributions of CAOA, RWAOA, and LFAOA in SCUC problem are provided.

1.6 CONCLUSIONS

The present chapter serves as the backbone of the thesis, providing a detailed outline of the research work carried out. It offers a comprehensive overview of the different chapters in the thesis and summarizes them briefly, highlighting the research's significance.

Furthermore, the chapter explores the current scenario of security constrained unit commitment problems, bringing together the different perspectives and solutions offered in the field. The research study presented in this thesis contributes to the existing body of knowledge by providing a novel approach to solving this problem.

In addition, the chapter offers an introduction to the thesis topic, providing a background to the research work. It sets the stage for the research problem and presents the objectives and methodology employed in the study. The introduction aims to provide a clear understanding of the research problem, its importance, and the scope of the study. Overall, the chapter provides a comprehensive overview of the thesis, serving as a guide for the reader. It lays out the research's foundation, highlighting the problem's significance and the approach taken to address it.

CHAPTER- 2

LITERATURE REVIEW

2.1 INTRODUCTION

SCUC is a critical concern in the operation and planning of power systems. The primary objective of the SCUC problem is to identify the optimal generation schedule that meets system demand while ensuring the safety and reliability of the power grid. Over the past few years, significant strides have been made in the development of efficient optimization algorithms for addressing the SCUC problem. The field of optimization research is constantly expanding due to new challenges and opportunities, driving further advancements in this area.

The different new procedures or strategies for various improvement issues are needed to effectively settle. To overcome the shortcomings of the current methods, the research is rapidly developing a hybrid combination of optimization algorithms. The current chapter provides an overview of the literature available on various optimization methods utilized to effectively address the challenges posed by security constraints in unit commitment problems. The SCUC problem related issues became more complicated when renewable energy sources like solar, wind, and others were involved. Additionally, the numerous constraints have made SCUC problem more complicated, including the charging and discharging of PEVs. In order to improve the system's reliability and boost the system’s generation profits, the power scheduling selections and allocations are more crucial in the security constraint unit commitment problem.

2.2 REVIEW OF LITERATURE

Optimization is a huge area of research in power systems, where research activities are used to design various optimization techniques. Numerous researchers have developed optimization techniques to address a variety of issues in a variety of fields. In order to improve the existing optimizer's efficiency, numerous researchers are successfully

developing new optimizers and modifying existing algorithms using chaotic and hybrid techniques [11]. The successfully implemented methods, including SCUC problem, can be divided into three groups for issues in the real world: conventional techniques, non-conventional techniques, and hybrid techniques. The researchers are eager to discover novel approaches and methods for resolving problems involving security constraint unit commitment. Additionally, optimization is a huge field in which research is moving quickly. The researchers are successful in locating solutions by attempting to apply various methods to various issues. In order to address any shortcomings in the methods that are currently in use, research is ongoing to discover new algorithms and hybrid versions of existing algorithms. The review of literature has been divided into three subsections viz. (i) Review of SCUC problem, (ii) Review of SCUC problem by considering renewable energy sources, (iii) Review of SCUC problem by considering the PEVs.

2.2.1 Review of Security Constraint Unit Commitment Problem

A metaheuristic technique was created by Yang et al. [12] to address the unit commitment problem with renewable energy sources. The tool included a revolutionary method for sampling several zones and considered the clever control of PEV charging and discharging. The analysis of four different unit commitment scenarios in various weather and season circumstances made up the entirety of the study. To completely analyse and assess the economic impacts of various scenarios, the average economic cost index is utilised [13].

Imani Hosseini et al. The utilisation of a V2G system is taken into consideration in the SCUC problem. They discussed the scheduling and management of power systems utilising V2G. The expanded IEEE 30 bus system and the IEEE 6 bus system are two case studies that have used the suggested methodology. In this study, two simulated scenarios were provided: The SCUC problem was initially evaluated separately and then with a few electrical cars connected to the lattice. The results demonstrate a reduction in the overall cost of operating. The administrator can also establish the appropriate number of cars needed to depart every hour by employing the suggested method. The findings of this study

could prove useful for system designers and operators in the design, planning, and operation of power systems [14].

In their work, Muralikrishna et al. conducted a thorough examination of evolutionary optimization methods utilized for solving UC problems. They gathered information from several peer-reviewed publications and divided their analysis into multiple sections, using a range of evolutionary optimization techniques. The aim was to provide assistance to new researchers in addressing modern UC problems in various power system scenarios [15].

Wang and Hobbs, along with other researchers, conducted an investigation into unit commitments in the real-time market with a focus on ramp or Flexi-ramp capability. The Flexi-ramp was defined as the reserve committed unit's ability to handle sudden changes in demand resulting from the increased penetration of renewable energy. This study highlighted the need for flexible generators to better handle such scenarios. To further advance the research, the team incorporated a multitude of complex constraints, including meeting load demands, power generation limits, minimum up and free time, as well as spinning reserves [13].

Abujarad et al. done a review of the UC concepts, goals, and limitations in the literature. The need for alternative optimization strategies for UC solutions is the subject of this study. The effects of installing energy storage devices on UC models and the fluctuation in power generation caused by them are discussed [16].

V. K. Kambhoj et al. for further developing the double ability to deal and worldwide execution of the DE calculation, a novel and mixture variant of the DE calculation is introduced, and furthermore, presents a DE algorithm in the hybrid form for calculation joined with a random search for the arrangement of a solitary region UCP. Experimental investigation was conducted on benchmark systems containing 4, 10, 20, and 40 generating units to evaluate the effectiveness of the hybrid DE random search method. The results of the study demonstrate the efficacy of the proposed hybrid algorithm and its ability to produce global solutions for the UCP problem [17].

Ghasemi et al. introduced a stochastic model for security-constrained unit commitment (SCUC) to enable the smooth integration of wind power into reconfigurable transmission networks [18]. The model was not only presented but also implemented in practice [18]. While accommodating transmission constraints, the proposed model makes use of network reconfiguration to reduce costs associated with energy, spinning reserve, wind curtailment, and load shedding. The Benders decomposition method is used to formulate and solve the associated optimization problem. Using IEEE 118-bus and 6-bus test systems, the proposed model's performance is thoroughly examined [18].

Talebizadeh et al. have suggested an appropriate charging and discharging schedule for PEVs based on load variations [3]. Integral PEVs are incorporated into the proposed method; referred to as parking lots; into the issue of unit commitment [3]. The effects of PEVs on generation scheduling are examined using a 10-unit IEEE test system. Significant technological and financial savings can be seen in the simulation analysis results [3].

Zheng et al. conducted a review of stochastic optimization-based unit commitment techniques. These techniques have been widely utilized in the power sector to facilitate decision-making processes for dispatch and power generation planning. Unit commitment is a critical aspect of power generation, and this review highlighted two main areas of research: unit commitment improvement and ongoing operations [19].

Cai et al. developed a mathematical model based on the conventional SCUC formulation to address the problem of power system dispatching including plug-in hybrid electric vehicles (PHEVs) [20]. The model takes into account not only the financial gains for PHEV owners but also the costs associated with carbon dioxide emissions, while ensuring the safe operation of the power system. The UC model and the EVs scheduling model, both of which incorporate AC power flow constraints, are then used to decouple the developed model from the PHEVs as mobile energy storage units [20].

Nikolaidis and others analyzed annual data from the isolated power system on the island of Cyprus to assess the effect of intermittent renewable energy sources on total production

costs. They recognized electrical energy stockpiling as a feasible way to deal with upgrade adaptability and dependability. To model and evaluate the selected EES facilities, a life-cycle cost analysis was carried out with cost metrics and characteristics based on actual values found in the literature [21]. According to the findings of the uncertainty analysis, the vanadium-redox flow battery exhibited the highest net present value compared to other evaluated electrical energy storage facilities [22]. Nevertheless, the sodium-sulphur battery system was identified as the most secure investment, in terms of both the uncertainty range and mean value, followed by the lead-acid battery system. On the other hand, even though the lithium-ion battery system had high capital costs, its overall cost performance was still poor, as indicated by its negative mean NPV well below zero [22].

Panagiotis et al. concentrated on UC models that employ several strategies to control the unpredictability of renewable energy sources and integrate large amounts of wind power output. The IEEE RTS 96 power system was chosen by the researchers as their test platform [23]. To evaluate the effectiveness of different electrical energy storage facilities in enhancing flexibility and reliability, a life-cycle cost analysis was conducted by considering the most realistic values found in the literature. The vanadium-redox flow battery was found to have the highest NPV among the EES facilities evaluated, while the sodium-sulphur and lead-acid battery systems were deemed the most secure investments based on their uncertainty range and mean value. Additionally, simulation results showed that an optimized charging strategy was more effective than a random charging strategy in terms of total operating costs and capacity to integrate additional EVs [23]. The most reliable UC model has higher overall operating expenses as compared to the other models as a result of its more conservative approach to handling the stochastic nature of wind. There is a non-linear trade-off between power system robustness and overall operating cost, which also influences EV uptake, depending on the features of each power system [23].

According to Wang et al., the growth in PEV ownership in recent years has been sparked by favourable regulatory changes, a greater availability of charging infrastructure, and reduced beginning prices. PEV adoption boosts grid-based power consumption, which may

either make supply shortages worse or level off demand curves. It is essential to have the best coordination and commitment of power production units while also making it feasible for more PEVs to connect to the grid in order to minimise the cost and pollution generated by thermal power generation systems as well as make the transition to a smarter grid [24].

The inclusion of stochastic charging behaviour of PEVs with flexible demand side management poses new challenges for optimizing complex power systems, rendering existing mathematical methods inadequate. This study aimed to tackle the challenge of large-scale unit commitment problems that involve mixed-integer variables and multiple constraints commonly found in PEV-integrated grids. To achieve this, a novel parallel competitive SOA was developed, which combines binary and real-valued optimizers, and can handle simultaneous UC problem and demand side management of PEVs. The proposed method was tested in numerical case studies, which included different scales of unit numbers and a variety of demand-side management strategies for plug-in electric vehicles. The results of these studies demonstrated that the parallel competitive swarm optimization-based method outperformed other approaches in effectively addressing the complex optimization problem. Plug-in electric vehicles' adaptable demand-side management strategies have demonstrated significant economic potential [9].

The importance of performing stochastic analysis on the security-constrained unit commitment problem has been emphasized by Mehrtash et al.[25]. This is particularly relevant in the current electricity market where renewable energy sources are being increasingly deployed on the generation side, and variable loads are emerging on the demand side. Additionally, the growing popularity of plug-in electric vehicles that rely on electricity instead of fossil fuels presents both opportunities and challenges for modern-day electric power systems. As such, there is a need for continued research in this area to ensure safe and efficient operation of the electricity market [25].

Table 2.2.1 Literature Review on Security Constraint Unit Commitment Problem

Author	Year	Research Gaps	Findings	Test Systems Used
Bertsimas, D. et al.[26]	2005	Integration of uncertainty in unit commitment	Showed that the incorporation of uncertainty led to more robust and flexible unit commitment solutions	IEEE RTS-96
Zhang, N. et al. [27]	2009	Uncertainty modeling in unit commitment	Identified the need for improved modeling techniques to capture the effects of uncertainty on unit commitment	IEEE 118-bus system
Guan, Y. et al. [28]	2011	RES integration with UCP	Showed that the integration of renewable energy sources can significantly reduce the operational cost of power systems	IEEE 118-bus system
Wu, L. et al. [28]	2013	Multi-objective unit commitment	Identified the need for better optimization techniques to handle the conflicting objectives of unit commitment	IEEE 30-bus system
Liu, C. et al.[29]	2015	Unit commitment under transmission network constraints	Showed that the inclusion of transmission network constraints can lead to more efficient and reliable unit commitment solutions	IEEE 118-bus system
Rogier et al. [30]	2021	All security constraints are not considered	Solved the unit commitment problem by considering ramping constraints	10 Unit, New algorithm
Wenjun et al.[31]	2022	Some limited constraints of SCUC problems are considered	Fastly detect the redundant constraints in the security constraint unit commitment problem.	IEEE-30 Bus system
Ayani N. et al.[9]	2022	Not considering the wind power generation as RES source	Profit based unit commitment problem is solved with hybrid algorithm.	10. 20 generating unit system are considered

Table 2.2.2 Hierarchy, Timescale of problems in the operation and planning of Power Systems

Hierarchy	Timescale	Problems	References
Strategic	Long-Term (Years)	Resource Planning, Infrastructure Development, Regulatory Compliance, Integration of Renewable Energy Sources	[32][33][34]
Tactical	Medium-Term (Months-Years)	Capacity Expansion Planning, Transmission Network Upgrades, Load Forecasting and Demand Management, Market Design and Policy Changes	[35][36][37] [38][13][39]
Operational	Short-Term (Minutes-Hours)	Real-Time Grid Operations, Contingency Management, Voltage and Frequency Control, Emergency Response	[40][41][42] [43][44][41]
Technical	Very Short-Term (Seconds)	Fault Detection and Diagnostics, Grid Stability and Resilience, Cybersecurity	[45][46][47]
Procedural	Immediate (Real-Time)	Operator Training and Procedures, Communication Protocols, Control Room Coordination	[48][49][16][50]

Effective management and day-ahead scheduling of plug-in electric vehicles presents an opportunity to address the challenges faced by power system operation and planning. To address the security-constrained unit commitment problem involving wind power generation and plug-in electric vehicles, this study proposes a novel approach that utilizes interior point optimization techniques. The method offers the advantages of conventional scenario-based approaches while overcoming their limitations. The algorithm was implemented on two networks: a large-scale 118-bus test system and a 6-bus test system. The results of the study demonstrate that the proposed method is accurate and effective, particularly for large-scale power systems with varying levels of uncertainty [25].

2.2.2 A comprehensive literature review on SCUC problems with RES

In the planning of the operation of power systems, the SCUC problems is a crucial optimisation issue. Finding the best unit commitment schedule for generators while ensuring the power system complies with operational requirements, such as security and reliability limitations, is the goal of the SCUC issue [6]. New difficulties in SCUC issues have emerged as a result of the growing penetration of renewable energy sources (RESs) in power networks. An overview of current studies on security-constrained unit commitment issues with renewable energy sources is provided in this literature review [51].

Several research have looked into SCUC issues with renewable energy. A 2-stage strategy was suggested by Zhang et al. (2021) for resolving the SCUC issue using renewable energy sources. In the first step, a unit commitment issue with no security requirements is solved, and in the second stage, security constraints are added. A case study employing wind and solar energy sources was employed in the study to show the usefulness of the mixed-integer linear programming model [52].

Studies have also been done on stochastic SCUC issues using renewable energy sources. A stochastic SCUC model that takes into account wind and solar power as uncertain variables was proposed by Fouladgar et al. (2018). The study used a chance-constrained programming approach to handle the uncertainty in the stochastic SCUC problem. The results showed that the proposed model could effectively handle the uncertainty in the stochastic SCUC problem [18].

Multi-objective SCUC issues with renewable energy sources have been examined in a number of research. A bi-level, multi-objective SCUC model that takes into account both economic and environmental goals was presented by Li et al. in 2019. The bi-level multi-objective SCUC issue was solved using a non-dominated sorting genetic algorithm II (NSGA-II) in the study. The findings demonstrated that the suggested model could successfully balance the SCUC problem's economic and environmental objectives while using renewable energy sources [53].

To enhance the performance of SCUC issues, battery energy storage systems have been combined with renewable energy sources. A SCUC model that takes battery energy storage systems into account to manage the unpredictability and uncertainty of renewable energy sources was proposed by Huang and colleagues in 2020. The findings of the study demonstrated that the suggested model could successfully handle the unpredictability and uncertainty of renewable energy sources. The study employed a two-stage strategy to address the SCUC problem using BESSs. There are a number of research gaps in the literature, as indicated in the table, including the neglect of voltage stability in SCUC issues, the absence of thorough analyses of optimisation models for SCUC with renewables, and the disregard for chance-constrained programming. However, there have been several findings, including the effectiveness of GA-based and SCUC approaches in handling uncertainty and variability of renewables, the significant impact on RES [54].

Table 2.2.3 Literature review on security constraint unit commitment problem with RES

Author & Year	References	Research Gaps	Findings	Test System Used
Galiana, F. D., & Wu, L. (2010).	[50]	Lack of comprehensive review of optimization models for SCUC	Reviewed various optimization models for SCUC with renewables	Power system with SCUC
Ortega-Vazquez, M. A., & Kirschen, D. S. (2013).	[55]	Lack of assessment of wind power's impact on system flexibility	Wind power can significantly reduce operational flexibility	Power system with wind power
Yang, H., Sun, Y., & Shahidehpour, M. (2016).	[56]	Lack of consideration for chance-constrained programming	The proposed approach can handle the uncertainty of renewables	Power system with wind power and solar power
Li, X., Fouladgar, M. M., & Ahmadi-Khatir, A. (2019).	[57]	Lack of multi-objective approach to SCUC with renewables	A proposed bi-level multi-objective approach for SCUC with RE	Power system with wind power and solar power

Zhang, L., Xu, H., & Gao, F. (2021).	[58]	Lack of consideration for two-stage approach to SCUC with RE	Proposed two-stage approach for SCUC with renewables	Power system with RES

The test systems used in these studies vary, with some studies using power systems with wind power and/or solar power, while others do not specify a test system.

2.2.3 A comprehensive literature review on security constraint unit commitment problems with plug-in electric vehicles

As shown in the table, there are several research gaps in the literature, including the lack of consideration for PEVs in SCUC, the lack of analysis on the impacts of PEVs on system operation, and the lack of consideration for the charging behaviours of PEVs.

Table 2.2.4 Literature review on security constraint unit commitment problem with electric vehicles

Author & Year	References	Research Gaps	Findings	Test System Used
Li, Liu & Wang (2012).	[28]	Lack of consideration for electric vehicles in SCUC	Proposed approach can effectively model PEVs in SCUC	IEEE 30-bus system with PEVs and wind power
Saberi & Vahidinasab (2013).	[59]	Lack of analysis on impacts of EVs on system operation	Proposed approach can effectively manage PEVs in SCUC	IEEE 14-bus system with PEVs
Ding, Li & Li (2016).	[60]	Lack of consideration for charging behaviors of PEVs	Proposed approach can model EV charging behaviors in SCUC	IEEE 33-bus system with PEVs and wind power
Kucuk & Kucuk (2018).	[61]	Lack of analysis on effects of charging infrastructure	Proposed approach can manage PEV charging infrastructure in SCUC	IEEE 30-bus system with EVs and charging infrastructure
Zhang & Cui (2019).	[62]	Lack of analysis on impacts of stochastic PEVs	Proposed approach can effectively manage stochastic PEVs in SCUC	IEEE 118-bus system with PEVs and wind power

Bai, Wang & Li (2020).	[63]	Lack of analysis on effects of bidirectional charging	Proposed approach can manage bidirectional PEV charging in SCUC	IEEE 33-bus system with PEVs and solar power
Rahimi, Safari & Moradi (2020).	[37]	Lack of consideration for uncertainty in PEV charging	Proposed approach can handle uncertainty in EV charging for SCUC	IEEE 33-bus system with PEVs and wind power
Zhang, Huang & Han (2021).	[58]	Lack of analysis on effects of V2G services	Proposed approach can manage V2G services in SCUC	IEEE 118-bus system with PEVs and wind power
Zangeneh et al. (2015)	[64]	Electric vehicle charging and discharging impact on power system reliability is absent.	To maximise the integration of electric cars into the power grid while retaining dependability, a security-constrained unit commitment model was proposed.	IEEE 118-bus test system
Haji et al. (2016)	[65]	Lack of consideration of the uncertainty of electric vehicle arrival and departure times.	Proposed a robust security-constrained unit commitment model that considers the uncertainty of electric vehicle arrival and departure times.	IEEE 57-bus test system
Asrari et al. (2017)	[14]	The effects of electric car charging on the distribution system have not been well examined.	Proposed a security-constrained unit commitment model that takes the distribution system's effect of PEV charging into account.	IEEE 33-bus distribution system
Teng et al. (2018)	[66]	The UC problem's implications for battery deterioration in electric vehicles are not taken into account.	A security-constrained unit commitment model that takes the effect of battery deterioration on the ideal charging and discharging schedule into account has been proposed.	IEEE 118-bus test system
Safdarian et al. (2019)	[13]	Lack of analysis of the impact of electric vehicle parking lots on the power system.	Proposed a SCUC model that considers the impact of electric vehicle parking lots on the power system.	IEEE 118-bus test system

Li et al. (2020)	[60]	Lack of consideration of the multi-objective nature of the UCP.	Proposed a SCUC that considers the multi-objective nature of the problem and optimizes the economic and environmental objectives.	IEEE 118-bus test system
Mousavi et al. (2021)	[67]	Lack of consideration of the impact of electric vehicle charging on the power system voltage stability.	Proposed a SCUC model that takes into account how charging electric vehicles affects the stability of the power system's voltage.	IEEE 39-Bus Test system

However, there have been several findings, including the effectiveness of proposed approaches in effectively modelling and managing PEVs in SCUC, the importance of analyzing the effects of bidirectional charging and V2G services, and the effectiveness of approaches in handling uncertainty in PEV charging. Some of these studies employ IEEE 30-bus, IEEE 33-bus, and IEEE 118-bus systems with electric vehicles, wind, solar, and/or charging infrastructure, while other studies do not identify a test system [68].

2.2.4 A comprehensive literature review on security constraint unit commitment problems with PEVs and renewable energy sources

Table 2.2.5 Literature review on SCUC problem with PEVs and RES.

Author	References	Research Gaps	Findings	Test System
Carrión, M et al. (2006). SCUC with Wind Power Plants	[69]	Incorporating wind power plants into SCUC models	Wind power plants can be successfully included into the SCUC issue and the uncertainties related to wind power generation can be handled by the provided model and solution method.	IEEE 118-bus system
Morales-España, G., Gómez-Lázaro, E., & Pérez-Molina, J. (2013). SCUC	[67]	How to effectively incorporate large-scale wind farms into SCUC models	The proposed model and algorithm can effectively handle large-scale wind farms in SCUC problems, while considering	IEEE 118-bus system

with large-scale wind integration.			transmission constraints and voltage stability.	
Ranjbar, A. M., & Taherian, H. (2016). Unit commitment problem with solar and wind energy sources.	[70]	Incorporating solar power plants into SCUC models, including consideration of the variability and uncertainty of solar power generation	The proposed model and solution algorithm can effectively handle the uncertainties associated with solar power generation in SCUC problems.	IEEE 30-bus system
Zhang, J., Li, G., & Wu, L. (2017). Multi-objective UC with Wind Generating power, and Energy storage	[41]	Incorporating wind and energy storage into SCUC models	The proposed multi-objective optimization algorithm can effectively handle wind power and energy storage in SCUC problems while considering multiple objectives.	IEEE 118-bus system and a modified version of the PJM system
Luo, F., Lu, Q., Chen, Y., & Chen, C. (2018).	[62]	How to effectively handle high wind power penetration in SCUC problems and improve the optimization algorithm	The proposed algorithm can effectively handle high wind power penetration in SCUC problems.	IEEE 39-bus system
Ayani N. et al (2020)	[71]	Solution to the UCP considering with EVs	The proposed algorithm scheduled the power demand	10, 20 Generating unit system
Ayani N. et al. (2021)	[51]	Solve the UCP problem with RES, considering the photovoltaic as renewable energy source.	The algorithm in question has been specifically designed to tackle the UCP problem, which is essentially a profit-based unit commitment problem.	10, 20, 40 generating unit system considered

M. Abdelateef Mostafa et al. (2022)	[72]	Wind energy conversion system	The proposed work focused on the wind energy conversion system integrated with grid.	Soft Computing Methods

Table 2.2.6 Literature review on SCUC problem with PEVs and RES

Author Name and Year	References	Research Gaps	Findings	Test System
Gao et al. (2020)	[24]	Lack of investigation on the coordination of SCUC with the charging and discharging of EVs	Proposed an integrated SCUC and EV charging scheduling model	IEEE 118 Bus System
Lin et al. (2021)	[53]	The limited consideration of power system uncertainty in SCUC problems with RESs and EVs	Developed a two-stage stochastic SCUC model taking into account the EV and RES uncertainties	IEEE 30-bus system
Niu et al. (2021)	[50]	Lack of investigation on the joint scheduling of wind power and EVs in SCUC	Proposed a joint wind power and EV charging scheduling model for SCUC	IEEE 118-bus system
Wang et al. (2022)	[20]	Limited research on the impact of EV charging on the power system voltage stability in SCUC	Developed an SCUC model considering the voltage stability constraint under EV charging	IEEE 30-bus system
Zhang et al. (2022)	[31]	Limited consideration of the interaction between EVs and RESs in SCUC	Developed a coordinated EV charging and RES scheduling model for SCUC	IEEE 118-bus system

Furthermore, there is still a lot of examination to be finished around here, for example, exploring the effect of various PEVs infiltration levels and charging methodologies on

SCUC issues, growing more precise and productive models for RESs, and tending to the difficulties of coordinating PEVs and RESs into power frameworks at an enormous scope.

2.2.5 A comprehensive literature review on the metaheuristic's optimization technique

In a variety of fields, including engineering, computer science, management, and others, metaheuristic optimization techniques are frequently used to solve optimization problems. Intelligent search algorithms are the foundation of these strategies, which are capable of rapidly locating high-quality solutions to challenging optimization issues. This section of the chapter presents a literature review in table format, offering a summary of the most significant metaheuristic optimization techniques developed and implemented between 2005 and 2023.

Table 2.2.7 Literature review on the metaheuristic optimization algorithms.

References	Algorithm Name	Author & Year	Research Gaps	Findings
[73]	Harmony Search Algorithm	Z. W. Geem et al. (2005)	Need for efficient update mechanisms, sensitivity to parameter settings.	Effective at solving engineering optimization problems
[74]	Artificial Bee Colony	Karaboga and Basturk (2007)	Need for more efficient update mechanisms, sensitivity to parameter settings.	Effective at solving real-world optimization problems, outperforms other algorithms
[75]	Cuckoo Search Algorithm[75]	X. S. Yang and S. Deb (2009) [75]	Need for efficient update mechanisms, sensitivity to parameter settings.	Effective at solving complex optimization problems
[76]	Bat Algorithm	X.-S. Yang (2010)	Need for efficient update mechanisms, sensitivity to parameter settings	Effective at solving continuous optimization problems with noisy objective functions
[77]	Firefly Algorithm	Yang (2010)	Need for better search strategy, parameter tuning.	High efficiency and flexibility, able to solve complex

				optimization problems
[78]	Artificial Bee Colony Algorithm	D. Karaboga and B. Akay (2010)	Need for efficient update mechanisms, sensitivity to parameter settings.	Effective at solving continuous optimization problems
[79]	Krill Herd Algorithm	Gandomi and Alavi (2012)	Need for more efficient update mechanisms, sensitivity to parameter settings.	Effective at solving real-world optimization problems, outperforms other algorithms
[80]	Flower Pollination Algorithm	X.-S. Yang (2012)	Need for efficient update mechanisms, sensitivity to parameter settings.	Effective at solving continuous optimization problems with non-linear constraints
[81]	Grey Wolf Optimizer	Mirjalili et al. (2014)	Lack of diversity in population, sensitivity to parameter settings.	Outperforms other optimization algorithms in accuracy and efficiency
[82]	Teaching-Learning-Based Optimization Algorithm	R. Kumar and P. Kumar (2014)	Need for efficient update mechanisms, sensitivity to parameter settings.	Effective at solving a variety of optimization problems
[83]	Moth-Flame Optimization Algorithm	Mirjalili (2015)	Need for more efficient update mechanisms, sensitivity to parameter settings.	Outperforms other optimization algorithms in accuracy and efficiency
[84]	Whale Optimization Algorithm	Mirjalili and Lewis (2016)	Need for more efficient update mechanisms, sensitivity to parameter settings.	Effective at solving complex optimization problems, outperforms other algorithms
[85]	Grasshopper Optimization Algorithm	S. Mirjalili (2019)	Need for efficient update mechanisms, sensitivity to parameter settings.	Effective at solving real-world optimization problems

[86]	Biogeography-Based Optimization	X. Liu et al. (2020)	Need for efficient update mechanisms, sensitivity to parameter settings.	Effective at solving real-world optimization problems
[2]	Arithmetic Optimization Algorithm (AOA)	Abualigah (2021)	Arithmetic Operator for Exploration and Exploitation	Engineering design problem.

Table 2.2.8 Literature review on the metaheuristic optimization algorithms.

Year	Metaheuristic Technique	Application	Key Features	References
2005	Particle Swarm Optimization (PSO)	Image Segmentation	Social learning and global optimization	[87]
2006	Genetic Algorithm (GA)	Supply Chain Management	Chromosome encoding and crossover	[34]
2007	Ant Colony Optimization (ACO)	Routing Optimization	Pheromone trail and heuristic function	[88]
2008	Differential Evolution (DE)	Power System Optimization	Mutation and crossover operators	[89]
2009	Artificial Bee Colony (ABC)	Data Clustering	Employed bees and onlooker bees phases	[78]
2010	Harmony Search (HS)	Sensor Placement Optimization	Memory consideration and improvisation rate	[6]
2011	Firefly Algorithm (FA)	Feature Selection	Attraction and distance-based light intensity	[77]
2012	Grey Wolf Optimizer (GWO)	Wireless Sensor Networks	Alpha, beta, and delta wolf positions	[81]
2013	Cuckoo Search (CS)	Resource Allocation	Random walk and Lévy flight	[90]
2014	Bat Algorithm (BA)	Image Classification	Echolocation and frequency tuning	[91]
2015	Teaching-Learning-Based Optimization (TLBO)	Economic Load Dispatch	Teacher and learner phases	[82]
2016	Moth-Flame Optimization (MFO)	Portfolio Optimization	Moth and flame attraction and movement	[83]

2017	Whale Optimization Algorithm (WOA)	Artificial Neural Network Training	Encircling and bubble-net hunting	[84]
2018	Dragonfly Algorithm (DA)	Task Scheduling	Swarming and territorial behaviour	[92]
2019	Water Cycle Algorithm (WCA)	Image Enhancement	Evaporation and precipitation phases	[93]
2021	Arithmetic Optimization Algorithm (AOA)	Engineering Design	Arithmetic Operator for Exploration and Exploitation	[2]
2021	Elephant Herding Optimization (EHO)	Image Retrieval	Herd behavior and migration	[94]
2021	Chaotic Slime Mold Algorithm	Engineering Design	Chaotic Slime mold	[95]
2022	Manta ray foraging optimization	Image processing	Manta ray foraging	[96]

Ultimately, it can be concluded that extensive exploration is still underway concerning metaheuristic optimization approaches, with a plethora of novel algorithms being put forward and rigorously assessed for their efficacy in resolving intricate optimization problems. However, there are still research gaps that need to be filled, such as the requirement for update mechanisms that are more effective and the sensitivity to set parameters. In general, metaheuristic optimization methods are still useful tools for resolving challenging optimization issues in a variety of contexts.

The No Free Lunch Theorem (NFL) is a concept that originates in the field of optimization and machine learning. It was introduced by David Wolpert and William Macready in 1997. In essence, the theorem suggests that there is no one-size-fits-all optimization algorithm that performs optimally on all possible problems. The fundamental idea behind the No Free Lunch Theorem is that the performance of any optimization algorithm is highly dependent on the specific characteristics of the problem it is applied to. Therefore, while an algorithm may excel at solving certain types of problems, it is expected to perform poorly on others.

The theorem has important implications, especially in the context of machine learning and artificial intelligence. It implies that there is no universal algorithm that can outperform all

others across diverse sets of problems. Consequently, researchers and practitioners must carefully choose or design algorithms based on the specific characteristics and constraints of the problems they are trying to solve. The No Free Lunch Theorem underscores the importance of understanding the problem at hand and selecting or designing optimization algorithms tailored to its unique features. It encourages a thoughtful and problem-specific approach to algorithm selection, acknowledging that there is no universal solution that guarantees superior performance across all possible scenarios [97].

The literature review reveals a gap in the existing research, as it is noted that there is a lack of consideration for the combination of various cases involving different generating units and uncertain renewable energy sources. Furthermore, the impact of these uncertain energy sources has not been adequately addressed. Additionally, some authors have faced challenges in conducting cost comparisons for different combinations of generating units. This identified gap emphasizes the need for further investigation into the integration of diverse generating units and the implications of uncertain renewable energy sources, as well as the necessity for comprehensive cost assessments in such scenarios.

2.3 SCOPE OF RESEARCH

The SCUC is an important optimization problem in power system operation and planning. It aims to determine the optimal commitment and dispatch schedules of generators while ensuring the security of the power system. The conventional optimization algorithms used for solving the SCUC problem, such as mixed-integer linear programming and mixed-integer quadratic programming, have been widely studied and applied. However, there are still several research gaps that need to be addressed. Upon reviewing the available literature, it has been observed that a number of numerical optimization techniques have been employed to address the complex unit commitment problem. Every optimization algorithm possesses its unique set of benefits and drawbacks. However, it should be noted that no optimization algorithm can achieve optimal results for all optimization problems.

One of the research gap is related to the computational efficiency of conventional optimization algorithms. The SCUC problem involves a large number of variables and constraints, which make it computationally expensive to solve using conventional optimization algorithms. Although various techniques such as decomposition methods and heuristic algorithms have been proposed to improve computational efficiency, there is still a need for further research to develop more efficient algorithms for solving the SCUC problem. Another research gap is related to the modeling of security constraints. The security constraints in the SCUC problem are typically modeled using deterministic or probabilistic approaches. However, these approaches may not fully capture the uncertainties and dynamics of the power system, which can lead to suboptimal solutions or even system failure. Therefore, there is a need for further research to develop more accurate and robust models for the security constraints in the SCUC problem.

An area of research that necessitates further focus is the impact of renewable energy sources on the SCUC problem. As renewable energy sources such as wind and solar power continue to expand, they pose new challenges to the SCUC problem. These challenges include the erratic and fluctuating behaviour of these sources. Several methods have been suggested to tackle these obstacles, such as using forecasting models and storage systems. Nevertheless, additional research is necessary to design more productive and economical ways for integrating renewable energy sources into the SCUC problem. In order to overcome the limitation of conventional arithmetic optimization algorithms, new three hybrid combinations are proposed namely as a chaotic arithmetic optimization algorithm, random walk arithmetic optimization algorithm, and levy flight strategies based arithmetic optimization algorithm presented in the proposed research. The algorithms in question possess several advantageous traits, such as their capability to evade local minima, their independence from differential gradients, and their immunity to divergence. Additionally, they possess a robust ability to explore various solution regions, coupled with an exceptional aptitude for both exploration and exploitation. The chaotic arithmetic optimisation algorithm, random walk arithmetic optimisation method, and levy fly arithmetic optimisation algorithm are among the innovative and hybrid optimisation

algorithms introduced by the suggested study. These algorithms are renowned for having outstanding exploration and exploitation capabilities. SCUC problem integration with PEVs and RES is the goal inside a single, multi-objective framework for the contemporary power system.

2.4 RESEARCH OBJETIVES

The primary objective of the proposed research is to utilize a hybrid meta-heuristics optimization algorithm to resolve the security constraint unit commitment problem. The study aims to achieve the following objectives:

(i) To develop a Hybrid Optimization Algorithm by combing a Local Search Algorithm with a Modern Global Search Algorithm for security-constraint unit commitment problems.

(ii) The aim of the study is to apply a hybrid optimization algorithm to address the SCUC problem in power systems.

(iii) To solve Security Constrained Unit Commitment Problem of the electrical power system by considering the impact of PEVs, and renewable energy sources using the proposed hybrid optimization algorithm.

(iv) Analysis and validation of results of proposed hybrid optimization algorithms with other recently proposed optimization algorithms.

2.5 CONCLUSIONS

In this chapter, multiple metaheuristic approaches are explored in the context of addressing the SCUC problem, with specific emphasis on the charging and discharging behaviours of PEVs, as well as RES. The table provided offers an overview of the erratic nature of RES, including solar and wind power. Furthermore, the effect of PEVs on the UCP and SCUC problem is examined, with any probable research gaps being identified.

This review of the literature gives an overview of current studies on SCUC problem connected to RES. The studies reviewed in this literature review demonstrate the effectiveness of various optimization techniques in handling the challenges introduced by renewable energy sources in SCUC problems. Future research efforts may focus on developing optimization strategies that are more competent and successful in handling SCUC challenges that incorporate RES in order to increase the reliability of the systems.

CHAPTER-3

OPTIMIZATION METHODOLOGIES AND TESTING OF HYBRID OPTIMIZER FOR SCUC PROBLEM

3.1 INTRODUCTION

Today, electrical power plays a crucial role in both the community's daily life and the growth of various economic sectors. The cutting-edge economy is, truth be told absolutely reliant upon power as a fundamental unit. Every facet of modern life is affected by the technological revolution. Power engineers employed by utilities and manufacturers are seeing their work environments transformed by rapidly evolving computer technologies. The power system's components, networks, and facilities can now be designed with greater precision thanks to new software, as can more urbane operational approaches that improve system reliability. In a variety of fields, there are numerous real-world examples of optimization techniques. Optimization problems are common in research for a variety of reasons, including engineering, design, manufacturing, the unpredictability of some constraints, and so on. As a result, finding solutions to complex problems can be challenging. Selecting a couple of explicit enhancers with upgrades in optimization techniques has been valuable to tackle complex streamlining issues [5].

There are two main types of problems that are frequently encountered in the field of optimization: problems related to engineering design and standard benchmarks. Standard benchmark issues are generally utilized in the improvement of the local area to look at the exhibition of various streamlining calculations. It is simple to evaluate an algorithm's performance because these problems are frequently well-defined and have known optimal solutions. The Rosenbrock function, Rastrigin function, and Griewank function are examples of typical benchmark problems. Typically, these functions are used to assess how well optimization algorithms perform on continuous optimization problems [68].

In contrast, engineering design issues are real-world issues that must be optimized in order to find the best solution. Multiple objectives, constraints, and decision variables are common in these problems, which are frequently intricate. Designing different mechanical problems, a chemical process, optimizing the layout of a manufacturing plant, or designing an aircraft wing are all examples of engineering design issues. To find the best solution to these issues, it is necessary to have knowledge of optimization algorithms in addition to expertise in the subject at hand. Figure 3.1 illustrates the categorization of different algorithm. These algorithms are inspired from different constraints [98].

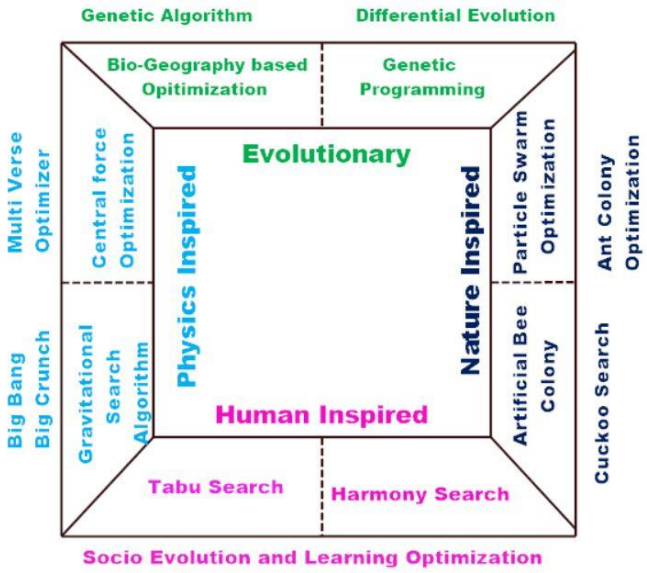

Figure 3.1: Categorization of algorithms

The main difference between engineering design problems and standard benchmark problems is that engineering design problems are real-world problems that need to be optimized to find the best solution, whereas standard benchmark problems are often used to test the performance of optimization algorithms. In addition, engineering design problems frequently involve constraints and goals that are more intricate than those found in standard benchmark problems. In general, optimization issues such as engineering design issues and standard benchmark issues are significant. Standard benchmark problems are good for comparing how well different algorithms work, and engineering design

problems are important for finding the best solutions to problems in the real world. Optimization researchers and practitioners can continue to develop new and more efficient optimization methods for complex problem-solving by studying both types of problems.

Security Constraint Unit Commitment is a significant issue in the electricity industry that involves optimizing power plant scheduling to meet a variety of operational constraints, such as transmission line capacity, ramping constraints, and startup costs, while simultaneously ensuring that electricity supply meets demand. To effectively and efficiently solve the problem, a variety of optimization methods have been developed due to their vast scale and complexity [71].

3.2 OPTIMIZATION METHODOLOGIES

The formulation of the problem in a mathematical format that is acceptable to an optimization algorithm is an important part of the optimal design process. All engineering problems can be formulated in a variety of ways. There are many different kinds of problems, such as design, decision-making, management, scheduling, operation, maintenance, etc. In various problems and situations, various techniques must be investigated. The formulation procedure's goal is to develop a mathematical model of the ideal problem that can be used to solve it with an optimization algorithm. The first step in formulating an optimization problem is to identify the design or decision variables that underlie it. These variables are primarily altered during the optimization process. There could be a lot of decision parameters, some of which are extremely important to the strategy's operation, and the user will likely decide which ones to use. Design variables refer to these parameters. After selecting the design variables, the next step is to determine the optimization problem's constraints. Certain physical phenomena and resource constraints are met by the constraints, which are functional relationships between design variables and other design parameters. The majority of considerations result in two types of constraints. There are constraints on equality and constraints on inequality. Correspondence imperatives are normally more challenging to deal with and in this manner, should be stayed away from whenever the situation allows. The next step in the

formulation process is to determine the objective function with respect to the design variables and other problem parameters. Depending on the situation, the objective function can be either minimized or maximized [71].

Each of the recently developed heuristic, metaheuristic, evolutionary, and nature-inspired algorithms have its own advantages and disadvantages. Additionally, the majority of these search algorithms cannot be universally accepted because they are not applicable to all kinds of optimization problems. In addition, the No Free Lunch Theorem states that if an algorithm based on the optimization technique is applied to all possible types of tasks, it will perform similarly to the recommended algorithm on average. NFL asserts that the algorithms cannot theoretically be regarded as the most effective type of optimizer for all purposes [51]. As a result, the NFL theorem encourages the development and penetration of more efficient algorithms based on optimization techniques. Inspired by the NFL theorem, the presented research has been taken to give one more remarkable optimizer, which depends on an arithmetic mathematical operation like expansion, deduction, division and duplication and turbulent guide, irregular walk, and duty flight procedures. In addition, hybrid variations are achieved by combining random walk and levy flight strategies with an arithmetic optimization algorithm, such as RWAOA, LFAOA, and tent chaotic map with CAOA.

3.3 METHODOLOGIES FOR GLOBAL OPTIMIZATION

The process of finding the best solution in a search space with multiple local optima is known as global optimization. Because it requires efficiently exploring a large search space, this is a difficult problem. It is used to solve problems with few variables and a high priority on finding the truly global solution.

3.3.1 Arithmetic Optimization Algorithm

The Arithmetic Optimization Algorithm uses mathematical modeling of arithmetic operations like addition, multiplication, division, and subtraction to solve a variety of optimization problems, including continuous, discrete, constraint, and unconstraint issues.

In a short period, various variants and several arithmetic optimization algorithms have been developed by several researchers. A wide range of arithmetic optimization algorithms and their various variants have been employed to tackle optimization problems in diverse fields such as pattern recognition, image processing, manufacturing, and engineering design. To enable accurate comparison and interpretation of these algorithms, several studies from major research variations have been selected. One such study by Laith Abualigah et al. presents an arithmetic optimization algorithm that can efficiently address a range of optimization problems through mathematical modeling [2]. To demonstrate the significance of the arithmetic optimization algorithm, the authors tested its performance on 29 benchmark functions and a few real designing plan challenges. Several scenarios were used to evaluate the execution, combination techniques, and mathematical complexity of AOA. The arithmetic optimization algorithm has been tested on various benchmark functions using different mathematical operators. This new meta-heuristic method uses arithmetic operators like multiplication, subtraction, addition, and division and focuses on their distribution behavior. By exploring a wide range of search spaces, the arithmetic optimization algorithm is modeled and implemented for optimization purposes. Figure 3.1b demonstrates the exploration and exploitation of the arithmetic optimization algorithm. It is a population-based meta-heuristic algorithm that can solve optimization problems without requiring the calculation of derivatives. Numerous studies have utilized the arithmetic optimization algorithm to address optimization problems across various domains, including manufacturing, pattern recognition, image processing, and engineering design. Some specific research variations of arithmetic optimization algorithms have been selected for comparison and interpretation purposes. Laith Abualigah et al. introduced an arithmetic optimization algorithm that is capable of solving various optimization problems through mathematical modeling [2]. The hierarchical structure of arithmetic operators is illustrated in Figure 3.3, where the intensity of the hierarchy decreases from the top to the bottom. This structure is essential in developing the arithmetic optimization algorithm. The inspiration behind arithmetic optimization algorithms is the extensive use of arithmetic operators in various mathematical calculations used to solve arithmetic problems. The

process illustrated in Figure 3.2 begins from the outer layer and proceeds towards the inner layer, comprising of two stages - diversification and intensification. The math optimizer accelerated (MOA) represents the optimization process. Figure 3.4 displays how the different mathematical operators gradually converge towards the optimal solution.

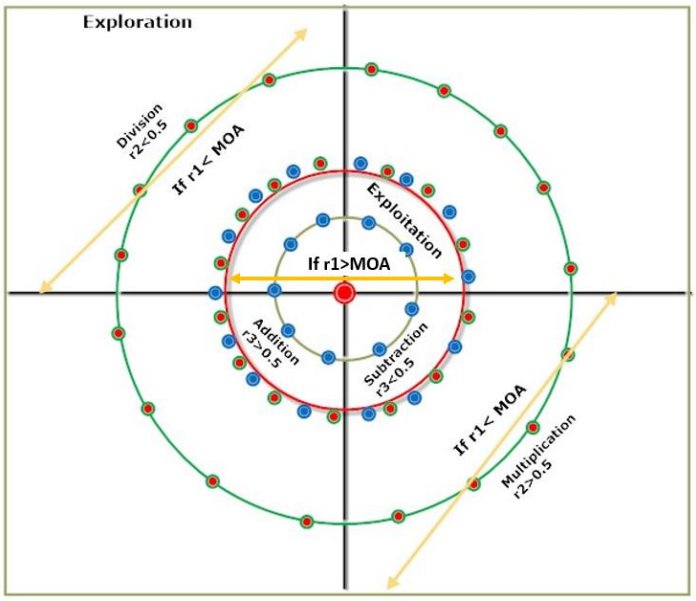

Figure 3.2 Arithmetic Optimization Algorithm Search phases

In Figure 3.4, the position of the math operator-model is updated to find the optimum area in AOA. Different mathematical operators, including division, multiplication, subtraction, and addition, are present in the figure. To move towards the optimum area, the mathematical operators change their position, and a random number, r2, is used in the process. Division and multiplication operators play a vital role in the diversification search mechanism as they have high decisions or distributed values [98].

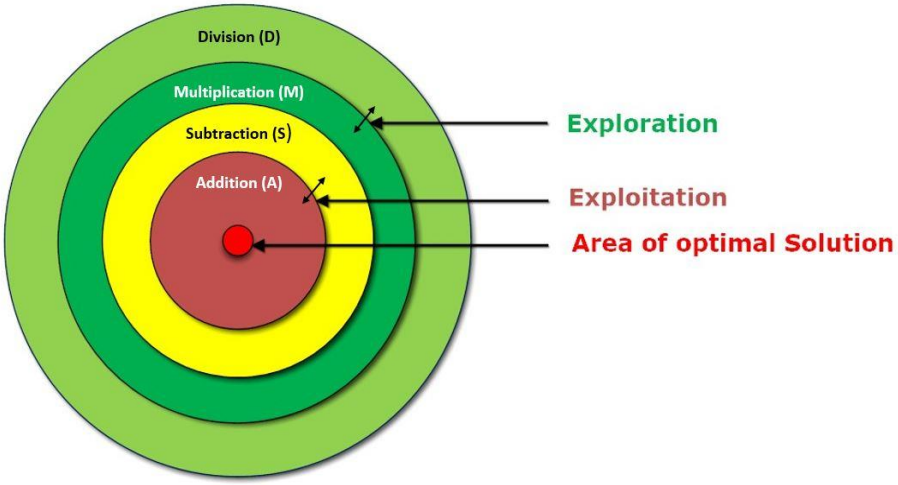

Figure 3.3 Arithmetic Operators Hierarchy intensity decreases from top to bottom [98].

3.3.1.1 Arithmetic Optimization Algorithm- Initialization phase

The optimization process of the Arithmetic Optimization Algorithm involves generating a group of candidate solutions in the initial step, which are usually generated randomly. The best candidate solution obtained from each iteration is then considered as the best-obtained solution throughout the optimization process. This process can be represented mathematically using equation (3.1) and helpful solving the problem effectively [98].

$$X = \begin{bmatrix} x_{1,1} & \cdots & \cdots & x_{1,k} & x_{1,n-1} & x_{1,n} \\ x_{2,1} & \cdots & \cdots & x_{2,k} & \cdots & x_{2,n} \\ \cdots & \cdots & \cdots & \cdots & \cdots & \cdots \\ \cdots & \cdots & \cdots & \cdots & \cdots & \cdots \\ x_{(m-1),1} & \cdots & \cdots & x_{(m-1),k} & \cdots & x_{(m-1),n} \\ x_{m,1} & \cdots & \cdots & x_{m,k} & x_{m,n-1} & x_{m,n} \end{bmatrix} \tag{3.1}$$

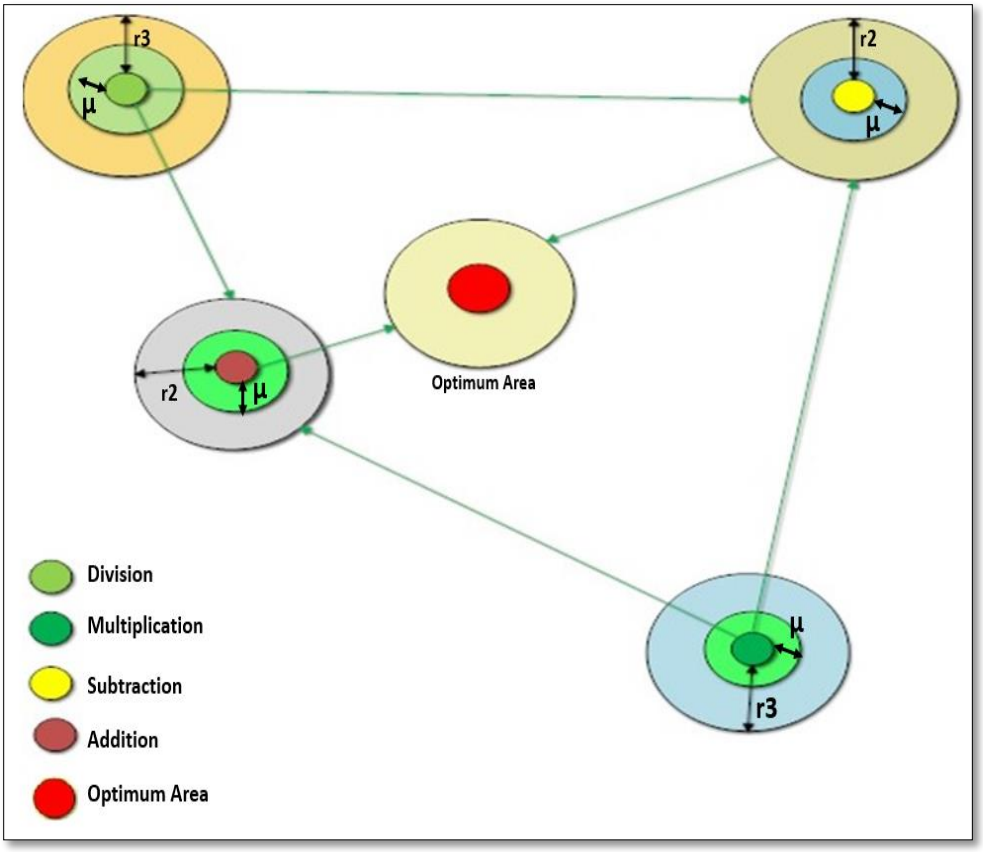

Figure 3.4: Mathematical Operator Model

Before initiating the Arithmetic Optimization Algorithm, it is essential to choose the exploration and exploitation phases. In these phases, the Math Optimizer Accelerated function is crucial as it helps to determine the coefficient by using equation (3.2).

$$MOA(C_{Iter}) = min + C_{Iter} \times \left(\frac{max - min}{Z_{Iter}} \right) \tag{3.2}$$

In equation (3.2), $MOA(C_{Iter})$ represent the function value for the t^{th} iteration. C_{Iter} indicate the current iteration. Z_{Iter} denote the maximum iteration [98].

3.3.1.2 Exploration phase

The Arithmetic Optimization Algorithm employs exploration operators that randomly investigate numerous locations within the search space to find better solutions using two

main search techniques: division (D) and multiplication (M). [89]. Equation (3.3) describes the two primary search methods used in the Arithmetic Optimization Algorithm for the exploration phase. The exploration is carried out by either division (D) or multiplication search methods, as shown in Figure 3.4, for the condition where r1 is a random number. These operators converge towards the optimal region, as depicted in Figure 3.1. In this phase, according to equation (3.1), the first step is to use the division operator (D) if r2<0.5. The multiplication operator will not be considered until the division operator completes its current task. If the condition is not met, the multiplication operator (M) will be assigned to complete the current task [98]. Here, r2 is also a random number. To introduce more diversification and explore other parts of the search space, a method that mimics the behavior of arithmetic operators was used [2].

$$x_{l,k}(C_{Iter}+1)=\begin{cases} LB_k+[best(x_k)\div(MOP+\eta)\times((UB_j-LB_k)\times v]; & r_2<0.5 \\ LB_k+[best(x_k)\times MOP\times((UB_k-LB_k)\times v]; & otherwise \end{cases} \tag{3.3}$$

The equation (3.3) represents the arithmetic optimization algorithm where the next solution is represented by $x_{l,k}(C_{Iter}+1)$ and the position of the current solution is $x_{l,k}(C_{Iter})$. The best-obtained solution is denoted by $best(x_k)$ and it is located at the position k^{th}, η which is a small integer number. The lower and upper bound values of the position are represented by LB_k and UB_k, respectively. To regulate the search process, a control parameter v is used, and its value is set to 0.5.

$$MOP(C_{Iter})=\left[1-\left(\frac{C_{Iter}}{Z_{Iter}}\right)^{1/\alpha}\right] \tag{3.4}$$

Here, MOP = Math optimizer probability. It is a coefficient

$MOP(C_{Iter})$ = Function value at the t^{th} iteration.

C_{Iter} = Represent present iteration

Z_{Iter} = Represent the maximum number of iterations.

A key parameter in the arithmetic optimization algorithm is the accuracy of the exploitation phase relative to the number of iterations, denoted by α. This is a highly sensitive parameter, with a fixed value of 5.

3.3.1.3 Exploitation phase

The exploitation phase is a critical component of the arithmetic optimization algorithm, playing a vital role in achieving the optimal solution. Addition and subtraction are highly effective mathematical operators in the intensification or diversification search mechanism. During the exploitation phase, the addition (A) and subtraction (S) operators are particularly significant. The exploitation phase in the Arithmetic Optimization Algorithm is crucial for obtaining the optimum solution. The addition and subtraction mathematical operators play a significant role in the intensification or diversification finding mechanism because they provide effective results. By utilizing these two operators, the exploitation phase can be modified by the value of the Math Optimizer Accelerated (MOA) function, as described in equation (3.2), for the condition of a value of $r_1 \le MOA(C_{Iter})$. Exploring the search area over the populated space and finding the optimal solution heavily relies on the use of operators. In AOA, there are two primary exploitation operators that play a crucial role in this process. The mathematical expression for the exploitation phase in AOA is represented by equation (3.5) which is very important in the AOA.

$$x_{l,k}(C_{Iter}+1) = \begin{cases} LB_k + [best(x_k) - MOP \times (UB_k - LB_k) \times v]; & r_3 < 0.5 \\ LB_k + [best(x_k) + MOP \times (UB_k - LB_k) \times v]; & \text{otherwise} \end{cases} \quad (3.5)$$

During the exploitation phase, the initial operator that is executed is the subtraction operator (S) which is carried out according to the equation (3.5). It's important to note that the addition operator (A) is not taken into consideration until the subtraction operation is completed. The effectiveness of the algorithm is analyzed through the examination of the boundary limitations, which are defined in equation (3.6). This equation has their own importance

$$LB_k \le x_{l,k} \le UB_k, \qquad \text{k} = 1, 2, ..., n \quad (3.6)$$

Here, LB_k = Lower bound of the position x_{lk}

UB_k = Upper bound of the position x_{lk}

n = Number of given positions

The generalized constrained problem is given by as shown in the equation (3.7 & 3.8)

$$\begin{aligned} &Function: \min f(X) \\ &Where,\ X = \left\{x_{11}, x_{1j}, ..., x_{1n}\right\} \end{aligned} \tag{3.7}$$

Subject to

$$\begin{aligned} &g_i(X) \le 0, i = 1, 2, ..., m \\ &h_p(X) = 0,\ p = 1, 2, ..., q \\ &LB_k \le x_{l,k} \le UB_k, \qquad \text{k} = 1, 2, ..., n \end{aligned} \tag{3.8}$$

Here, m is the number of various constraints, l is the constraints belong to equilibrium.

Equation (3.9a) can be used to represent the optimization problem that incorporates all of the given constraints.

$$f(X) = f(X)\sum_{k=1}^{m} Pe_k \max\left\{g_l(X), 0\right\} + \sum_{p=1}^{n} Pe_p \max\left\{\left|h_p(X) - \varepsilon\right|, 0\right\} \tag{3.9a}$$

The equation (3.9a) represents the optimization problem. Here, Pe_k & Pe_p are the charged function and cost functions, ε = equilibrium constraint error.

$$\psi = rand() \tag{3.9b}$$

$$r_1 = 2.3 \times \psi^2 \times sin(\pi\psi) \tag{3.9c}$$

3.4 Optimizer for Local Search

One of the heuristic strategies used in optimization to deal with problems of the computationally complex kind is the use of local search optimizers. It can be developed on problems that can be described as selecting an expanding model solution from a variety of candidate solutions. By employing neighborhood change, these kinds of searches in the

field of optimization can move from one solution to another in the search area until the best solutions are found and sufficient time has passed.

Most of the time, the local search methods are used to solve a lot of hard simulation problems, like software engineering. This is especially true in the fields of artificial intelligence, operation research, mathematics, bioinformatics, and engineering. The majority of these optimizers consider side constraints that do not involve equality limitation. It can be handled effectively by simply implementing it in the optimizer. The best algorithms will never disregard any of the constraints that are provided.

A type of optimization algorithm called "local search optimization" is used to find the best solution to a problem within a certain set of constraints. Local search optimization is based on the basic idea of starting with one solution and iteratively improving on it by making small changes and evaluating the new ones. The fundamental steps of a local search optimization algorithm are as follows:

Initialization: Begin with a preliminary solution to the issue.

Evaluation: Utilize a cost function or an objective function to evaluate the quality of the initial solution.

Modification: Using a set of rules or operators that define the search space, make minor changes to the solution.

Selection: Choose the new solution with the highest objective function value or cost.

Termination: When a stopping criterion (such as a certain number of iterations or a certain level of improvement) is met, the search is halted.

Local search optimization is based on the idea that it is a heuristic algorithm that often finds a good solution to a problem quickly but does not always find the best one. To increase the likelihood of finding the best solution, local search optimization is frequently used in combination with other optimization methods.

3.4.1 Chaotic Search Strategies

A subset of optimization techniques known as chaotic search strategies is derived from the natural behavior of chaotic systems. The search space is explored and the best solution to a problem is found using these methods, which make use of chaotic dynamics. The

principles of chaos theory, which emphasize the system's sensitivity to minor changes in the initial conditions, drive the search process in this strategy. In complex, high-dimensional, and non-convex optimization problems, chaotic search strategies are especially useful for finding the global optimum [99]. In many real-world applications, such as engineering design, financial modeling, and machine learning, these issues are common. Gradient-based algorithms, for instance, are an example of a traditional search strategy that frequently fails to locate the global optimum because it gets bogged down in local optima.

To explore the search space, chaotic search strategies employ a variety of strategies. Utilizing chaotic maps like the logistic or Henon maps to generate a sequence of numbers that act as pseudo-random guides is a common strategy. These maps can effectively explore the search space and evade local optima thanks to their rich and intricate behavior. To explore the search space and locate the best solution, these algorithms make use of a population of agents that interact with one another. A wide range of applications, including neural network training, data clustering, and image processing, have demonstrated the efficacy of chaotic search strategies. However, they may require careful tuning to achieve good performance due to their potential sensitivity to parameter selection. Additionally, the unpredictability and non-determinism of the search trajectories can make it challenging to analyze and interpret the process. In conclusion, utilizing the principles of chaos theory, chaotic search strategies present a promising strategy for resolving challenging optimization issues [64]. These methods are powerful tools for exploring the search space and locating the global optimum, despite their difficulty in application. Different types of chaotic maps are given in the Figure 3.5.

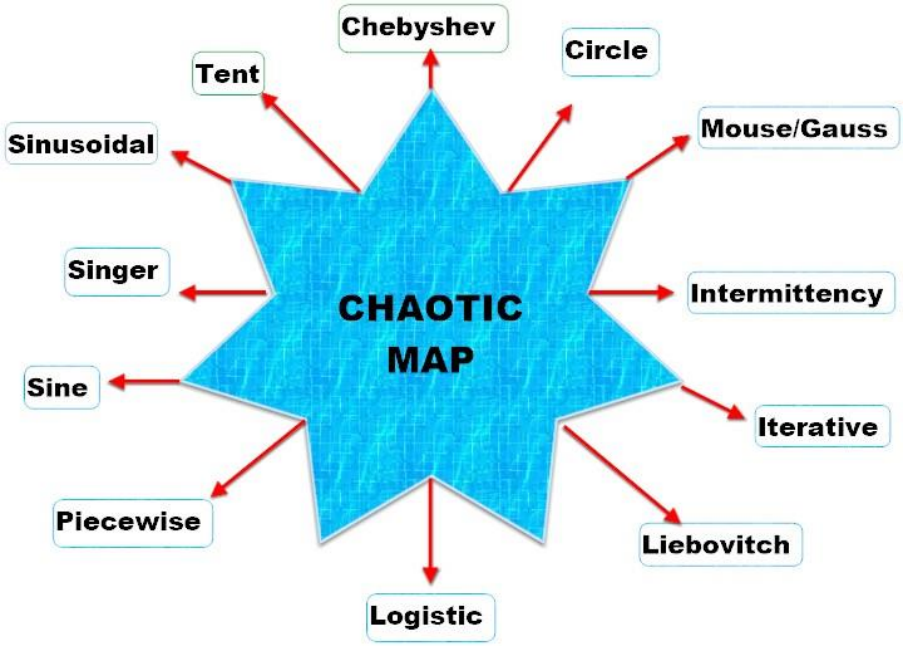

Figure 3.5: Chaotic Maps

3.4.2 Random Walk Strategies

In random walk is nothing but random process and in this random process included random steps which are very important for the solution [100]. Random walk mathematically expressed in equation (3.10).

$$R_N = \sum_{j=1}^{N} S_j \tag{3.10}$$

Where, S_j is a random/ arbitrary step that can be taken from any random distribution. This random step can be taken from arbitrary appropriation. The consecutive random walks, occurring in pairs, exhibit a connection between each successive pair. This relationship is expressed in the following equation (3.11).

$$R_N = \sum_{j=1}^{N} S_j = \sum_{j=1}^{N-1} S_j + F_N = R_{N-1} + S_N \tag{3.11}$$

In the above equation (3.11) current state R_{N-1} is very important because R_N is dependent on this current state. In this process of random walk steps are changed from current step to the next step. The most important things in random walk are step size S_j. This step size may be varied or may be fixed. Now suppose an arithmetic algorithm starting with point f_0 and its end position is f_N, so in this case, we can define the random walk as mention in the equation (3.12).

$$f_n = f_0 + \alpha_1 s_1 + \alpha_2 s_2 + \ldots + \alpha_N s_N = f_0 + \sum_{j=1}^{N} \alpha_j S_j \tag{3.12}$$

Here, $\alpha_j > 0$ is plays an important role in controlling the step size S_j in every iteration

3.4.3 Levy Flight Strategies

The Levy Flight is mainly focus on the zigzag deceptive motions of prey during evading phase. In aging condition, Levy Flight is utilized for the optimum activities, in Levy Flight different optimum tactics are utilized for predators in noncorrosive [98]. The detection of LF-based patterns is the primary application of Levy Flight and is especially significant in tracking the movement patterns of various animals such as sharks and monkeys. This benefit of LF is leveraged in the arithmetic calculation for obtaining the optimal solution. Equation (3.13) outlines the mathematical procedure that is employed for this purpose.

$$M = LF(Y) \times V + Y \tag{3.13}$$

Here, V is a random vector of size $1 \times Y$ and dimension of the problem is indicated by Y, LF is the Levy Flight function and this Levy Flight function is calculated by Equation (3.13)

$$LF(x) = \frac{\delta \times \omega}{|\rho|^{\frac{1}{\beta}}} \times 0.01, \ \omega = \left(\frac{\sin\left(\frac{\pi\beta}{2}\right) \times \tau(1+\beta)}{2^{\left(\frac{\beta-1}{2}\right)} \times \beta \times \tau\left(\frac{1+\beta}{2}\right)} \right) \tag{3.14}$$

Where, δ and ω are random values inside (0, 1), default constant β is set to 1.5.

The final optimum solution is obtained by updating the position and for that Equation (3.15) is utilized.

$$X(n+1) = \begin{Bmatrix} N & \text{if } F(N) < F(X(n)) \\ P & \text{if F}(P) < F(X(n)) \end{Bmatrix} \tag{3.15}$$

Here N and P are obtained from Equation (3.15)

3.5 Hybrid Optimization Methodologies

The term "hybrid optimization methodologies" refers to methods that combine two or more different optimization approaches in order to solve more difficult optimization problems with greater precision and efficiency. Hybrid methodologies can improve performance by combining various optimization algorithms to take advantage of their strengths and overcome their weaknesses [101].

The development of hybrid optimization methodologies can be approached in a number of ways, including:

- *Hybridation in succession:* In this method, optimization algorithms are applied sequentially to a problem in a predetermined order. A genetic algorithm, for instance, can be used to generate initial solutions, and a local search algorithm can further refine the solutions.
- *Hybridization in parallel:* This approach includes running numerous enhancement calculations all the while to track down the ideal arrangement. For instance, various parameters or search strategies can be used to run multiple genetic algorithms simultaneously.

- *Hybridization based on models:* In order to boost the efficiency of the optimization process, this strategy combines evolutionary algorithms or swarm intelligence with mathematical models like linear or nonlinear programming.
- *Hybridization in collaboration:* In this strategy, various algorithms are combined in a cooperative fashion, with each algorithm being accountable for a specific subproblem or task. The best solution is obtained by combining the solutions produced by each algorithm.
- *Hybridization in competition:* Multiple optimization algorithms compete with one another to find the best solution in this strategy. The algorithm with the best solution is chosen, and the results of that algorithm's search are used to narrow the search space for the other algorithms.

In a variety of fields, including engineering, finance, and healthcare, hybrid optimization methodologies have been extensively utilized to resolve challenging optimization issues. When compared to individual algorithms, the integration of various optimization algorithms has demonstrated significant improvements in terms of solution quality and convergence speed. However, the selection of appropriate algorithms and their integration can be challenging, and hybrid optimization methodologies necessitate expertise in both optimization algorithms and problem domain knowledge [102].

3.5.1 Hybrid Chaotic Arithmetic Optimization Algorithm

A class of optimization algorithms known as chaotic arithmetic optimization algorithms enhances the efficiency of conventional optimization strategies by combining chaotic maps with arithmetic operations. To explore the search space and escape local optima, CAOAs make use of chaotic maps' randomness and sensitivity to initial conditions. CAOAs are a promising approach to optimization that has the potential to assist in overcoming some of the limitations imposed by conventional methods of optimization. These algorithms, on the other hand, can perform differently depending on the problem at hand, and their effectiveness is influenced by a number of different factors [103].

The Arithmetic Optimization Algorithm is a metaheuristic approach that utilizes distribution behaviors for various mathematical parameters such as division, subtraction, addition, and multiplication [77]. These operators inherently possess the ability to explore both global maxima and minima. However, the local search in the fundamental Arithmetic Optimization Algorithm is sluggish and exhibits a slow convergence rate due to its weak exploitation capacity [104]. To overcome this limitation, the proposed research introduces a Chaotic Map based improved Arithmetic Optimization Algorithm that enhances the exploration and exploitation phases of the existing algorithm [91]. The efficacy of the proposed optimizer is validated through testing on 23 standard benchmark problems and 10 real-life engineering design problems, with a comparison to classical algorithms such as Biogeography-based optimization algorithm [105], Moth-flame optimization algorithm [106], Genetic algorithm [107], and many more [80]. The obtained results demonstrate that the proposed hybrid Chaotic Arithmetic Optimization Algorithm performs exceptionally well, with superior fitness values and convergence rates on various test functions and engineering design problems [108]. This research is significant in improving the exploitation capacity of arithmetic optimization algorithms for global engineering optimization problems [81], [98]. Figures 3.6 and 3.7 show the pseudo code and flow chart for the proposed hCAOA method.

Step – 1: Initialize the Arithmetic Optimization Algorithm *i.e.*, α, v.
Step – 2: Initialize the solution's status randomly. (Solutions:l=1,...,n.)
Step – 3: **While** $(C_{Iter} < M_{Iter})$ **do**
Step – 4: Find out the fitness function (FF) for the given solutions
Step – 5: Calculate the best solution $\left(\text{Calculated best so far}\right)$.
Step – 6: Upgrade the *MOA* value using equation $\left(3.2\right)$.
Step – 7: Upgrade the *MOP* value using equation $\left(3.4\right)$.
Step – 8: **for** $l = (1\ to$ Solutions) **do**
Step – 9: **for** k= (1 to Positions) **do**
Step – 10: Update r_1, r_2, and r_3 using chaotic map function
Step – 11: **if** $r_1 > MOA$ **then**
Step – 12: **Exploration phase**
Step – 13: **if** $r_2 > 0.5$ **then**
Step – 14: Use the division (D '÷ ') math operator.
Step – 15: Upgrade the l^{th} solutions position using the first rule in equation $\left(3.3\right)$.
Step – 16: **else**
Step – 17: Apply the multiplication math operator (M '× ').
Step – 18: Upgrade the l^{th} solutions position by the 2nd rule in equation $\left(3.3\right)$.
Step – 19: **end if**
Step – 20: **else**
Step – 21: **Exploitation phase**
Step – 22: **if** $r_3 > 0.5$ **then**
Step – 23: Apply the subtraction mathematical operator (S '– ').
Step – 24: Upgrade the l^{th} solutions position by the first rule in equation $\left(3.5\right)$.
Step – 25: **else**
Step – 26: Apply the addition mathematical operator (A '+ ').
Step – 27: Upgrade the l^{th} solutions position by the 2nd rule in equation $\left(3.5\right)$.
Step – 28 Further updated the position vector using chaotic map mechanism
Step – 29: **end if**
Step – 30: **end if**
Step – 31: **end for**
Step – 32: **end for**
Step – 33: $C_{Iter} = C_{Iter+1}$
Step – 34: **end while**
Step – 35: Return the best solution (x).

Figure 3.6 PSEUDO code for the hCAOA algorithm

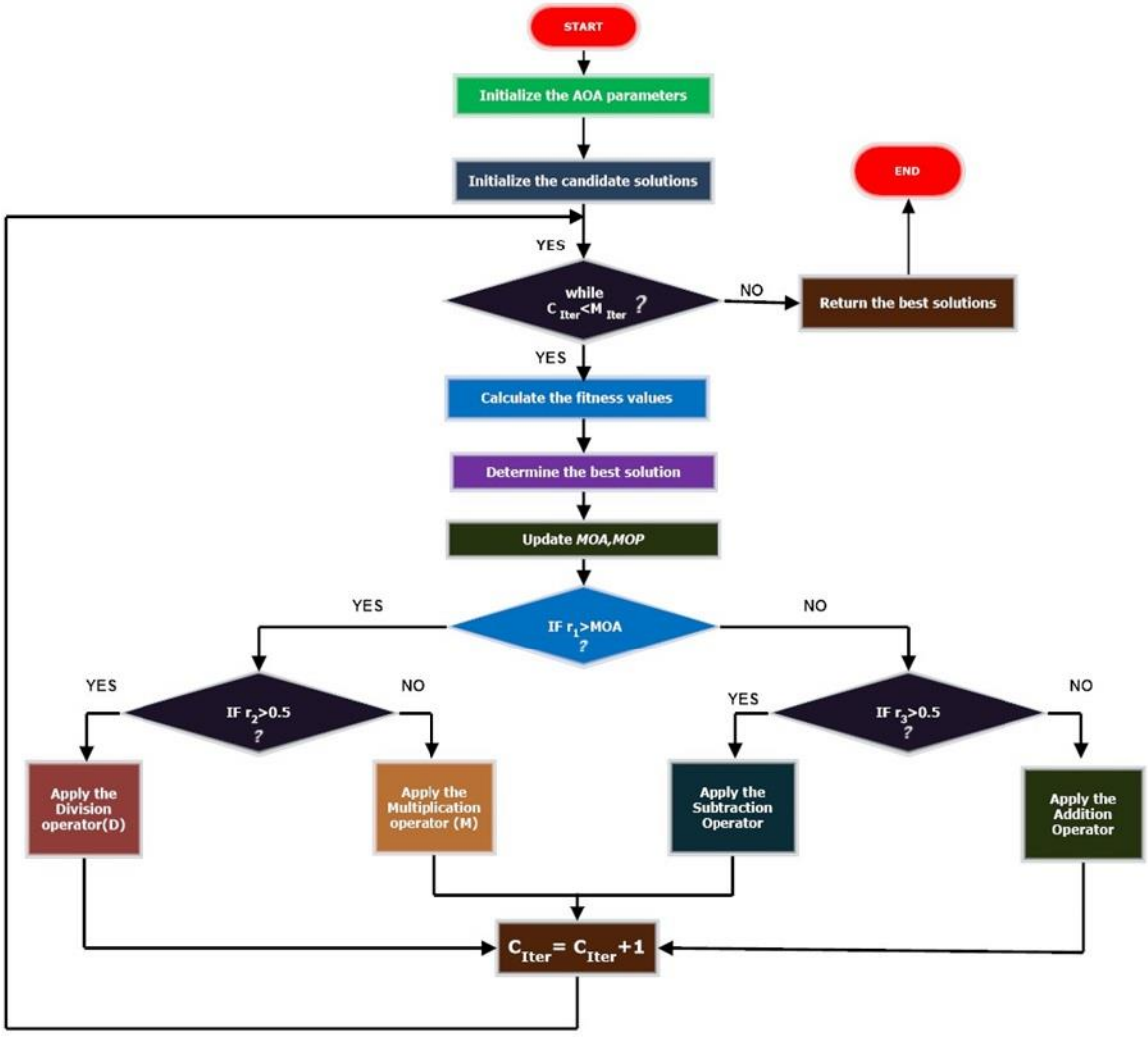

Figure 3.7: A new hybrid CAOA search algorithm Flowchart.

3.5.2 Hybrid Random Walk based Arithmetic Optimization Algorithm

A stochastic optimization algorithm known as the Random Walk Arithmetic Optimization Algorithm makes use of random walks to explore the search space and locate the best possible solutions. When the optimization problem is non-linear and the search space is large, this algorithm is especially useful.

The algorithm's basic concept is to begin at a random point in the search space and proceed in a series of random directions. The objective function is evaluated by the algorithm at each step, and the best current solution is recorded. This process is then repeated by the algorithm for a predetermined number of times or until a satisfactory solution is found. The algorithm can be used to solve a wide variety of optimization issues, including discrete and continuous optimization issues. It is a popular choice for many optimization issues due to its ease of implementation and minimal parameter tuning requirements.

The Arithmetic Optimization Algorithm is a meta-heuristic algorithm that investigates global maxima and minima by employing various mathematical operators. In this proposed study, the Random Walk-inspired Arithmetic Optimization Algorithm is suggested as a way to improve the exploitation phase of the current arithmetic optimizer algorithm. The proposed RWAOA algorithm has also been tested on engineering design problems and standard benchmarks. A meta-heuristics algorithm that makes use of mathematical distributions for the various parameters is the current Arithmetic Optimization Algorithm. The inherent capability to investigate global maxima and minima exists in a variety of mathematical operators, including division, addition, multiplication, and subtraction. Due to its limited exploitation capacity, the local search of the fundamental Arithmetic Optimization Algorithm is sluggish and has a slow convergence rate. The Random Walk strategies of the Arithmetic Optimization Algorithm have been used to improve the exploration and exploitation phase of the algorithm in the current work. For the hybrid Random Walk Arithmetic Optimization Algorithm, 23 standard functions have been tested and simulated, and ten different engineering design-related optimization problems are also tested. Figures 3.8 and 3.9 show the pseudo code and flow chart for the proposed hybrid RWAOA method.

Step – 1: Initialize the Arithmetic Optimization Algorithm *i.e.*, α, v.
Step – 2: Initialize the solution's status randomly. (Solutions:l=1,...,n.)
Step – 3: **While** ($C_{Iter} < M_{Iter}$) **do**
Step – 4: Find out the fitness function (FF) for the given solutions
Step – 5: Calculate the best solution (Calculated best so far).
Step – 6: Upgrade the *MOA* value using equation (3.2).
Step – 7: Upgrade the *MOP* value using equation (3.4).
Step – 8: **for** $l = (1\ to$ Solutions) **do**
Step – 9: **for** k= (1 to Positions) **do**
Step – 10: Update r_1, r_2, and r_3 using random walk function using equation (3.11).
Step – 11: **if** $r_1 > MOA$ **then**
Step – 12: **Exploration phase**
Step – 13: **if** $r_2 > 0.5$ **then**
Step – 14: Use the division (D '÷ ') math operator.
Step – 15: Upgrade the l^{th} solutions position using the first rule in equation (3.3).
Step – 16: **else**
Step – 17: Apply the multiplication math operator (M '× ').
Step – 18: Upgrade the l^{th} solutions position by the 2nd rule in equation (3.3).
Step – 19: **end if**
Step – 20: **else**
Step – 21: **Exploitation phase**
Step – 22: **if** $r_3 > 0.5$ **then**
Step – 23: Apply the subtraction mathematical operator (S '– ').
Step – 24: Upgrade the l^{th} solutions position by the first rule in equation (3.5).
Step – 25: **else**
Step – 26: Apply the addition mathematical operator (A '+ ').
Step – 27: Upgrade the l^{th} solutions position by the 2nd rule in equation (3.5).
Step – 28 Further updated the position vector using random walk mechanism using equation (3.11)
Step – 29: **end if**
Step – 30: **end if**
Step – 31: **end for**
Step – 32: **end for**
Step – 33: $C_{Iter} = C_{Iter+1}$
Step – 34: **end while**
Step – 35: Return the best solution (x).

Figure 3.8 PSEUDO code for RWAOA

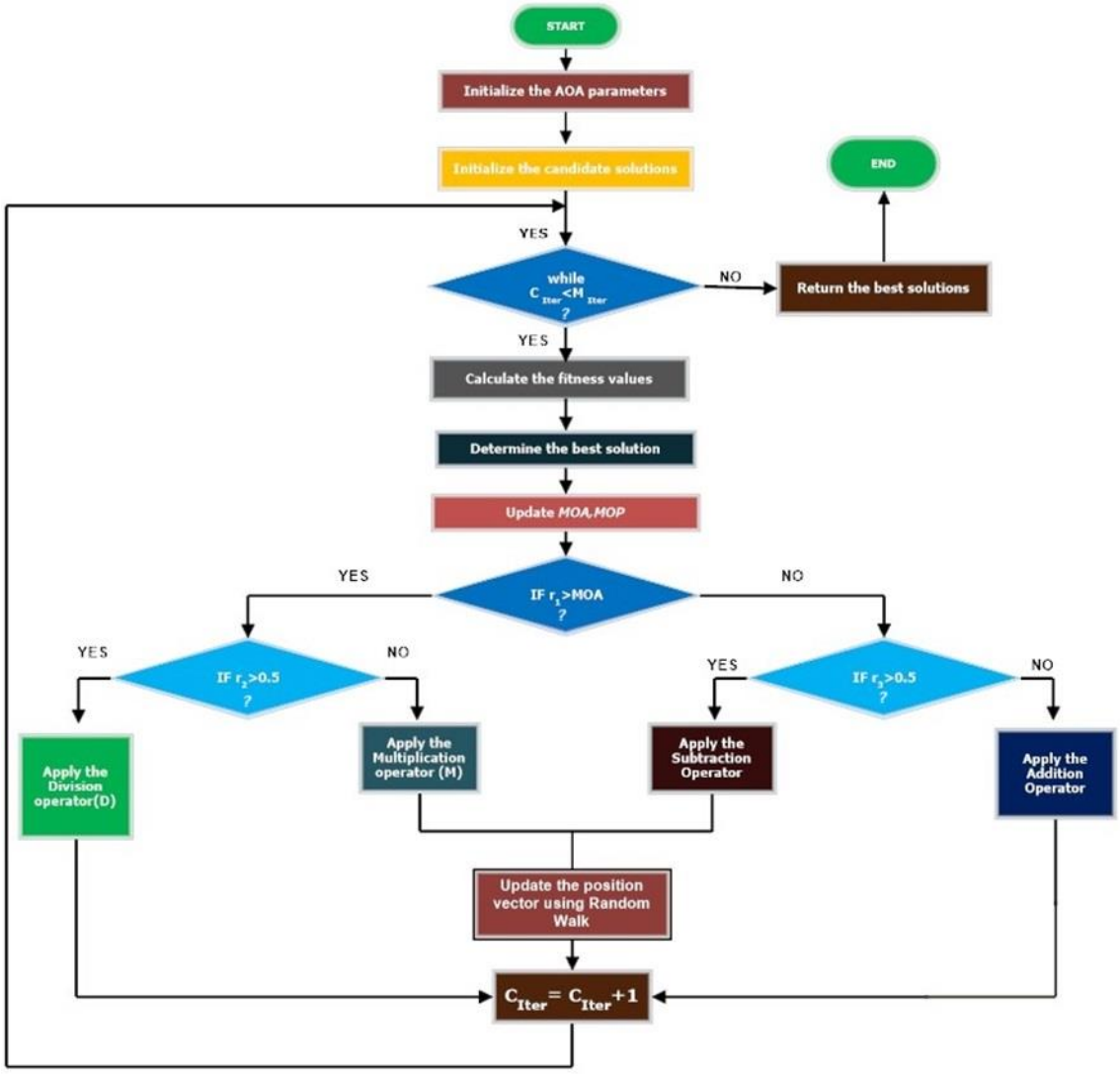

Figure 3.9: A new flowchart for RWAOA

3.5.3 Hybrid Levy Flight strategies based Arithmetic Optimization Algorithm

The Levy Flight Arithmetic Optimization Algorithm is a metaheuristic optimization approach that draws inspiration from the behavior of Levy flights observed in nature. Levy flights are characterized by a type of random walk where the step sizes follow a heavy-

tailed probability distribution. The LFAOA leverages this concept to facilitate its search process for optimal solutions in various applications. This means that there is a small probability of taking a very large step, which allows the walker to explore the search space more efficiently than a standard random walk. The LFA algorithm applies this idea to optimization problems by using Levy flights to generate candidate solutions. In LFAOA, each candidate solution is represented as a vector of real-valued variables, and the algorithm uses Levy flights to update the values of these variables in order to find a solution with the best objective function value [98].

Compared to other metaheuristic optimization algorithms, LFAOA has several advantages, including its ability to handle multimodal and non-convex optimization problems, its low computational cost, and its flexibility in handling different types of optimization problems. Levy Flight-based improved arithmetic optimization algorithms for better optimal solutions to various engineering design issues have been proposed in the research. Due to its limited exploitation capacity, the local search of the fundamental Arithmetic Optimization Algorithm is slow and has a slow convergence rate. In the proposed research, the Levy Flight mechanism is employed to enhance the exploration and exploitation phases of the existing Arithmetic Optimization Algorithm. The improved algorithm is then put to the test on 23 standard benchmark problems as well as 10 real-world engineering design problems to validate the effectiveness of the proposed optimizer. This approach aims to improve the algorithm's search capabilities and accuracy in finding optimal solutions for a diverse range of applications [98]. Figures 3.10 and 3.11 show the pseudo code and flow chart for the proposed hybrid LFAOA method.

Step – 1: Initialize the Arithmetic Optimization Algorithm *i.e.*, α, v.
Step – 2: Initialize the solution's status randomly. (Solutions:l=1,...,n.)
Step – 3: **While** ($C_{Iter} < M_{Iter}$) **do**
Step – 4: Find out the fitness function (FF) for the given solutions
Step – 5: Calculate the best solution (Calculated best so far).
Step – 6: Upgrade the *MOA* value using equation (3.2).
Step – 7: Upgrade the *MOP* value using equation (3.4).
Step – 8: **for** $l = (1$ *to* Solutions) **do**
Step – 9: **for** k= (1 to Positions) **do**
Step – 10: Update r_1, r_2, and r_3 using levy flight strategies using equation (3.13).
Step – 11: **if** $r_1 > MOA$ **then**
Step – 12: **Exploration phase**
Step – 13: **if** $r_2 > 0.5$ **then**
Step – 14: Use the division (D '÷ ') math operator.
Step – 15: Upgrade the l^{th} solutions position using the first rule in equation (3.3).
Step – 16: **else**
Step – 17: Apply the multiplication math operator (M '× ').
Step – 18: Upgrade the l^{th} solutions position by the 2nd rule in equation (3.3).
Step – 19: **end if**
Step – 20: **else**
Step – 21: **Exploitation phase**
Step – 22: **if** $r_3 > 0.5$ **then**
Step – 23: Apply the subtraction mathematical operator (S '– ').
Step – 24: Upgrade the l^{th} solutions position by the first rule in equation (3.5).
Step – 25: **else**
Step – 26: Apply the addition mathematical operator (A '+ ').
Step – 27: Upgrade the l^{th} solutions position by the 2nd rule in equation (3.5).
Step – 28 Further updated the position vector using levy flight mechanism using equation (3.13)
Step – 29: **end if**
Step – 30: **end if**
Step – 31: **end for**
Step – 32: **end for**
Step – 33: $C_{Iter} = C_{Iter+1}$
Step – 34: **end while**
Step – 35: Return the best solution (x).

Figure 3.10 PSEUDO code for hybrid LFAOA

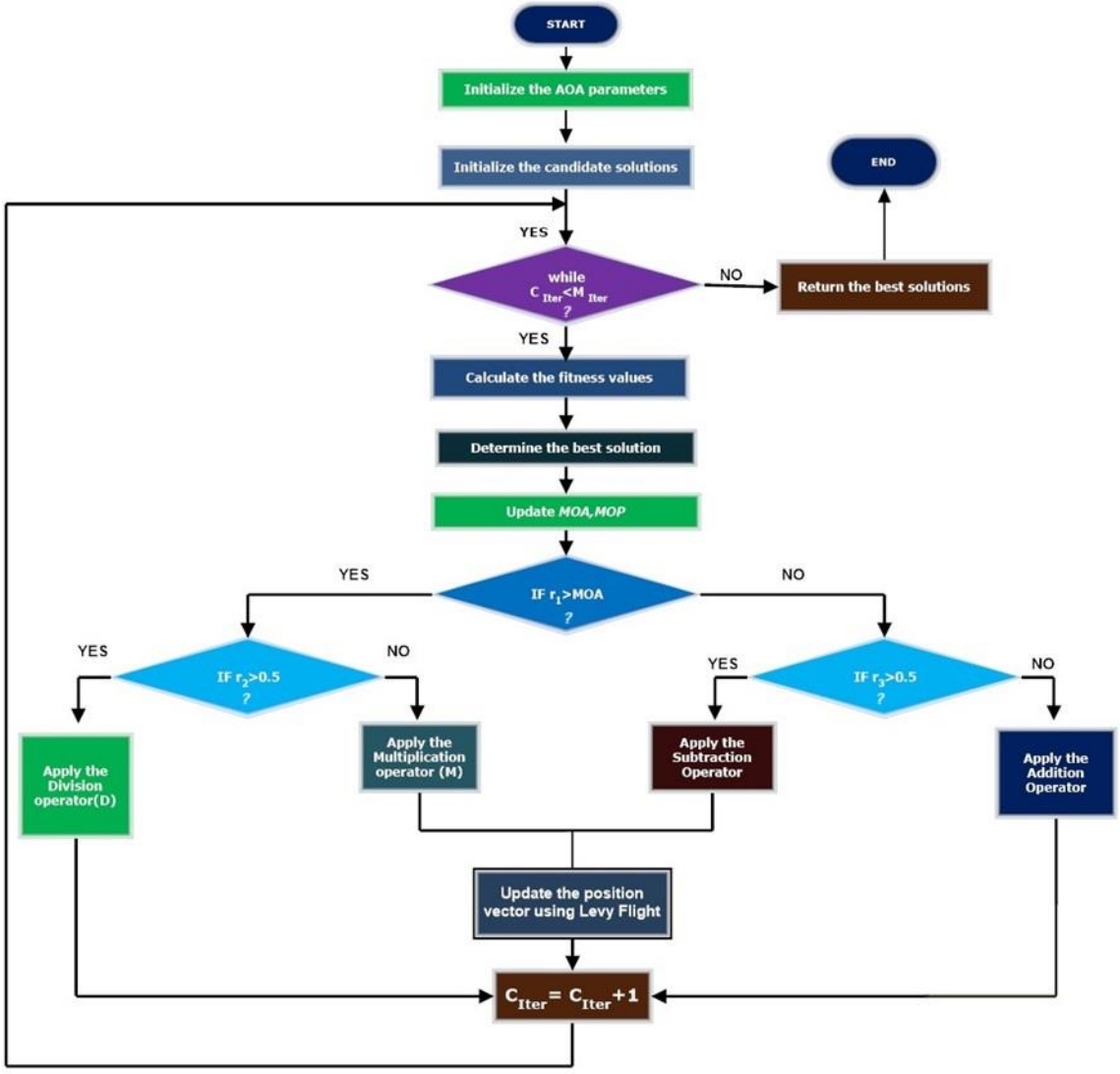

Figure 3.11: A new flowchart for hybrid LFAOA

3.6 TESTING FOR HYPOTHESIS

A statistical technique called hypothesis testing is used to test a hypothesis about a population using sample data. A null hypothesis and an alternative hypothesis must be formulated, a statistical test must be chosen, and a test statistic and a p-value must be calculated. We reject the null hypothesis and draw the conclusion that the alternative hypothesis is correct if the p-value falls below a predetermined significance level. We fail

to reject the null hypothesis if the p-value is greater than the significance level. In statistical analysis, hypothesis testing is an important tool for drawing conclusions about a population from sample data. The security constraint unit commitment problem is solved using the proposed algorithm by testing the following hypotheses.

3.6.1 Wilcoxon Rank Sum Test for the Hypothesis

The Wilcoxon Rank Total Test, otherwise called the Mann-Whitney U test, is a nonparametric measurable test used to look at two free gatherings of information. The purpose of the test is to ascertain whether or not the medians of the two groups differ significantly. The Wilcoxon Rank Sum Test works by comparing the total ranks of the two groups and ranking all of the data values from lowest to highest. We can conclude that the two groups have different medians if the total ranks of one group are consistently higher or lower than those of the other group.

The test necessitates the presumption that the two groups share a similar distribution shape but may be located in distinct locations (median). When the data do not meet the assumptions of the t-test, such as when the sample size is small or the data are not normally distributed, the Wilcoxon Rank Sum Test is frequently used. We first determine the sum of the ranks for each group before beginning the Wilcoxon Rank Sum Test. A test statistic is then calculated using a formula based on the rank sums. Using statistical software, we determine the p-value or compare the calculated value of U to a critical value from a table of critical values. We reject the null hypothesis and conclude that the two groups have significantly different medians if the p-value is less than a predetermined significance level (typically 0.05). We fail to reject the null hypothesis and conclude that there is insufficient evidence to support the alternative hypothesis if the p-value is greater than the significance level. In conclusion, the Wilcoxon Rank Sum Test is a nonparametric statistical test used to compare two independent data sets and determine whether or not their medians differ significantly. The test uses rank sums and a formula to calculate the test statistic and is useful when the data do not meet the t-test's assumptions [109].

3.6.2 t-Test for Hypothesis

The t-test is a factual strategy used to look at the method for two free gatherings of information. A parametric test, assumes that the data have equal variances and are normally distributed. In hypothesis testing, the test is frequently used to determine whether the difference in means between the two groups is statistically significant or merely random

3.7 HYBRID ARITHMETIC OPTIMIZATION ALGORITHM

A class of optimization techniques known as arithmetic optimization algorithms update the search space in order to locate the best possible solution. A wide range of optimization issues can benefit from these simple and effective algorithms. The optimization problem's particular characteristics and the problem at hand influence the choice of algorithm. In a variety of fields, such as engineering, finance, and data analysis, researchers have been able to solve complex optimization issues by utilizing these algorithms. In the point number 3.1 to 3.6, the hybrid chaotic-based algorithm CAOA, the random walk strategies-based RWAOA, and Levy Flight strategies-based AOA was hybridized and their flowchart is shown in Figure 3.7, Figure 3.9, Figure 3.11 respectively. The experimental results for CAOA, RWAOA, and LFOAA have been investigated for a variety of benchmark problems in this chapter.

3.8 STANDARD BENCHMARK PROBLEMS

In this chapter, the performance of the proposed hybrid algorithm has been tested for Uni-modal [110], Multi-modal [110], and fixed dimensions problems [110]. The performance of the optimizer also has been tested for multi-disciplinary engineering design problems [110]. The mathematical formulation for Uni-modal, multi-modal, and fixed dimensions is shown in Table 3.1, Table 3.2, and Table 3.3 respectively. Figures 3.12, 3.13, and 3.14 represent the three-dimensional views of unimodal, multimodal, and fixed benchmark functions, respectively [98].

Table 3.1: Standard Uni-modal Benchmark Functions [98]

Functions	Dimensions	Range	$f_{\min}$
$F_1(\eta) = \sum_{m=1}^{z} \eta_m^2$	30	[-100, 100]	0
$F_2(\eta) = \sum_{m=1}^{z} \lvert\eta_m\rvert + \prod_{m=1}^{z} \lvert\eta_m\rvert$	30	[-10, 10]	0
$F_3(\eta) = \sum_{m=1}^{z} (\sum_{n-1}^{m} \eta_n)^2$	30	[-100, 100]	0
$F_4(\eta) = \max_m\{\lvert\eta_m\rvert, 1 \le m \le z\}$	30	[-100, 100]	0
$F_5(\eta) = \sum_{m=1}^{z-1} [100(\eta_{m+1} - \eta_m^2)^2 + (\eta_m - 1)^2]$	30	[-38, 38]	0
$F_6(\eta) = \sum_{m=1}^{z} ([\eta_m + 0.5])^2$	30	[-100, 100]	0
$F_7(\eta) = \sum_{m=1}^{z} m\eta_m^4 +$ random [0,1]	30	[-1.28, 1.28]	0

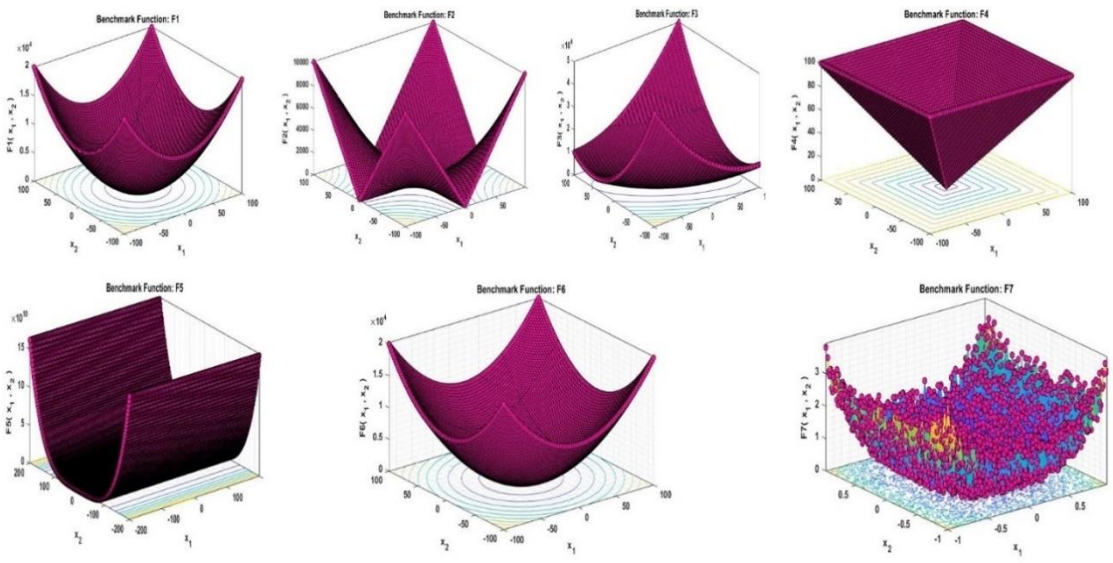

Figure 3.12: 3D view of standard Unimodal Benchmark Functions

Table 3.2: Standard Multi-modal Benchmark Functions [98]

Multimodal Benchmark Functions (F8-F13)	Dim.	Range	$f_{\min}$
$F_8(\eta) = \sum_{m=1}^{z} -\eta_m \sin(\sqrt{\lvert\eta_m\rvert})$	30	[-500,500]	-418.98295
$F_9(\eta) = \sum_{m=1}^{z} [\eta_m^2 - 10\cos(2\pi\eta_m) + 10]$	30	[-5.12,5.12]	0
$F_{10}(\eta) = -20\exp\left(-0.2\sqrt{\left(\frac{1}{z}\sum_{m=1}^{z}\eta_m^2\right)}\right) - \exp\left(\frac{1}{z}\sum_{m=1}^{z}\cos(2\pi\eta_m)\right) + 20 + \mathrm{d}$	30	[-32,32]	0
$F_{11}(\eta) = 1 + \sum_{m=1}^{z}\frac{\eta_m^2}{4000} - \Pi_{m=1}^{z}\cos\frac{\eta_m}{\sqrt{m}}$	30	[-600, 600]	0
$F_{12}(\eta) = \frac{\pi}{z}\left\{10\sin(\pi\tau_1) + \sum_{m=1}^{z-1}(\tau_m - 1)^2[1 + 10\sin^2(\pi\tau_{m+1})] + (\tau_z - 1)^2\right\} + \sum_{m=1}^{z}\mathrm{u}(\eta_m, 10,100,4)$ $\tau_m = 1 + \frac{\eta_m + 1}{4}$ $\mathrm{u}(\eta_m, x, i, b) = \begin{cases} \mathrm{x}(\eta_m - \mathrm{b})^i & \eta_m > b \\ 0 & -\mathrm{b} < \eta_m < b \\ \mathrm{x}(-\eta_m - \mathrm{b})^i & \eta_m < -b \end{cases}$	30	[-50,50]	0
$F_{13}(\eta) = 0.1\left\{\sin^2(3\pi\eta_m) + \sum_{m=1}^{z}(\eta_m - 1)^2[1 + \sin^2(3\pi\eta_m + 1)] + (\mathrm{x}_z - 1)^2[1 + \sin^2]\right\}$	30	[-50,50]	0

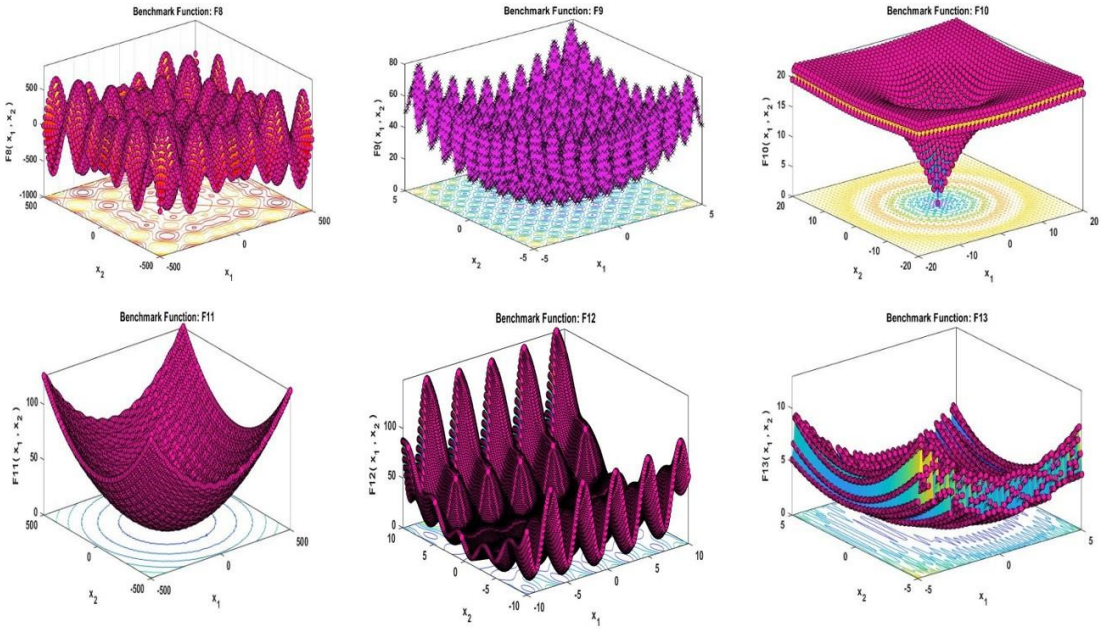

Figure 3.13: 3D view of standard Multi-modal Benchmark Functions

Table 3.3: Standard Fixed Dimensions Benchmark Functions [98]

Fixed Dimension Function [F14-F23]	Dimension	Range	$f_{\min}$
$F_{14}(\eta) = [\frac{1}{500} + \sum_{n=1}^{2} 5 \frac{1}{n+\sum_{m=1}^{z}(\eta_m - b_{mn})6}]^{-1}$	2	[-65.536, 65.536]	1
$F_{15}(\eta) = \sum_{m=1}^{11}[b_m - \frac{\eta_1(a_m^2+a_m\eta_2)}{a_m^2+a_m\eta_3+\eta_4}]^2$	4	[-5, 5]	0.00030
$F_{16}(\eta) = 4\eta_1^2 - 2.1\eta_1^4 + \frac{1}{3}\eta_1^6 + \eta_1\eta_2 - 4\eta_2^2 + 4\eta_2^4$	2	[-5, 5]	-1.0316
$F_{17}(\eta) = (\eta_2 - \frac{5.1}{4\pi 2}\eta_1^2 + \frac{5}{\pi}\eta_1 - 6)^2 + 10(1-\frac{1}{8\pi})\cos\eta_1 + 10$	2	[-5, 5]	0.398
$F_{18}(\eta)=[1+(\eta_1+\eta_2+1)^2(19-14\eta_1+3\eta_1^2-14\eta_2+6\eta_1\eta_2+3\eta_2^2)]$ x $[30+(2\eta_1-3\eta_2)^2$ x $(18-32\eta_1+12\eta_1^2+48\eta_2-36\eta_1\eta_2+27\eta_2^2)]$	2	[-2,2]	3
$F_{19}(\eta) = -\sum_{m=1}^{4} d_m \exp(-\sum_{n=1}^{3}\eta_{mn}(\eta_m - q_{mn})^2)$	3	[1, 3]	-3.32
$F_{20}(\eta) = -\sum_{m=1}^{4} d_m \exp(-\sum_{n=1}^{6}\eta_{mn}(\eta_m - q_{mn})^2)$	6	[0, 1]	-3.32
$F_{21}(\eta) = -\sum_{m=1}^{5}[(\eta - b_m)(\eta - b_m)^T + d_m]^{-1}$	4	[0,10]	-10.1532

$F_{22}(\eta) = -\sum_{m=1}^{7}[(\eta - b_m)(\eta - b_m)^{T}+d_m]^{-1}$	4	[0, 10]	-10.4028
$F_{23}(\eta) = -\sum_{m=1}^{7}[(\eta - b_m)(\eta - b_m)^{T}+d_m]^{-1}$	4	[0, 10]	-10.5363

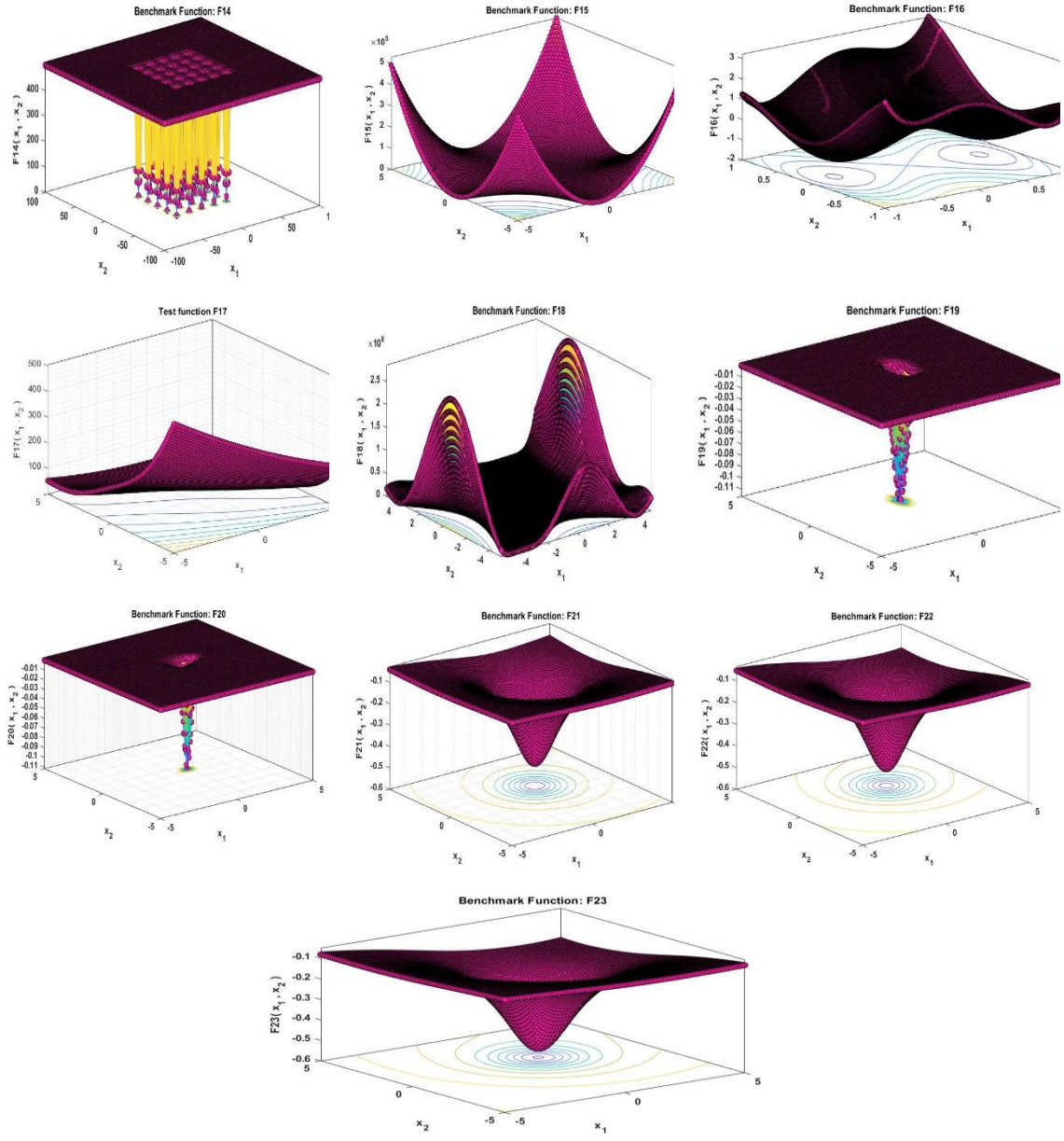

Figure 3.14: 3D view of standard Fixed Dimensions Benchmark Functions

3.9 STANDARD ENGINEERING BENCHMARK PROBLEMS

The Pressure Vessel problem [111], the Three-Bar Truss problem [111], the Welded Beam problem [111], the Cantilever Beam Design problem [111], the Tension/compression Spring Design problem, the Gear Train Design problem, the Speed Reducer, the Belleville spring [111], the Coil Compression problem, and the Multidisc Clutch are some of the eleven types of engineering design problems that are taken into consideration in order to verify the efficacy of the proposed algorithms in the context of multidisciplinary engineering design optimizations problems [111]. The following section provides a comprehensive description of these kinds of engineering design issues.

3.9.1 THREE TRUSS BAR PROBLEM

The engineering focus on the truss design problem is entirely on reducing weight. The truss bar design problem typically consists of three types of constraints warping, stress, and deflection which are optimized to achieve the desired result [112]. The mathematical model of the Three truss bar problem is shown from equation (3.16) to equation (3.20) and the Figure 3.15 shows the model of the Truss Bar problem [98]. Table 3.62 illustrate the result for Three Truss Bar problem comparing other algorithm [112].

Let us consider,

$$\vec{y} = [y_1, y_2] = [A_1, A_2] \tag{3.16}$$

Minimize

$$f(\vec{y}) = \left(2\sqrt{2}y_1 + y_2\right) \times l \tag{3.17}$$

Subject to:

$$g_1(\vec{y}) = \frac{\sqrt{2}y_1 + y_2}{\sqrt{2}y_1^2 + 2y_1y_2} P - \sigma \leq 0 \tag{3.18}$$

$$g_2(\vec{y}) = \frac{y_2}{\sqrt{2}y_1^2 + 2y_1y_2} P - \sigma \leq 0 \tag{3.19}$$

$$g_3(\vec{y}) = \frac{1}{\sqrt{2}y_2 + y_1} P - \sigma \leq 0 \tag{3.20}$$

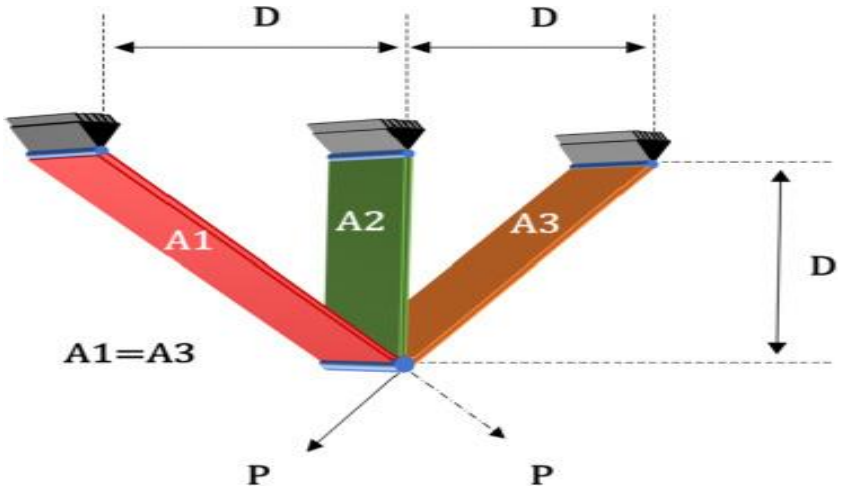

Figure 3.15: Three Bar Truss Design [3]

3.9.2 Speed Reducer Design Problem

In the design engineering world, the speed reducer design problem is considered an extreme problem, and this problem is generally related to seven engineering design parameters [113]. The main objective of this design problem is to minimize the weight of the speed reducer [113]. This type of design problem consists of six continuous variables and eleven constraints as shown in Figure (3.16). These variables are facing width (z_1), teeth module (z_2), pinion teeth (z_3), first shaft length (z_4), second shaft length (z_5), first shaft diameter (z_6), and last parameter is second shaft diameter (z_7)[113]. In this parameter, z_3 is not the continuous parameter while others are continuous parameters because z_3 has an integer value. Equation (3.21) to (3.31) illustrate mathematical modeling for the optimal design of the speed reducer problem [98]. The result for Speed Reducer Design problem is shown in the Table 3.60.

Minimizing;

$$f(\vec{z}) = 0.7854 z_1 z_2 (3.3333 z_3^2 + 14.9334 z_3 - 43.0934) - 1.508 z_1 (z_6^2 + z_7^2) + 7.4777 (z_6^3 + z_7^3) + 0.7854 (z_4 z_6^2 + z_5 z_7^2)$$

Subject to;

$$g_1(\vec{z}) = \frac{(27)}{(z_1 z_2^2 z_3)} - (1 \le 0) \tag{3.21}$$

$$g_2(\vec{z}) = \frac{(397.5)}{(z_1 z_2^2 z_3^2)} - (1 \le 0) \tag{3.22}$$

$$g_3(\vec{z}) = \frac{(1.93 z_4^3)}{(z_2 z_3 z_6^4)} - (1 \le 0) \tag{3.23}$$

$$g_4(\vec{z}) = \frac{1.93 z_5^3}{z_2 z_3 z_7^4} - 1 \le 0 \tag{3.24}$$

$$g_5(\vec{z}) = \frac{1}{110 z_6^3} \sqrt{\left(\frac{745.0 z_4}{z_2 z_3}\right)^2 + 16.9 \times 10^6} - 1 \le 0 \tag{3.25}$$

$$g_6(\vec{z}) = \frac{1}{85 z_7^3} \sqrt{\left(\frac{745.0 z_5}{z_2 z_3}\right)^2 + 157.5 \times 10^6} - 1 \le 0 \tag{3.26}$$

$$g_7(\vec{z}) = \frac{z_2 z_3}{40} - 1 \le 0 \tag{3.27}$$

$$g_8(\vec{z}) = \frac{5 z_2}{z_1} - 1 \le 0 \tag{3.28}$$

$$g_9(\vec{z}) = \frac{z_1}{12 z_2} - 1 \le 0 \tag{3.29}$$

$$g_{10}(\vec{z}) = \frac{(1.5 z_6 + 1.9)}{(12 z_2)} - (1 \le 0) \tag{3.30}$$

$$g_{11}(\vec{z}) = \frac{(1.1z_7 + 1.9)}{z_5} - (1 \le 0) \tag{3.31}$$

Here,

$0.7 \le z_2 \le 0.8,\ 2.6 \le z_1 \le 3.6,\ 17 \le z_3 \le 28, 7.3 \le z_4 \le 8.3,\ 7.8 \le z_5 \le 8.3, 2.9 \le z_6 \le 3.9$ *and* $5 \le z_7 \le 5.5$

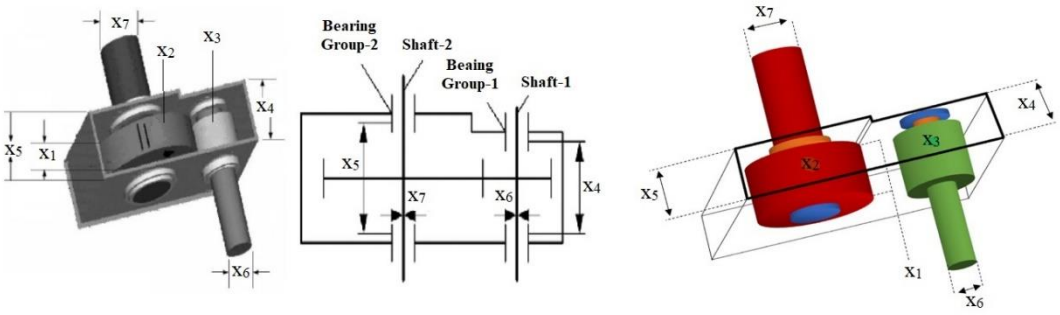

Figure 3.16: Speed reducer design problem [3]

3.9.3 Pressure Vessel Design Problem

Figure 3.17 shows the design specifications for the pressure vessel engineering issue. The Optimization Algorithm's implementation results in lower costs. The main expenses are the cost of welding and the materials used to make the cylinder-shaped vessel. The shell thickness (T_s), the head thickness (T_h), the inner radius (R), and the length of the cylindrical unit (L_h) are the four different variables that are utilized during the process of designing a pressure vessel [113]. The numerical displaying for this issue is represented in equation (3.32) to (3.37).

Consider:

$$\vec{s} = [s_1 s_2 s_3 s_4] = [T_s T_h R L_h] \tag{3.32}$$

Minimize:

$$f(\vec{s}) = 0.6224 s_1 s_3 s_4 + 1.7781 s_2 s_3^2 + 3.1661 s_1^2 s_4 + 19.84 s_1^2 s_3 \quad (3.33)$$

Subject to:

$$g_1(\vec{s}) = (-s_1 + 0.0193 s_3) \leq 0 \quad (3.34)$$

$$g_2(\vec{s}) = (s_3 + 0.00954 s_3) \leq 0 \quad (3.35)$$

$$g_3(\vec{s}) = 1296000 \leq 0 + (-\pi s_3^2 s_4 - \frac{4}{3}\pi s_3^3) \quad (3.36)$$

$$g_4(\vec{s}) = s_4 - 240 \leq 0 \quad (3.37)$$

Variable range $0 \leq s_1 \leq 99$, $0 \leq s_2 \leq 99$, $10 \leq s_3 \leq 200$, $10 \leq s_4 \leq 200$

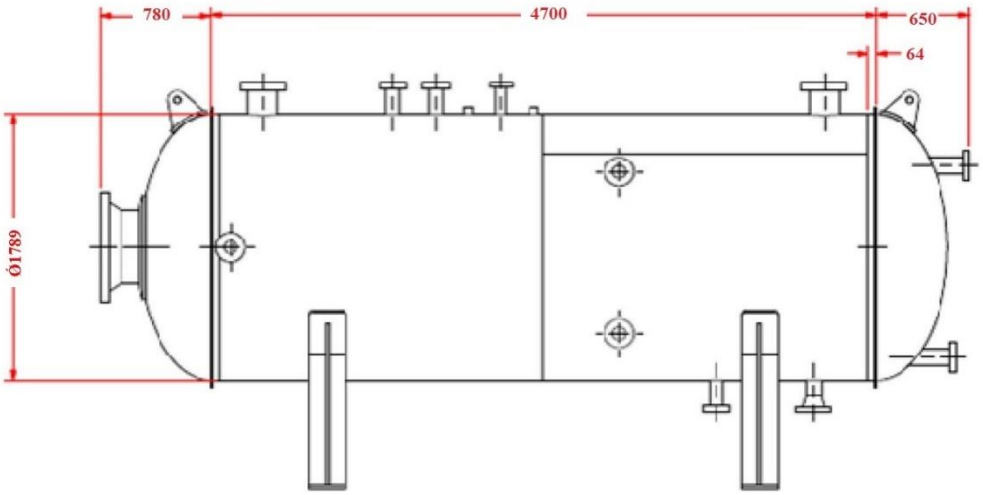

Figure 3.17: Pressure Vessel Design Problem [98]

3.9.4 Cantilever Beam Engineering Design Problem

As depicted in Figure 3.18, the primary objective of the cantilever beam design engineering problem is to keep the beam's weight as low as possible. In this design problem, for the most part, five components are available. The goal of this engineering design issue is to reduce the cantilever beam's weight to a minimum. The numerical demonstrating of the cantilever shaft configuration is shown from equations (3.38) to (3.40). During the design of the cantilever beam, it is crucial that the beam's finishing not be disrupted by the displacement of the vertical constraint in order to achieve the ultimate optimal solution.

$$\text{Consider, } \vec{l} = [l_1 l_2 l_3 l_4 l_5] \tag{3.38}$$

Minimize

$$f(\vec{l}) = 0.6224(l_1 + l_2 + l_3 + l_4 + l_5), \tag{3.39}$$

Subject to

$$g(\vec{l}) = \frac{61}{l} + \frac{37}{l_2^3} + \frac{19}{l_3^3} + \frac{7}{l_4^3} + \frac{1}{l_5^3} \leq 1 \tag{3.40}$$

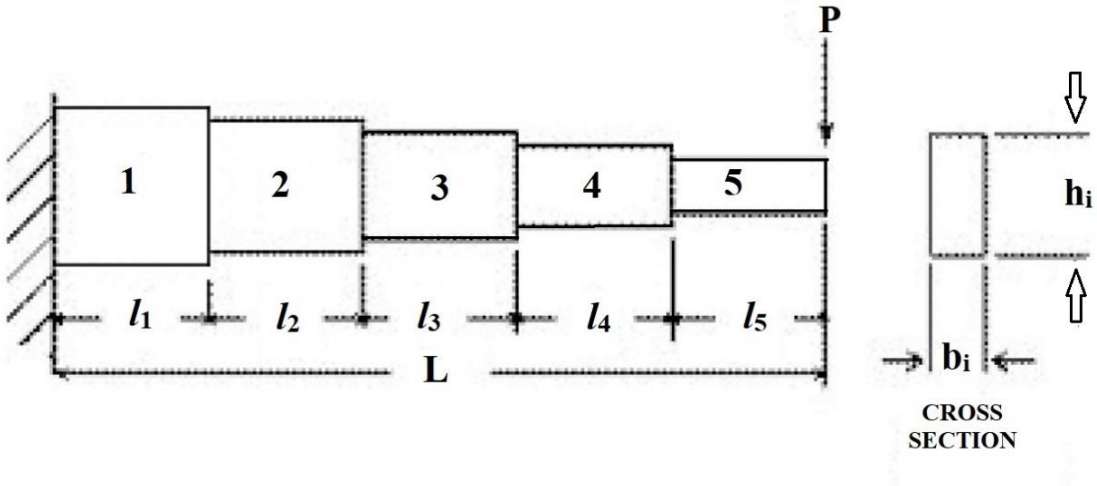

Figure 3.18: Cantilever Beam Design Problem [98]

3.9.5 Compression Spring

As shown in Figure 3.19, this problem is related to mechanical engineering. The primary objective of the spring design problem in compression is to reduce weight. Wire diameter (*dr*), active coils (*Nc*), and coil diameter (*Dm*) are three crucial variables in the compression spring design problem. The mathematical modelling of compression spring design is shown in equations (3.41) to (3.47).

Consider;

$$\vec{y} = \left[y_1 y_2 y_3 \right] = \left[drDmNc \right], \tag{3.41}$$

$$\text{Minimize } f(\vec{y}) = \left(y_3 + 2 \right) y_2 y_1^2, \tag{3.42}$$

Subject to:

$$g_1(\vec{y}) = 1 - \frac{y_2^3 y_3}{71785 y_1^4} \leq 0, \tag{3.43}$$

$$g_2(\vec{y}) = \frac{4y_2^2 - y_1 y_2}{12566\left(y_2 y_1^3 - y_1^4 \right)} + \frac{1}{5108 y_1^2} \leq 0, \tag{3.44}$$

$$g_2(\vec{y}) = \frac{4y_2^2 - y_1 y_2}{12566\left(y_2 y_1^3 - y_1^4 \right)} + \frac{1}{5108 y_1^2} \leq 0, \tag{3.45}$$

$$g_3(\vec{y}) = 1 - \frac{140.45 y_1}{y_2^2 y_3} \leq 0, \tag{3.46}$$

$$g_4(\vec{y}) = \frac{y_1 + y_2}{1.5} - 1 \leq 0, \tag{3.47}$$

Variable rang is given by $0.005 \leq y_1 \leq 2.00$, $0.25 \leq y_2 \leq 1.30$, $2.00 \leq y_3 \leq 15.0$

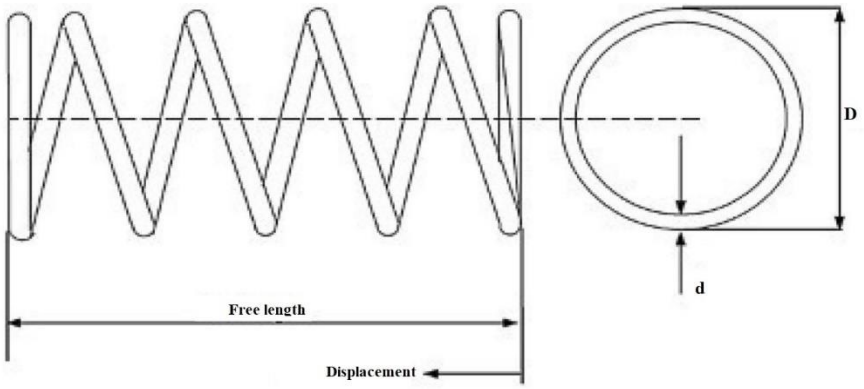

Figure 3.19: Compression Spring Design Problem [98]

3.9.6 Engineering design problem of Rolling Element Bearing [114]

As shown in Figure 3.20, the primary objective of the rolling element bearing design problem is to increase the rolling element's dynamic load-bearing capacity [114]. Ten parameters play a crucial role in increasing rolling elements' load-carrying capacity. Only five of these ten parameters are taken into consideration [111]. The outer curvature coefficient, the inner curvature coefficient, the diameter pitch (DIMP), and the number of balls (*Nb*) are all crucial variables. The inner part of the design geometry is influenced in an indirect way by the remaining five variables. The mathematical modelling is illustrated as follows [98].

Maximum;

$$C_D = f_c DIM_B^{1.8} N^{2/3} \tag{3.48}$$

If $(DIM \le 25.4mm)$

$$C_D = 3.647 DIM_B^{1.4} N^{2/3} f_C \tag{3.49}$$

If $(DIM \ge 25.4mm)$ (3.50)

Subjected to;

$$r_1(x) = \frac{\theta_0}{2\sin^{-1}\left(\frac{DIM_B}{DIM_{MAX}}\right)} - N + 1 \ge 0 \tag{3.51}$$

$$r_2(x) = 2DIM_B - K_{DIM_{MIN}}(DIM - \dim) \geq 0 \quad (3.52)$$

$$r_3(x) = K_{DIM_{MAX}}(DIM - \dim) \geq 0 \quad (3.53)$$

$$r_4(x) = \beta B_W - DIM_B \leq 0 \quad (3.54)$$

$$r_4(x) = DIM_{MAX} - 0.5(DIM + \dim) \geq 0 \quad (3.55)$$

$$r_5(x) = DIM_{MAX} - 0.5(DIM + \dim) \geq 0 \quad (3.56)$$

$$r_6(x) = (0.5 + re)(DIM + \dim) \geq 0 \quad (3.57)$$

$$r_7(x) = 0.5(DIM - DIM_{MAX} - DIM_B) - \alpha DIM_B \geq 0 \quad (3.58)$$

$$r_8(x) = f_I \geq (0.515) \quad (3.59)$$

$$r_9(x) = f_0 \geq (0.515) \quad (3.60)$$

here,

$$f_c = (37.91)\left[1+\left\{(1.04)\left(\frac{1-\varepsilon}{1+\varepsilon}\right)^{1.72}\left(\frac{f_I(2f_0-1)}{f_0(2f_I-1)}\right)^{0.41}\right\}^{10/3}\right]^{-0.3} \times\left[\frac{\varepsilon^{0.3}(1-\varepsilon)^{1.39}}{(1+\varepsilon)^{1/3}}\right]\left[\frac{(2f_I)}{(2f_I-1)}\right]^{0.41}$$

$$\theta_0 = (2\pi - 2\cos^{-1})\left(\frac{\left[\{(DIM-\dim)/2-3(t/4)\}^2+(DIM/2-t/4-DIM_B)^2-\{\dim/2+t/4\}^2\right]}{2\{(DIM-\dim)/2-3(t/4)\}\{D/2-t/4-DIM_B\}}\right)$$

$$\varepsilon = \frac{DIM_B}{(DIM_{MAX})},\ f_I = \frac{R_I}{(DIM_B)},\ f_0 = \frac{R_0}{(DIM_B)},\ t = (DIM - \dim - 2DIM_B)$$

$DIM = 160,\ \dim = 90,\ B_W = 30,\ R_I = R_0 = 11.033$

$0.5(DIM + \dim.) \leq DIM_{MAX} \leq 0.6(DIM + \dim.), 0.15(DIM - \dim.) \leq DIM_B \leq 0.45(DIM - \dim.), 4 \leq N \leq 50$

$(f_0 \leq 0.6)$ and $(0.515 \leq f_I)$

$(0.4 \leq K_{DIM_{MIN}} \leq 0.5),\ (0.6 \leq K_{DIM_{MAX}} \leq 0.7),\ (0.3 \leq re \leq 0.1),\ (0.02 \leq re \leq 0.1),\ (0.6 \leq \beta \leq 0.85)$

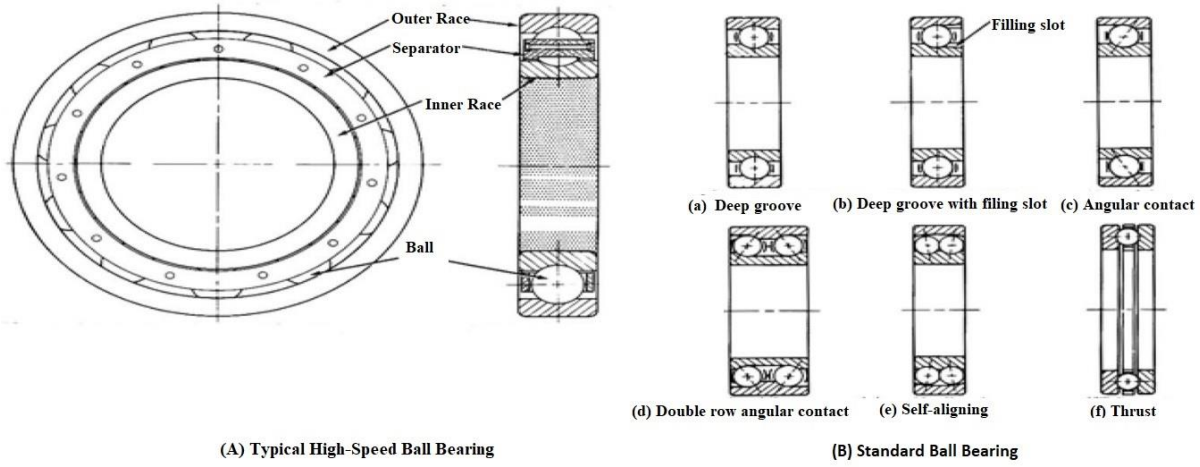

Figure 3.20: Rolling Element Bearing [98]

3.9.7 Welded Beam Design problem

Figure 3.21 depicts the process of welding, in which molten metal is used to blend the various sections together. The goal of this kind of design problem is to make the beam as cheap as possible. There are four main variables in the welded beam design problem. Weld thickness (h), bar height (h), and bar thickness (b) are these variables. The formulation of this design problem's mathematical modelling is shown in equations (3.61) to (3.75). Another significant thing is numerical display, relying on the requirements of imperatives and boundaries [98].

Consider,

$$\vec{y} = \left[y_1 y_2 y_3 y_4 \right] = \left[hltb \right] \tag{3.61}$$

Minimize,

$$f(\vec{y}) = 0.04811 y_3 y_4 \left(14.0 + y_2\right) + (1.10471 y_1^2 y_2) \tag{3.62}$$

Subject to

$$g_1(\vec{y}) = [\tau(\vec{y}) - \tau_{\text{maxi}}] \le 0, \tag{3.63}$$

$$g_2(\vec{y}) = [\sigma(\vec{y}) - \sigma_{\text{maxi}}] \le 0, \tag{3.64}$$

$$g_3(\vec{y}) = [\delta(\vec{y}) - \delta_{\text{maxi}}] \le 0, \tag{3.65}$$

$$g_4(\vec{y}) = [y_1 - y_4] \le 0, \tag{3.66}$$

$$g_5(\vec{y}) = [P_i - P_c(\vec{y})] \le 0, \tag{3.67}$$

$$g_6(\vec{y}) = [0.125 - y_1] \le 0, \tag{3.68}$$

$$g_7(\vec{y}) = [1.10471 y_1^2] + [0.04811 y_3 y_4 (14.0 + y_2)] - [5.0] \le 0 \tag{3.69}$$

Variable range is given by

$(0.1 \le y_1 \le 2),\ (0.1 \le y_2 \le 10),\ (0.1 \le y_3 \le 10),\ (0.1 \le y_4 \le 2),$

Where,

$$\tau(\vec{y}) = \sqrt{(\tau')^2 + 2\tau'\tau'' \frac{y_2}{2R} + (\tau'')^2}, \tag{3.70}$$

$$\tau' = \frac{P_i}{\sqrt{2} y_1 y_2}, \tau'' = \frac{MR}{J}, M = P_i\left(L + \frac{y_2}{2}\right), \tag{3.71}$$

$$R = \sqrt{\frac{y_2^2}{4} + \left(\frac{y_1 + y_3}{2}\right)^2}, \tag{3.72}$$

$$J = 2\left\{\sqrt{2} y_1 y_2 \left[\frac{y_2^2}{4} + \left(\frac{y_1 + y_3}{2}\right)^2\right]\right\}, \tag{3.73}$$

$$\sigma(\vec{y}) = \frac{6 P_i L}{y_4 y_3^2}, \delta(\vec{y}) = \frac{6 P_i L^3}{E y_2^2 y_4}, \tag{3.74}$$

$$P_c(\vec{y}) = \frac{(4.013 E \frac{\sqrt{(y_3^2 y_4^6)}}{36})}{L^2}\left(1 - \frac{y_3}{2L}\sqrt{\frac{E}{(4G)}}\right), \tag{3.75}$$

$(G = 12 \times 10^6\ psi),\ (P_i = 6000 lb),\ (E = 30 \times 1^6\ psi),\ (L = 14 in),\ (\delta_{\max i} = 0.25 in),$
$\sigma_{\text{maxi}} = 3000\, psi,\ \tau_{\text{maxi}} = 13600\, psi,$

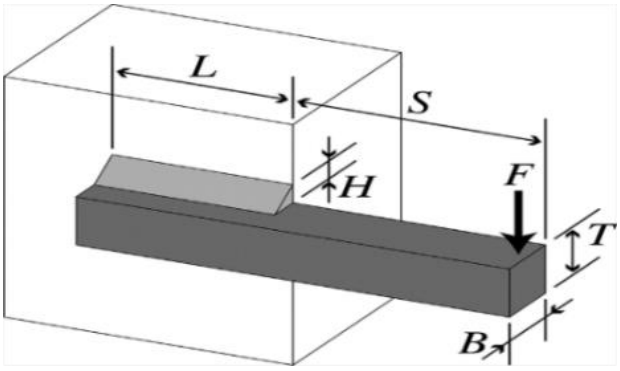

Figure 3.21 Design of Welded Beam [98]

3.9.8 Belleville Spring Design

This design problem's primary objective is to meet a number of constraints while keeping the weight as low as possible. Any parameter is minimized from the constraints that are available using this approach, and the ratios of the designed variables are used to make this selection. The internal spring diameter (DIM_I), the outer spring diameter (DIM_E), the spring height (S_H), and then the spring width are the primary variables in this problem. The equation used to perform the mathematical modelling is (3.76) to (3.83). The Belleville spring design problem is depicted in Figure 3.22.

Minimizing;

$$f(x) = 0.07075\pi(DIM_E^2 - DIM_I^2)t \tag{3.76}$$

Subject to:

$$b_1(x) = G - \frac{4P\lambda_{\max}}{(1-\delta^2)\alpha DIM_E}\left[\delta(S_H - \frac{\lambda \max}{2}) + \mu t\right] \geq 0 \tag{3.77}$$

$$b_2(x) = \left(\frac{4P\lambda_{\max}}{(1-\delta^2)\alpha DIM_E}\left[(S_H - \frac{\lambda}{2})(S_H - \lambda)t + t^3\right]\right)_{\lambda_{\max}} - P_{MAX} \geq 0 \tag{3.78}$$

$$b_3(x) = (\lambda_1 - \lambda_{\max}) \geq 0 \tag{3.79}$$

$$b_4(x) = (H - S_H - t) \geq 0 \tag{3.80}$$

$$b_5(x) = (DIM_{MAX} - DIM_E) \geq 0 \tag{3.81}$$

$$b_6(x) = (DIM_E - DIM_I) \geq 0 \tag{3.82}$$

$$b_7(x) = (0.3) - \left(\frac{S_H}{(DIM_E - DIM_I)} \right) \geq 0 \qquad (3.83)$$

Here, $\alpha = \frac{6}{(\pi \ln J)} \left(\frac{J-1}{J} \right)^2$

$\delta = \frac{6}{(\pi \ln J)} \left(\frac{J-1}{\ln J} - 1 \right)$

$\mu = \frac{6}{(\pi \ln J)} \left(\frac{J-1}{2} \right)$

$P_{MAX} = (5400lb)$

$(P = 30e6\,psi), (\lambda_{\max} = 0.2in), (\delta = 0.3), (G = 200Kpsi), (H = 2in), (DIM_{MAX} = 12.01in),$

$(J = \frac{DIM_E}{DIM_I}), \lambda_1 = f(a)a, a = \frac{S_H}{t}$

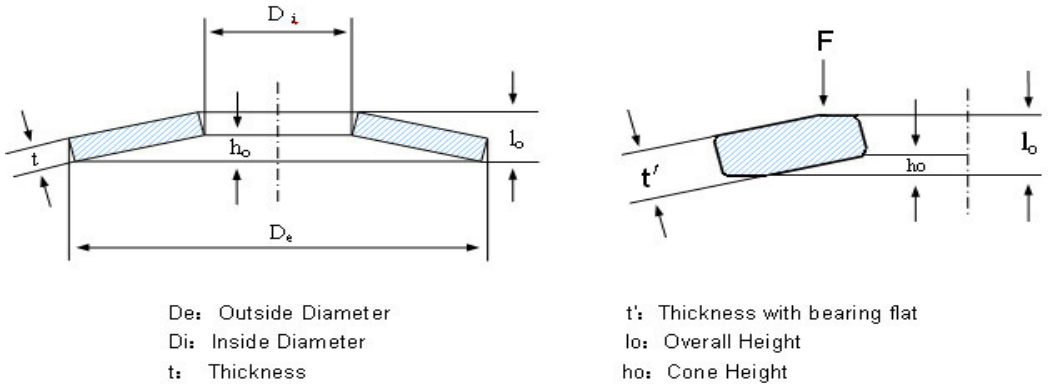

Figure 3.22: Belleville Spring Design [113]

3.9.9 Gear Train Design Problem

The mathematical modelling is presented through equations (3.84) to (3.85). The four variables that play a significant role in the restructuring of this method to reduce the tooth ratio and scalar value are depicted in Figure 3.23.

Considering;

$$\vec{g} = [g_1, g_2, g_3, g_4] = [M_A, M_B, M_C, M_D] \qquad (3.84)$$

Minimizing;

$$f(\vec{g}) = \left(\frac{1}{6.931} - \frac{g_3 g_4}{g_1 g_4} \right)^2 \tag{3.85}$$

Subject to: $12 \le (g_1, g_2, g_3, g_4) \le 60$

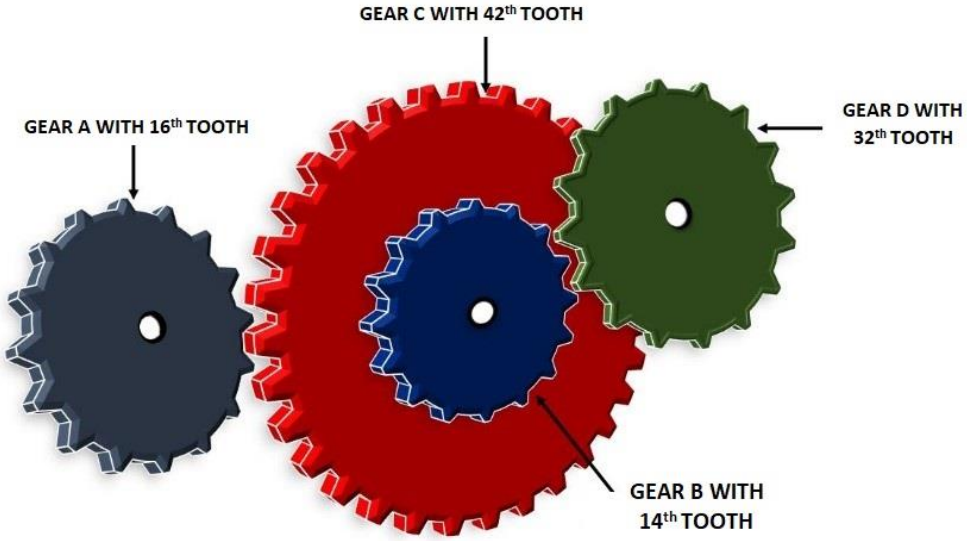

Figure 3.23: Gear Train Design Problem

3.9.10 Multi-Disc Clutch Design Problem

Brake design is considered one of the most crucial engineering design issues. The primary objective of designing a clutch is to minimize its overall weight, which is achieved through careful design considerations. The clutch design involves five significant design parameters, namely, the outer surface radius, the inner surface radius, the disc thickness, the number of friction surfaces, and the actuating force. Figure 3.24 illustrates the design challenge associated with multi-disc clutches, while equations (3.86) through (3.94) present the mathematical model for the multi-disc brake design problem.

Minimizing;

$$f\left(Th, S_f, R_{in}, R_O\right) = \pi Th\gamma\left(S_f + 1\right)\left(R_0^2 - R_{in}^2\right) \tag{3.86}$$

Where,

$R_{in} \in (60, 61, 62....80);$

$R_o \in (90, 91, ...110);$

$Th \in (1, 1.5, 2, 2.5, 3);$

$F_{ac} \in (600, 610, 620, 1000);$

$S_f \in (2, 3, 4, 5, 6, 7, 8, 9)$

Subject to,

$$m_1 = R_0 - R_{in} - \Delta R \geq 0 \quad (3.87)$$

$$m_2 = L_{MAX} - (S_f + 1)(Th + \alpha) \geq 0 \quad (3.88)$$

$$m_3 = PM_{MAX} - PM_{\pi} \geq 0 \quad (3.89)$$

$$m_4 = PM_{MAX} Y_{MAX} + PM_{\pi} Y_{SR} \geq 0 \quad (3.90)$$

$$m_5 = Y_{SR_{MAX}} - Y_{SR} \geq 0 \quad (3.91)$$

$$m_6 = t_{MAX} - t \geq 0 \quad (3.92)$$

$$m_7 = DC_h - DC_f \geq 0 \quad (3.93)$$

$$m_8 = t \geq 0 \quad (3.94)$$

Where, $PM_{\pi} = \dfrac{F_{ac}}{\Pi\left(R_0^2 - R_{in}^2\right)}$

$$Y_{SR} = \frac{2\pi n\left(R_0^3 - R_{in}^3\right)}{90\left(R_0^2 - R_{in}^2\right)}$$

$$t = \frac{i_x \pi n}{30\left(DC_h + DC_f\right)}$$

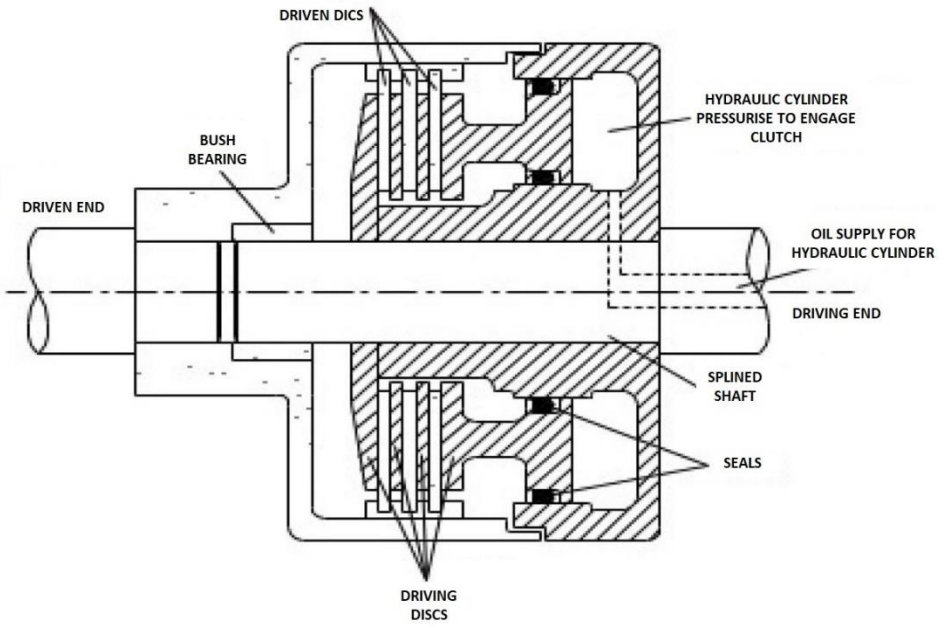

Figure 3.24: Multi-disc Clutch Break Design Problem [113]

3.9.11 I-Beam Engineering Design Problem

A type of structural member used in engineering and construction is the I-beam. The distinctive shape of the beam, which resembles the capital "I," gives it its name. The beam has two flanges on either side of a central web. The web is typically oriented along the beam's length and is typically perpendicular to the flanges.

The cross-sectional elements of the shaft are basic to its solidarity and firmness properties. Typically, these dimensions are chosen to strike a balance between the requirements for strength and the constraints imposed by material and fabrication costs. The design problem is to ensure that the beam can withstand the loads that will be applied to it without failing while also meeting any relevant design criteria, such as deflection limits or serviceability requirements. The mathematical formulation for the I-Beam Engineering Design problem is given by equations (3.95) to (3.97). The figure for the I-Beam design problem is shown in figure 3.25.

$$B = 2.B_f + \Delta.\rho \qquad (3.95)$$

$$I = \frac{\rho^2}{4} \times \left(2.B_f + \frac{\Delta.\rho}{3} \right) \tag{3.96}$$

$$M = \frac{\rho}{2} \times \left(2.B_f + \frac{\Delta.\rho}{3} \right) \tag{3.97}$$

Where, B is defined as cross sectional region, I represented as inertia moment of the cross section of xx axis and M denoted as module of cross section, ρ represent the thickness, B_f represent the chord's cross sectional area. Δ represent the thickness [111].

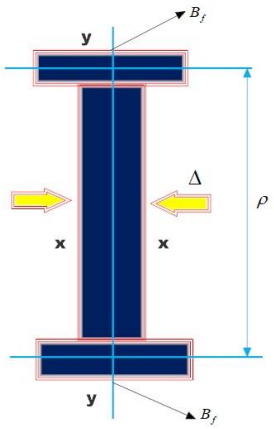

Figure 3.25: I-Beam Design Problem

3.10 RESULT & DISCUSSION

The results of the study are presented and discussed in this section. The data collected from the research has been analyzed, and the findings are summarized below. Each of the objective functions has been estimated for index, average values, standard deviation [68], best value, worst value, and median values in order to validate the results in the stochastic environment of the proposed optimization algorithms [68].

When measuring the p-value and h-value for standard benchmarks that take into account unimodal, multimodal, and fixed-dimension functions with proposed optimizers, the Wilcoxon rank-sum test and the t-test are taken into consideration. The tables display the minimum fitness value, number of trails, maximum fitness value, mean fitness, median fitness, semi-inter-quartile deviation, number of outliers, and standard deviations for the first quartile (25th percentile), second quartile (50th percentile), and third quartile (75th percentile).

3.10.1 Testing of Unimodal Benchmark Functions

The process of searching for the optimal position for any algorithm totally depends on its capability to reach closer to that optimal area or origin. During this process of finding the optimal location or best position, different agents may be entrapped nearby or far as per the defined exploration and exploitation. The proposed CAOA, RWAOA, and LFAOA optimisation algorithms are tested for Uni-modal Benchmark Functions (F1 to F7) for 10, 30, 50, 100 dimensions, 30 trial runs, and 500 iterations [68]. The objective fitness function results of the unimodal test functions of CAOA, RWAOA, and LFAOA in terms of the best time, mean, median, worst time, and standard deviation have been shown in **Tables 3.5**, **3.6, 3.7,** and **3.8** for 10, 30, 50, and 100 dimensions, respectively. The Wilcoxon sum test and statistical T-test results have been performed to examine the usefulness of the solution. The quartile results of CAOA, RWAOA, and LFAOA for multi-modal benchmark functions are shown in **Tables 3.9, 3.10, 3.11,** and **3.12** for 10, 30, 50, and 100 dimensions, respectively. The results of the Wilcoxon sum test and statistical T-test of CAOA, RWAOA, and LFAOA have been shown in **Tables 3.13, 3.14, 3.15**, and **3.16** for 10, 30, 50, and 100 dimensions, respectively. The simulation time required for the Multi-Model Benchmark Function using CAOA, RWAOA, and LFAOA for 10, 30, 50, and 100 dimensions is shown in **Tables 3.17, 3.18, 3.19**, and **3.20**, respectively. The comparison results for the unimodal benchmark function of the Chaotic, Random Walk, and Levy Flight Arithmetic Optimisation Algorithm have been shown in **Table 3.21**, where CAOA, RWAOA, and LFAOA are compared with other known meta-heuristics search algorithms such as Genetic Algorithm, PSO, BBO, FPA, GWO, BAT, FA, CS, MFO, GSA, DE, and AOA in terms of standard deviation and average time for 10, 30, 50, and 100 dimensions. The comparison convergence curve of CAOA, RWAOA, and LFAOA for the unimodal benchmark function has been shown in Figure 3.26. The test result of multi-modal with increased convergence by CAOA, RWAOA, and LFAOA shows the effectiveness of this algorithm [115].

Table 3.5: Test result of Uni-modal Benchmark Function for Objective fitness functions for CAOA, RWAOA, LFAOA (10 Dimensions)

Function No.	CAOA	RWAOA	LFAOA	CAOA	RWAOA	LFAOA	CAOA	RWAOA	LFAOA	CAOA	RWAOA	LFAOA	CAOA	RWAOA	LFAOA	CAOA	RWAOA	LFAOA
	Index	Index	Index	Mean	Mean	Mean	Std.	Std.	Std.	Best	Best	Best	Worst	Worst	Worst	Median	Median	Median
F1	1	1	1	0	0	1.46E-190	0	0	0	0	0	0	0	0	4.37E-189	0	0	0
F2	1	1	1	0	0	0	0	0	0	0	0	0	0	0	0	0	0	0
F3	1	1	1	0	4.09E-257	0	0	0	0	0	0	0	0	1.23E-255	0	0	0	0
F4	1	2	2	8.68E-157	5.40E-173	2.74E-54	4.76E-156	0	1.50E-53	0	0	0	2.61E-155	1.62E-171	8.22E-53	0	0	0
F5	25	12	29	5.763658	6.593295	6.558106	0.336263	0.316239	0.396009	4.874147	6.123462	5.809852	6.463738	7.325205	7.448476	5.836879	6.519671	6.514729
F6	16	2	27	1.1315	0.024108	0.027501	0.170991	0.011605	0.013394	0.834647	0.006341	0.011438	1.472082	0.058218	0.067957	1.124892	0.021627	0.026595
F7	18	20	5	5.96E-05	7.47E-05	6.09E-05	5.99E-05	6.77E-05	6.83E-05	1.37E-06	7.54E-07	1.95E-06	0.000235	0.000253	0.000283	4.98E-05	4.75E-05	3.58E-05

Table 3.6: Test result of Uni-modal Benchmark Function for Objective fitness functions for CAOA, RWAOA, LFAOA (30 Dimensions)

Function No.	CAOA	RWAOA	LFAOA	CAOA	RWAOA	LFAOA	CAOA	RWAOA	LFAOA	CAOA	RWAOA	LFAOA	CAOA	RWAOA	LFAOA	CAOA	RWAOA	LFAOA
	Index	Index	Index	Mean	Mean	Mean	Std.	Std.	Std.	Best	Best	Best	Worst	Worst	Worst	Median	Median	Median
F1	1	1	14	1.19E-251	2.34E-24	6.02E-31	0	1.28E-23	3.30E-30	0	3.37E-167	1.61E-160	3.56E-250	7.02E-23	1.81E-29	0	1.30E-96	3.02E-79
F2	1	1	1	0	0	0	0	0	0	0	0	0	0	0	0	0	0	0
F3	1	5	5	1.85E-293	0.006314	0.006292	0	0.012077	0.011735	0	3.08E-134	4.09E-119	5.56E-292	0.046447	0.052021	0	6.44E-27	5.31E-22
F4	7	29	15	0.003416	0.024651	0.025639	0.009886	0.020556	0.020221	0	3.06E-44	2.89E-49	0.042955	0.050551	0.048614	3.94E-244	0.039326	0.039483
F5	23	8	13	27.52772	28.51794	28.45713	0.715691	0.300947	0.292458	26.15785	27.7572	27.65634	28.63521	28.91593	28.90474	27.50334	28.51406	28.4714
F6	13	25	26	6.254627	3.138059	3.174603	0.255096	0.246767	0.28494	5.624777	2.543627	2.540394	6.656821	3.790637	3.700038	6.310744	3.126337	3.247782
F7	23	7	11	6.40E-05	6.01E-05	6.37E-05	5.77E-05	4.63E-05	8.20E-05	2.10E-06	7.02E-06	2.22E-06	0.000229	0.000199	0.000436	3.61E-05	5.20E-05	5.27E-05

Table 3.7: Test result of Uni-modal Benchmark Function for Objective fitness functions for CAOA, RWAOA, LFAOA (50 Dimensions)

Function No.	CAOA	RWAOA	LFAOA	CAOA	RWAOA	LFAOA	CAOA	RWAOA	LFAOA	CAOA	RWAOA	LFAOA	CAOA	RWAOA	LFAOA	CAOA	RWAOA	LFAOA
	Index	Index	Index	Mean	Mean	Mean	Std.	Std.	Std.	Best	Best	Best	Worst	Worst	Worst	Median	Median	Median
F1	1	2	27	0	0.000466	0.000616	0	0.001338	0.001631	0	3.19E-88	1.41E-63	0	0.006008	0.007687	0	4.83E-18	2.97E-22
F2	1	24	27	0	1.57E-179	1.73E-178	0	0	0	0	8.25E-276	1.47E-257	0	4.72E-178	5.17E-177	0	2.60E-219	1.16E-227
F3	1	13	2	0.000487	0.096162	0.073774	0.002666	0.132076	0.041409	0	1.96E-41	0.002347	0.0146	0.634769	0.174862	0	0.048345	0.068661
F4	27	28	12	0.024899	0.047978	0.048932	0.039229	0.009089	0.014396	1.07E-262	0.031683	4.13E-06	0.153351	0.071281	0.069679	0.007847	0.046451	0.050245
F5	15	27	4	47.9003	48.67957	48.73295	0.595159	0.235867	0.183431	46.56329	48.08766	48.39324	48.60945	48.92234	48.93971	48.08201	48.70699	48.77124
F6	25	7	1	11.38891	7.224709	7.181049	0.256114	0.367543	0.398565	10.39602	6.54057	6.454521	11.77567	8.042734	7.843837	11.40538	7.241782	7.234707
F7	18	29	7	6.39E-05	7.14E-05	6.22E-05	4.02E-05	6.20E-05	7.37E-05	6.65E-07	2.75E-06	8.83E-07	0.000167	0.000251	0.000375	5.86E-05	5.93E-05	4.31E-05

Table 3.8: Test result of Uni-modal Benchmark Function for Objective fitness functions for CAOA, RWAOA, LFAOA (100 Dimensions)

Function No.	CAOA	RWAOA	LFAOA	CAOA	RWAOA	LFAOA	CAOA	RWAOA	LFAOA	CAOA	RWAOA	LFAOA	CAOA	RWAOA	LFAOA	CAOA	RWAOA	LFAOA
	Index	Index	Index	Mean	Mean	Mean	Std.	Std.	Std.	Best	Best	Best	Worst	Worst	Worst	Median	Median	Median
F1	12	3	20	0.003119	0.027498	0.023725	0.002283	0.010312	0.00805	0	0.012165	0.0091	0.008846	0.052138	0.039748	0.002793	0.028495	0.024517
F2	1	14	30	0	9.89E-56	2.89E-65	0	5.42E-55	1.58E-64	0	1.74E-124	2.55E-119	0	2.97E-54	8.66E-64	0	2.40E-89	3.37E-90
F3	9	8	21	0.058415	0.894559	0.729194	0.03339	0.664391	0.441787	4.72E-239	0.307839	0.325039	0.149722	3.731743	2.312983	0.054283	0.753455	0.54545
F4	17	11	19	0.058814	0.090713	0.088532	0.026461	0.010108	0.009289	0.030332	0.069272	0.068598	0.125558	0.110653	0.113581	0.049987	0.087654	0.087608
F5	6	29	21	98.30327	98.87152	98.86718	0.375895	0.10381	0.116504	96.77066	98.46341	98.52826	98.86983	98.99185	98.98432	98.39147	98.90103	98.92107
F6	13	15	22	24.27647	18.2342	18.31291	0.245	0.589895	0.588171	23.71392	16.56132	16.69428	24.64553	19.19342	19.2827	24.34808	18.32137	18.45554
F7	6	2	3	0.000112	7.44E-05	4.26E-05	0.0001	8.73E-05	4.35E-05	4.96E-06	1.79E-06	1.73E-06	0.000387	0.000459	0.000177	8.02E-05	5.07E-05	2.23E-05

Table 3.9: Quartile result for Uni-modal Test function using CAOA, RWAOA, LFAOA (10 Dim.)								
Algorithm	**Function No.**	**F1**	**F2**	**F3**	**F4**	**F5**	**F6**	**F7**
CAOA	No. of trials	30	30	30	30	30	30	30
RWAOA	No. of trials	30	30	30	30	30	30	30
LFAOA	No. of trials	30	30	30	30	30	30	30
CAOA	Minimum value	0	0	0	0	4.874146547	0.83464735	1.37E-06
RWAOA	Minimum value	0	0	0	0	6.123461926	0.006340875	7.54E-07
LFAOA	Minimum value	0	0	0	0	5.809852328	0.011438088	1.95E-06
CAOA	Maximum value	0	0	0	2.61E-155	6.463737931	1.472082341	0.000234602
RWAOA	Maximum value	0	0	1.23E-255	1.62E-171	7.325205089	0.058218226	0.000253003
LFAOA	Maximum value	4.36E-189	0	0	8.22E-53	7.448475875	0.067956753	0.000282693
CAOA	Mean Value	0	0	0	8.68E-157	5.763657963	1.131499651	5.96E-05
RWAOA	Mean Value	0	0	4.09E-257	5.40E-173	6.593295189	0.024108002	7.47E-05
LFAOA	Mean Value	1.45E-190	0	0	2.74E-54	6.558106427	0.027500504	6.09E-05
CAOA	Median	0	0	0	0	5.836878651	1.124892176	4.98E-05
RWAOA	Median	0	0	0	0	6.519671409	0.021627081	4.75E-05
LFAOA	Median	0	0	0	0	6.514729312	0.026595237	3.58E-05
CAOA	First quartile (25th Percentile)					5.453826778	1.008950814	1.45E-05
RWAOA	First quartile (25th Percentile)	-	-	-	-	6.423162666	0.016814359	2.21E-05
LFAOA	First quartile 25th Percentile)	-	-	-	-	6.288813448	0.018135659	1.30E-05
CAOA	Second quartile (50th Percentile)	0	0	0	0	5.836878651	1.124892176	4.98E-05
RWAOA	Second quartile (50th Percentile)	0	0	0	0	6.519671409	0.021627081	4.75E-05
LFAOA	Second quartile (50th Percentile)	0	0	0	0	6.514729312	0.026595237	3.58E-05
CAOA	Third quartile (75th Percentile)	-	-	-	2.61E-155	5.98012879	1.242650851	8.71E-05
RWAOA	Third quartile (75th Percentile)	-	-	1.23E-255	4.80E-280	6.748994063	0.029090776	0.000114791
LFAOA	Third quartile (75th Percentile)	4.36E-189	-	-	1.19E-269	6.793622776	0.029940686	8.72E-05
CAOA	Semi Interquartile Deviation	-	-	-	-	0.263151006	0.116850018	3.63E-05
RWAOA	Semi Interquartile Deviation	-	-	-	-	0.162915699	0.006138209	4.63E-05

LFAOA	Semi Interquartile Deviation	-	-	-	-	0.252404664	0.005902514	3.71E-05
CAOA	Outliers	0	0	0	0	0	0	1
RWAOA	Outliers	0	0	0	0	0	1	0
LFAOA	Outliers	0	0	0	0	0	3	2
CAOA	Standard Deviation	0	0	0	4.76E-156	0.33626263	0.170991105	5.99E-05
RWAOA	Standard Deviation	0	0	0	0	0.316239072	0.01160521	6.77E-05
LFAOA	Standard Deviation	0	0	0	1.50E-53	0.396009329	0.013393713	6.83E-05

Table 3.10: Quartile result for Uni-modal Test function using CAOA, RWAOA, LFAOA (30 Dim.)

Algorithm	**Function No.**	**F1**	**F2**	**F3**	**F4**	**F5**	**F6**	**F7**
CAOA	No. of trials	30	30	30	30	30	30	30
RWAOA	No. of trials	30	30	30	30	30	30	30
LFAOA	No. of trials	30	30	30	30	30	30	30
CAOA	Minimum value	0	0	0	0	26.157853	5.6247772	2.10E-06
RWAOA	Minimum value	3.37E-167	0	3.08E-134	3.06E-44	27.75720193	2.543626727	7.02E-06
LFAOA	Minimum value	1.61E-160	0	4.09E-119	2.89E-49	27.656336	2.5403941	2.22E-06
CAOA	Maximum value	3.56E-250	0	5.56E-292	0.0429553	28.635206	6.6568209	0.0002293
RWAOA	Maximum value	7.02E-23	0	0.046447471	0.050550972	28.9159301	3.790637167	0.000198774
LFAOA	Maximum value	1.81E-29	0	0.0520213	0.0486136	28.90474	3.7000377	0.0004361
CAOA	Mean Value	1.19E-251	0	1.85E-293	0.0034162	27.52772	6.254627	6.40E-05
RWAOA	Mean Value	2.34E-24	0	0.00631434	0.024650944	28.51794056	3.138059317	6.01E-05
LFAOA	Mean Value	6.02E-31	0	0.0062922	0.0256386	28.457134	3.1746032	6.37E-05
CAOA	Median	0	0	0	3.94E-244	27.503343	6.3107436	3.61E-05
RWAOA	Median	1.30E-96	0	6.44E-27	0.039326409	28.51405718	3.126336842	5.20E-05
LFAOA	Median	3.02E-79	0	5.31E-22	0.0394833	28.471396	3.2477819	5.27E-05
CAOA	First quartile (25th Percentile)	-	-	-	2.36E-299	26.966641	6.0924285	2.82E-05
RWAOA	First quartile (25th Percentile)	2.05E-111	-	1.56E-49	1.87E-17	28.35758635	3.035319259	2.75E-05
LFAOA	First quartile (25th Percentile)	1.53E-104		4.78E-78	2.08E-10	28.312937	2.9433277	1.75E-05
CAOA	Second quartile (50th Percentile)	0	0	0	3.94E-244	27.503343	6.3107436	3.61E-05
RWAOA	Second quartile (50th Percentile)	1.30E-96	0	6.44E-27	0.039326409	28.51405718	3.126336842	5.20E-05

LFAOA	Second quartile (50th Percentile)	3.02E-79	0	5.31E-22	0.0394833	28.471396	3.2477819	5.27E-05
CAOA	Third quartile (75th Percentile)	3.56E-250		5.56E-292	5.02E-109	28.191969	6.421998	8.01E-05
RWAOA	Third quartile (75th Percentile)	2.38E-74	-	0.007093825	0.042709811	28.75447033	3.24357219	8.14E-05
LFAOA	Third quartile (75th Percentile)	6.69E-62	-	0.0107464	0.0423624	28.6821	3.39766	7.77E-05
CAOA	Semi Interquartile Deviation				2.51E-109	0.6126642	0.1647848	2.59E-05
RWAOA	Semi Interquartile Deviation	1.19E-74	-	0.003546913	0.021354905	0.198441989	0.104126465	2.70E-05
LFAOA	Semi Interquartile Deviation	3.35E-62	-	0.0053732	0.0211812	0.1845816	0.2271662	3.01E-05
CAOA	Number of outliers	0	0	0	7	0	0	2
RWAOA	Number of outliers	6	0	4	0	0	1	1
LFAOA	Number of outliers	7	0	1	0	0	0	1
CAOA	Standard Deviation	0	0	0	0.0098857	0.7156909	0.2550962	5.77E-05
RWAOA	Standard Deviation	1.28E-23	0	0.012077442	0.020555671	0.300946654	0.24676702	4.63E-05
LFAOA	Standard Deviation	3.30E-30	0	0.0117352	0.0202212	0.2924578	0.2849396	8.20E-05

Table 3.11: Quartile result for Uni-modal Test function using CAOA, RWAOA, LFAOA (50 Dim.)

Algorithm	**Function No.**	**F1**	**F2**	**F3**	**F4**	**F5**	**F6**	**F7**
CAOA	No. of trials	30	30	30	30	30	30	30
RWAOA	No. of trials	30	30	30	30	30	30	30
LFAOA	No. of trials	30	30	30	30	30	30	30
CAOA	Minimum value	0	0	0	1.07E-262	46.5632892	10.3960173	6.65E-07
RWAOA	Minimum value	3.19E-88	8.25E-276	1.96E-41	0.03168326	48.087664	6.5405702	2.75E-06
LFAOA	Minimum value	1.41E-63	1.50E-257	0.002347	4.13E-06	48.39324	6.454521	8.83E-07
CAOA	Maximum value	0	0	0.01460029	0.1533513	48.6094516	11.7756726	0.00016691
RWAOA	Maximum value	0.00600783	4.72E-178	0.63476879	0.07128094	48.9223434	8.04273391	0.0002506
LFAOA	Maximum value	0.007687	5.20E-177	0.174862	0.069679	48.93971	7.843837	0.000375
CAOA	Mean Value	0	0	0.00048668	0.02489881	47.9003002	11.388912	6.39E-05
RWAOA	Mean Value	0.00046597	1.57E-179	0.09616188	0.04797812	48.6795681	7.22470931	7.14E-05
LFAOA	Mean Value	0.000616	1.70E-178	0.073774	0.048932	48.73295	7.181049	6.22E-05

CAOA	Median	0	0	0	0.00784689	48.0820072	11.4053785	5.86E-05
RWAOA	Median	4.83E-18	2.60E-219	0.04834456	0.04645101	48.7069932	7.24178155	5.93E-05
LFAOA	Median	2.97E-22	1.20E-227	0.068661	0.050245	48.77124	7.234707	4.31E-05
CAOA	First quartile (25th Percentile)				3.08E-188	47.6077703	11.3331184	2.97E-05
RWAOA	First quartile (25th Percentile)	7.18E-33	2.39E-235	0.02647395	0.04261345	48.5710715	7.01788398	2.87E-05
LFAOA	First quartile (25th Percentile)	2.40E-33	8.90E-248	0.042973	0.045284	48.57573	6.916985	2.03E-05
CAOA	Second quartile (50th Percentile)	0	0	0	0.00784689	48.0820072	11.4053785	5.86E-05
RWAOA	Second quartile (50th Percentile)	4.83E-18	2.60E-219	0.04834456	0.04645101	48.7069932	7.24178155	5.93E-05
LFAOA	Second quartile (50th Percentile)	2.97E-22	1.20E-227	0.068661	0.050245	48.77124	7.234707	4.31E-05
CAOA	Third quartile (75th Percentile)			1.37E-248	0.03485824	48.3979928	11.5182459	9.26E-05
RWAOA	Third quartile (75th Percentile)	4.13E-07	1.05E-210	0.1315006	0.05259703	48.8893685	7.44098927	8.06E-05
LFAOA	Third quartile (75th Percentile)	1.61E-13	1.40E-214	0.104216	0.05869	48.90579	7.492536	7.78E-05
CAOA	Semi Interquartile Deviation				0.01742912	0.39511126	0.09256374	3.15E-05
RWAOA	Semi Interquartile Deviation	2.07E-07	5.24E-211	0.05251332	0.00499179	0.15914853	0.21155265	2.59E-05
LFAOA	Semi Interquartile Deviation	8.06E-14	7.20E-215	0.030621	0.006703	0.165032	0.287775	2.87E-05
CAOA	Number of outliers	0	0	0	2	0	1	0
RWAOA	Number of outliers	7	7	2	0	0	0	2
LFAOA	Number of outliers	7	7	0	1	0	0	2
CAOA	Standard Deviation	0	0	0.00266564	0.03922932	0.59515857	0.25611399	4.02E-05
RWAOA	Standard Deviation	0.00133809	0	0.13207551	0.0090887	0.23586674	0.36754288	6.20E-05
LFAOA	Standard Deviation	0.001631	0	0.041409	0.014396	0.183431	0.398565	7.37E-05

Table 3.12: Quartile result for Uni-modal Test function using CAOA, RWAOA, LFAOA (100 Dim.)								
Algorithm	Function No.	F1	F2	F3	F4	F5	F6	F7
CAOA	No. of trials	30	30	30	30	30	30	30
RWAOA	No. of trials	30	30	30	30	30	30	30
LFAOA	No. of trials	30	30	30	30	30	30	30
CAOA	Minimum value	1.41E-63	1.50E-257	0.002347	4.13E-06	48.39324	6.454521	8.83E-07
RWAOA	Minimum value	0.0121654	1.74E-124	0.307839	0.0692717	98.463406	16.561323	1.79E-06
LFAOA	Minimum value	0.0091	2.60E-119	0.325039	0.068598	98.52826	16.69428	1.73E-06
CAOA	Maximum value	0.007687	5.20E-177	0.174862	0.069679	48.93971	7.843837	0.000375
RWAOA	Maximum value	0.0521382	2.97E-54	3.7317433	0.1106532	98.991847	19.193422	0.0004595
LFAOA	Maximum value	0.039748	8.66E-64	2.312983	0.113581	98.98432	19.2827	0.000177
CAOA	Mean Value	0.000616	1.70E-178	0.073774	0.048932	48.73295	7.181049	6.22E-05
RWAOA	Mean Value	0.0274984	9.89E-56	0.8945592	0.0907126	98.871521	18.234201	7.44E-05
LFAOA	Mean Value	0.023725	2.89E-65	0.729194	0.088532	98.86718	18.31291	4.26E-05
CAOA	Median	2.97E-22	1.20E-227	0.068661	0.050245	48.77124	7.234707	4.31E-05
RWAOA	Median	0.0284949	2.40E-89	0.7534552	0.0876543	98.901028	18.321373	5.07E-05
LFAOA	Median	0.024517	3.37E-90	0.54545	0.087608	98.92107	18.45554	2.23E-05
CAOA	First quartile (25th Percentile)	2.40E-33	8.90E-248	0.042973	0.045284	48.57573	6.916985	2.03E-05
RWAOA	First quartile (25th Percentile)	0.0182885	1.01E-100	0.5725357	0.0824328	98.832727	17.973013	1.95E-05
LFAOA	First quartile (25th Percentile)	0.017495	4.24E-98	0.423132	0.082573	98.82575	18.08796	1.12E-05
CAOA	Second quartile (50th Percentile)	2.97E-22	1.20E-227	0.068661	0.050245	48.77124	7.234707	4.31E-05
RWAOA	Second quartile (50th Percentile)	0.0284949	2.40E-89	0.7534552	0.0876543	98.901028	18.321373	5.07E-05
LFAOA	Second quartile (50th Percentile)	0.024517	3.37E-90	0.54545	0.087608	98.92107	18.45554	2.23E-05
CAOA	Third quartile (75th Percentile)	1.61E-13	1.40E-214	0.104216	0.05869	48.90579	7.492536	7.78E-05
RWAOA	Third quartile (75th Percentile)	0.0338811	2.95E-81	0.9319574	0.0976391	98.929056	18.547529	9.58E-05

LFAOA	Third quartile (75th Percentile)	0.028955	1.33E-82	0.999589	0.094731	98.93731	18.67388	8.17E-05
CAOA	Semi Interquartile Deviation	8.06E-14	7.20E-215	0.030621	0.006703	0.165032	0.287775	2.87E-05
RWAOA	Semi Interquartile Deviation	0.0077963	1.47E-81	0.1797109	0.0076032	0.0481644	0.2872577	3.81E-05
LFAOA	Semi Interquartile Deviation	0.00573	6.64E-83	0.288228	0.006079	0.055777	0.292962	3.53E-05
CAOA	Number of outliers	7	7	0	1	0	0	2
RWAOA	Number of outliers	0	6	2	0	1	0	1
LFAOA	Number of outliers	0	7	1	0	0	0	0
CAOA	Standard Deviation	0.001631	0	0.041409	0.014396	0.183431	0.398565	7.37E-05
RWAOA	Standard Deviation	0.0103121	5.42E-55	0.6643912	0.0101075	0.1038102	0.5898947	8.73E-05
LFAOA	Standard Deviation	0.00805	1.58E-64	0.441787	0.009289	0.116504	0.588171	4.35E-05

Table 3.13: Statistical Test result of Unimodal Benchmark Functions for CAOA, RWAOA, LFAOA (10 Dimensions)

Algorithm	CAOA				RWAOA				LFAOA			
Function No.	Wilcoxon rank sum test		T-Test		Wilcoxon rank sum test		T-Test		Wilcoxon rank sum test		T-Test	
	p-rank	h-rank	p-test	t-test	p-rank	h-rank	p-test	t-test	p-rank	h-rank	p-test	t-test
F1	--	0	--	--	-	0	-	-	0.3337107	0	1	0
F2	--	0		--	-	0	-	-		0		
F3	0.3337107	0	1	0	1	0	1	0	0.3337107	0	1	0
F4	0.00424959	1	0	0.32558199	0.90729642	0	0	0.32558199	0.43204406	0	0	0.32558199
F5	3.82E-10	1	1	1.54E-09	0.56922016	0	0	0.569455	0.38709978	0	0	0.41333039
F6	3.02E-11	1	1	1.24E-25	0.31118764	0	0	0.16676545	0.02708632	1	1	0.01973526
F7	0.52978249	0	0	0.6575717	0.73939882	0	0	0.5828317	0.59968948	0	0	0.77104149

Table 3.14: Statistical Test result of Unimodal Benchmark Functions for CAOA, RWAOA, LFAOA (30 Dimensions)

Algorithm	CAOA				RWAOA				LFAOA[98]			
Function No.	Wilcoxon rank sum test		T-Test		Wilcoxon rank sum test		T-Test		Wilcoxon rank sum test		T-Test	
	p-rank	h-rank	p-test	t-test	p-rank	h-rank	p-test	t-test	p-rank	h-rank	p-test	t-test
F1	1.72E-12	1	0	0.325579	0.33285469	0	0	0.32558251	0.06786886	0	0	0.32557885
F2	--	0	--	--	-	0	-	-	-	0	-	-
F3	1.72E-12	1	1	0.006595	0.39526701	0	0	0.52681462	0.68432259	0	0	0.48477225
F4	6.51E-09	1	1	9.94E-07	0.34028847	0	0	0.45666011	0.37903631	0	0	0.54614669
F5	4.80E-07	1	1	3.22E-06	0.23984999	0	0	0.25862192	0.62040372	0	0	0.67067031
F6	3.02E-11	1	1	2.64E-30	0.89999504	0	0	0.82771559	0.44641944	0	0	0.52110848
F7	0.620404	0	0	0.701174	0.50114367	0	0	0.85399422	0.93519197	0	0	0.75962765

Table 3.15: Statistical Test result of Unimodal Benchmark Functions for CAOA, RWAOA, LFAOA (50 Dimensions)

Algorithm	CAOA				RWAOA				LFAOA			
Function No.	Wilcoxon rank sum test		T-Test		Wilcoxon rank sum test		T-Test		Wilcoxon rank sum test		T-Test	
	p-rank	h-rank	p-test	t-test	p-rank	h-rank	p-test	t-test	p-rank	h-rank	p-test	t-test
F1	1.21E-12	1	0	0.0539346	0.02708632	1	0	0.34736231	0.06786886	0	0	0.23038971
F2	1.21E-12	1	0	0.32558199	0.20620549	0	0	0.32558199	0.84180145	0	0	0.32558199
F3	1.51E-11	1	1	0.00013613	0.51059794	0	0	0.82009535	0.98230705	0	0	0.24554218
F4	4.12E-06	1	1	0.00165309	0.42038633	0	0	0.24810654	0.80727495	0	0	0.53404955
F5	1.69E-09	1	1	1.57E-07	0.94695594	0	0	0.80588987	0.30417682	0	0	0.48456687
F6	3.02E-11	1	1	8.82E-30	0.79584554	0	0	0.72890589	0.59968948	0	0	0.47381165
F7	0.12967023	0	0	0.06122919	0.27070534	0	0	0.17722485	0.040595	1	0	0.15154438

Table 3.16: Statistical Test result of Unimodal Benchmark Functions for CAOA, RWAOA, LFAOA (100 Dimensions)

Algorithm	CAOA				RWAOA				LFAOA			
Function No.	Wilcoxon rank sum test		T-Test		Wilcoxon rank sum test		T-Test		Wilcoxon rank sum test		T-Test	
	p-rank	h-rank	p-test	t-test	p-rank	h-rank	p-test	t-test	p-rank	h-rank	p-test	t-test
F1	5.49E-11	1	1	8.92E-12	0.2225729	0	0	0.16666146	0.63087629	0	0	0.81708626
F2	1.21E-12	1	0	0.32556084	0.86499371	0	0	0.3940845	0.78445977	0	0	0.32556084
F3	3.02E-11	1	1	1.93E-07	0.68432259	0	0	0.72805608	0.37107703	0	0	0.15629828
F4	2.15E-06	1	1	6.89E-07	0.51059794	0	0	0.41224113	0.14127751	0	0	0.07345329
F5	4.62E-10	1	1	2.78E-08	0.36322231	0	0	0.63318939	0.85338174	0	0	0.58682251
F6	3.02E-11	1	1	5.36E-32	0.65204362	0	0	0.89475981	0.30417682	0	0	0.54989648
F7	0.91170898	0	0	0.70010743	0.05368525	0	0	0.09922052	0.00058737	1	1	0.00143501

Table 3.17: Simulation Time for Uni-Model Benchmark Function using CAOA, RWAOA, LFAOA (10 Dimensions)

Function No.	CAOA	RWAOA	LFAOA	CAOA	RWAOA	LFAOA	CAOA	RWAOA	LFAOA
	Best Time (Sec)	Best Time (Sec)	Best Time (Sec)	Avg. Time (Sec.)	Avg. Time (Sec.)	Avg. Time (Sec.)	Worst Time (Sec)	Worst Time (Sec)	Worst Time (Sec)
F1	0.03125	0.125	0.03125	0.066666667	0.179166667	0.078125	0.265625	0.578125	0.25
F2	0.03125	0.125	0.03125	0.066145833	0.182291667	0.077604167	0.28125	0.53125	0.34375
F3	0.0625	0.15625	0.0625	0.093229167	0.186979167	0.094270833	0.15625	0.25	0.171875
F4	0.03125	0.109375	0.03125	0.059895833	0.1671875	0.065104167	0.125	0.3125	0.140625
F5	0.046875	0.140625	0.046875	0.074479167	0.163020833	0.08125	0.140625	0.21875	0.140625
F6	0.03125	0.125	0.03125	0.0578125	0.152604167	0.061979167	0.140625	0.203125	0.09375
F7	0.0625	0.140625	0.0625	0.0796875	0.1703125	0.084895833	0.109375	0.25	0.125

Table 3.18: Simulation Time for Uni-Model Benchmark Function using CAOA, RWAOA, LFAOA (30 Dimensions)

Function No.	CAOA	RWAOA	LFAOA	CAOA	RWAOA	LFAOA	CAOA	RWAOA	LFAOA
	Best Time (Sec)	Best Time (Sec)	Best Time (Sec)	Avg. Time (Sec.)	Avg. Time (Sec.)	Avg. Time (Sec.)	Worst Time (Sec)	Worst Time (Sec)	Worst Time (Sec)
F1	0.046875	0.375	0.046875	0.105208333	0.659375	0.102083333	0.25	1.296875	0.328125
F2	0.046875	0.390625	0.0625	0.09375	0.6078125	0.104166667	0.296875	1.546875	0.3125
F3	0.171875	0.546875	0.171875	0.191145833	0.6921875	0.197395833	0.234375	0.890625	0.234375
F4	0.046875	0.3125	0.0625	0.077604167	0.565104167	0.089583333	0.109375	0.9375	0.1875
F5	0.0625	0.328125	0.0625	0.080208333	0.576041667	0.080729167	0.109375	0.8125	0.109375
F6	0.046875	0.34375	0.0625	0.063020833	0.580729167	0.071875	0.078125	1.015625	0.109375
F7	0.109375	0.359375	0.109375	0.124479167	0.585416667	0.1296875	0.140625	0.796875	0.171875

Table 3.19: Simulation Time for Uni-Model Benchmark Function using CAOA, RWAOA, LFAOA (50 Dimensions)									
Function No.	**CAOA**	**RWAOA**	**LFAOA**	**CAOA**	**RWAOA**	**LFAOA**	**CAOA**	**RWAOA**	**LFAOA**
	Best Time (Sec)	**Best Time (Sec)**	**Best Time (Sec)**	**Avg. Time (Sec.)**	**Avg. Time (Sec.)**	**Avg. Time (Sec.)**	**Worst Time (Sec)**	**Worst Time (Sec)**	**Worst Time (Sec)**
F1	0.078125	0.359375	0.078125	0.1421875	0.384375	0.141666667	0.5	0.421875	0.421875
F2	0.078125	0.453125	0.078125	0.130729167	0.765625	0.125	0.421875	1.25	0.375
F3	0.28125	0.71875	0.28125	0.307291667	0.895833333	0.327604167	0.375	1.125	0.859375
F4	0.078125	0.515625	0.078125	0.102604167	0.684375	0.1125	0.203125	1.078125	0.1875
F5	0.09375	0.5	0.09375	0.109375	0.748958333	0.114583333	0.140625	1.015625	0.15625
F6	0.078125	0.4375	0.078125	0.0984375	0.6859375	0.099479167	0.15625	0.90625	0.171875
F7	0.171875	0.578125	0.171875	0.201041667	0.810416667	0.208854167	0.21875	1.015625	0.3125

Table 3.20: Simulation Time for Uni-Model Benchmark Function using CAOA, RWAOA, LFAOA (100 Dimensions)									
Function No.	**CAOA**	**RWAOA**	**LFAOA**	**CAOA**	**RWAOA**	**LFAOA**	**CAOA**	**RWAOA**	**LFAOA**
	Best Time (Sec)	**Best Time (Sec)**	**Best Time (Sec)**	**Avg. Time (Sec.)**	**Avg. Time (Sec.)**	**Avg. Time (Sec.)**	**Worst Time (Sec)**	**Worst Time (Sec)**	**Worst Time (Sec)**
F1	0.125	0.734375	0.140625	0.200520833	1.095833333	0.222395833	0.546875	2.09375	0.90625
F2	0.140625	0.75	0.140625	0.209375	1.09375	0.2015625	0.765625	1.671875	0.5625
F3	0.5625	1.234375	0.59375	0.653645833	1.505208333	0.65625	0.984375	1.859375	0.875
F4	0.125	0.71875	0.140625	0.151041667	0.9640625	0.157291667	0.234375	1.34375	0.203125
F5	0.140625	0.703125	0.140625	0.173958333	0.993229167	0.172395833	0.328125	1.375	0.359375
F6	0.125	0.828125	0.125	0.147916667	0.969270833	0.161458333	0.1875	1.21875	0.265625
F7	0.3125	0.828125	0.328125	0.332291667	1.180729167	0.343229167	0.5	1.75	0.375

Table 3.21 Comparison of Uni-modal test functions of CAOA, RWAOA, LFAOA[98]

Algorithms	Parameter	Uni-modal Test Functions 30 Dimensions						
		F_1	F_2	F_3	F_4	F_5	F_6	F_7
GA[98]	Ave	01.03E+003	02.47E+001	02.65E+004	05.17E+001	01.95E+004	09.01E+002	01.91E-01
	Std.	05.79E+002	05.68E+000	03.44E+003	01.05E+001	01.31E+004	02.84E+002	01.50E-01
PSO[116]	Ave	01.83E+004	03.58E+002	04.05E+004	04.39E+001	01.96E+007	01.87E+004	01.07E+01
	Std.	03.01E+003	01.35E+003	08.21E+003	03.64E+000	06.25E+006	02.92E+003	03.05E+00
BBO[116]	Ave	07.59E+001	01.36E-003	01.21E+004	03.02E+001	01.82E+003	06.71E+001	02.91E-03
	Std.	02.75E+001	07.45E-003	02.69E+003	04.39E+000	09.40E+002	02.20E+01	01.83E-03
FPA[98]	Ave	02.01E+013	03.22E+001	01.41E+003	02.38E+001	03.17E+005	01.70E+003	03.44E-01
	Std.	05.60E+002	05.55E+000	05.59E+002	02.77E+000	01.75E+005	03.13E+002	01.10E-01
GWO[81]	Ave	01.18E-027	09.71E-017	05.12E-005	01.24E-006	02.70E+001	08.44E-001	01.70E-03
	Std.	01.47E-027	05.60E-017	02.03E-004	01.94E-006	07.78E-001	03.18E-001	01.06E-03
BAT[98]	Ave	06.59E+004	02.71E+008	01.38E+005	08.51E+001	02.10E+008	06.69E+004	04.57E+01
	Std.	07.51E+003	01.30E+009	04.72E+004	02.95E+000	04.17E+007	05.87E+003	07.82E+00
FA [116]	Ave	07.11E-003	04.34E-001	01.66E+003	01.11E-001	07.97E+001	06.94E-003	06.62E-02
	Std.	03.21E-003	01.84E-001	06.72E+002	04.75E-002	07.39E+001	03.61E-003	04.23E-02
CS [117]	Ave	09.06E-004	01.49E-001	02.10E-001	09.65E-002	02.76E+001	03.13E-003	07.29E-02
	Std.	04.55E-004	02.79E-002	05.69E-002	01.94E-002	04.51E-001	01.30E-003	02.21E-02
MFO [83]	Ave	01.01E+003	03.19E+001	02.34E+004	07.00E+001	07.35E+003	02.68E+003	04.50E+00
	Std.	03.05E+003	02.06E+001	01.41E+004	07.06E+000	02.26E+004	05.84E+003	09.21E+00
GSA [118]	Ave	06.08E+002	02.27E+001	01.35E+005	07.87E+001	07.41E+002	03.08E+003	01.12E-01
	Std.	04.64E+002	03.36E+00	04.86E+004	02.81E+000	07.81E+002	08.98E+002	03.76E-02
DE [119]	Ave	01.33E-003	06.83E-003	03.97E+004	01.15E+001	01.06E+002	01.44E-003	05.24E-02
	Std.	05.92E-004	02.06E-003	05.37E+003	02.37E+000	01.01E+002	05.38E-004	01.37E-02
AOA[2]	Ave	06.67E-007	00.00E+000	06.87E-006	01.40E-003	02.49E+001	03.47E-004	03.92E-06
	Std.	07.45E-007	00.00E+000	06.87E-006	01.90E-003	03.64E-001	03.47E-004	03.92E-06
CAOA	**Ave**	**1.19E-251**	**0**	**1.85E-293**	**0.0034162**	**27.52772**	**6.254627**	**6.40E-05**
	Std.	**0**	**0**	**0**	**0.0098857**	**0.7156909**	**0.2550962**	**5.77E-05**
RWAOA	**Ave**	**2.34E-24**	**0**	**0.0063143**	**0.0246509**	**28.517941**	**3.1380593**	**6.01E-05**
	Std.	**1.28E-23**	**0**	**0.0120774**	**0.0205557**	**0.3009467**	**0.246767**	**4.63E-05**
LAOA	**Ave**	**6.02E-31**	**0**	**0.00629218**	**0.02563863**	**28.4571341**	**3.17460324**	**6.37E-05**
	Std.	**3.30E-30**	**0**	**0.01173523**	**0.02022121**	**0.29245785**	**0.28493956**	**8.20E-05**

.

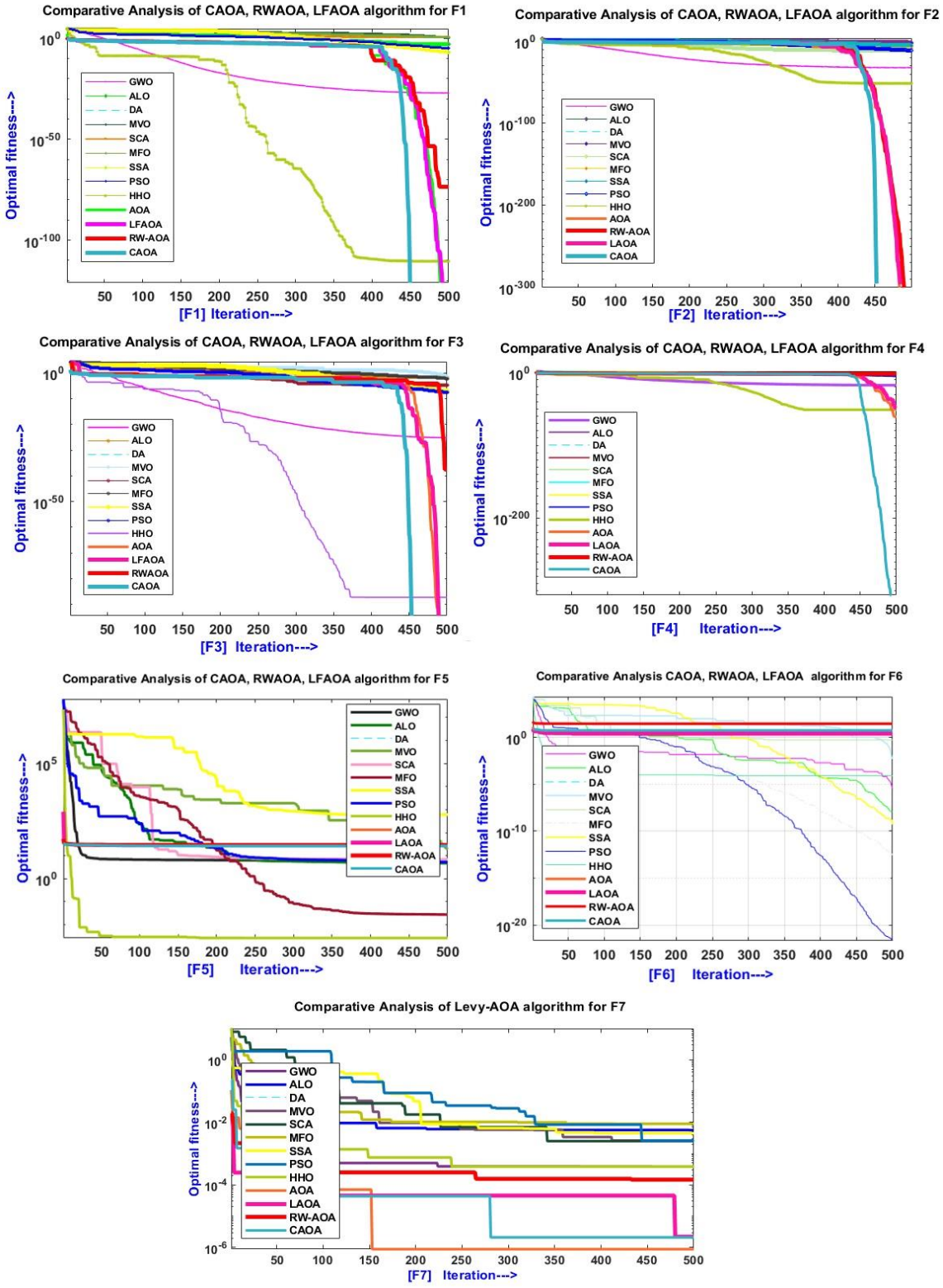

Figure 3.26 Comparison convergence curve for Uni-modal Benchmark Functions (F1-F7)

3.10.2 Testing of Multi-modal Benchmark Functions

The multi-modal Benchmark Functions (F8 to F13) were used to test the effectiveness of the CAOA, RWAOA, and Levy Flight Arithmetic Optimization Algorithm. The experiments were conducted for 10, 30, 50, and 100 dimensions, with 30 trial runs and 500 iterations. **Tables 3.23 to 3.25** display the results of the multi-modal test functions for each dimension. To evaluate the usefulness of the solutions, the Wilcoxon sum test and statistical T-test results were computed. The quartile results of CAOA, RWAOA, and LFAOA for multi-modal benchmark functions are presented in **Tables 3.26 to 3.29** for 10, 30, 50, and 100 dimensions. **Tables 3.30 to 3.33** display the results of the Wilcoxon sum test and statistical T-test for CAOA, RWAOA, and LFAOA for each dimension. Additionally, **Tables 3.34 to 3.37** show the simulation time required for the Multi-Model Benchmark Function using CAOA, RWAOA, and LFAOA for each dimension.

To compare the effectiveness of the Chaotic, Random Walk, and Levy Flight Arithmetic Optimization Algorithm with other known meta-heuristics search algorithms such as Genetic Algorithm, PSO, BBO, FPA, GWO, BAT, FA, CS, MFO, GSA, DE, and AOA, the comparison results for the multi-modal benchmark function are presented in **Table 3.38** in terms of standard deviation and average time for 10, 30, 50, and 100 dimensions. Finally, the comparison convergence curve of CAOA, RWAOA, and LFAOA for the multi-modal benchmark function has been depicted in **Figure 3.27**. The test results reveal the effectiveness of this algorithm in achieving increased convergence for multi-modal optimization problems.

Table 3.22: Test result of Multi-modal Benchmark Function for Objective fitness functions for CAOA, RWAOA, LFAOA (10 Dimensions)

Function No.	CAOA	RWAOA	LFAOA	CAOA	RWAOA	LFAOA	CAOA	RWAOA	LFAOA	CAOA	RWAOA	LFAOA	CAOA	RWAOA	LFAOA	CAOA	RWAOA	LFAOA
	Index	Index	Index	Mean	Mean	Mean	Std.	Std.	Std.	Best	Best	Best	Worst	Worst	Worst	Median	Median	Median
F8	24	20	23	-1734.371	-2811.486	-2850.43	197.7648	274.7437	257.1771	-2219.434	-3264.289	-3367.355	-1201.366	-2171.013	-2372.641	-1743.461	-2839.639	-2859.361
F9	1	1	1	0	0	0	0	0	0	0	0	0	0	0	0	0	0	0
F10	1	1	1	8.87E-16	8.87E-16	8.87E-16	0	0	0	8.87E-16	8.87E-16	8.87E-16	8.87E-16	8.87E-16	8.87E-16	8.87E-16	8.87E-16	8.87E-16
F11	1	1	1	0	2.67E-10	3.71E-12	0	1.46E-09	2.03E-11	0	0	0	0	8.02E-09	1.11E-10	0	0	0
F12	3	28	1	0.558022	0.027092	0.027692	0.078817	0.008617	0.006921	0.388923	0.012956	0.016178	0.683227	0.046773	0.04437	0.57854	0.024566	0.027934
F13	15	15	14	0.89792	0.872596	0.860297	0.086376	0.107949	0.128551	0.698127	0.588627	0.549517	0.998363	0.995354	0.995658	0.893131	0.894699	0.884453

Table 3.23: Test Result of Multi-Modal Benchmark Function for Objective Fitness Functions for CAOA, RWAOA, LFAOA (30 Dimensions)

Function No.	CAOA	RWAOA	LFAOA	CAOA	RWAOA	LFAOA	CAOA	RWAOA	LFAOA	CAOA	RWAOA	LFAOA	CAOA	RWAOA	LFAOA	CAOA	RWAOA	LFAOA
	Index	Index	Index	Mean	Mean	Mean	Std.	Std.	Std.	Best	Best	Best	Worst	Worst	Worst	Median	Median	Median
F8	21	19	8	-2849.658	-5221.357	-5121.334	360.2603	380.7035	443.8498	-3593.412	-6034.022	-6437.323	-2083.7	-4566.286	-4317.872	-2858.494	-5166.625	-5090.45
F9	1	1	1	0	0	0	0	0	0	0	0	0	0	0	0	0	0	0
F10	1	1	1	8.87E-16	8.87E-16	8.87E-16	0	0	0	8.87E-16	8.87E-16	8.87E-16	8.87E-16	8.87E-16	8.87E-16	8.87E-16	8.87E-16	8.87E-16
F11	3	28	22	3.29E-07	0.1957	0.189366	1.67E-06	0.152275	0.137668	0	0.003887	0.01795	9.13E-06	0.522348	0.472264	0	0.140521	0.171467
F12	28	4	25	1.020885	0.522437	0.510007	0.029816	0.043487	0.043297	0.938339	0.427404	0.421172	1.090108	0.599395	0.592129	1.022028	0.51899	0.513492
F13	20	7	18	2.875993	2.838214	2.830882	0.076801	0.080463	0.091525	2.7413	2.707066	2.557182	2.991007	2.943452	2.996984	2.88307	2.848733	2.830613

Table 3.24: Test result of Multi-modal Benchmark Function for Objective fitness functions for CAOA, RWAOA, LFAOA (50 Dimensions)

Function No.	CAOA	RWAOA	LFAOA	CAOA	RWAOA	LFAOA	CAOA	RWAOA	LFAOA	CAOA	RWAOA	LFAOA	CAOA	RWAOA	LFAOA	CAOA	RWAOA	LFAOA
	Index	Index	Index	Mean	Mean	Mean	Std.	Std.	Std.	Best	Best	Best	Worst	Worst	Worst	Median	Median	Median
F8	8	10	19	-3673.392	-6814.26	-6972.898	560.4298	447.1978	432.7812	-4829.409	-7513.611	-7778.371	-2717.921	-6001.204	-5883.546	-3624.218	-6752.302	-7012.487
F9	1	1	1	0	0	0	0	0	0	0	0	0	0	0	0	0	0	0
F10	01	01	01	8.87E-16	8.87E-16	8.87E-16	0	0	0	8.87E-16	8.87E-16	8.87E-16	8.87E-16	8.87E-16	8.87E-16	8.87E-16	8.87E-16	8.87E-16
F11	23	19	3	0.017977	1.353511	1.287844	0.03171	1.491352	0.614718	0.000297	0.596256	0.465704	0.096788	8.884027	3.481201	0.001482	1.047028	1.075953
F12	12	4	8	1.10786	0.719726	0.730831	0.02658	0.031246	0.027107	1.06946	0.660472	0.667205	1.183918	0.789094	0.778194	1.105037	0.717573	0.737038
F13	19	21	16	4.916112	4.878615	4.861873	0.059616	0.096027	0.103893	4.776627	4.610043	4.66393	4.991623	4.99654	5.010965	4.918261	4.900088	4.874001

Table 3.25: Test result of Multi-modal Benchmark Function for Objective fitness functions for CAOA, RWAOA, LFAOA (100 Dimensions)

Function No.	CAOA	RWAOA	LFAOA	CAOA	RWAOA	LFAOA	CAOA	RWAOA	LFAOA	CAOA	RWAOA	LFAOA	CAOA	RWAOA	LFAOA	CAOA	RWAOA	LFAOA
	Index	Index	Index	Mean	Mean	Mean	Std.	Std.	Std.	Best	Best	Best	Worst	Worst	Worst	Median	Median	Median
F8	2	20	2	-5507.669	-9778.683	-9946.689	991.0596	853.1979	767.3219	-7235.421	-11646.91	-11259.57	-3238.41	-7776.608	-8075.022	-5613.767	-9805.79	-9959.651
F9	1	1	1	0	0	0	0	0	0	0	0	0	0	0	0	0	0	0
F10	1	1	1	8.88E-16	0.000239	0.000672	0	0.000618	0.001103	8.88E-16	8.88E-16	8.88E-16	8.88E-16	0.002316	0.003568	8.88E-16	8.88E-16	8.88E-16
F11	4	27	21	0.043708	587.5424	596.3999	0.049159	142.801	181.4274	0.008311	363.5091	232.8222	0.185092	1039.195	927.7727	0.022903	591.5407	589.2233
F12	9	24	13	1.190578	0.912288	0.903276	0.027934	0.021449	0.021584	1.152306	0.865221	0.857602	1.262264	0.946007	0.94594	1.186953	0.913563	0.904086
F13	14	10	8	9.964364	9.958024	9.956183	0.035624	0.055109	0.067823	9.854697	9.845558	9.698846	9.997424	10.04573	10.02458	9.976775	9.958422	9.968506

Table 3.26: Quartile Result Analysis of Multi-modal Test Function using CAOA, RWAOA, and LFAOA (10 Dim.)							
Algorithm	**Function No.**	**F_8**	**F_9**	**F_{10}**	**F_{11}**	**F_{12}**	**F_{13}**
CAOA	No. of trials	30	30	30	30	30	30
RWAOA	No. of trials	30	30	30	30	30	30
LFAOA	No. of trials	30	30	30	30	30	30
CAOA	Minimum value	-2219.434266	0	8.88E-16	0	0.388923203	0.698126757
RWAOA	Minimum value	-3264.288881	0	8.88E-16	0	0.012956406	0.58862712
LFAOA	Minimum value	-3367.355	0	8.88E-16	0	0.0161779	0.5495171
CAOA	Maximum value	-1201.366077	0	8.88E-16	0	0.68322718	0.99836257
RWAOA	Maximum value	-2171.013295	0	8.88E-16	8.02E-09	0.046772505	0.995353601
LFAOA	Maximum value	-2372.641	0	8.88E-16	1.11E-10	0.0443696	0.9956581
CAOA	Mean Value	-1734.371154	0	8.88E-16	0	0.558022136	0.897920339
RWAOA	Mean Value	-2811.485542	0	8.88E-16	2.67E-10	0.027091725	0.872595987
LFAOA	Mean Value	-2850.43	0	8.88E-16	3.71E-12	0.0276916	0.8602966
CAOA	Median	-1743.460653	0	8.88E-16	0	0.578540097	0.893130673
RWAOA	Median	-2859.361	0	8.88E-16	0	0.0279343	0.8844531
LFAOA	Median	-2859.361	0	8.88E-16	0	0.0279343	0.8844531
CAOA	First quartile (25th Percentile)	-1829.313205	-	-	-	0.481474913	0.84681472
RWAOA	First quartile (25th Percentile)	-2999.587241	-	-	-	0.020816802	0.811703252
LFAOA	First quartile (25th Percentile)	-3031.732	-	-	-	0.0212042	0.844347
CAOA	Second quartile (50th Percentile)	-1743.460653	0	8.88E-16	0	0.578540097	0.893130673
RWAOA	Second quartile (50th Percentile)	-2839.638644	0	8.88E-16	0	0.024566396	0.89469937
LFAOA	Second quartile (50th Percentile)	-2859.361	0	8.88E-16	0	0.0279343	0.8844531
CAOA	Third quartile (75th Percentile)	-1593.231132	-	-	-	0.612410424	0.993860858
RWAOA	Third quartile (75th Percentile)	-2628.887709	-	-	2.08E-13	0.033909005	0.939219297
LFAOA	Third quartile (75th Percentile)	-2727.692	-	-	5.57E-11	0.0320797	0.939061
CAOA	Semi Interquartile Deviation	118.0410366	-	-	-	0.065467755	0.073523069
RWAOA	Semi Interquartile Deviation	185.3497658	-	-	-	0.006546101	0.063758023
LFAOA	Semi Interquartile Deviation	152.01969	-	-	-	0.0054377	0.047357
CAOA	Number of Outliers	00	00	00	00	00	00
RWAOA	Number of Outliers	00	00	00	00	00	00
LFAOA	Number of Outliers	00	00	00	00	00	1
CAOA	Standard Deviation	197.7647741	0	0	0	0.078816737	0.086376323
RWAOA	Standard Deviation	274.7436983	0	0	1.46E-09	0.008617397	0.107948562
LFAOA	Standard Deviation	257.17713	0	0	2.03E-11	0.0069211	0.1285511

Table 3.27: Quartile Result Analysis of Multi-modal Test Function using CAOA, RWAOA, and LFAOA (30 Dim.)							
Algorithm	**Function No.**	**F8**	**F9**	**F10**	**F11**	**F12**	**F13**
CAOA	No. of trials	30	30	30	30	30	30
RWAOA	No. of trials	30	30	30	30	30	30
LFAOA	No. of trials	30	30	30	30	30	30
CAOA	Minimum value	-3593.412076	0	8.88E-16	0	0.938338679	2.741299917
RWAOA	Minimum value	-6034.02246	0	8.88E-16	0.00388669	0.427403646	2.707065643
LFAOA	Minimum value	-6437.32	0	8.88E-16	0.01795	0.421172	2.557182
CAOA	Maximum value	-2083.699764	0	8.88E-16	9.13E-06	1.090107592	2.991007434
RWAOA	Maximum value	-4566.285991	0	8.88E-16	0.522348465	0.599395034	2.943452241
LFAOA	Maximum value	-4317.87	0	8.88E-16	0.472264	0.592129	2.996984
CAOA	Mean Value	-2849.657583	0	8.88E-16	3.29E-07	1.020885349	2.875993176
RWAOA	Mean Value	-5221.357188	0	8.88E-16	0.195699936	0.522437122	2.838214169
LFAOA	Mean Value	-5121.33	0	8.88E-16	0.189366	0.510007	2.830882
CAOA	Median	-2858.49437	0	8.88E-16	0	1.022028138	2.883070367
RWAOA	Median	-5166.624983	0	8.88E-16	0.140520813	0.51899007	2.848732517
LFAOA	Median	-5090.45	0	8.88E-16	0.171467	0.513492	2.830613
CAOA	First quartile (25th Percentile)	-3084.762078				1.009067744	2.812129798
RWAOA	First quartile (25th Percentile)	-5583.795956	-	-	0.076224261	0.505619956	2.754939109
LFAOA	First quartile (25th Percentile)	-5346.52	-	-	0.066652	0.47345	2.782429
CAOA	Second quartile (50th Percentile)	-2858.49437	0	8.88E-16	0	1.022028138	2.883070367
RWAOA	Second quartile (50th Percentile)	-5166.624983	0	8.88E-16	0.140520813	0.51899007	2.848732517
LFAOA	Second quartile (50th Percentile)	-5090.45	0	8.88E-16	0.171467	0.513492	2.830613
CAOA	Third quartile (75th Percentile)	-2599.482065			5.99E-11	1.03475506	2.945839676
RWAOA	Third quartile (75th Percentile)	-4945.909681	-	-	0.291778	0.540634531	2.898541231
LFAOA	Third quartile (75th Percentile)	-4827.89	-	-	0.256276	0.538682	2.886724
CAOA	Semi Interquartile Deviation	242.6400066	-	-	-	00.012843658	00.066854939
RWAOA	Semi Inter-quartile Deviation	318.9431372	-	-	00.107776869	00.017507287	00.071801061
LFAOA	Semi Inter-quartile Deviation	259.312	-	-	00.094812	00.032616	00.052147
CAOA	Number of outliers	00	00	00	00	01	00
RWAOA	Number of outliers	00	00	00	00	00	00
LFAOA	Number of outliers	00	00	00	00	00	00
CAOA	Standard Deviation	360.2603018	0	0	1.67E-06	0.029816289	0.076801279
RWAOA	Standard Deviation	380.7035328	0	0	0.152275141	0.0434873	0.080463123
LFAOA	Standard Deviation	443.8498	0	0	0.137668	0.043297	0.091525

Table 3.28: Quartile Result Analysis of Multi-modal Test Function using CAOA, RWAOA, and LFAOA in (50 Dim.)							
Algorithm	**Function No.**	**F8**	**F9**	**F10**	**F11**	**F12**	**F13**
CAOA	No. of trials	30	30	30	30	30	30
RWAOA	No. of trials	30	30	30	30	30	30
LFAOA	No. of trials	30	30	30	30	30	30
CAOA	Minimum value	-4829.40869	0	8.88E-16	0.000297244	1.069459927	4.776626719
RWAOA	Minimum value	-7513.61126	0	8.88E-16	0.596255717	0.6604717	4.610043011
LFAOA	Minimum value	-11259.6	0	8.88E-16	232.8222	0.857602	9.698846
CAOA	Maximum value	-2717.92146	0	8.88E-16	0.096787541	1.183918338	4.991623306
RWAOA	Maximum value	-6001.2037	0	8.88E-16	8.884027107	0.789094439	4.996539772
LFAOA	Maximum value	-8075.02	0	0.003568	927.7727	0.94594	10.02458
CAOA	Mean Value	-3673.39243	0	8.88E-16	0.017977437	1.107860127	4.916112368
RWAOA	Mean Value	-6814.25972	0	8.88E-16	1.353511185	0.719726068	4.878614894
LFAOA	Mean Value	-9946.69	0	0.000672	596.3999	0.903276	9.956183
CAOA	Median	-3624.21848	0	8.88E-16	0.00148244	1.105036718	4.918261253
RWAOA	Median	-6752.30234	0	8.88E-16	1.047028119	0.717573311	4.900088356
LFAOA	Median	-9959.65	0	8.88E-16	589.2233	0.904086	9.968506
CAOA	First quartile (25th Percentile)	-4049.06415	-	-	0.000742225	1.091453763	4.867164504
RWAOA	First quartile (25th Percentile)	-7235.15301	-	-	0.921475568	0.695279599	4.849090592
LFAOA	First quartile (25th Percentile)	-10554.4	-	0	500.0965	0.887647	9.927189
CAOA	Second quartile (50th Percentile)	-3624.21848	0	8.88E-16	0.00148244	1.105036718	4.918261253
RWAOA	Second quartile (50th Percentile)	-6752.30234	0	8.88E-16	1.047028119	0.717573311	4.900088356
LFAOA	Second quartile (50th Percentile)	-9959.65	0	8.88E-16	589.2233	0.904086	9.968506
CAOA	Third quartile (75th Percentile)	-3150.46951	-	-	0.004947676	1.122971163	4.977279926
RWAOA	Third quartile (75th Percentile)	-6446.94541	-	-	1.15443814	0.74244727	4.943754237
LFAOA	Third quartile (75th Percentile)	-9626.94	-	0.002077	744.2696	0.917979	10.00467
CAOA	Semi Interquartile Deviation	449.2973226	-	-	0.002102725	0.0157587	0.055057711
RWAOA	Semi Interquartile Deviation	394.1037984	-	-	0.116481286	0.023583835	0.047331822
LFAOA	Semi Interquartile Deviation	463.7405	-	-	122.0865	0.015166	0.038743
CAOA	Number of outliers	00	00	00	07	00	00
RWAOA	Number of outliers	00	00	00	02	00	00
LFAOA	Number of outliers	00	00	00	00	00	00
CAOA	Standard Deviation	560.4298463	0	0	0.031709698	0.02657997	0.059616328
RWAOA	Standard Deviation	447.1978123	0	0	1.491352366	0.031246413	0.096026811
LFAOA	Standard Deviation	767.3219	0	0.001103	181.4274	0.021584	0.067823

Table 3.29: Quartile Result Analysis of Multi-modal Test Function using CAOA, RWAOA, and LFAOA (100 Dim.)							
Algorithm	**Function No.**	**F8**	**F9**	**F10**	**F11**	**F12**	**F13**
CAOA	No. of trials	30	30	30	30	30	30
RWAOA	No. of trials	30	30	30	30	30	30
LFAOA	No. of trials	30	30	30	30	30	30
CAOA	Minimum value	-7235.42068	0	8.88E-16	0.008310858	1.152306078	9.854696623
RWAOA	Minimum value	-11646.90928	0	8.88E-16	363.5090905	0.865220863	9.845558027
LFAOA	Minimum value	-11259.6	0	8.88E-16	232.8222	0.857602	9.698846
CAOA	Maximum value	-3238.409742	0	8.88E-16	0.185091748	1.262264274	9.997423615
RWAOA	Maximum value	-7776.608079	0	0.002316303	1039.195059	0.946006909	10.04572924
LFAOA	Maximum value	-8075.02	0	0.003568	927.7727	0.94594	10.02458
CAOA	Mean Value	-5507.668919	0	8.88E-16	0.04370755	1.190577588	9.964364131
RWAOA	Mean Value	-9778.682679	0	0.0002389	587.5424145	0.912287866	9.958023754
LFAOA	Mean Value	-9946.69	0	0.000672	596.3999	0.903276	9.956183
CAOA	Median	-5613.767026	0	8.88E-16	0.022902793	1.186952981	9.976775158
RWAOA	Median	-9805.789752	0	8.88E-16	591.5407049	0.913563378	9.958421759
LFAOA	Median	-9959.65	0	8.88E-16	589.2233	0.904086	9.968506
CAOA	First quartile (25th Percentile)	-6321.503466			0.016004166	1.16940323	9.971514811
RWAOA	First quartile (25th Percentile)	-10577.44282	-	-	468.106047	0.899219	9.919350749
LFAOA	First quartile (25th Percentile)	-10554.4	-	0	500.0965	0.887647	9.927189
CAOA	Second quartile (50th Percentile)	-5613.767026	0	8.88E-16	0.022902793	1.186952981	9.976775158
RWAOA	Second quartile (50th Percentile)	-9805.789752	0	8.88E-16	591.5407049	0.913563378	9.958421759
LFAOA	Second quartile (50th Percentile)	-9959.65	0	8.88E-16	589.2233	0.904086	9.968506
CAOA	Third quartile (75th Percentile)	-4737.399221			0.029928147	1.208722749	9.980499053
RWAOA	Third quartile (75th Percentile)	-9243.80493	-	2.76E-06	637.6100347	0.932562629	10.00662979
LFAOA	Third quartile (75th Percentile)	-9626.94	-	0.002077	744.2696	0.917979	10.00467
CAOA	Semi Interquartile Deviation	792.0521223			0.006961991	0.019659759	0.004492121
RWAOA	Semi Interquartile Deviation	666.8189425	-	-	84.75199386	0.016671814	0.043639522
LFAOA	Semi Interquartile Deviation	463.7405	-	-	122.0865	0.015166	0.038743
CAOA	Number of Outliers	00	00	00	06	00	05
RWAOA	Number of Outliers	00	00	00	01	00	00
LFAOA	Number of Outliers	00	00	00	00	00	00
CAOA	Standard Deviation	991.0595792	0	00	0.049158533	0.02793436	0.035623834
RWAOA	Standard Deviation	853.1978684	0	0.000617669	142.8010313	0.021448581	0.055108734
LFAOA	Standard Deviation	767.3219	0	0.001103	181.4274	0.021584	0.067823

Table 3.30: Statistical Test result of Multi-modal Benchmark Functions for CAOA, RWAOA, LFAOA (10 Dimensions)

Algorithm	CAOA				RWAOA				LFAOA			
Function No.	Wilcoxon rank sum test		T-Test		Wilcoxon rank sum test		T-Test		Wilcoxon rank sum test		T-Test	
	p-rank	h-rank	p-test	t-test	p—test	h—test	p—test	t--test	p—test	h—test	p-test	t--test
F08	3.02E-11	01	01	2.95E-21	0.66273476	0	0	0.45963469	0.97051605	0	00	0.9132262
F09	-	00	-	-	-	00	-	-	-	00	-	-
F10	-	00	-	-	-	00	-	-	-	00	-	-
F11	00.16080212	00	00	0.32557393	0.63261384	00	00	0.32682014	0.98636118	00	00	0.43057824
F12	03.02E-11	01	01	9.96E-26	0.89999504	00	00	0.85017453	0.66273476	00	00	0.61918686
F13	0.07727198	00	00	0.06409857	0.42896339	00	00	0.21160983	0.39526701	00	00	0.6061278

Table 3.31: Statistical Test result of Multi-modal Benchmark Functions for CAOA, RWAOA, LFAOA (30 Dimensions)

Algorithm	CAOA				RWAOA				LFAOA			
Function No.	Wilcoxon rank sum test		T-Test		Wilcoxon rank sum test		T-Test		Wilcoxon rank sum test		T-test	
	p-rank	h-rank	p-test	t-test	p-rank	h-rank	p-test	t-test	p-rank	h-rank	p-test	t-test
F08	3.02E-11	1	1	1.01E-21	0.07727198	0	0	0.0991717	0.01383162	1	1	0.0199548
F09	---	0	---	--	--	00	--	-	-	00	-	-
F10	---	0	--	---	--	00	--	-	-	00	-	-
F11	1.96E-11	1	1	2.05E-07	0.50114367	0	0	0.53246164	0.52978249	0	0	0.62536249
F12	3.02E-11	1	1	1.56E-28	0.64142352	0	0	0.44002951	0.76182835	0	0	0.78658571
F13	0.000318	1	1	7.90E-05	0.02812867	1	1	0.0246209	0.04514621	1	0	0.08458966

Table 3.32: Statistical Test result of Multi-modal Benchmark Functions for CAOA, RWAOA, LFAOA (50 Dimensions)												
Algorithm	**CAOA**				**RWAOA**				**LFAOA**			
Function No.	**Wilcoxon rank sum test**		**T-Test**		**Wilcoxon rank sum test**		**T-Test**		**Wilcoxon rank sum test**		**T-Test**	
	p-rank	**h-rank**	**p-test**	**t-test**	**p-rank**	**h-rank**	**p-test**	**t-test**	**p-rank**	**h-rank**	**p-test**	**t-test**
F8	3.02E-11	1	1	2.48E-19	0.36322231	0	0	0.33059721	0.64142352	0	0	0.93806412
F9		0			-	0	-	-	-	0	-	-
F10		0			-	0	-	-	-	0	-	-
F11	3.02E-11	1	1	9.24E-15	0.46427291	0	0	0.58372455	0.73939882	0	0	0.56043925
F12	3.02E-11	1	1	6.34E-29	0.63087629	0	0	0.93622591	0.07727198	0	0	0.24189072
F13	0.01836796	1	1	0.01142289	0.30417682	0	0	0.62633642	0.98230705	0	0	0.84028016

Table 3.33: Statistical Test result of Multi-modal Benchmark Functions for CAOA, RWAOA, LFAOA (100 Dimensions)												
Algorithm	**CAOA**				**RWAOA**				**LFAOA**			
Function No.	**Wilcoxon rank sum test**		**T-Test**		**Wilcoxon rank sum test**		**T-Test**		**Wilcoxon rank sum test**		**T-Test**	
	p-rank	**h-rank**	**p-test**	**t-test**	**p-rank**	**h-rank**	**p-test**	**t-test**	**p-rank**	**h-rank**	**p-test**	**t-test**
F8	3.02E-11	1	1	4.06E-19	0.04358355	1	1	0.03271263	0.27070534	0	0	0.10976515
F9		0			-	0	-	-	-	0	-	-
F10	0.00031349	1	1	0.00614263	0.83931901	0	0	0.20120278	0.66656508	0	0	0.47022737
F11	3.02E-11	1	1	2.42E-18	0.49178296	0	0	0.61110068	0.8766349	0	0	0.7591375
F12	3.02E-11	1	1	1.17E-29	0.4825169	0	0	0.42531213	0.37107703	0	0	0.4122382
F13	0.21701683	0	0	0.20425307	0.59968949	0	0	0.5487882	0.42896339	0	0	0.72329891

Table 3.34: Simulation Time for Multi-Model Benchmark Function using CAOA, RWAOA, LFAOA (10 Dimensions)[98]									
Function No.	**CAOA**	**RWAOA**	**LFAOA**	**CAOA**	**RWAOA**	**LFAOA**	**CAOA**	**RWAOA**	**LFAOA**
	Best Time (Sec)	**Best Time (Sec)**	**Best Time (Sec)**	**Avg. Time (Sec.)**	**Avg. Time (Sec.)**	**Avg. Time (Sec.)**	**Worst Time (Sec)**	**Worst Time (Sec)**	**Worst Time (Sec)**
F08	00.046875	00.125	00.03125	00.066666667	00.159375	00.074479167	00.109375	00.234375	00.15625
F09	00.03125	00.125	00.03125	00.056770833	00.165104167	00.061458333	00.078125	00.40625	00.109375
F10	00.03125	00.125	00.046875	00.058333333	00.164583333	00.0640625	00.09375	00.40625	00.09375
F11	00.046875	00.140625	00.046875	00.0796875	00.165625	00.078125	00.125	00.234375	00.125
F12	00.140625	00.203125	00.140625	00.1578125	00.253125	00.1671875	00.1875	00.328125	00.25
F13	00.140625	00.203125	00.140625	00.155729167	00.247916667	00.159895833	00.203125	00.296875	00.1875

Table 3.35: Simulation Time for Multi-Model Benchmark Function using CAOA, RWAOA, LFAOA (30 Dimensions)									
Function No.	**CAOA**	**RWAOA**	**LFAOA**	**CAOA**	**RWAOA**	**LFAOA**	**CAOA**	**RWAOA**	**LFAOA**
	Best Time (Sec)	**Best Time (Sec)**	**Best Time (Sec)**	**Avg. Time (Sec.)**	**Avg. Time (Sec.)**	**Avg. Time (Sec.)**	**Worst Time (Sec)**	**Worst Time (Sec)**	**Worst Time (Sec)**
F08	00.046875	00.3125	00.03125	00.079166667	00.5828125	00.0875	00.109375	00.15625	00.125
F09	00.03125	00.375	00.03125	00.069270833	00.576041667	00.072916667	00.09375	00.109375	00.125
F10	00.03125	00.3125	00.046875	00.075	00.594791667	00.075	00.109375	00.09375	00.109375
F11	00.046875	00.328125	00.046875	00.080729167	00.5875	00.0890625	00.109375	00.125	00.125
F12	00.140625	00.546875	00.140625	00.256770833	00.846875	00.265625	00.296875	00.25	00.3125
F13	00.140625	00.5	00.140625	00.245833333shrey	00.776041667	00.247395833	00.34375	00.1875	00.28125

Table 3.36: Simulation Time for Multi-Model Benchmark Function using CAOA, RWAOA, LFAOA (50 Dimensions)									
Function No.	**CAOA**	**RWAOA**	**LFAOA**	**CAOA**	**RWAOA**	**LFAOA**	**CAOA**	**RWAOA**	**LFAOA**
	Best Time (Second)	**Best Time (Second)**	**Best Time (Second)**	**Avg. Time (Second)**	**Avg. Time (Second)**	**Avg. Time (Second)**	**Worst Time (Second)**	**Worst Time (Second)**	**Worst Time (Second)**
F8	0.09375	0.421875	0.109375	0.1203125	0.743229167	0.133854167	0.15625	0.921875	0.171875
F9	0.09375	0.546875	0.09375	0.105729167	0.775520833	0.122916667	0.140625	1.1875	0.1875
F10	0.078125	0.53125	0.09375	0.110416667	0.719270833	0.117708333	0.140625	1	0.203125
F11	0.09375	0.484375	0.109375	0.121354167	0.722916667	0.136458333	0.21875	0.96875	0.21875
F12	0.34375	0.75	0.328125	0.371354167	0.9671875	0.365104167	0.40625	1.34375	0.40625
F13	0.3125	0.8125	0.328125	0.360416667	0.996875	0.36875	0.421875	1.3125	0.421875

Table 3.37: Simulation Time for Multi-Model Benchmark Function using CAOA, RWAOA, LFAOA (100 Dimensions)									
Function No.	**CAOA**	**RWAOA**	**LFAOA**	**CAOA**	**RWAOA**	**LFAOA**	**CAOA**	**RWAOA**	**LFAOA**
	Best Time (Sec.)	**Best Time (Sec.)**	**Best Time (Sec.)**	**Avg. Time (Sec.)**	**Avg. Time (Sec.)**	**Avg. Time (Sec.)**	**Worst Time (Sec.)**	**Worst Time (Sec.)**	**Worst Time (Sec.)**
F8	0.15625	0.828125	0.171875	0.1828125	1.031770833	0.206770833	0.203125	1.328125	0.3125
F9	0.140625	0.6875	0.140625	0.155208333	0.965104167	0.165104167	0.171875	1.40625	0.28125
F10	0.140625	0.84375	0.140625	0.160416667	1.0671875	0.168229167	0.1875	1.625	0.265625
F11	0.15625	0.78125	0.1875	0.176041667	1.058854167	0.2171875	0.234375	1.453125	0.28125
F12	0.59375	1.140625	0.59375	0.605729167	1.494270833	0.624479167	0.640625	1.84375	0.640625
F13	0.5625	1.203125	0.578125	0.5921875	1.43125	0.600520833	0.640625	1.84375	0.640625

Table 3.38 Comparison of Multi-Modal Test Functions for CAOA, RWAOA, LFAOA[98]

Algorithms	Parameter	Test Functions- Multi-modal					
		F8	F9	F10	F11	F12	F13
GA[98]	Ave.	-01.26E+04	09.04E+00	01.36E+01	01.01E+01	04.77E+00	01.52E+01
	Std.	04.51E+00	04.58E+00	01.51E+00	02.43E+00	01.56E+00	04.52E+00
PSO[120]	Ave	-03.86E+03	02.87E+02	01.75E+01	01.70E+02	01.51E+07	05.73E+07
	Std.	02.49E+02	01.95E+01	03.67E-01	03.17E+01	09.88E+06	02.68E+07
BBO [2]	Ave.	-01.24E+04	00.00E+00	02.13E+00	01.46E+00	06.68E-01	01.82E+00
	Std.	03.50E+01	00.00E+00	03.53E-01	01.69E-01	02.62E-01	03.41E-01
FPA[98]	Ave.	-06.45E+03	01.82E+02	07.14E+00	01.73E+01	03.05E+02	09.59E+04
	Std.	03.03E+02	01.24E+01	01.08E+00	03.63E+00	01.04E+03	01.46E+05
GWO [81]	Ave	-05.91E+03	02.19E+00	01.03E-03	04.76E-03	04.83E-02	05.96E-01
	Std.	07.10E+02	03.69E+00	01.70E-14	08.57E-03	02.12E-02	02.23E-01
BAT [121]	Ave.	-02.33E+03	01.92E+02	01.92E+01	06.01E+02	04.71E+08	09.40E+08
	Std.	02.96E+02	03.56E+01	02.43E-01	05.50E+01	01.54E+08	01.67E+08
FA[2]	Ave	-05.85E+03	03.82E+01	04.58E-02	04.23E-03	03.13E-04	02.08E-03
	Std.	01.16E+03	01.12E+01	01.20E-02	01.29E-03	01.76E-04	09.62E-04
CS [98]	Ave.	-05.19E+01	01.51E+01	03.29E-02	04.29E-05	05.57E-05	08.19E-03
	Std.	01.76E+01	01.25E+00	07.93E-03	02.00E-05	04.96E-05	06.74E-03
MFO [83]	Ave.	-08.48E+03	01.59E+02	01.74E+01	03.10E+01	02.46E+02	02.73E+07
	Std.	07.98E+02	03.21E+01	04.95E+00	05.94E+01	01.21E+03	01.04E+08
GSA [118]	Ave.	-02.35E+03	03.10E+01	03.74E+00	04.86E-01	04.63E-01	07.61E+00
	Std.	03.82E+02	01.36E+01	01.71E-01	04.97E-02	01.37E-01	01.22E+00
DE [122]	Ave.	-06.82E+03	01.58E+02	01.21E-02	03.52E-02	02.25E-05	09.12E-03
	Std.	03.94E+02	01.17E+01	03.30E-03	07.20E-02	01.70E-03	01.16E-02
AOA[2]	Ave.	-01.22E+04	03.42E-07	08.88E-16	00.00E+00	04.28E-06	03.10E-01
	Std.	01.22E+03	3.42E-07	08.88E-16	00.00E+00	04.28E-06	03.10E-01
CAOA	**Ave.**	**-2849.658**	**0**	**8.88E-16**	**3.29E-07**	**1.0208853**	**2.8759932**
	Std.	**360.2603**	**0**	**0**	**1.67E-06**	**0.0298163**	**0.0768013**
RWAOA	**Ave.**	**-2849.658**	**0**	**8.88E-16**	**3.29E-07**	**1.0208853**	**2.8759932**
	Std.	**360.2603**	**0**	**0**	**1.67E-06**	**0.0298163**	**0.0768013**
LAOA	**Ave**	**-5121.33357**	**0**	**8.88E-16**	**0.18936639**	**0.51000717**	**2.83088185**
	Std.	**443.849808**	**0**	**0**	**0.13766838**	**0.04329661**	**0.09152525**

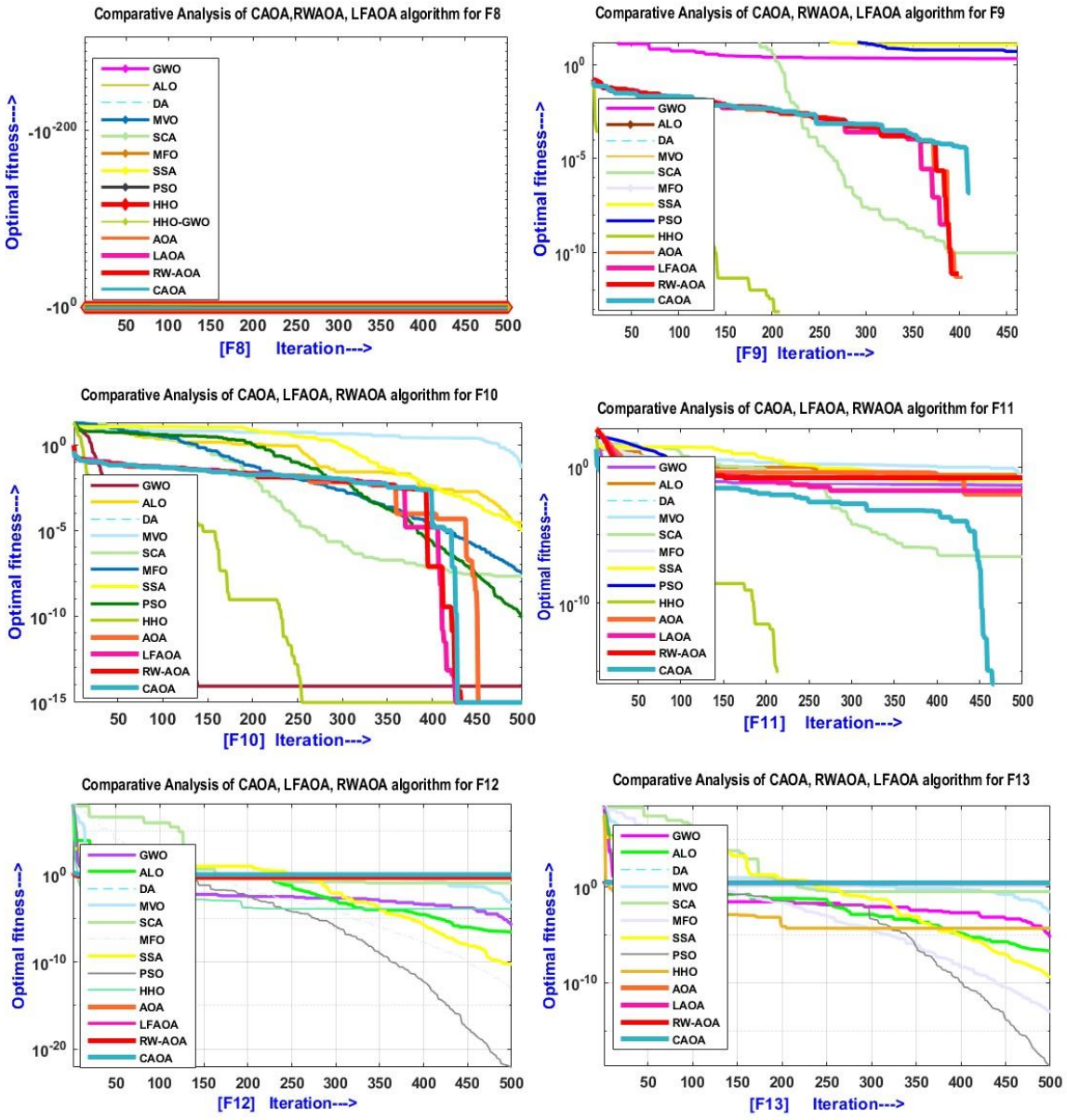

Figure 3.27: Comparison convergence curve for Multi-modal (F8-F13) Benchmark Functions of CAOA, RWAOA, LFAOA with competitive algorithm.

3.10.3 Fixed Benchmark Functions- Testing

The performance of the CAOA, RWAOA, and LFAOA algorithms was evaluated on fixed benchmark functions (F14 to F23) by conducting 30 trial runs and 500 iterations for each of the 10, 30, 50, and 100 dimensions. **Tables 3.39 to 3.54** depict the results obtained from the fixed test functions for 10, 30, 50, and 100 dimensions. The Wilcoxon sum test and statistical T-test were utilized to evaluate the usefulness of the solution. **Tables 3.47, 3.48, 3.49,** and **3.50** showcase the results of the Wilcoxon sum test and statistical T-test for 10, 30, 50, and 100 dimensions, respectively. The efficacy of the algorithm is established through the increased convergence of fixed benchmark functions by CAOA, RWAOA, and LFAOA. **Table 3.39** illustrates the test result of the fixed-dimension benchmark function for objective fitness functions using CAOA, RWAOA, and LFAOA for 10 dimensions. **Table 3.40** illustrates the test result of the fixed-dimension benchmark function for objective fitness functions using CAOA, RWAOA, and LFAOA for 30 dimensions. Table 3.41 illustrates the test result of the fixed-dimension benchmark function for objective fitness functions using CAOA, RWAOA, and LFAOA (50 dimensions). **Table 3.42** illustrates the test result of the fixed-dimension benchmark function for objective fitness functions using CAOA, RWAOA, and LFAOA (100 dimensions). **Table 3.43** illustrates the quartile result for the fixed benchmark test function using CAOA, RWAOA, and LFAOA (10 dim.). **Table 3.44** illustrates the quartile result for the fixed benchmark test function using CAOA, RWAOA, and LFAOA (30 dim.). **Table 3.45** illustrates the quartile result for the fixed benchmark test function using CAOA, RWAOA, and LFAOA (50 dim.). **Table 3.46** illustrates the quartile result for the fixed benchmark test function using CAOA, RWAOA, and LFAOA (100 dim.). **Table 3.47** illustrates the statistical test results of fixed-dimension benchmark functions for CAOA, RWAOA, and LFAOA (10 dimensions). **Table 3.48** illustrates the statistical test results of fixed-dimension benchmark functions for CAOA, RWAOA, and LFAOA (30 dimensions). **Table 3.49** illustrates the statistical test results of fixed-dimension benchmark functions for CAOA, RWAOA, and LFAOA (50 dimensions). **Table 3.50** illustrates the statistical test results of the fixed-

dimension benchmark functions for CAOA, RWAOA, and LFAOA (100 dimensions). The runtime performance of the CAOA, RWAOA, and LFAOA algorithms on fixed benchmark functions is shown in **Tables 3.51 to 3.54** for 10, 30, 50, and 100 dimensions, respectively. Additionally, **Figure 3.28** illustrates a comparison of the convergence curve for Fixed Dimensions (F14–F23) benchmark functions.

Table 3.39: Test result of Fixed Dimension Benchmark Function for objective fitness functions using CAOA, RWAOA, LFAOA (10 Dimensions)

Function No.	CAOA	RWAOA	LFAOA	CAOA	RWAOA	LFAOA	CAOA	RWAOA	LFAOA	CAOA	RWAOA	LFAOA	CAOA	RWAOA	LFAOA	CAOA	RWAOA	LFAOA
	Index	Index	Index	Mean	Mean	Mean	Std.	Std.	Std.	Best	Best	Best	Worst	Worst	Worst	Median	Median	Median
F14	29	21	20	10.6408	10.1545	8.95862	3.6913	4.14959	4.68855	0.998	0.998	0.998	12.6705	12.6705	12.6705	12.6705	12.6705	11.7187
F15	28	11	26	0.01047	0.00962	0.01604	0.01801	0.01292	0.03096	0.00034	0.00041	0.00035	0.08015	0.06132	0.12075	0.00063	0.00512	0.00191
F16	7	1	28	-1.03161	-1.03163	-1.03163	6.11E-06	1.00E-07	1.34E-07	-1.03163	-1.03163	-1.03163	-1.0316	-1.03163	-1.03163	-1.03161	-1.03163	-1.03163
F17	29	30	14	0.84628	0.41346	0.41234	0.44059	0.01595	0.00982	0.4329	0.3981	0.3995	2.1983	0.47623	0.44101	0.68535	0.40828	0.41065
F18	4	5	17	20.2691	5.70149	9.3	31.9447	8.23797	11.6149	3	3	3	146.283	30	30	3.00006	3	3
F19	29	4	18	-3.52431	-3.85084	-3.85057	0.18834	0.0046	0.00588	-3.82295	-3.86058	-3.85783	-2.72038	-3.8413	-3.82983	-3.54193	-3.85202	-3.85163
F20	30	1	5	-2.30135	-3.05168	-3.04106	0.25541	0.10087	0.09212	-2.81805	-3.18726	-3.23505	-1.73375	-2.71719	-2.8634	-2.27241	-3.07518	-3.05838
F21	18	8	6	-3.43934	-3.72944	-3.74796	1.39311	0.93112	1.38006	-5.69408	-5.20625	-8.60371	-1.21413	-1.824	-1.79483	-4.02183	-3.65874	-3.55453
F22	14	27	13	-3.46672	-3.42199	-3.50864	1.54186	1.23987	1.46628	-7.21725	-6.94361	-6.87603	-1.29287	-1.54203	-1.39188	-3.71163	-3.30375	-3.58709
F23	24	9	26	-3.34872	-3.77532	-4.16565	1.62769	0.92356	1.69045	-7.94784	-5.69922	-8.21259	-1.28013	-1.73084	-1.6651	-3.36965	-3.7067	-3.90621

Table 3.40: Test result of Fixed Dimension Benchmark Function for objective fitness functions using CAOA, RWAOA, LFAOA (30 Dimensions)

Function No.	CAOA	RWAOA	LFAOA	CAOA	RWAOA	LFAOA	CAOA	RWAOA	LFAOA	CAOA	RWAOA	LFAOA	CAOA	RWAOA	LFAOA	CAOA	RWAOA	LFAOA
	Index	Index	Index	Mean	Mean	Mean	Std.	Std.	Std.	Best	Best	Best	Worst	Worst	Worst	Median	Median	Median
F14	11	14	30	9.89974	8.865361	9.2958827	4.0621941	4.5106136	3.708035	0.9980038	0.9980038	1.9920309	12.670506	12.670506	12.670506	12.670506	11.24094	10.763181
F15	9	28	29	0.0093635	0.0153665	0.0169005	0.0127572	0.0260077	0.0327302	0.0003746	0.0003666	0.0003475	0.0452419	0.116729	0.1162259	0.0029661	0.0045066	0.0010714
F16	21	13	30	-1.031615	-1.031628	-1.031628	6.70E-06	1.35E-07	1.15E-07	-1.031626	-1.031628	-1.031628	-1.031602	-1.031628	-1.031628	-1.031615	-1.031628	-1.031628
F17	8	17	16	0.9503106	0.408804	0.4097653	0.4763681	0.0104698	0.010759	0.3981556	0.3979466	0.399306	2.3155067	0.4379595	0.4491349	0.8712412	0.4048806	0.406472
F18	12	20	7	16.337499	12.901135	11.10058	21.859273	13.232705	12.584091	3	3	3	98.991245	30.000018	30.00002	3.000059	3	3
F19	14	3	4	-3.514905	-3.851534	-3.850895	0.1833019	0.0045117	0.0035879	-3.81513	-3.859146	-3.857879	-2.895255	-3.83724	-3.842513	-3.528365	-3.852421	-3.851732
F20	1	5	7	-2.415127	-3.080955	-3.101836	0.3039548	0.0790838	0.0778961	-2.943966	-3.215955	-3.249474	-1.649953	-2.893159	-2.898031	-2.482055	-3.104828	-3.11237
F21	3	12	18	-2.975096	-3.429211	-4.258822	1.5494601	1.0064295	1.5273327	-6.902406	-5.373432	-8.929123	-1.211925	-1.685525	-2.014846	-2.469007	-3.358496	-3.834521
F22	10	15	30	-3.410715	-4.234742	-3.800713	1.6337523	1.8364665	1.4745621	-8.682326	-9.606045	-8.058339	-1.088643	-1.640566	-1.453697	-3.587198	-3.672918	-3.726861
F23	8	29	12	-2.604408	-3.765198	-4.541238	1.2302613	1.4925453	1.6560109	-6.00509	-7.244342	-8.761818	-1.250982	-1.51428	-2.001318	-1.957601	-3.739343	-4.216748

Table 3.41: Test result of Fixed Dimension Benchmark Function for objective fitness functions using CAOA, RWAOA, LFAOA (50 Dimensions)

Function No.	CAOA	RWAOA	LFAOA	CAOA	RWAOA	LFAOA	CAOA	RWAOA	LFAOA	CAOA	RWAOA	LFAOA	CAOA	RWAOA	LFAOA	CAOA	RWAOA	LFAOA
	Index	Index	Index	Mean	Mean	Mean	Std.	Std.	Std.	Best	Best	Best	Worst	Worst	Worst	Median	Median	Median
F14	23	1	17	9.7345	9.08767	9.55023	4.37094	4.66164	3.87079	0.998	0.998	0.998	12.6705	12.6705	12.6705	12.6705	11.7168	10.7632
F15	5	2	8	0.02114	0.01511	0.01811	0.03311	0.02497	0.03154	0.00035	0.00037	0.00035	0.11714	0.10654	0.10892	0.0084	0.00513	0.00431
F16	24	25	6	-1.03161	-1.03163	-1.03163	4.40E-06	1.03E-07	1.75E-07	-1.03162	-1.03163	-1.03163	-1.0316	-1.03163	-1.03163	-1.03161	-1.03163	-1.03163
F17	24	14	30	1.00173	0.4141	0.41306	0.6445	0.0132	0.01382	0.41279	0.39935	0.39968	2.89966	0.45282	0.45572	0.79804	0.40909	0.40769
F18	2	14	18	10.5132	8.4017	8.40054	18.0186	10.9838	10.9844	3	3	3	82.2474	30	30	3.00006	3	3
F19	15	10	3	-3.58661	-3.84892	-3.85183	0.15006	0.00778	0.0042	-3.85861	-3.85817	-3.86033	-3.16048	-3.81859	-3.8393	-3.57701	-3.85056	-3.85254
F20	2	15	5	-2.39924	-3.03121	-3.07096	0.24203	0.13316	0.10563	-3.03077	-3.24128	-3.22613	-1.91154	-2.69717	-2.77249	-2.40015	-3.08982	-3.10608
F21	4	11	5	-3.11029	-4.14427	-3.50798	1.21046	1.47715	1.15973	-4.99049	-8.13278	-6.30952	-1.19635	-1.78183	-1.3909	-3.14469	-3.89565	-3.37041
F22	4	1	14	-3.07096	-3.66693	-3.55785	1.3679	1.50121	1.1441	-6.89177	-6.53941	-6.60297	-1.27968	-1.1852	-1.72776	-3.48158	-3.42104	-3.57931
F23	17	29	10	-2.75158	-3.70131	-3.66506	1.47079	1.36445	1.82601	-7.52406	-7.36815	-8.58343	-1.22982	-1.53891	-1.34077	-2.06798	-3.5207	-3.51495

Table 3.42: Test Result of Fixed Dimension Benchmark Function for Objective Fitness Functions Using CAOA, RWAOA, LFAOA (100 Dimensions)

Function No.	CAOA	RWAOA	LFAOA	CAOA	RWAOA	LFAOA	CAOA	RWAOA	LFAOA	CAOA	RWAOA	LFAOA	CAOA	RWAOA	LFAOA	CAOA	RWAOA	LFAOA
	Index	Index	Index	Mean	Mean	Mean	Std.	Std.	Std.	Best	Best	Best	Worst	Worst	Worst	Median	Median	Median
F14	28	10	27	9.3585426	10.610992	10.444576	3.8142686	3.5401679	4.0003265	0.9980038	1.9920309	0.9980038	12.670506	12.670506	12.670506	10.763181	12.670506	12.670506
F15	24	3	12	0.0184065	0.0097721	0.0097	0.0265917	0.0168959	0.1689	0.0003624	0.0003438	0.00035	0.101808	0.0611054	0.0601105	0.0085974	0.0010224	0.001123
F16	8	5	15	-1.031616	-1.031628	-1.03512	5.17E-06	9.62E-08	9.60E-06	-1.031626	-1.031628	-1.03E+00	-1.031606	-1.031628	-1.03E+00	-1.031616	-1.031628	-1.03E+00
F17	22	15	27	0.8510901	0.4106737	0.4127692	0.3277233	0.0090875	0.0110477	0.4151938	0.3979135	0.3987943	1.4766241	0.4365189	0.4428635	0.7327505	0.4089637	0.4105367
F18	2	20	18	20.537192	6.6000679	7.5000008	29.07797	9.335117	10.234325	3.0000022	3	3	96.043625	30.000015	30.000011	3.0000571	3	3
F19	6	5	8	-3.545768	-3.853267	-3.852858	0.1618398	0.0040244	0.0047404	-3.794575	-3.862491	-3.861191	-3.069853	-3.847035	-3.836353	-3.559406	-3.85267	-3.853641
F20	24	28	12	-2.358696	-3.066813	-3.073051	0.2645883	0.0869092	0.0945628	-2.725891	-3.17735	-3.251341	-1.815574	-2.821159	-2.848968	-2.403609	-3.085258	-3.099351
F21	3	11	30	-3.075704	-3.671157	-3.834278	1.5758597	1.0345725	1.1648219	-8.717403	-6.002072	-6.355369	-1.257704	-1.728972	-1.769785	-2.244356	-3.793496	-3.595541
F22	8	13	21	-2.960904	-4.266825	-3.501941	1.8624454	1.5060564	1.1145269	-8.471397	-9.268822	-5.105268	-1.124959	-1.156168	-1.601393	-2.294747	-4.519846	-3.620801
F23	5	11	11	-3.452269	-3.510268	-3.813213	1.3343065	1.6987649	1.6634419	-6.78871	-7.643446	-8.230561	-1.599281	-1.483115	-1.380206	-3.786571	-3.016605	-3.715185

Table 3.43: Quartile result for Fixed Benchmark Test function using CAOA, RWAOA, LFAOA (10 Dim.)											
Algorithm	**Function No.**	**F14**	**F15**	**F16**	**F17**	**F18**	**F19**	**F20**	**F21**	**F22**	**F23**
CAOA	No. of trials	30	30	30	30	30	30	30	30	30	30
RWAOA	No. of trials	30	30	30	30	30	30	30	30	30	30
LFAOA	No. of trials	30	30	30	30	30	30	30	30	30	30
CAOA	Minimum value	0.998004	0.000338	-1.031628	0.4329	3	-3.82295	-2.818055	-5.694077	-7.217248	-7.947839
RWAOA	Minimum value	0.998004	0.000405	-1.031628	0.398098	3	-3.860576	-3.187263	-5.20625	-6.943608	-7.643446
LFAOA	Minimum value	0.998004	0.000348	-1.031628	0.3995	3	-3.857826	-3.235046	-8.603711	-6.876026	-8.212587
CAOA	Maximum value	12.67051	0.080151	-1.031602	2.1983	146.2833	-2.720382	-1.733745	-1.214131	-1.29287	-1.280128
RWAOA	Maximum value	12.67051	0.061316	-1.031628	0.476226	30	-3.841298	-2.717191	-1.823998	-1.542028	-1.483115
LFAOA	Maximum value	12.67051	0.120747	-1.031628	0.441005	30.00001	-3.829832	-2.863404	-1.794827	-1.391883	-1.665099
CAOA	Mean Value	10.6408	0.010469	-1.031614	0.846278	20.26915	-3.524308	-2.301351	-3.439342	-3.466721	-3.348719
RWAOA	Mean Value	10.15447	0.009619	-1.031628	0.413462	5.701493	-3.85084	-3.05168	-3.729443	-3.421991	-3.510268
LFAOA	Mean Value	8.958619	0.016038	-1.031628	0.412342	9.300001	-3.850568	-3.041062	-3.747962	-3.508642	-4.165654
CAOA	Median	12.67051	0.000633	-1.031614	0.685348	3.000061	-3.541932	-2.272413	-4.021829	-3.71163	-3.369647
RWAOA	Median	12.67051	0.00512	-1.031628	0.408282	3	-3.852022	-3.07518	-3.65874	-3.303755	-3.016605
LFAOA	Median	11.7187	0.001912	-1.031628	0.410649	3	-3.851633	-3.058383	-3.554529	-3.587089	-3.906213
CAOA	First quartile (25th Percentile)	10.76318	0.000402	-1.031617	0.489251	3.000052	-3.588531	-2.42387	-4.487803	-4.25614	-4.502801
RWAOA	First quartile (25th Percentile)	10.76318	0.000567	-1.031628	0.403287	3	-3.853221	-3.123511	-4.511989	-4.271098	-4.698748
LFAOA	First quartile (25th Percentile)	2.982105	0.000398	-1.031628	0.404804	3	-3.854023	-3.100055	-4.797739	-4.355181	-4.886637
CAOA	Second quartile (50th Percentile)	12.67051	0.000633	-1.031614	0.685348	3.000061	-3.541932	-2.272413	-4.021829	-3.71163	-3.369647
RWAOA	Second quartile (50th Percentile)	12.67051	0.00512	-1.031628	0.408282	3	-3.852022	-3.07518	-3.65874	-3.303755	-3.016605
LFAOA	Second quartile (50th Percentile)	11.7187	0.001912	-1.031628	0.410649	3	-3.851633	-3.058383	-3.554529	-3.587089	-3.906213
CAOA	Third quartile (75th Percentile)	12.67051	0.012342	-1.03161	0.981694	30.00021	-3.494192	-2.111133	-1.905689	-2.134033	-1.735965
RWAOA	Third quartile (75th Percentile)	12.67051	0.015558	-1.031628	0.419282	3	-3.847513	-2.988374	-2.961412	-2.606102	-2.107209
LFAOA	Third quartile (75th Percentile)	12.67051	0.012268	-1.031628	0.417018	3	-3.849013	-2.964197	-2.866853	-2.004937	-2.953976
CAOA	Semi Interquartile Deviation	0.953663	0.00597	3.73E-06	0.246222	13.50008	0.04717	0.156369	1.291057	1.061054	1.383418
RWAOA	Semi Interquartile Deviation	0.953663	0.007496	6.53E-08	0.007997	1.86E-08	0.002854	0.067569	0.775289	0.832498	1.29577
LFAOA	Semi Interquartile Deviation	4.8442	0.005935	8.74E-08	0.006107	3.90E-08	0.002505	0.067929	0.965443	1.175122	0.966331
CAOA	Number of outliers	4	2	0	1	2	2	0	0	0	0
RWAOA	Number of outliers	5	1	0	1	5	0	1	0	0	0
LFAOA	Number of outliers	0	5	0	0	7	2	0	0	0	0
CAOA	Standard Deviation	3.691301	0.018013	6.11E-06	0.440589	31.94472	0.188339	0.25541	1.393107	1.541861	1.627694
RWAOA	Standard Deviation	4.149593	0.012916	1.00E-07	0.015954	8.237968	0.004599	0.10087	0.931119	1.239872	1.698765
LFAOA	Standard Deviation	4.688551	0.030964	1.34E-07	0.009825	11.61495	0.00588	0.09212	1.380064	1.466279	1.690452

Table 3.44: Quartile result for Fixed Benchmark Test function using CAOA, RWAOA, LFAOA (30 Dim.)

Algorithm	Function No.	F14	F15	F16	F17	F18	F19	F20	F21	F22	F23
CAOA	No. of trials	30	30	30	30	30	30	30	30	30	30
RWAOA	No. of trials	30	30	30	30	30	30	30	30	30	30
LFAOA	No. of trials	30	30	30	30	30	30	30	30	30	30
CAOA	Minimum value	0.998004	0.000375	-1.031626	0.398156	3	-3.81513	-2.943966	-6.902406	-8.682326	-6.00509
RWAOA	Minimum value	0.998004	0.000367	-1.031628	0.397947	3	-3.859146	-3.215955	-5.373432	-9.606045	-7.244342
LFAOA	Minimum value	1.992031	0.000348	-1.03163	0.399306	3	-3.85788	-3.24947	-8.92912	-8.05834	-8.76182
CAOA	Maximum value	12.67051	0.045242	-1.031602	2.315507	98.99124	-2.895255	-1.649953	-1.211924	-1.088643	-1.250982
RWAOA	Maximum value	12.67051	0.116729	-1.031628	0.437959	30.00002	-3.83724	-2.893159	-1.685525	-1.640566	-1.51428
LFAOA	Maximum value	12.67051	0.116226	-1.03163	0.449135	30.00002	-3.84251	-2.89803	-2.01485	-1.4537	-2.00132
CAOA	Mean Value	9.89974	0.009364	-1.031614	0.950311	16.3375	-3.514905	-2.415127	-2.975096	-3.410715	-2.604407
RWAOA	Mean Value	8.865361	0.015366	-1.031628	0.408804	12.90113	-3.851534	-3.080955	-3.429211	-4.234742	-3.765198
LFAOA	Mean Value	9.295883	0.016901	-1.03163	0.409765	11.10058	-3.85089	-3.10184	-4.25882	-3.80071	-4.54124
CAOA	Median	12.67051	0.002966	-1.031615	0.871241	3.000059	-3.528365	-2.482055	-2.469007	-3.587198	-1.957601
RWAOA	Median	11.24094	0.004507	-1.031628	0.404881	3	-3.852421	-3.104828	-3.358496	-3.672918	-3.739343
LFAOA	Median	10.76318	0.001071	-1.03163	0.406472	3	-3.85173	-3.11237	-3.83452	-3.72686	-4.21675
CAOA	First quartile (25th Percentile)	7.873993	0.000447	-1.031618	0.540538	3.000052	-3.606414	-2.617635	-4.03812	-4.364942	-3.771007
RWAOA	First quartile (25th Percentile)	2.982105	0.00045	-1.031628	0.401501	3	-3.853922	-3.124335	-4.083652	-5.38118	-4.609194
LFAOA	First quartile (25th Percentile)	6.903336	0.000425	-1.03163	0.402304	3	-3.85303	-3.15205	-4.97619	-4.59725	-5.98771
CAOA	Second quartile (50th Percentile)	12.67051	0.002966	-1.031615	0.871241	3.000059	-3.528365	-2.482055	-2.469007	-3.587198	-1.957601
RWAOA	Second quartile (50th Percentile)	11.24094	0.004507	-1.031628	0.404881	3	-3.852421	-3.104828	-3.358496	-3.672918	-3.739343
LFAOA	Second quartile (50th Percentile)	10.76318	0.001071	-1.03163	0.406472	3	-3.85173	-3.11237	-3.83452	-3.72686	-4.21675
CAOA	Third quartile (75th Percentile)	12.67051	0.017009	-1.031609	1.181921	30.00063	-3.474016	-2.177103	-1.532586	-2.066064	-1.605141
RWAOA	Third quartile (75th Percentile)	12.67051	0.022686	-1.031628	0.414318	30	-3.850096	-3.048169	-2.56229	-2.999236	-3.029218
LFAOA	Third quartile (75th Percentile)	12.67051	0.017472	-1.03163	0.413105	30	-3.84802	-3.07989	-3.13408	-2.93309	-3.29856
CAOA	Semi Interquartile Deviation	2.398256	0.008281	4.77E-06	0.320692	13.50029	0.066199	0.220266	1.252767	1.149439	1.082933
RWAOA	Semi Interquartile Deviation	4.8442	0.011118	8.71E-08	0.006408	13.5	0.001913	0.038083	0.760681	1.190972	0.789988
LFAOA	Semi Interquartile Deviation	2.883585	0.008523	8.13E-08	0.0054	13.5	0.002508	0.036081	0.921058	0.83208	1.344571
CAOA	Number of outliers	0	0	0	0	1	3	0	0	0	0
RWAOA	Number of outliers	0	2	0	0	0	1	1	0	0	0
LFAOA	Number of outliers	0	3	0	1	0	0	1	0	0	0
CAOA	Standard Deviation	4.062194	0.012757	6.70E-06	0.476368	21.85927	0.183302	0.303955	1.54946	1.633752	1.230261
RWAOA	Standard Deviation	4.510614	0.026008	1.35E-07	0.01047	13.23271	0.004512	0.079084	1.00643	1.836466	1.492545
LFAOA	Standard Deviation	3.708035	0.03273	1.15E-07	0.010759	12.58409	0.003588	0.077896	1.527333	1.474562	1.656011

Table 3.45: Quartile result for Fixed Benchmark Test function using CAOA, RWAOA, LFAOA (50 Dim.)

Algorithm	Function No.	F14	F15	F16	F17	F18	F19	F20	F21	F22	F23
CAOA	No. of trials	30	30	30	30	30	30	30	30	30	30
RWAOA	No. of trials	30	30	30	30	30	30	30	30	30	30
LFAOA	No. of trials	30	30	30	30	30	30	30	30	30	30
CAOA	Minimum value	0.998004	0.000355	-1.031621	0.412789	3	-3.858611	-3.030775	-4.990491	-6.891767	-7.524065
RWAOA	Minimum value	0.998004	0.000375	-1.031628	0.399349	3	-3.858168	-3.241276	-8.132781	-6.539407	-7.368153
LFAOA	Minimum value	0.998004	0.000353	-1.03163	0.399682	3	-3.86033	-3.22613	-6.30952	-6.60297	-8.58343
CAOA	Maximum value	12.67051	0.117139	-1.031604	2.899663	82.24742	-3.160481	-1.911545	-1.196352	-1.279678	-1.229819
RWAOA	Maximum value	12.67051	0.106539	-1.031628	0.452823	30.00003	-3.818591	-2.697168	-1.781834	-1.185197	-1.538908
LFAOA	Maximum value	12.67051	0.108918	-1.03163	0.455719	30.00001	-3.8393	-2.77249	-1.3909	-1.72776	-1.34077
CAOA	Mean Value	9.734501	0.021142	-1.031613	1.001727	10.51324	-3.586609	-2.39924	-3.110287	-3.070958	-2.751578
RWAOA	Mean Value	9.087669	0.015112	-1.031628	0.414103	8.401698	-3.848918	-3.031209	-4.144275	-3.666925	-3.701307
LFAOA	Mean Value	9.550234	0.018105	-1.03163	0.413056	8.400538	-3.85183	-3.07096	-3.50798	-3.55785	-3.66506
CAOA	Median	12.67051	0.008401	-1.031613	0.798039	3.000058	-3.57701	-2.400154	-3.144691	-3.48158	-2.067984
RWAOA	Median	11.71684	0.005125	-1.031628	0.409093	3	-3.850556	-3.089819	-3.895647	-3.421042	-3.520698
LFAOA	Median	10.76318	0.004306	-1.03163	0.407686	3	-3.85254	-3.10608	-3.37041	-3.57931	-3.51495
CAOA	First quartile (25th Percentile)	7.873993	0.000565	-1.031615	0.542686	3.000018	-3.696443	-2.570406	-4.24906	-3.940421	-3.956709
RWAOA	First quartile (25th Percentile)	2.982105	0.000932	-1.031628	0.404258	3	-3.852804	-3.12013	-4.841257	-4.743435	-4.143094
LFAOA	First quartile (25th Percentile)	7.873993	0.000392	-1.03163	0.402741	3	-3.85402	-3.12942	-4.48799	-4.04615	-4.75072
CAOA	Second quartile (50th Percentile)	12.67051	0.008401	-1.031613	0.798039	3.000058	-3.57701	-2.400154	-3.144691	-3.48158	-2.067984
RWAOA	Second quartile (50th Percentile)	11.71684	0.005125	-1.031628	0.409093	3	-3.850556	-3.089819	-3.895647	-3.421042	-3.520698
LFAOA	Second quartile (50th Percentile)	10.76318	0.004306	-1.03163	0.407686	3	-3.85254	-3.10608	-3.37041	-3.57931	-3.51495
CAOA	Third quartile (75th Percentile)	12.67051	0.036142	-1.031611	1.106487	3.000067	-3.51042	-2.190452	-2.138094	-1.499535	-1.653536
RWAOA	Third quartile (75th Percentile)	12.67051	0.021727	-1.031628	0.425705	3.017583	-3.847626	-2.932499	-3.307642	-2.278425	-3.069058
LFAOA	Third quartile (75th Percentile)	12.67051	0.020357	-1.03163	0.42037	3.001781	-3.85011	-3.01441	-2.77835	-2.77205	-2.08499
CAOA	Semi Interquartile Deviation	2.398256	0.017789	2.30E-06	0.281901	2.42E-05	0.093012	0.189977	1.055483	1.220443	1.151586
RWAOA	Semi Interquartile Deviation	4.8442	0.010398	5.51E-08	0.010724	0.008792	0.002589	0.093815	0.766807	1.232505	0.537018
LFAOA	Semi Interquartile Deviation	2.398256	0.009983	8.03E-08	0.008814	0.00089	0.001955	0.057504	0.854822	0.637052	1.332866
CAOA	Number of outliers	0	2	0	3	7	0	0	0	0	0
RWAOA	Number of outliers	0	2	1	0	6	2	0	0	0	1
LFAOA	Number of outliers	0	4	1	1	7	1	1	0	0	0
CAOA	Standard Deviation	4.370938	0.033113	4.40E-06	0.644496	18.01859	0.150061	0.242029	1.210457	1.367901	1.470792
RWAOA	Standard Deviation	4.661637	0.024973	1.03E-07	0.013198	10.98377	0.007782	0.133165	1.47715	1.501205	1.364452
LFAOA	Standard Deviation	3.870795	0.031536	1.75E-07	0.013823	10.98436	0.004201	0.105627	1.15973	1.144103	1.826007

Table 3.46: Quartile result for Fixed Benchmark Test function using CAOA, RWAOA, LFAOA (100 Dim.)

Algorithm	Function No.	F14	F15	F16	F17	F18	F19	F20	F21	F22	F23
CAOA	No. of trials	30	30	30	30	30	30	30	30	30	30
RWAOA	No. of trials	30	30	30	30	30	30	30	30	30	30
LFAOA	No. of trials	30	30	30	30	30	30	30	30	30	30
CAOA	Minimum value	0.998004	0.000362	-1.031626	0.415194	3.000002	-3.794575	-2.725891	-8.717403	-8.471397	-6.78871
RWAOA	Minimum value	1.992031	0.000344	-1.031628	0.397914	3	-3.862491	-3.17735	-6.002072	-9.268822	-7.643446
LFAOA	Minimum value	0.998004	0.000356	-1.03163	0.398794	3	-3.86119	-3.25134	-6.35537	-5.10527	-8.23056
CAOA	Maximum value	12.67051	0.101808	-1.031606	1.476624	96.04363	-3.069853	-1.815574	-1.257704	-1.124959	-1.599281
RWAOA	Maximum value	12.67051	0.061105	-1.031628	0.436519	30.00001	-3.847035	-2.821159	-1.728972	-1.156168	-1.483115
LFAOA	Maximum value	12.67051	0.104987	-1.03163	0.442864	30.00001	-3.83635	-2.84897	-1.76978	-1.60139	-1.38021
CAOA	Mean Value	9.358543	0.018407	-1.031616	0.85109	20.53719	-3.545768	-2.358696	-3.075704	-2.960904	-3.452269
RWAOA	Mean Value	10.61099	0.009772	-1.031628	0.410674	6.600068	-3.853267	-3.066813	-3.671157	-4.266825	-3.510268
LFAOA	Mean Value	10.44458	0.020974	-1.03163	0.412769	7.500001	-3.85286	-3.07305	-3.83428	-3.50194	-3.81321
CAOA	Median	10.76318	0.008597	-1.031616	0.73275	3.000057	-3.559406	-2.403609	-2.244356	-2.294747	-3.786571
RWAOA	Median	12.67051	0.001022	-1.031628	0.408964	3	-3.85267	-3.085258	-3.793496	-4.519846	-3.016605
LFAOA	Median	12.67051	0.005446	-1.03163	0.410537	3	-3.85364	-3.09935	-3.59554	-3.6208	-3.71519
CAOA	First quartile (25th Percentile)	7.873993	0.000547	-1.031619	0.597732	3.000022	-3.639438	-2.589383	-3.984782	-3.928974	-4.350468
RWAOA	First quartile (25th Percentile)	10.76318	0.000404	-1.031628	0.403286	3	-3.85422	-3.131736	-4.361661	-4.91799	-4.698748
LFAOA	First quartile (25th Percentile)	10.76318	0.000724	-1.03163	0.404284	3	-3.85535	-3.13617	-4.59042	-4.54337	-4.34758
CAOA	Second quartile (50th Percentile)	10.76318	0.008597	-1.031616	0.73275	3.000057	-3.559406	-2.403609	-2.244356	-2.294747	-3.786571
RWAOA	Second quartile (50th Percentile)	12.67051	0.001022	-1.031628	0.408964	3	-3.85267	-3.085258	-3.793496	-4.519846	-3.016605
LFAOA	Second quartile (50th Percentile)	12.67051	0.005446	-1.03163	0.410537	3	-3.85364	-3.09935	-3.59554	-3.6208	-3.71519
CAOA	Third quartile (75th Percentile)	12.67051	0.01617	-1.031612	1.232128	30.00093	-3.503185	-2.150971	-1.95552	-1.501889	-2.032166
RWAOA	Third quartile (75th Percentile)	12.67051	0.012303	-1.031628	0.417468	3	-3.850382	-2.980953	-2.829377	-3.229949	-2.107209
LFAOA	Third quartile (75th Percentile)	12.67051	0.023358	-1.03163	0.419541	3	-3.8497	-3.03319	-2.91296	-2.49375	-2.65391
CAOA	Semi Interquartile Deviation	2.398256	0.007812	3.65E-06	0.317198	13.50046	0.068126	0.219206	1.014631	1.213542	1.159151
RWAOA	Semi Interquartile Deviation	0.953663	0.00595	5.45E-08	0.007091	1.19E-08	0.001919	0.075391	0.766142	0.844021	1.29577
LFAOA	Semi Interquartile Deviation	0.953663	0.011317	8.38E-08	0.007629	1.34E-08	0.002825	0.051492	0.838729	1.024811	0.846836
CAOA	Number of outliers	0	4	0	0	1	1	0	0	0	0
RWAOA	Number of outliers	4	3	0	0	6	0	0	0	0	0
LFAOA	Number of outliers	5	4	0	0	5	1	0	0	0	0
CAOA	Standard Deviation	3.814269	0.026592	5.17E-06	0.327723	29.07797	0.16184	0.264588	1.57586	1.862445	1.334306
RWAOA	Standard Deviation	3.540168	0.016896	9.62E-08	0.009087	9.335117	0.004024	0.086909	1.034572	1.506056	1.698765
LFAOA	Standard Deviation	4.000326	0.031331	1.15E-07	0.011048	10.23433	0.00474	0.094563	1.164822	1.114527	1.663442

Table 3.47: Statistical Test result of Fixed Dimension Benchmark Functions for CAOA, RWAOA, LFAOA (10 Dimensions)												
Algorithm	**CAOA**				**RWAOA**				**LFAOA**			
Function No.	**Wilcoxon rank sum test**		**T-Test**		**Wilcoxon rank sum test**		**T-Test**		**Wilcoxon rank sum test**		**T-Test**	
	p-rank	**h-rank**	**p-test**	**t-test**	**p-rank**	**h-rank**	**p-test**	**t-test**	**p-rank**	**h-rank**	**p-test**	**t-test**
F14	0.149448706	0	0	0.09581603	0.20620549	0	0	0.41728829	1	0	0	0.88325653
F15	0.270705338	0	0	0.252032428	0.78445977	0	0	0.08700574	0.30417682	0	0	0.79732188
F16	3.02E-11	1	1	1.21E-13	0.31118764	0	0	0.34349183	0.21156124	0	0	0.35018738
F17	3.69E-11	1	1	9.20E-06	0.25188082	0	0	0.91238001	0.53951032	0	0	0.52428661
F18	0.001952677	1	0	0.110059513	0.18089953	0	0	0.09607184	0.6952154	0	0	0.78647964
F19	3.02E-11	1	1	2.36E-10	0.92344213	0	0	0.61527579	0.79584554	0	0	0.79014103
F20	3.02E-11	1	1	3.63E-16	0.42038633	0	0	0.2362264	0.12597019	0	0	0.16090947
F21	0.830255284	0	0	0.755899361	0.31118764	0	0	0.42610616	0.71718881	0	0	0.52286367
F22	0.153667235	0	0	0.162151749	0.09049036	0	0	0.11058683	0.2009489	0	0	0.13874029
F23	0.739398819	0	0	0.992827093	0.13345409	0	0	0.13169673	0.07012659	0	1	0.04155308

Table 3.48: Statistical Test result of Fixed Dimension Benchmark Functions for CAOA, RWAOA, LFAOA (30 Dimensions)[98]												
Algorithm	**CAOA**				**RWAOA**				**LFAOA**			
Function No.	**Wilcoxon rank sum test**		**T-Test**		**Wilcoxon rank sum test**		**T-Test**		**Wilcoxon rank sum test**[98]		**T-Test**	
	p-rank	**h-rank**	**p-test**	**t-test**	**p-rank**	**h-rank**	**p-test**	**t-test**	**p-rank**	**h-rank**	**p-test**	**t-test**
F14	0.520145	0	0	0.471522	0.16237502	0	0	0.12001829	0.096262831	0	0	0.152869181
F15	0.750587232	0	0	0.249501873	0.77311994	0	0	0.97814598	0.491782957	0	0	0.808216304
F16	3.02E-11	1	1	4.01E-12	0.25188082	0	0	0.28492132	0.761828346	0	0	0.789463877
F17	1.86E-09	1	1	8.10E-07	0.50114367	0	0	0.97759933	0.264326213	0	0	0.807877294
F18	1.19E-06	1	1	0.03830275	0.01221194	1	0	0.0504197	0.171450047	0	0	0.169431678
F19	3.02E-11	1	1	6.38E-11	0.6952154	0	0	0.93784239	0.510597937	0	0	0.440433815
F20	4.50E-11	1	1	2.00E-12	0.76182835	0	0	0.84706892	0.222572896	0	0	0.251684594
F21	0.011227764	1	1	0.02175062	0.21156124	0	0	0.18264571	0.270705338	0	0	0.226847844
F22	0.325526587	0	0	0.408791052	0.38709978	0	0	0.18043427	0.8766349	0	0	0.824173703
F23	0.000769729	1	1	0.003165676	0.98230705	0	0	0.88430541	0.074827008	0	1	0.011835674

Table 3.49: Statistical Test result of Fixed Dimension Benchmark Functions for CAOA, RWAOA, LFAOA (50 Dimensions)												
Algorithm	**CAOA**				**RWAOA**				**LFAOA**[98]			
Function No.	**Wilcoxon rank sum test**		**T-Test**		**Wilcoxon rank sum test**		**T-Test**		**Wilcoxon rank sum test**		**T-Test**	
	p-rank	**h-rank**	**p-test**	**t-test**	**p-rank**	**h-rank**	**p-test**	**t-test**	**p-rank**	**h-rank**	**p-test**	**t-test**
F14	0.217016825	0	0	0.739283893	0.739398819	0	0	0.818908424	0.93519197	0	0	0.87895956
F15	0.061451911	0	1	0.02758378	0.149448706	0	0	0.06179697	0.65204362	0	0	0.0736713
F16	3.02E-11	1	1	4.24E-18	0.122352926	0	0	0.160633501	0.97051605	0	0	0.96797196
F17	9.92E-11	1	1	2.47E-05	0.899995037	0	0	0.527901252	0.7282653	0	0	0.80467975
F18	9.51E-06	1	0	0.285211497	0.520144612	0	0	0.488670206	0.93519197	0	0	0.53628936
F19	5.07E-10	1	1	1.46E-10	0.569220164	0	0	0.370359482	0.27070534	0	0	0.18837475
F20	8.15E-11	1	1	3.72E-15	0.739398819	0	0	0.728426145	0.09925761	0	0	0.15476367
F21	0.003338612	1	1	0.000658581	0.784459769	0	0	0.860991999	0.0191124	1	1	0.00990763
F22	0.371077032	0	0	0.201087101	0.750587232	0	0	0.638562425	0.73939882	0	0	0.84652556
F23	0.001952677	1	1	0.010131735	0.982307053	0	0	0.58262391	0.38709978	0	0	0.56560174

Table 3.50: Statistical Test result of Fixed Dimension Benchmark Functions for CAOA, RWAOA, LFAOA (100 Dimensions)												
Algorithm	**CAOA**				**RWAOA**				**LFAOA**			
Function No.	**Wilcoxon rank sum test**		**T-Test**		**Wilcoxon rank sum test**		**T-Test**		**Wilcoxon rank sum test**		**T-Test**	
	p-rank	**h-rank**	**p-test**	**t-test**	**p-rank**	**h-rank**	**p-test**	**t-test**	**p-rank**	**h-rank**	**p-test**	**t-test**
F14	0.610007552	0	0	0.359141405	0.446419436	0	0	0.693763574	0.379036311	0	0	0.854855186
F15	0.27718919	0	0	0.912245299	0.559230536	0	0	0.283394211	0.297271689	0	0	0.606215158
F16	3.02E-11	1	1	9.62E-14	0.318304227	0	0	0.68673343	0.717188814	0	0	0.803038766
F17	1.61E-10	1	1	4.69E-08	0.379036311	0	0	0.092337053	0.818745653	0	0	0.434506508
F18	0.000212646	1	0	0.10169482	0.290472149	0	0	0.133918124	0.11536236	0	0	0.160710928
F19	3.02E-11	1	1	2.61E-11	0.641423523	0	0	0.260239974	0.270705338	0	0	0.397041358
F20	3.02E-11	1	1	1.75E-14	0.818745653	0	0	0.835382255	0.750587232	0	0	0.914222625
F21	0.005569939	1	1	0.034162786	0.706171488	0	0	0.684317243	0.8766349	0	0	0.863595511
F22	0.001114256	1	1	0.023979999	0.641423523	0	0	0.825344607	0.096262831	0	0	0.082513861
F23	0.695215399	0	0	0.9373123	0.994101921	0	0	0.9506226	0.318304227	0	0	0.386318326

Table 3.51: Simulation Time for Fixed Benchmark Function using CAOA, RWAOA, LFAOA (10 Dimensions)									
Function No.	**CAOA**	**RWAOA**	**LFAOA**	**CAOA**	**RWAOA**	**LFAOA**	**CAOA**	**RWAOA**	**LFAOA**
	Best Time (Sec)	**Best Time (Sec)**	**Best Time (Sec)**	**Avg. Time (Sec.)**	**Avg. Time (Sec.)**	**Avg. Time (Sec.)**	**Worst Time (Sec)**	**Worst Time (Sec)**	**Worst Time (Sec)**
F14	0.34375	0.34375	0.03125	0.376041667	0.39947917	0.053645833	0.4375	0.453125	0.09375
F15	0.03125	0.046875	0.03125	0.059375	0.08177083	0.053645833	0.09375	0.125	0.09375
F16	0.03125	0.03125	0.03125	0.047916667	0.05989583	0.054166667	0.078125	0.09375	0.09375
F17	0.03125	0.03125	0.03125	0.061979167	0.07604167	0.077604167	0.171875	0.21875	0.171875
F18	0.015625	0.03125	0.015625	0.0421875	0.06041667	0.048958333	0.078125	0.125	0.078125
F19	0.03125	0.046875	0.03125	0.054166667	0.07916667	0.0640625	0.140625	0.171875	0.09375
F20	0.03125	0.078125	0.03125	0.059375	0.10989583	0.061458333	0.09375	0.140625	0.109375
F21	0.046875	0.0625	0.046875	0.074479167	0.09479167	0.069791667	0.125	0.21875	0.109375
F22	0.046875	0.078125	0.0625	0.072916667	0.10572917	0.0796875	0.109375	0.15625	0.109375
F23	0.0625	0.09375	0.0625	0.086458333	0.11666667	0.09375	0.171875	0.203125	0.171875

Table 3.52: Simulation Time for Fixed Benchmark Function using CAOA, RWAOA, LFAOA (30 Dimensions)									
Function No.	**CAOA**	**RWAOA**	**LFAOA**	**CAOA**	**RWAOA**	**LFAOA**	**CAOA**	**RWAOA**	**LFAOA**
	Best Time (Sec)	**Best Time (Sec)**	**Best Time (Sec)**	**Avg. Time (Sec.)**	**Avg. Time (Sec.)**	**Avg. Time (Sec.)**	**Worst Time (Sec)**	**Worst Time (Sec)**	**Worst Time (Sec)**
F14	0.34375	0.359375	0.359375	0.385416667	0.386979167	0.386979167	0.4375	0.4375	0.46875
F15	0.03125	0.046875	0.03125	0.046875	0.070833333	0.041145833	0.078125	0.09375	0.09375
F16	0.03125	0.03125	0.03125	0.038020833	0.052083333	0.041666667	0.0625	0.078125	0.078125
F17	0.015625	0.03125	0.03125	0.052083333	0.072916667	0.054166667	0.28125	0.25	0.1875
F18	0.015625	0.03125	0.015625	0.0296875	0.044791667	0.030729167	0.046875	0.09375	0.046875
F19	0.03125	0.046875	0.03125	0.044791667	0.061458333	0.047395833	0.0625	0.125	0.09375
F20	0.03125	0.078125	0.03125	0.048958333	0.102083333	0.05	0.078125	0.15625	0.0625
F21	0.046875	0.078125	0.03125	0.0609375	0.091666667	0.0640625	0.109375	0.234375	0.140625
F22	0.046875	0.078125	0.046875	0.063541667	0.097395833	0.0703125	0.078125	0.15625	0.109375
F23	0.0625	0.09375	0.0625	0.077604167	0.10625	0.08125	0.109375	0.203125	0.125

Table 3.53: Simulation Time for Fixed Benchmark Function using CAOA, RWAOA, LFAOA (50 Dimensions)									
Function No.	**CAOA**	**RWAOA**	**LFAOA**	**CAOA**	**RWAOA**	**LFAOA**	**CAOA**	**RWAOA**	**LFAOA**
	Best Time (Sec)	**Best Time (Sec)**	**Best Time (Sec)**	**Avg. Time (Sec.)**	**Avg. Time (Sec.)**	**Avg. Time (Sec.)**	**Worst Time (Sec)**	**Worst Time (Sec)**	**Worst Time (Sec)**
F14	0.34375	0.359375	0.34375	0.374479167	0.384375	0.384375	0.421875	0.421875	0.4375
F15	0.015625	0.046875	0.03125	0.055208333	0.0796875	0.058333333	0.125	0.109375	0.109375
F16	0.015625	0.046875	0.03125	0.045833333	0.070833333	0.053645833	0.078125	0.09375	0.125
F17	0.015625	0.03125	0.015625	0.05625	0.080729167	0.066145833	0.171875	0.265625	0.171875
F18	0.015625	0.03125	0.03125	0.043229167	0.058854167	0.047395833	0.078125	0.140625	0.0625
F19	0.03125	0.046875	0.03125	0.069270833	0.086979167	0.065625	0.125	0.265625	0.15625
F20	0.046875	0.078125	0.046875	0.073958333	0.121354167	0.072916667	0.109375	0.171875	0.125
F21	0.046875	0.078125	0.03125	0.071354167	0.1109375	0.073958333	0.125	0.171875	0.109375
F22	0.0625	0.09375	0.0625	0.093229167	0.121354167	0.0875	0.15625	0.171875	0.140625
F23	0.0625	0.09375	0.0625	0.092708333	0.1203125	0.099479167	0.140625	0.1875	0.15625

Table 3.54: Simulation Time for Fixed Benchmark Function using CAOA, RWAOA, LFAOA (100 Dimensions)									
Function No.	**CAOA**	**RWAOA**	**LFAOA**	**CAOA**	**RWAOA**	**LFAOA**	**CAOA**	**RWAOA**	**LFAOA**
	Best Time (Sec)	**Best Time (Sec)**	**Best Time (Sec)**	**Avg. Time (Sec.)**	**Avg. Time (Sec.)**	**Avg. Time (Sec.)**	**Worst Time (Sec)**	**Worst Time (Sec)**	**Worst Time (Sec)**
F14	0.34375	0.359375	0.03125	0.3703125	0.373958333	0.051041667	0.453125	0.4375	0.09375
F15	0.03125	0.046875	0.03125	0.052604167	0.075	0.051041667	0.078125	0.203125	0.09375
F16	0.03125	0.03125	0.03125	0.051041667	0.059375	0.052604167	0.078125	0.078125	0.078125
F17	0.015625	0.03125	0.015625	0.052604167	0.079166667	0.0609375	0.140625	0.234375	0.171875
F18	0.015625	0.03125	0.015625	0.039583333	0.051041667	0.044270833	0.0625	0.09375	0.0625
F19	0.03125	0.046875	0.03125	0.052604167	0.075	0.052604167	0.09375	0.1875	0.09375
F20	0.03125	0.078125	0.03125	0.057291667	0.097395833	0.0546875	0.078125	0.171875	0.078125
F21	0.046875	0.0625	0.046875	0.061979167	0.096354167	0.068229167	0.09375	0.234375	0.109375
F22	0.046875	0.078125	0.046875	0.071875	0.100520833	0.078645833	0.09375	0.203125	0.09375
F23	0.0625	0.078125	0.0625	0.0875	0.111458333	0.0796875	0.109375	0.203125	0.171875

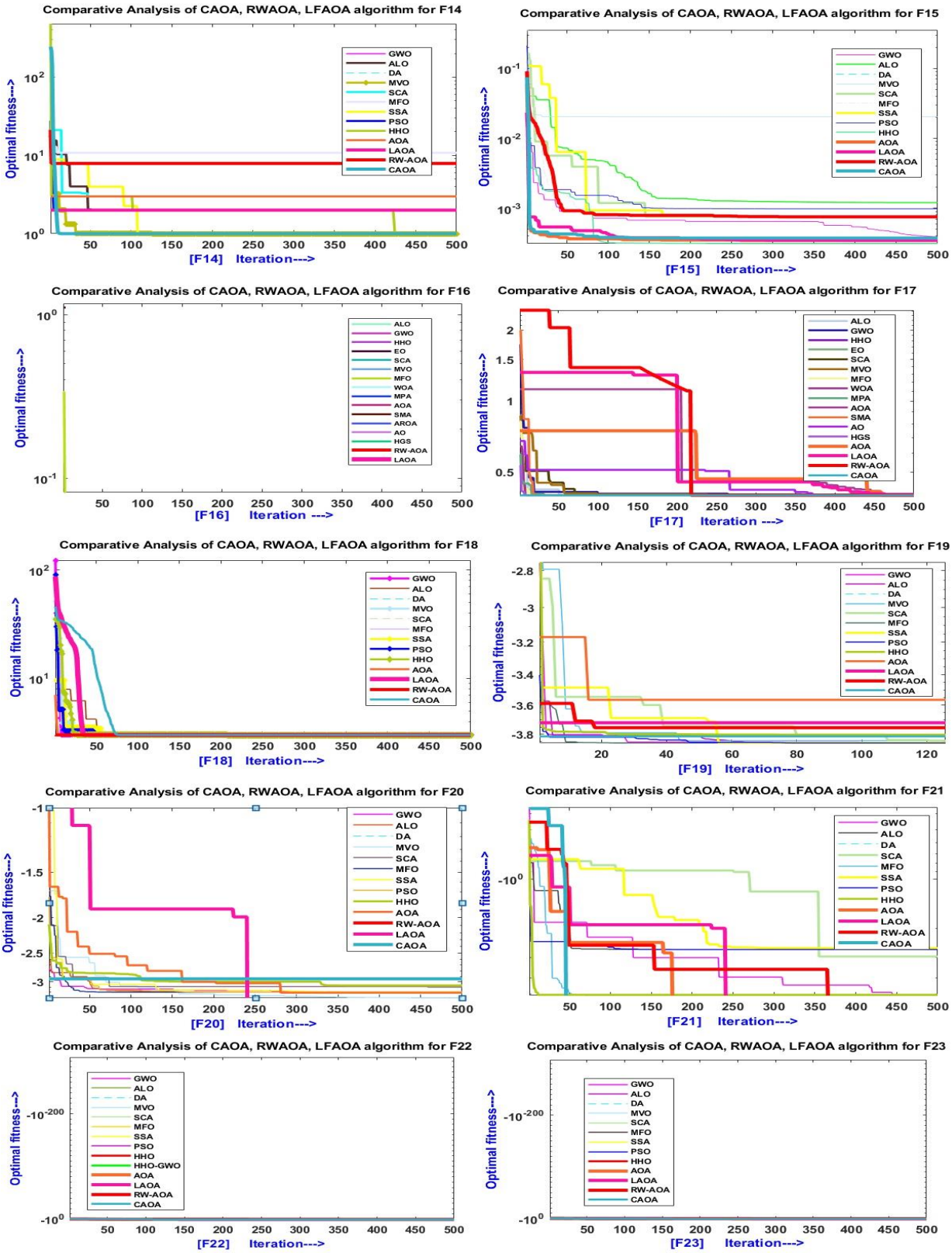

Figure 3.28: Comparison convergence curve for Fixed Dimensions (F14-F23)

3.11 Multidisciplinary Engineering Design Problem

The explanations for each engineering design problem are provided in this section. Each multidisciplinary engineering design problem's numerical analysis and constraints are also taken into account. In-depth explanations are provided for eleven types of engineering design issues. The three-bar truss issue, the compression design, the pressure-vessel design, the welded beam, the gear train, the cantilever beam design, the speed reducer, the rolling elements, the Belleville spring, the multi-disc clutch brake issue, and the I-beam design issue are all put through their paces. The proposed optimization techniques are used to simulate each design problem. The results of engineering design issues using CAOA, RWAOA, and LFAOA are presented in the tables. **Table 3.55** illustrate the Engineering Design Problems Functions result using CAOA, RWAOA, LFAOA. **Table 3.56** illustrate the Quartile Result for Engineering Function (EF1 to EF11). **Table 3.57** illustrate the Simulation time for EF1 to EF10 Function (EF) using CAOA, RWAOA, LFAOA. **Table 3.58** illustrate the Comparative result analysis of Gear Train problem with other methods. **Table 3.59** illustrate the Relative analysis of RWAOA for multiple disc clutch brake design with other algorithms. **Table 3.60** illustrate the Speed reducer design problem cost comparison with other methods. **Table 3.61** illustrate the Rolling Element Design variables result of LAOA comparing with other methods. **Table 3.62** illustrate the Three Bar Truss Design Result of CAOA, RWAOA, LFAOA compared with other methods. **Table 3.63** illustrate the Comparative analysis of CAOA, RWAOA, LFAOA with classical heuristic algorithms for Pressure Vessel Design problem. **Table 3.64** illustrate the Cantilever Beam Design problem comparing result with other methods. **Table 3.65** illustrate the Compression Spring Design problem result by comparing with other methods. **Table 3.66** illustrate the Welded Beam Design problem result comparing with other methods. **Table 3.67** illustrate the Comparative result of Belleville spring design variables using others methods. **Figure 3.29** illustrate the Convergence curve for Special Engineering Design Problem (S1-S11) with CAOA, RWAOA, LFAOA optimization algorithm. **Figure 3.30** Box Diagram of Special trial run for Engineering Design Problem (EF1-EF11).

Table 3.55: Engineering Design Problems Functions Result Using CAOA, RWAOA, LFAOA												
Algorithm	**Engineering Functions**	**EF1**	**EF2**	**EF3**	**EF4**	**EF5**	**EF6**	**EF7**	**EF8**	**EF9**	**EF10**	**EF11**
CAOA	**Index**	15	7	21	8	2	12	4	13	13	15	2
RWAOA	**Index**	22	13	7	23	10	23	2	10	4	27	10
LFAOA	**Index**	21	27	23	2	1	9	8	8	7	20	11
CAOA	**Mean**	271.09277	3190.9216	161074.11	3.93E+13	2.226E+10	-76357.85	0.527282	1.66E-08	2.8621162	3.4835619	0.0066263
RWAOA	**Mean**	266.44745	3173.5001	53669.388	0.0153418	2.2605018	-75432	0.4472692	1.04E-08	2.5246558	2.7579927	0.0066265
LFAOA	**Mean**	265.53066	3150.4186	47284.705	0.0156939	2.2624421	-72052.86	0.4470799	5.90E-09	2.6458473	2.2443859	0.0066264
CAOA	**Std.**	7.5045249	26.098656	112914.48	3.46E+13	1.14E+11	3786.8146	0.0209854	2.05E-08	0.3621563	1.6819333	1.90E-07
RWAOA	**Std.**	4.5983362	39.607177	66252.646	0.0056024	0.2970651	4586.9303	0.010844	1.81E-08	0.2199146	0.9890221	5.16E-07
LFAOA	**Std.**	3.3438434	49.084262	58077.701	0.0063847	0.2674583	7115.0931	0.0090621	7.21E-09	0.2758555	0.6536162	3.70E-07
CAOA	**Best**	264.05097	3100.0423	35717.104	0.0131927	1.8811312	-82732.4	0.5070689	8.43E-13	2.4663515	1.6234197	0.0066262
RWAOA	**Best**	263.9501	3086.3419	8817.463	0.0131946	1.8631382	-84060.05	0.4103601	9.48E-12	2.2223211	1.4309722	0.0066261
LFAOA	**Best**	263.94986	3061.7011	10379.513	0.0131947	1.8683383	-82452.74	0.4203728	1.78E-12	2.1393908	1.5735425	0.0066261
CAOA	**Worst**	282.84271	3218.6864	442030.1	1.13E+14	6.25E+11	-66536.3	0.5592473	9.63E-08	4.5461866	7.6432546	0.0066269
RWAOA	**Worst**	282.84271	3219.4399	284621.57	0.0320299	2.8962656	-64688.74	0.4678317	6.81E-08	3.1001085	5.5021134	0.0066286
LFAOA	**Worst**	282.84271	3218.7713	266625.43	0.0329073	2.7636071	-56056.53	0.4613565	2.44E-08	3.3285856	4.4559467	0.0066279
CAOA	**Median**	267.3573	3194.5627	122914.33	5.32E+13	2.6835015	-76578.43	0.5165322	1.25E-08	2.7745231	2.8443156	0.0066262
RWAOA	**Median**	265.25475	3191.1147	31647.462	0.0132479	2.2874112	-76369.13	0.4484954	1.69E-09	2.4922491	2.5972564	0.0066262
LFAOA	**Median**	264.87307	3160.0031	21884.333	0.0132357	2.2735629	-73049.4	0.4469935	1.91E-09	2.7196299	2.0985774	0.0066265
CAOA	**p-rank**	2.52E-05	0.0060971	1.17E-09	6.04E-07	1.34E-05	0.0467558	3.01E-11	0.0070611	1.87E-05	0.0107626	0.0020898
RWAOA	**p-rank**	0.166819	0.1023263	0.1808995	0.3749706	0.5792942	0.1761275	0.2972717	0.8014577	0.9234421	0.2518808	0.2164042
LFAOA	**p-rank**	1	0.7282653	0.5996895	0.7958317	0.7618284	0.6414235	0.2282301	0.835943	0.0849997	0.2972717	0.1206367
CAOA	**h-rank**	1	1	1	1	1	1	1	1	1	1	1
RWAOA	**h-rank**	0	0	0	0	0	0	0	0	0	0	0
LFAOA	**h-rank**	0	0	0	0	0	0	0	0	0	0	0
CAOA	**p-test**	1	1	1	1	0	1	1	0	1	1	1
RWAOA	**p-test**	0	0	0	0	0	0	0	0	0	0	0
LFAOA	**p-test**	0	0	0	0	0	0	0	0	0	0	0
CAOA	**t-test**	0.0008177	0.0001315	4.60E-07	8.58E-07	0.2940103	0.0157847	6.04E-18	0.1508253	0.0014518	0.0157535	0.0039608
RWAOA	**t-test**	0.3967785	0.1037324	0.0601048	0.8521757	0.6203164	0.0674277	0.5362232	0.8570219	0.6857684	0.3727323	0.2465038
LFAOA	**t-test**	0.9860599	0.809229	0.0776232	0.6954606	0.6221746	0.7336031	0.4218321	0.3637952	0.301771	0.2388317	0.1139455

Table 3.56: Quartile Result for Engineering Function (EF1 to EF11)												
Function		**F1**	**F2**	**F3**	**F4**	**F5**	**F6**	**F7**	**F8**	**F9**	**F10**	**F11**
Algorithm	**No. of trials**	**30**	**30**	**30**	**30**	**30**	**30**	**30**	**30**	**30**	**30**	**30**
CAOA	**Min. value**	264.05097	3100.0423	35717.104	0.0131927	1.8811312	-82732.4	0.507069	8.43E-13	2.4663515	1.6234197	0.0066262
RWAOA	**Min. value**	263.9501	3086.3419	8817.463	0.0131946	1.8631382	-84060.05	0.4103601	9.48E-12	2.2223211	1.4309722	0.0066261
LFAOA	**Min. value**	263.94986	3061.7011	10379.513	0.0131947	1.8683383	-82452.74	0.4203728	1.78E-12	2.1393908	1.5735425	0.0066261
CAOA	**Max. value**	282.84271	3218.6864	442030.1	1.13E+14	6.25E+11	-66536.3	0.5592473	9.63E-08	4.5461866	7.6432546	0.0066269
RWAOA	**Max. value**	282.84271	3219.44	284621.57	0.0320299	2.8962656	-64688.74	0.4678317	6.81E-08	3.1001086	5.5021134	0.0066286
LFAOA	**Max. value**	282.84271	3218.7713	266625.43	0.0329073	2.7636071	-56056.53	0.4613565	2.44E-08	3.3285856	4.4559467	0.0066279
CAOA	**Mean Value**	271.09277	3190.9216	161074.11	3.93E+13	2.23E+10	-76357.85	0.527282	1.66E-08	2.8621162	3.4835619	0.0066263
RWAOA	**Mean Value**	266.44745	3173.5001	53669.388	0.0153418	2.2605018	-75432	0.4472692	1.04E-08	2.5246558	2.7579927	0.0066265
LFAOA	**Mean Value**	265.53065	3150.4186	47284.705	0.0156939	2.2624421	-72052.86	0.4470799	5.90E-09	2.6458473	2.2443859	0.0066264
CAOA	**Median**	267.3573	3194.5627	122914.33	5.32E+13	2.6835015	-76578.43	0.5165322	1.25E-08	2.7745231	2.8443156	0.0066262
RWAOA	**Median**	265.25475	3191.1147	31647.462	0.0132479	2.2874112	-76369.13	0.4484954	1.69E-09	2.4922491	2.5972564	0.0066262
LFAOA	**Median**	264.87307	3160.0031	21884.333	0.0132357	2.2735629	-73049.4	0.4469934	1.91E-09	2.7196299	2.0985774	0.0066265
CAOA	**First Quartile (25th Percentile)**	265.4456	3189.3163	64253.706	0.0133815	2.5182815	-78660.74	0.5080571	3.14E-09	2.7446235	2.175503	
RWAOA	**First Quartile (25th Percentile)**	264.47978	3142.2869	15761.64	0.0132155	1.9949453	-78999.62	0.4423581	2.68E-10	2.3882415	1.9911562	0.0066261
LFAOA	**First Quartile (25th Percentile)**	264.39297	3103.7019	15497.596	0.0132047	2.0198316	-76983.63	0.4413711	3.10E-10	2.3817813	1.7161303	0.0066262

CAOA	**Second Quartile (50th Percentile)**	267.3573	3194.5627	122914.33	5.32E+13	2.6835015	-76578.43	0.5165322	1.25E-08	2.7745231	2.8443156	0.0066262
RWAOA	**Second Quartile (50th Percentile)**	265.25475	3191.1147	31647.462	0.0132479	2.2874112	-76369.13	0.4484954	1.69E-09	2.4922491	2.5972564	0.0066262
LFAOA	**Second Quartile (50th Percentile)**	264.87307	3160.0031	21884.333	0.0132357	2.2735629	-73049.4	0.4469934	1.91E-09	2.7196299	2.0985774	0.0066265
CAOA	**Third Quartile (75th Percentile)**	282.84271	3201.6875	255372.45	6.66E+13	3.0487238	-74359.02	0.5520741	1.63E-08	2.8714859	4.3874931	0.0066265
RWAOA	**Third Quartile (75th Percentile)**	265.77243	3199.0987	54048.393	0.0133407	2.4224016	-72325.96	0.4534976	1.37E-08	2.6366328	3.4943778	0.0066267
LFAOA	**Third Quartile (75th Percentile)**	265.49006	3194.9573	45904.715	0.0132649	2.5200803	-66871.43	0.4544259	9.05E-09	2.8141054	2.5345532	0.0066265
CAOA	**Semi Interquartile Deviation**	8.6985581	6.1855888	95559.37	3.33E+13	0.2652211	2150.864	0.0220085	6.59E-09	0.0634312	1.1059951	
RWAOA	**Semi Interquartile Deviation**	0.6463267	28.405871	19143.376	6.26E-05	0.2137282	3336.8292	0.0055698	6.74E-09	0.1241956	0.7516108	3.06E-07
LFAOA	**Semi Interquartile Deviation**	0.5485434	45.627689	15203.56	3.01E-05	0.2501244	5056.1017	0.0065274	4.37E-09	0.2161621	0.4092115	1.67E-07
CAOA	**Number of outliers**	0	2	0	0	5	0	0	2	2	0	0
RWAOA	**Number of outliers**	3	0	2	4	0	0	0	4	0	0	1
LFAOA	**Number of outliers**	1	0	4	4	0	0	0	0	0	1	1
CAOA	**Std.**	7.5045249	26.098656	112914.48	3.46E+13	1.14E+11	3786.8146	0.0209854	2.05E-08	0.3621563	1.6819333	1.90E-07
RWAOA	**Std.**	4.5983362	39.607177	66252.646	0.0056024	0.2970651	4586.9303	0.010844	1.81E-08	0.2199146	0.9890221	5.16E-07
LFAOA	**Std.**	3.3438434	49.084262	58077.701	0.0063847	0.2674583	7115.0931	0.0090621	7.21E-09	0.2758555	0.6536162	3.70E-07

Table 3.57: Simulation time for EF1 to EF10 Function (EF) using CAOA, RWAOA, LFAOA

Algorithm	CAOA	RWAOA	LFAOA	CAOA	RWAOA	LFAOA	CAOA	RWAOA	LFAOA
Engineering Function	**Best Time (Sec)**	**Best Time (Sec)**	**Best Time (Sec)**	**Average Time (Sec.)**	**Average Time (Sec.)**	**Average Time (Sec.)**	**Worst Time (Sec)**	**Worst Time (Sec)**	**Worst Time (Sec)**
EF1	0.0625	0.09375	0.0625	0.146875	0.2046875	0.165104167	0.40625	0.609375	0.46875
EF2	0.09375	0.234375	0.125	0.2015625	0.3421875	0.205729167	0.609375	0.890625	0.625
EF3	0.078125	0.140625	0.078125	0.117708333	0.19375	0.121875	0.1875	0.28125	0.21875
EF4	0.078125	0.109375	0.078125	0.1140625	0.161979167	0.115625	0.171875	0.25	0.1875
EF5	0.078125	0.15625	0.09375	0.131770833	0.239583333	0.14375	0.359375	0.8125	0.484375
EF6	0.109375	0.640625	0.125	0.1609375	0.954166667	0.166666667	0.265625	1.328125	0.375
EF7	0.078125	0.1875	0.09375	0.1125	0.221875	0.121354167	0.171875	0.28125	0.15625
EF8	0.046875	0.140625	0.0625	0.086979167	0.177604167	0.094791667	0.140625	0.234375	0.125
EF9	0.0625	0.15625	0.078125	0.114583333	0.189583333	0.116666667	0.28125	0.25	0.1875
EF10	0.078125	0.1875	0.078125	0.114583333	0.23125	0.121875	0.203125	0.3125	0.15625
EF11	0.0625	0.140625	0.078125	0.1	0.188020833	0.108333333	0.171875	0.234375	0.171875

Table 3.58: Comparative result analysis of Gear Train problem with other methods

METHOD		CAOA	RWAOA	LFAOA	GeneAS [98]	Kannan and Kramer [98]	Sandgren [113]
Optimal values for variables	$g1$	55	55	55	50	41	60
	$g2$	33	35	33	33	33	45
	$g3$	14	15	14	14	15	22
	$g4$	17	16	16	17	13	18
Optimum fitness		0.141321	0.14213	0.141123	0.144242	0.144242	0.144124

Table 3.59: Relative analysis of RWAOA for multiple disc clutch brake design with other algorithms

METHOD		CAOA	RWAOA	LFAOA	NSGA-II[98]	TL-BO[82]	AM-DE
Fitness variables	$x1$	50	50	50	70	70	70
	$x2$	80	80	80	90	90	90
	$x3$	1.734092	1.784092	1.764092	3	3	3
	$x4$	5	5	5	1.5	1	1
	$x5$	50	50	50	1000	810	810
Optimum fitness		0.0065012	0.006738	0.006626	0.4704	0.31365	0.3136566

Table 3.60: Speed reducer design problem cost comparison with other methods

Method		CAOA	RWAOA	LFAOA	MDE[98]	PSO-DE[112]	MBA[98]
Variables of Fitness Values	z_1	3.6	3.6	3.6	3.50001	3.5	3.5
	z_2	0.7	0.7	0.7	0.7	0.7	0.7
	z_3	17	17	17	17	17	17
	z_4	7.3	7.3	8.3	7.300156	7.3	7.300033
	z_5	8.3	8.3	8.007456	7.800027	7.8	7.715772
	z_6	3.354388	3.354388	3.358835	3.350221	3.350214	3.350218
	z_7	5.367489	5.367489	5.303089	5.286685	5.286683	5.286654
Optimum Cost		3100.042	3086.3419	3061.70114	2996.35669	2996.34817	2994.48245

Table 3.61: Rolling Element Design variables result of LAOA comparing with other methods.

METHODS		CAOA	RWAOA	LFAOA	WCA [65]	SCA [51]	MFO [66]	MVO [7]
Values for Variables	r_1	0125	0125	0125	0125.72	0125	0125	0125.6002
	r_2	21.31895	21.30989	21.14436	21.423	21.03287	21.03287	21.3225
	r_3	10.6035	10.872	10.78227	10.0103	10.96571	10.96571	10.97338
	r_4	0.515	0.515	0.515	0.515	0.515	0.515	0.515
	r_5	0.515	0.515	0.515	0.515	0.515	0.515	0.515
	r_6	0.5	0.4	0.5	0.401514	0.5	0.5	0.5
	r_7	0.66529	0.7	0.7	0.659047	0.7	0.67584	0.68782
	r_8	00.3	00.3	00.3	00.300032	00.3	00.300214	00.301348
	r_9	00.02	00.02	00.02	00.040045	00.02778	00.02397	00.03617
	r_{10}	00.6	00.6	00.6	00.6	00.62912	00.61001	00.61061
Optimum fitness		**82732.3998**	**84060.1**	**82452.7**	85538.48	83431.11	84002.524	84491.266

Table 3.62: Three Bar Truss Design Result of CAOA, RWAOA, LFAOA compared with other methods							
ALOGRITHM		**CAOA**	**RWAOA**	**LFAOA**	**CS** [51]	**RAY AND SAY** [52]	**TSA** [52]
Optimal values for variables	*y*1	0.792215	0.78615	0.797268	0.789	0.795	0.788
	y2	0.399786	0.415934	0.384484	0.409	0.395	0.408
Optimal weight		264.051	263.9501	263.9498605	263.972	264.3	263.68

Table 3.63: Comparative analysis of CAOA, RWAOA, LFAOA with classical heuristic algorithms for Pressure Vessel Design problem												
Algorithm		CAOA	RWAOA	LFAOA	GWO [54]	GSA [18]	PSO [55]	GA [56]	DE [57]	ACO [23]	Lagrangian Multiplier [58]	Branch-bound [59]
Optimum Value	*Ts*	1.22888	1.02007	1.102815	0.8125	1.125	0.8125	0.8125	0.8125	0.8125	1.125	1.125
	Th	0.501813	0.75558	0.509999	0.4345	0.625	0.4375	0.4345	0.4375	0.4375	0.625	0.625
	R	40.85536	40.4069	47.08122	42.0892	55.9887	42.0913	40.3239	42.0984	42.1036	58.291	47.7
	L	194.8231	200	200	176.7587	84.4542	176.7465	200	176.6377	176.5727	43.69	117.701
Optimum Cost		6041.10399	8817.463	10379.5128	7016.962	6051.564	8538.84	6061.078	6059.75	6059.734	6059.089	7198.043

Table 3.64: Cantilever Beam Design problem comparing result with other methods									
Method		**CAOA**	**RWAOA**	**LFAOA**	**CS [61]**	**ALO [62]**	**SOS [63]**	**MMA [64]**	**GCA_I[64]**
Optimal values for variables	l1	0.05	0.05	0.05	6.0089	6.0181	6.0188	6.01	6.01
	l2	0.310416	0.310462	0.310463	5.3049	5.3114	5.3034	5.3	5.304
	l3	15	15	15	4.5023	4.4884	4.4959	4.49	4.49
	l4	0.05	0.05	0.05	3.5077	3.4975	3.499	3.49	3.498
	l5	0.310416	0.310462	0.310463	2.1504	2.1583	2.1556	2.15	2.15
Optimum weight		0.013192661	0.013195	0.01319467	1.33996	1.33996	1.33995	1.33999	1.34

Table 3.65: Compression Spring Design result by comparing with other methods											
METHOD		**CAOA**	**RWAOA**	**LFAOA**	**GWO**	**GSA**	**PSO**	**ES**	**GA**	**HS**	**DE**
Optimized value for Variables	'd'	0.189179	0.20082	0.199997	0.0516	0.0503	0.0517	0.052	0.0515	0.0512	0.0516
	'D'	3.792957	3.561784	3.53201	0.3567	0.3237	0.3576	0.364	0.3517	0.3499	0.3547
	'N'	9.820304	10	10	11.2889	13.5254	11.2445	10.89	11.632	12.076	11.4108
Optimum weight		1.88113115	1.863138	1.86833829	0.01195	0.01267	0.0127	0.0126	0.0126	0.0127	0.01267

Table 3.66: Welded Beam Design problem result comparing with other methods										
METHOD		**CAOA**	**RWAOA**	**LFAOA**	**GSA** [67]	**HS** [68]	**GA** [69]	**Random** [21]	**Simplex** [70]	**APPROX** [71]
Optimum Variables	**h**	80	78.10904	80	0.2442	0.1821	0.2489	0.4575	0.2792	0.2444
	l	104.8734	98.14844	100.0935	6.2231	3.857	6.173	4.7313	5.6256	6.2189
	t	1.5	1.5	1.5	8.2915	10	8.1789	5.0853	7.7512	8.2915
	b	1000	978.3937	1000	0.2443	0.2024	0.2533	0.66	0.2796	0.2444
Optimal Cost		0.507068948	0.41036	0.420373	1.88	2.3807	2.4331	4.1185	2.5307	2.3815

Table 3.67: Comparative result of Belleville spring design variables using others methods.						
Method		**CAOA**	**RWAOA**	**LFAOA**	**TLBO** [9]	**MBA** [72]
Values of Variables	$x1$	60	42.25549	11.07316	12.01	12.01
	$x2$	13.00186	13.40112	8.756127	10.0304	10.0304
	$x3$	39.94831	14.56819	0.209495	0.20414	0.20414
	$x4$	60	32.0235	0.2	0.2	0.2
Optimum fitness		8.43E-13	9.48E-12	2.139391	0.19896	0.19896

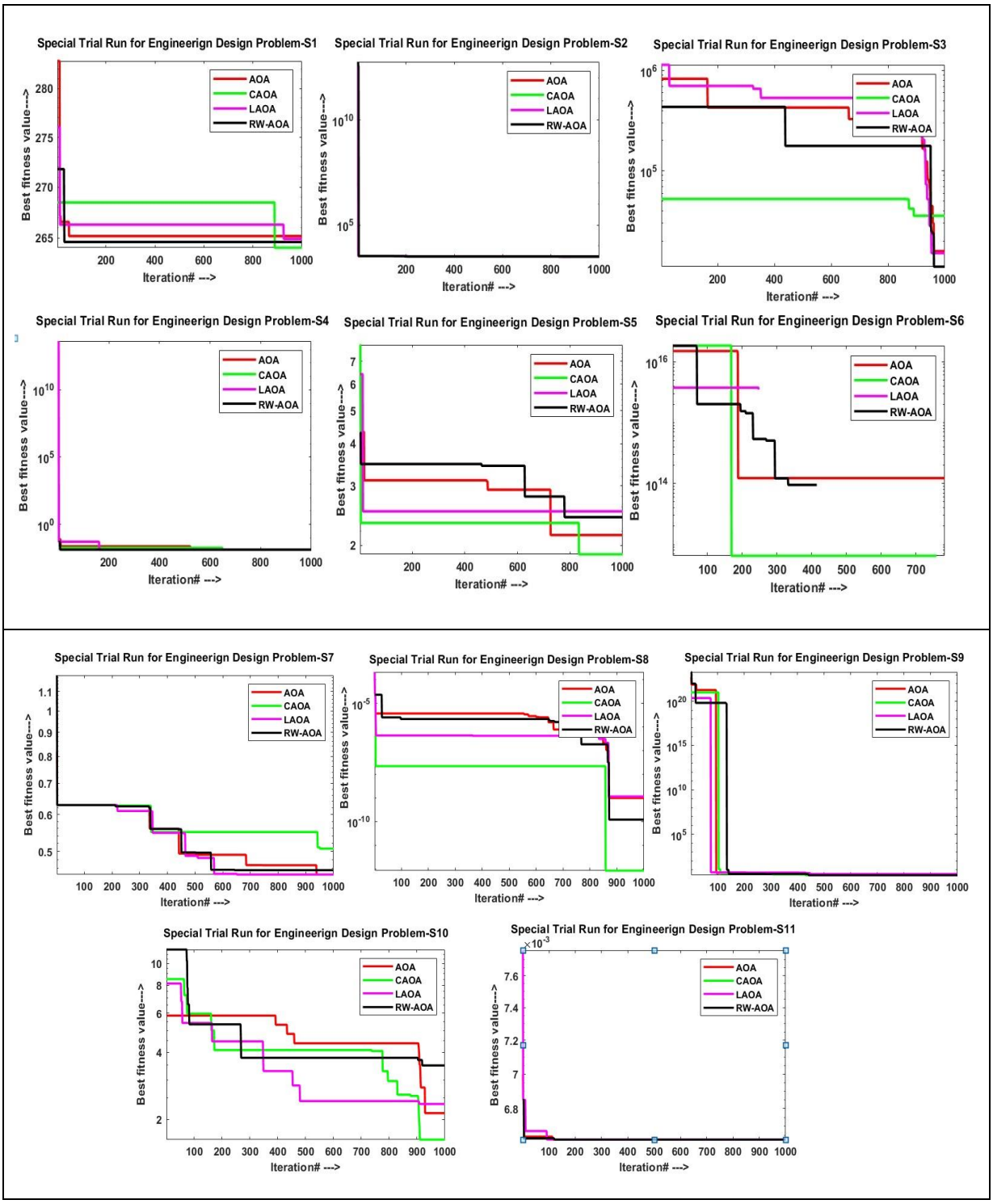

Figure 3.29: Convergence curve for Special Engineering Design Problem (S1-S11) with CAOA, RWAOA, LFAOA optimization algorithm

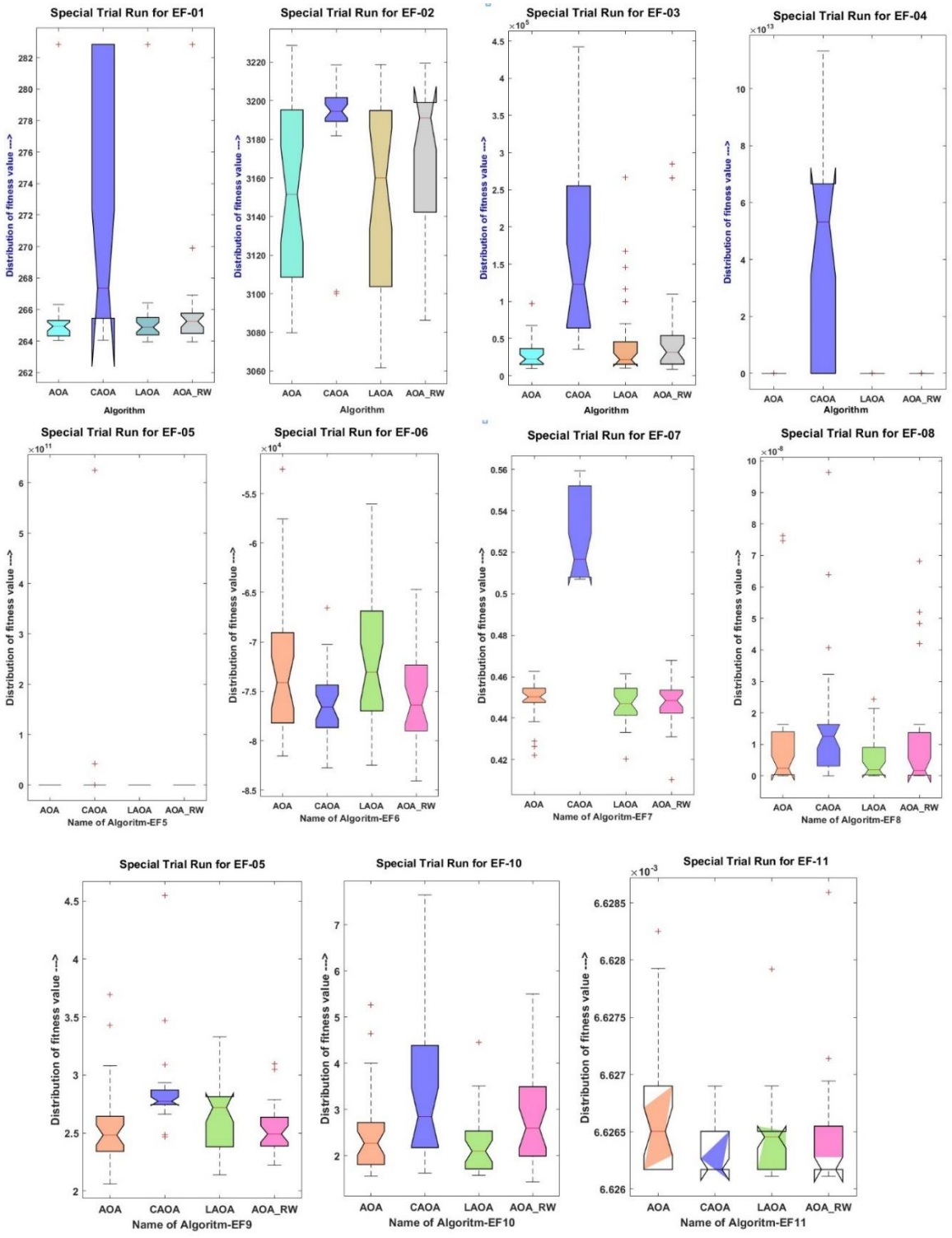

Figure 3.30: Box Diagram of Special trial run for Engineering Design Problem (EF1-EF11)

3.12 CONCLUSIONS

This chapter introduces novel optimization methodologies that utilize arithmetic operations, including addition, subtraction, multiplication, and division. The proposed algorithms, CAOA, RWAOA, and LFAOA, are based on chaotic map, random walk, and levy flight strategies, respectively. The algorithms are designed to improve the exploration and exploitation phases of existing arithmetic optimization algorithms. The detailed pseudocode and steps for each algorithm are presented. The focus of this chapter is on enhancing the exploitation phase of existing AOA optimizers using chaotic functions, namely CAOA, RWAOA, and LFAOA. Moreover, the exploration phase is enhanced using CAOA, RWAOA, and hRWAOA, and tested on both unimodal and multimodal standard benchmark issues, as well as multidisciplinary designing plan issues. The efficiency of the proposed optimization algorithms is validated through comparison with other existing optimization algorithms. In the upcoming chapters, the proposed algorithms will be used to solve various benchmark problems and the security constraint unit commitment problem, which integrates electric vehicles and renewable energy sources under different scenarios.

CHAPTER 4

SECURITY CONSTRAINT UNIT COMMITMENT PROBLEM

4.1 INTRODUCTION

An essential and difficult optimization problem in power systems is the security-constrained unit commitment problem. It involves taking into account a variety of operating and security constraints while scheduling the commitment and dispatch of power-generating units. The SCUC problem aims to reduce the total cost of producing electricity while maintaining the system's stability and dependability in a variety of situations. To ensure that the system operates within safe limits and can handle unexpected events like equipment failures, shifts in demand, or unexpected power outages, security constraints are added to the problem.

Because it contributes to ensuring the power grid's efficient, secure, and dependable operation, the SCUC issue is crucial for energy market participants and operators of power systems. The numerous generating units, transmission lines, and constraints that need to be taken into consideration make the issue complex. Subsequently, different numerical enhancement methods and calculations have been created to proficiently take care of the issue. Due to the increasing use of renewable energy sources and the requirement for power system operations that are both flexible and secure, the SCUC problem has received a significant amount of attention from researchers and practitioners in recent years [123].

This chapter aims to provide an overview of the SCUC problem and its significance to the operation of the power system in this context. Other power systems optimization tasks, such as economic dispatch, unit commitment, and optimal power flow, are also closely related to the SCUC problem. The large-scale, nonlinear, and dynamic nature of power systems, in addition to the uncertainties and variations in electricity demand, renewable energy sources, and contingencies, contribute to the complexity of SCUC. The SCUC problem can be solved using a variety of approaches, including dynamic programming,

mixed-integer linear programming, heuristic algorithms, and artificial intelligence. In order to enhance power system efficiency, dependability, and sustainability, researchers, engineers, and policymakers must have a thorough understanding of the SCUC problem [124]. The problem's main challenges and constraints are discussed, and various optimization strategies and algorithms that have been developed to address the issue are presented in the research. In addition, the research emphasizes recent advancements and potential future directions for SCUC research.

4.2 SECURITY CONSTRAINT UNIT COMMITMENT PROBLEM

The SCUC problem in power systems can be formulated mathematically as an optimization problem. The objective of the problem is to find the optimal dispatch of power generators subject to various constraints that ensure the reliable and secure operation of the power system. The formulation of the SCUC problem involves several decision variables, constraints, and an objective function. The decision variables in the SCUC problem are typically binary variables that represent the commitment status of the power generators. If a generator is committed, it must generate power during the optimization horizon, while if it is not committed, it must remain offline [17]. The power output of committed generators is represented by continuous variables. The constraints in the SCUC problem include various operational and physical constraints that must be satisfied. These constraints ensure that the power system operates within safe and stable limits. Some of the constraints include Generator ramping limits, Minimum and maximum power output limits, Start-up and shutdown costs, Transmission line capacity limits, Demand constraints etc.

When it comes to system security, a breach is an event that is deemed undesirable or seemingly impossible. In this particular case, the only security breach that has been taken into consideration is the inadequate generation capacity. To quantitatively measure the likelihood of the available generation capacity (which is the sum of the committed unit capacities) being lower than the load demand at a specific hour, a method known as Patton's security function has been developed and described.

$$S_p = \sum p_n r_n \tag{4.1}$$

Where, S_p= Patton's Security Functions

p_n= Probability or chance of the system being in state n.

r_n= A breach occurring while the system is in state n.

In the case where the available capacity is less than the loads, the value of r_n is set to 1; otherwise, it is set to 0. However, this condition only holds if the system load is deterministic, meaning it is known with complete certainty. The quantitative measure of system insecurity is denoted as S. Although, in theory, the sum over all possible system states is described by Equation (4.1) (which can be a very large number), practically, it is only necessary to consider states that reflect a relatively small number of units on forced outage. For instance, states where only two units are out are more realistic due to the low probability of occurrences of other types of states. At a specific load level, once the units to be committed have been determined based purely on economic considerations, the computation of the security function S is performed according to Equation (4.1). The equation that calculates the power output of each generator at a given t^{th} hour is a non-linear, non-smooth, and non-convex quadratic equation. The objective function of the security constraint unit commitment problem is revealed in the equation (4.2).

4.2.1 Objective Function

$$\min F_{k,t} = \sum_{k=1}^{NG}\sum_{t=1}^{NH}\left[(a_k P_{k,t}^2 + b_k P_{k,t} + c_k) \times U_{k,t} + SUC_k \times \{U_{k,t} \times (1 - U_{k,(t-1)})\} + SDC_k \times U_{k,t-1}(1 - U_{k,t}) \right] \tag{4.2}$$
$$\left(k = 1, 2, ..., NG(\text{Number of Generating Units}); \quad t = 1, 2, ..., \text{ Number of Hours}\right)$$

where, $F_{k,t}$ represent the cost associated with the k^{th} generating unit at the t^{th} hour and a_k, b_k, and c_k are its fuel and operational cost coefficients. $U_{k,t}$ and $(1 - U_{k,(t-1)})$ is the committed status of the k^{th} unit at t^{th} hour and $(t-1)^{th}$ hour respectively. SUC_k is the start-

up cost of the k^{th} unit at t^{th} hour. The total cost ($F_{k,t}$) for all the generating units (NG) for a particular time at t^{th} hour is given by the equation (4.1a).

4.2.2 Constraints of SCUC problem

The security constraint unit commitment problem is a complex optimization problem that involves multiple constraints. These constraints ensure that the power system operates safely, reliably, and efficiently. The following are some of the most common constraints that are considered in the SCUC problem:

4.2.2.1 System Power Balance

The power balance constraint ensures that the total power demanded by the power system is equal to the total power generated by the system, minus the power losses in the transmission lines. To ensure that the power system operates reliably and meets the demand for power, this constraint is essential [123]. In order for the system to be in power balance, the total power generated by the thermal unit needs to be the same as the amount of power needed during scheduled hours [125].

In the security constraint unit commitment problem, there is a load balance or system power balance constraint that ensures that the total generation of all the committed units at a particular hour 't' is greater than or equal to the power demand, P_D, at that hour t. This constraint is expressed mathematically as the sum of power generation, P, of all committed units, k, at hour t, being equal to P_{D_t}.

$$\sum_{k=1}^{NG} P_{tk} U_{tk} = P_{D_t} \qquad (\mathrm{t} = 1, 2, ..., Hours) \tag{4.3}$$

However, this equation does not take into account power loss in the system. If power loss is considered, then the equation can be modified to include hourly power loss, P_{L_t}.

$$\sum_{k=1}^{NG} P_{tk} U_{tk} = P_D + P_{Lk} \qquad (\mathrm{t} = 1, 2, ..., Hours) \tag{4.4}$$

To satisfy the power balance constraint and operating limit constraints, one unit is designated as the reference unit, and its power generation is constrained by the power balance equation. For random free unit power outputs, P_{tk}, where $k = (1, 2, ..., NG)$, and $P_{k(\min)} \le P_{tk} \le P_{k(\max)}$ are the minimum and maximum power outputs of unit k, the Rth reference unit's power output is constrained by the power balance equation at hour tR. This equation is expressed mathematically as the sum of power generation, P, of all committed units, k, at hour t, being equal to the power demand, P_{Dt}, plus the power loss, P_{Lt}, at that hour t, minus the power generation of the Rth reference unit at hour tR.

$$P_{tR} = P_t + P_{Lt} - \sum_{\substack{k=1 \\ k \neq R}}^{NG} P_{tk} \qquad (t = 1, 2, ..., Hour) \tag{4.5}$$

4.2.2.2 System Spinning Reserve Constraints

The Spinning Reserve Constraint (SRC) is a crucial element of the security constrained unit commitment method, which is a mathematical optimization model utilized for power system operation and planning. This model determines the best commitment and dispatch of generating units to satisfy electricity demand while also maintaining system security. The mathematical expression for spinning reserve constraints is given by equation (4.6).

$$\sum_{t=1}^{NG} P_{t(\max)} U_{tk} \ge P_{D_T} + SR_t \qquad (t = 1, 2, ..., Hour) \tag{4.6}$$

The optimal amount of spinning reserve is maintained in the SCUC problem process through the spinning reserve constraint, which is essential for ensuring system reliability and stability while minimizing costs. In equation (4.6) the maximum power for the time t hour is represented by $P_{t(max)}$, for the committed status U_{tk} is greater than or equal to maximum power demand P_{D_T} and spinning reserve SR_t for t hour. Skillful management of spinning reserves by system operators promotes efficient use of resources and enables customers to have access to power as needed.

4.2.2.3 Generating Unit Limits

The generation unit limits constraint is a significant aspect of the SCUC problem process that restricts the power output of each generating unit within certain minimum and maximum levels. By managing the available generating units to operate within these limits, system operators can ensure a dependable and economical supply of energy that meets the anticipated load, while also encouraging efficient use of resources.

$$P_{k(\min)} \le P_{tk} \le P_{k(\max)} \qquad (k = 1, 2, ..., NG; \quad \text{t=1,2,...,Hours}) \tag{4.7}$$

The generation unit limits constraint places restrictions on the amount of power that can be generated by each unit in the system. These constraints are usually expressed in terms of minimum and maximum power output levels, as well as a minimum up and down times for each unit.

4.2.2.4 Minimum up/Minimum down Time Constraints

In the SCUC problem process, the minimum up and down time constraint plays a significant role in regulating the amount of time that a generating unit must stay on or off before it can be turned on or off again. By carefully managing the use of generating units in adherence to these constraints, system operators can ensure the provision of dependable and cost-effective energy to fulfill the expected load, while also promoting the efficient use of resources.

$$T_{tk}^{ON} \ge MUT_k \qquad (\text{k} = 1, 2, ..., NG; \ t = 1, 2, ..., Hour) \tag{4.8}$$

In this equation, the symbol T_{tk}^{ON} represents the time duration that a unit k^{th} remains continuously operational in t hours, while MUT_k refers to the minimum time that a particular unit must remain active before it can be shut down again, also measured in hours. Both of these parameters are relevant to the k units being considered. After a unit has been turned off, it cannot be restarted until a certain minimum duration has elapsed, known as the "down-time" period. This constraint can be expressed mathematically as follows:

$$T_{tk}^{OFF} \ge MDT_k \qquad (\text{k} = 1, 2, ..., NG; \ t = 1, 2, ..., Hour) \tag{4.9}$$

In this context, the variable "T_{tk}^{OFF}" represents the length of time that the k^{th} unit has been continuously inactive in hours. Additionally, the parameter "MDT_k" refers to the minimum duration of inactivity required for that specific unit k, also measured in hours t.

4.2.2.5 Thermal Constraints for SCUC problem

Thermal constraints are a security constraint that is crucial to consider in the operation of power systems. These constraints set limits on the maximum power output of thermal generators, including coal, gas, or nuclear power plants. Such limits exist due to the physical constraints of their equipment or cooling systems. Typically, thermal constraints are stated as inequality constraints, which restrict the maximum power generation capacity of thermal generators. For instance, the capacity limit of a thermal generator could be articulated as follows:

$$P_{Thermal,t} \leq P_{Max} \tag{4.10}$$

Where $P_{Thermal,t}$ is the thermal output of the generator at time t, and P_{Max} is the maximum allowable thermal output. The operational limit of a thermal generator can be expressed as:

$$P_{Thermal,t} \leq \alpha \times P_{Max} \tag{4.11}$$

Where α is a safety factor that accounts for the generator's operating conditions and typically ranges between 0.85 to 0.95.

4.2.2.6 Crew Constraints

Crew constraints play a crucial role in ensuring the safe and efficient operation and maintenance of power systems. They establish a limit on the number of workers that can work on power system equipment, ensuring that maintenance and repair tasks are carried out effectively while maintaining a reliable power system. Crew constraints are usually expressed as a maximum limit on the number of workers assigned to a specific piece of equipment or area.

4.2.2.7 Initial Operating Status of Generation Units

In order to ensure that every unit meets its minimum up/down time requirements, the initial operating status of each unit must consider the previous day's schedule. This means that the starting status of each unit is influenced by its previous operating state and the minimum duration it must remain in that state before it can transition to another state. By factoring in these considerations, the initial operating status of each unit can be determined in a way that promotes system reliability and efficiency.

4.2.2.8 Transmission Line Loss Constraints

The inequality constraint, which restricts power flow on a transmission line based on its maximum capacity and anticipated resistance losses, is typically used to describe transmission line loss constraints. This constraint can be expressed mathematically as:

$$P_{mn} - R_{mn} \times (P_{mn}^2 + Q_{mn}^2)^{1/2} \leq S_{mn} \qquad (4.12)$$

where P_{mn} and Q_{mn} represent the transmission line's active and reactive power flows between nodes m and n, R_{mn} represents the line's resistance, and S_{mn} represents the maximum power flow limit on the line. The magnitude of the complex power flow is represented by the term $(P_{mn}^2 + Q_{mn}^2)^{1/2}$ which is used to calculate the losses caused by line resistance. The constraint ensures that the line's power flow does not exceed the maximum power flow limit, S_{mn}, while still taking these losses into account.

In the security-constrained unit commitment problem, where they are incorporated as constraints on the power flow between various power system nodes, transmission line loss constraints are an important consideration. These constraints ensure that power is not wasted or misdirected due to excessive losses on transmission lines and promote system reliability and efficiency.

4.3 METHODOLOGIES FOR SOLUTION OF THE SECURITY CONSTRAINT UNIT COMMITMENT PROBLEM

The study has utilized hybrid versions of the CAOA algorithm to solve a power system's security constraint unit commitment problem, taking into account physical constraints and the system of thermal power units. To create the hybrid optimizers, the general operators of various algorithms, such as the chaotic map, and the arithmetic optimization algorithm, have been combined recursively. The aim is to address various types of operational and physical constraints using stochastic and heuristic processes. In points, 4.3.1, 4.3.2, and 4.3.3, the constraints of the spinning reserve, minimum-up and minimum-down time, and de-commitment of excessive power-generating units, respectively, are described. The following sections discuss the suggested hybrid optimizers to obtain solutions for the profit-based unit commitment problem.

4.3.1 Spinning Reserve Constraint Repair

The minimum up-and-down time of each power unit and the duration of that k^{th} unit have been taken into consideration in order to meet the requirement for reserve capacity of various types of power units. According to the PSEUDO code shown in Figure 4.1, the reserve constraints need to be fixed.

Step 1: Arrange the power generators in a decreasing order based on their maximum capacity to generate power.

Step 2:

$$for\ k = 1\ to\ NG\ if\ u_{k,t} = 0 \quad then\ u_{k,t} = 1$$

$$else\ if\ \mathrm{T}_{k,t}^{OFF} \geq T_k^{MDT_k}$$

$$then\ T_{k,t}^{ON} = T_{k,t-1}^{ON} + 1 \ \text{ and } T_{k,t}^{OFF} = 0$$

Step 3: Check the newly generated power output of the units for validation.

Step 4: if $\sum_{k=1}^{NG} P_{k(\max)} u_{k,t} \geq P_{D_t} + R_t$.

If the condition is not met, proceed to step 2, otherwise terminate the algorithm.

Step 5: $T_{k,t}^{OFF} \leq T_k^{MDT_k}$ then do $l = t - T_{k,t}^{OFF} + 1$ and set $u_{k,t} = 1$

Step 6: Calculate $T_k^l = T_{k,l-1}^{ON} + 1$ and $T_{k,t}^{OFF} = 0$

Step 7: if $1 > t$, Check the power output of the generator to ensure its accuracy for

$$\sum_{k=1}^{NG} P_{k(\max)} U_{k,t} \geq P_{D_t} + R_t,$$

else, Increase the value of 1 by 1 and proceed to step 5.

Figure 4.1 PSEUDO code for Spinning Reserve Constraint

4.3.2 Addressing the Constraints related to Minimum up and Down time

The method utilized to meet the minimum downtime requirement of generating units involves the implementation of a particular repair mechanism.

The minimum up and down time restrictions necessitate specific power-generating units to remain active for a minimum duration prior to being shut down for maintenance or repairs. To ensure adherence to these requirements, a maintenance mechanism can be established.

for $t = 1$ *to* H

for $k = 1 : NG$, do $k = 1$

if $U_{k,t} = 1$, *do* $U_{k,(t-1)} = 0$, *if* $T_{k,t}^{OFF} < T_k^{MDT}$, do $U_{k,t} = 0$

else $U_{k,t} = 1$

end

end

if $U_{k,(t-1)} = 1$, *else if* $U_{k,t} = 0$, *if* $T_{k,t}^{OFF} < MUT_k$ *do* $U_{k,t} = 1$

else $U_{k,t} = 0$

if $k = NG$ *then* stop or else *do* $k = 1$ and follow the steps

else

end

end

Figure 4.2 PSEUDO code for Minimum up/down time constraints repairing

4.3.3 Excessive Generating Unit De-commitment

De-commitment of excessive generating units is a process that involves reducing the number of active generating units in a power system to optimize efficiency and reduce costs. This can be achieved through a de-commitment algorithm that determines which units are producing more power than is necessary and de-commits them.

```
for t = 1 : Hour(H)
    for k = 1 : NG
        do g = t(NG + 1 − k) and calculate generating power P_1 = P_k(max) × (U_tk)'
            if u_tk = 1 then
                if P_1 − P_max(g) ≥ P_Dt + R_t then
                    if T_t,g^ON > MUT_g | (T_t,g^ON = 1) then
                        do u_t,k = 0 and T_t,g^ON = 0
                        if t == 1 then
                            do T_t,g^OFF = T_t,g^OFF + 1
                        else
                        do T_t,g^OFF = T_t−1,g^OFF + 1
                        end
                    else
                      continue;
                    end
                else
                    interruption;
                end
            end
        end
```

Input:

- Active generating unit

- Power demand

- De-commitment threshold

Output:

- De-committed generating units

Algorithm:

1. Calculate total power output of all active generating units

2. If total power output exceeds power demand, proceed to step 3, otherwise return an empty list for de-committed units

3. Calculate excess power (total power output - power demand)

4. Sort active generating units by their incremental cost of producing power (i.e., the cost of producing an additional unit of power)

5. Iterate over the list of active generating units, starting with the unit with the highest incremental cost

6. For each unit, calculate the amount of power that can be de-committed without exceeding the de-commitment threshold (i.e., the minimum amount of power that can be produced by the unit)

7. If the de-committed power is less than the excess power, de-commit the unit and subtract the de-committed power from the excess power

8. Repeat step 6 to 7 for the next generating unit until the excess power is zero or all generating units have been considered

9. Return the list of de-committed generating units

4.3.4 Hybrid Chaotic Arithmetic Optimization Algorithm

The chaotic arithmetic optimization algorithm is a metaheuristic optimization technique inspired by the chaotic dynamics of non-linear systems. It has been applied to various optimization problems and has shown promising results in terms of convergence speed and solution quality. In this context, the CAOA algorithm is applied to solve the security-constrained unit commitment problem, which is a crucial task in power system planning and operation.

Pseudo code for the Chaotic Arithmetic Optimization algorithm for the SCUC problem:

The security-constrained unit commitment problem is a challenging optimization problem that involves determining the optimal schedule of power generators to meet the power

demand while satisfying several security constraints. The chaotic arithmetic optimization algorithm is a metaheuristic optimization algorithm that is inspired by the chaotic behavior of some nonlinear systems. Here is a procedure for solving the SCUC problem using the chaotic arithmetic optimization algorithm:

Step 1: Define the SCUC problem and its constraints.

The SCUC problem involves determining the optimal schedule of power generators subject to several constraints, such as power balance, generator ramp rates, and transmission line limits. Define these constraints and the objective function that measures the cost of the generation schedule.

Step 2: Initialize the chaotic arithmetic optimization algorithm.

Initialize the algorithm by setting the population size, the number of iterations, the chaos map parameters, and the other algorithmic parameters. Initialize the population randomly.

Step 3: Evaluate the fitness of the population.

Evaluate the fitness of each solution in the population by solving the SCUC problem for each solution. Evaluate the objective function and the constraints for each solution.

Step 4: Apply chaos to the population.

Apply a chaotic map to the population to introduce diversity and avoid premature convergence. The chaotic map generates a random number sequence that modifies the position of each individual in the population.

Step 5: Select parents and generate offspring.

Select parents from the population based on their fitness and generate offspring using crossover and mutation operators. Apply elitism to keep the best individuals in the population.

Step 6: Evaluate the fitness of the offspring.

Evaluate the fitness of the offspring by solving the SCUC problem for each solution. Evaluate the objective function and the constraints for each solution.

Step 7: Apply selection to update the population.

Apply selection to update the population by keeping the best individuals from the parents and offspring.

Step 8: Check the stopping criteria.

Check if the stopping criteria have been met. If not, repeat steps 4 to 7 until the stopping criteria are met.

Step 9: Output the best solution found.

Output the best solution found in the optimization process, which corresponds to the optimal schedule of power generators that meets the power demand while satisfying the security constraints.

In summary, the procedure for solving the SCUC problem using the chaotic arithmetic optimization algorithm involves initializing the algorithm, evaluating the fitness of the population, applying chaos to the population, generating offspring, evaluating their fitness, updating the population, and checking the stopping criteria. The best solution found corresponds to the optimal schedule of power generators that meets the power demand while satisfying the security constraints.

4.4 TEST SYSTEM

The SCUC problem was successfully solved by considering the limitations of power generation units and various system sizes, including small, medium, and large-scale systems. The mixed-integer constrained SCUC problem was solved for different system sizes, namely standard 10-generating unit systems, 10-generating unit systems (small scale), 20-generating unit systems (medium scale), and 40-generating unit systems (large scale). The article also discusses power demand in the electricity market and the attributes of power units with cost coefficient parameters.

4.4.1 Generation System for 10 units

Table 4.1 illustrates the parameters of the 10-generating unit system used in the test. These parameters include the maximum and minimum power generation limits of the system $P_{k(\max)}$ and $P_{k(\min)}$,fuel coefficient constraints (a_k , b_k , and c_k), up and down time constraints (T_k^{MUP} and T_k^{MDT}), cost for hot and cold start (HSU_k and CSU_k), cold start hour of the unit CSU_k , and the initial status of the system INS_k Meanwhile, Table 4.2 shows the load demand of the test system for 24 hours. The system was evaluated under different spinning reserve capacities, particularly 10%, using a 24-hour load demand pattern. For the analysis of the proposed system, the standard IEEE 10-unit, 39-bus test system with 24 hours of data has been taken into consideration for the study [126].

Table 4.1: Characteristics of the 10-generating unit system [126]

Parameter	Units	P_1	P_2	P_3	P_4	P_5	P_6	P_7	P_8	P_9	P_{10}
$P_{k(\max)}$	MW	455	455	130	130	162	80	85	55	55	55
$P_{k(\min)}$	MW	150	150	20	20	25	20	25	10	10	10
a_k	$/hour	1000	970	700	680	450	370	480	660	665	670
b_k	$/MWh	16.19	17.26	16.6	16.5	19.7	22.26	27.74	25.92	27.27	27.79
c_k	$/MW^{2}h	0.00048	0.0003	0.002	0.0021	0.004	0.0071	0.0008	0.0041	0.0022	0.0017
T_k^{MUP}	hour	8	8	5	5	6	3	3	1	1	1
T_k^{MDT}	hour	8	8	5	5	6	3	3	1	1	1
HSU_k	$	4500	5000	550	560	900	170	260	30	30	30

CSU_k	$	9000	10000	1100	1120	1800	340	520	60	60	60
T_k^{COLD}	hour	5	5	4	4	4	2	2	0	0	0
INS_k	hour	8	8	-5	-5	-6	-3	-3	-1	-1	-1

Table 4.2: Power demand for a system consisting of 10 generating units [126].

	Hourly Load data (Time in Hours)											
Power Demand (MW)	**t_1**	**t_2**	**t_3**	**t_4**	**t_5**	**t_6**	**t_7**	**t_8**	**t_9**	**t_{10}**	**t_{11}**	**t_{12}**
	700	750	850	950	1000	1100	1150	1200	1300	1400	1450	1500
	t_{13}	**t_{14}**	**t_{15}**	**t_{16}**	**t_{17}**	**t_{18}**	**t_{19}**	**t_{20}**	**t_{21}**	**t_{22}**	**t_{23}**	**t_{24}**
	1400	1300	1200	1050	1000	1100	1200	1400	1300	1100	900	800

4.5 RESULT AND DISCUSSION

To determine the effectiveness of the proposed techniques for the SCUC problem, standard test systems were utilized [126]. These test systems were classified into small-scale (10 generating units), medium-scale (20 generating units), and large-scale (40 generating units) systems. The performance of the proposed algorithms was evaluated using MATLAB 2021a (8.1.0.604) software on a 64-bit version of Windows 11 Home Basic, with a CPU operating at 2.10 GHz, 8 GB of RAM, and an Intel® CoreTM i5-2310M processor. According to statistical analysis, the CAOA algorithms proposed were found to be effective.

4.5.1 Hybrid Chaotic Arithmetic Optimization Algorithm and Levy Flight Arithmetic Optimization algorithm

The CAOA and LFAOA are novel hybrid algorithms that combine chaotic maps and levy flight strategies with arithmetic optimization techniques. These algorithms are designed to address optimization problems by incorporating both exploratory and exploitative phases, which are stimulated using arithmetic operations such as division, multiplication, addition, and subtraction. CAOA and LFAOA are population-based algorithm that do not rely on gradients, which makes them suitable for a wide range of optimization problems.

The CAOA and LFAOA algorithms are effective in the exploratory phase, where they generate a diverse set of solutions using chaotic maps. It also has a strong ability to adapt from the exploratory phase to the exploitative phase, where it refines the solutions using arithmetic operations. Overall, CAOA and LFAOA are powerful optimizers that can be applied to a variety of optimization problems. Its ability to combine chaotic maps with arithmetic optimization techniques makes it a promising algorithm that can effectively address complex optimization issues.

4.5.1.1 System of Ten Generating Units

The efficiency of the proposed CAOA and LFAOA optimizers has been tested using the standard IEEE 10-unit, 39-bus test system with 24 hours of data. The CAOA technique is subjected to evaluation through 100 iterations, while 30 trial runs verify the effectiveness of the CAOA and LFAOA algorithms. The convergence curve is shown in Figure 4.3. Details of the commitment status, optimal scheduling, and individual fuel costs of each of the 10 generating units are presented in **Table 4.3.1**, **Table 4.3.2**, and **Table 4.3.3**, respectively. **Table 4.3.1** illustrates the commitment status, while Table 4.3.2 displays the optimal scheduling of power-generating units during the 24-hour period. P_1 and P_2 operate continuously, supplying 455 MW and 245 MW of power, respectively. P_3 runs from the 5^{th} hour to the 23^{rd} hour, providing a power output of 130 MW when active (indicated as '1'), and is off (indicated as '0') otherwise. P_4 remains inactive during the 1^{st} to 5^{th} hours and the 22^{nd} to 24^{th} hours but is on from the 6^{th} hour to the 21^{st} hour, producing 130 MW of power per hour during operation. P_5 operates only from the 5^{th} to the 22^{nd} hour to meet the power demand.

Table 4.3.3 shows the individual fuel cost of that unit. For P_1 and P_2, maximum profit can be obtained as it is on for 24 hours. For P_3, the fuel cost value varies from 2891.8 $ only for the 5^{th} hour to the 21^{st} hour. **Table 4.4** illustrates the committed status and scheduling for a 10-generating unit system using LFAOA algorithm with conventional system (Thermal System). **Table 4.5** illustrates the Individual fuel cost for 10 generating units system using the LFAOA algorithm for a conventional generation systems.

Table 4.3.1: Committed status of 10 Generating Unit for Thermal system																								
Units/ Hour	**t_1**	**t_2**	**t_3**	**t_4**	**t_5**	**t_6**	**t_7**	**t_8**	**t_9**	**t_{10}**	**t_{11}**	**t_{12}**	**t_{13}**	**t_{14}**	**t_{15}**	**t_{16}**	**t_{17}**	**t_{18}**	**t_{19}**	**t_{20}**	**t_{21}**	**t_{22}**	**t_{23}**	**t_{24}**
U_1	1	1	1	1	1	1	1	1	1	1	1	1	1	1	1	1	1	1	1	1	1	1	1	1
U_2	1	1	1	1	1	1	1	1	1	1	1	1	1	1	1	1	1	1	1	1	1	1	1	1
U_3	0	0	0	0	1	1	1	1	1	1	1	1	1	1	1	1	1	1	1	1	1	0	0	0
U_4	0	0	0	0	0	1	1	1	1	1	1	1	1	1	1	1	1	1	1	1	1	0	0	0
U_5	0	0	1	1	1	1	1	1	1	1	1	1	1	1	1	1	1	1	1	1	1	1	0	0
U_6	0	0	0	0	0	0	0	0	1	1	1	1	1	1	0	0	0	0	0	1	1	1	1	0
U_7	0	0	0	0	0	0	0	0	1	1	1	1	1	1	0	0	0	0	0	1	1	1	0	0
U_8	0	0	0	0	0	0	0	0	0	1	1	1	1	0	0	0	0	0	0	1	0	0	0	0
U_9	0	0	0	0	0	0	0	0	0	0	1	1	0	0	0	0	0	0	0	0	0	0	0	0
U_{10}	0	0	0	0	0	0	0	0	0	0	0	1	0	0	0	0	0	0	0	0	0	0	0	0

Table 4.3.2: Scheduling of a 10- Generating unit Test system using CAOA algorithm for conventional thermal system														
Hour	**P_1**	**P_2**	**P_3**	**P_4**	**P_5**	**P_6**	**P_7**	**P_8**	**P_9**	**P_{10}**	**Generated Power (MW)**	**Load Demand (MW)**	**SUC ($)**	**FC ($)**
t_1	455	245	0	0	0	0	0	0	0	0	700	700	0	13683.13
t_2	455	295	0	0	0	0	0	0	0	0	750	750	1430	14554.5
t_3	455	370	0	0	25	0	0	0	0	0	850	850	900	16809.45
t_4	455	455	0	0	40	0	0	0	0	0	950	950	0	18597.67
t_5	455	390	130	0	25	0	0	0	0	0	1000	1000	0	20051.16
t_6	455	360	130	130	25	0	0	0	0	0	1100	1100	0	22387.04
t_7	455	410	130	130	25	0	0	0	0	0	1150	1150	0	23261.98
t_8	455	455	130	130	30	0	0	0	0	0	1200	1200	600	24150.34
t_9	455	455	130	130	85	20	25	0	0	0	1300	1300	0	27251.06
t_{10}	455	455	130	130	162	33	25	10	0	0	1400	1400	60	30057.55
t_{11}	455	455	130	130	162	73	25	10	10	0	1450	1450	60	31916.06
t_{12}	455	455	130	130	162	80	25	43	10	10	1500	1500	60	33890.16
t_{13}	455	455	130	130	162	33	25	10	0	0	1400	1400	0	30057.55
t_{14}	455	455	130	130	85	20	25	0	0	0	1300	1300	0	27251.06
t_{15}	455	455	130	130	30	0	0	0	0	0	1200	1200	0	24150.34
t_{16}	455	310	130	130	25	0	0	0	0	0	1050	1050	0	21513.66
t_{17}	455	260	130	130	25	0	0	0	0	0	1000	1000	0	20641.82
t_{18}	455	360	130	130	25	0	0	0	0	0	1100	1100	0	22387.04
t_{19}	455	455	130	130	30	0	0	0	0	0	1200	1200	0	24150.34
t_{20}	455	455	130	130	162	33	25	10	0	0	1400	1400	490	30057.55
t_{21}	455	455	130	130	85	20	25	0	0	0	1300	1300	0	27251.06
t_{22}	455	455	0	0	145	20	25	0	0	0	1100	1100	0	22735.52
t_{23}	455	425	0	0	0	20	0	0	0	0	900	900	0	17645.36
t_{24}	455	345	0	0	0	0	0	0	0	0	800	800	0	15427.42

Table 4.3.3: Individual fuel cost for Generation of 10 Unit Test System using CAOA algorithm for Thermal system												
Hours/ Units	**P_1**	**P_2**	**P_3**	**P_4**	**P_5**	**P_6**	**P_7**	**P_8**	**P_9**	**P_{10}**	**SUC ($)**	**FC ($)**
t_1	8465.82	5217.31	0	0	0	0	0	0	0	0	0	13683.1298
t_2	8465.82	6088.68	0	0	0	0	0	0	0	0	1430	14554.4998
t_3	8465.82	7398.64	0	0	944.988	0	0	0	0	0	900	16809.4485
t_4	8465.82	8887.48	0	0	1244.37	0	0	0	0	0	0	18597.6678
t_5	8465.82	7748.55	2891.8	0	944.988	0	0	0	0	0	0	20051.1605
t_6	8465.82	7223.78	2891.8	2860.66	944.988	0	0	0	0	0	0	22387.0445
t_7	8465.82	8098.71	2891.8	2860.66	944.988	0	0	0	0	0	0	23261.9795
t_8	8465.82	8887.48	2891.8	2860.66	1044.58	0	0	0	0	0	600	24150.3408
t_9	8465.82	8887.48	2891.8	2860.66	2153.26	818	1174	0	0	0	0	27251.056
t_{10}	8465.82	8887.48	2891.8	2860.66	3745.85	1112	1174	919.6	0	0	60	30057.5503
t_{11}	8465.82	8887.48	2891.8	2860.66	3745.85	2033	1174	919.6	937.9	0	60	31916.0611
t_{12}	8465.82	8887.48	2891.8	2860.66	3745.85	2196	1174	1782	937.9	948.1	60	33890.163
t_{13}	8465.82	8887.48	2891.8	2860.66	3745.85	1112	1174	919.6	0	0	0	30057.5503
t_{14}	8465.82	8887.48	2891.8	2860.66	2153.26	818	1174	0	0	0	0	27251.056
t_{15}	8465.82	8887.48	2891.8	2860.66	1044.58	0	0	0	0	0	0	24150.3408
t_{16}	8465.82	6350.39	2891.8	2860.66	944.988	0	0	0	0	0	0	21513.6595
t_{17}	8465.82	5478.56	2891.8	2860.66	944.988	0	0	0	0	0	0	20641.8245
t_{18}	8465.82	7223.78	2891.8	2860.66	944.988	0	0	0	0	0	0	22387.0445
t_{19}	8465.82	8887.48	2891.8	2860.66	1044.58	0	0	0	0	0	0	24150.3408
t_{20}	8465.82	8887.48	2891.8	2860.66	3745.85	1112	1174	919.6	0	0	490	30057.5503
t_{21}	8465.82	8887.48	2891.8	2860.66	2153.26	818	1174	0	0	0	0	27251.056
t_{22}	8465.82	8887.48	0	0	3390.18	818	1174	0	0	0	0	22735.521
t_{23}	8465.82	8361.49	0	0	0	818	0	0	0	0	0	17645.3638
t_{24}	8465.82	6961.6	0	0	0	0	0	0	0	0	0	15427.4198

Table 4.4: Committed status and scheduling for a 10-generating unit system using LFAOA algorithm with Conventional system (Thermal System)

Hour	U_1	U_2	U_3	U_4	U_5	U_6	U_7	U_8	U_9	U_{10}	Hour	P_1	P_2	P_3	P_4	P_5	P_6	P_7	P_8	P_9	P_{10}	Power Generated (MW)	SUC ($)	FC ($)
t_1	1	1	0	0	0	0	0	0	0	0	t_1	455	245	0	0	0	0	0	0	0	0	700	1620	13683.13
t_2	1	1	0	0	0	0	0	0	0	0	t_2	455	295	0	0	0	0	0	0	0	0	750	560	14554.5
t_3	1	1	0	0	1	0	0	0	0	0	t_3	455	370	0	0	25	0	0	0	0	0	850	0	16809.45
t_4	1	1	0	0	1	0	0	0	0	0	t_4	455	455	0	0	40	0	0	0	0	0	950	0	18597.67
t_5	1	1	0	1	1	0	0	0	0	0	t_5	455	390	0	130	25	0	0	0	0	0	1000	0	20020.02
t_6	1	1	1	1	1	0	0	0	0	0	t_6	455	360	130	130	25	0	0	0	0	0	1100	0	22387.04
t_7	1	1	1	1	1	0	0	0	0	0	t_7	455	410	130	130	25	0	0	0	0	0	1150	0	23261.98
t_8	1	1	1	1	1	0	0	0	0	0	t_8	455	455	130	130	30	0	0	0	0	0	1200	0	24150.34
t_9	1	1	1	1	1	1	1	0	0	0	t_9	455	455	130	130	85	20	25	0	0	0	1300	690	27251.06
t_{10}	1	1	1	1	1	1	1	1	0	0	t_{10}	455	455	130	130	162	33	25	10	0	0	1400	60	30057.55
t_{11}	1	1	1	1	1	1	1	1	1	0	t_{11}	455	455	130	130	162	73	25	10	10	0	1450	60	31916.06
t_{12}	1	1	1	1	1	1	1	1	1	1	t_{12}	455	455	130	130	162	80	25	43	10	10	1500	60	33890.16
t_{13}	1	1	1	1	1	1	1	1	0	0	t_{13}	455	455	130	130	162	33	25	10	0	0	1400	0	30057.55
t_{14}	1	1	1	1	1	1	1	0	0	0	t_{14}	455	455	130	130	85	20	25	0	0	0	1300	0	27251.06
t_{15}	1	1	1	1	1	0	0	0	0	0	t_{15}	455	455	130	130	30	0	0	0	0	0	1200	0	24150.34
t_{16}	1	1	1	1	1	0	0	0	0	0	t_{16}	455	310	130	130	25	0	0	0	0	0	1050	0	21513.66
t_{17}	1	1	1	1	1	0	0	0	0	0	t_{17}	455	260	130	130	25	0	0	0	0	0	1000	0	20641.82
t_{18}	1	1	1	1	1	0	0	0	0	0	t_{18}	455	360	130	130	25	0	0	0	0	0	1100	260	22387.04
t_{19}	1	1	1	1	1	0	0	0	0	0	t_{19}	455	455	130	130	30	0	0	0	0	0	1200	120	24150.34
t_{20}	1	1	1	1	1	1	1	1	0	0	t_{20}	455	455	130	130	162	33	25	10	0	0	1400	170	30057.55
t_{21}	1	1	1	1	1	1	1	0	0	0	t_{21}	455	455	130	130	85	20	25	0	0	0	1300	0	27251.06
t_{22}	1	1	0	0	1	1	1	0	0	0	t_{22}	455	455	0	0	145	20	25	0	0	0	1100	0	22735.52
t_{23}	1	1	0	0	1	0	0	0	0	0	t_{23}	455	420	0	0	25	0	0	0	0	0	900	0	17684.69
t_{24}	1	1	0	0	0	0	0	0	0	0	t_{24}	455	345	0	0	0	0	0	0	0	0	800	0	15427.42

Table 4.5: Individual fuel cost for 10 Generating Unit system using LFAOA algorithm for Conventional Generation system (Thermal)

Hours/ Units	P_1	P_2	P_3	P_4	P_5	P_6	P_7	P_8	P_9	P_{10}	SUC ($)	FC ($)
t_1	8465.82	5217.31	0	0	0	0	0	0	0	0	1620	13683.1
t_2	8465.82	6088.68	0	0	0	0	0	0	0	0	560	14554.5
t_3	8465.82	7398.64	0	0	944.988	0	0	0	0	0	0	16809.4
t_4	8465.82	8887.48	0	0	1244.37	0	0	0	0	0	0	18597.7
t_5	8465.82	7748.55	0	2860.66	944.988	0	0	0	0	0	0	20020
t_6	8465.82	7223.78	2891.8	2860.66	944.988	0	0	0	0	0	0	22387
t_7	8465.82	8098.71	2891.8	2860.66	944.988	0	0	0	0	0	0	23262
t_8	8465.82	8887.48	2891.8	2860.66	1044.58	0	0	0	0	0	0	24150.3
t_9	8465.82	8887.48	2891.8	2860.66	2153.26	818.048	1173.99	0	0	0	690	27251.1
t_{10}	8465.82	8887.48	2891.8	2860.66	3745.85	1112.33	1173.99	919.613	0	0	60	30057.6
t_{11}	8465.82	8887.48	2891.8	2860.66	3745.85	2032.92	1173.99	919.613	937.922	0	60	31916.1
t_{12}	8465.82	8887.48	2891.8	2860.66	3745.85	2196.37	1173.99	1782.2	937.922	948.073	60	33890.2
t_{13}	8465.82	8887.48	2891.8	2860.66	3745.85	1112.33	1173.99	919.613	0	0	0	30057.6
t_{14}	8465.82	8887.48	2891.8	2860.66	2153.26	818.048	1173.99	0	0	0	0	27251.1
t_{15}	8465.82	8887.48	2891.8	2860.66	1044.58	0	0	0	0	0	0	24150.3
t_{16}	8465.82	6350.39	2891.8	2860.66	944.988	0	0	0	0	0	0	21513.7
t_{17}	8465.82	5478.56	2891.8	2860.66	944.988	0	0	0	0	0	0	20641.8
t_{18}	8465.82	7223.78	2891.8	2860.66	944.988	0	0	0	0	0	260	22387
t_{19}	8465.82	8887.48	2891.8	2860.66	1044.58	0	0	0	0	0	120	24150.3
t_{20}	8465.82	8887.48	2891.8	2860.66	3745.85	1112.33	1173.99	919.613	0	0	170	30057.6
t_{21}	8465.82	8887.48	2891.8	2860.66	2153.26	818.048	1173.99	0	0	0	0	27251.1
t_{22}	8465.82	8887.48	0	0	3390.18	818.048	1173.99	0	0	0	0	22735.5
t_{23}	8465.82	8273.88	0	0	944.988	0	0	0	0	0	0	17684.7
t_{24}	8465.82	6961.6	0	0	0	0	0	0	0	0	0	15427.4

4.5.1.2 System of 20 Generating Units

The efficiency of the proposed CAOA and LFAOA optimizer are tested using a specialized system comprising 20 power-generating units that operate for 24 hours. The CAOA and LFAOA technique is subjected to evaluation through 100 iterations, while 30 trial runs verify the effectiveness of the CAOA and LFAOA algorithm [68]. The convergence graph in **Figure 4.3** illustrates the total profit. **Table 4.6** illustrate the Commitment status of 20 Generating Thermal Test Units system; **Table 4.7** illustrate the Scheduling of 20 Generation test unit system using hCAOA algorithm for conventional thermal system**. Table 4.8** illustrate the Individual fuel cost of 20 Unit Test System using CAOA for conventional Thermal system**. Table 4.9** illustrate the Scheduling for a 20-generating unit system using LFAOA algorithm with conventional Thermal system**. Table 4.10** illustrate the Scheduling for a 20-generating unit system using LFAOA algorithm with Conventional Thermal system**. Table 4.11** illustrate the Individual fuel cost for 20 Generating Unit system using LFAOA algorithm considering Thermal system**. Table 4.12** illustrate the statistical and hypothetical result of 20 Generating unit system using hCAOA. **Table 4.13** illustrate the statistical and hypothetical analysis of 20 Generating Unit System results for LFAOA optimization algorithms for thermal system.

Table 4.6 Commitment status of a 20 Generating Thermal Test Units systems with CAOA																				
Hour/ Units	**U_1**	**U_2**	**U_3**	**U_4**	**U_5**	**U_6**	**U_7**	**U_8**	**U_9**	**U_{10}**	**U_{11}**	**U_{12}**	**U_{13}**	**U_{14}**	**U_{15}**	**U_{16}**	**U_{17}**	**U_{18}**	**U_{19}**	**U_{20}**
t_1	1	1	0	0	0	0	0	0	0	0	1	1	0	0	0	0	0	0	0	0
t_2	1	1	0	0	0	0	0	0	0	0	1	1	0	0	0	0	0	0	0	0
t_3	1	1	0	1	0	0	0	0	0	0	1	1	0	0	0	0	0	0	0	0
t_4	1	1	0	1	1	0	0	0	0	0	1	1	0	0	0	0	0	0	0	0
t_5	1	1	0	1	1	0	0	0	0	0	1	1	0	1	0	0	0	0	0	0
t_6	1	1	0	1	1	0	0	0	0	0	1	1	0	1	1	0	0	0	0	10
t_7	1	1	0	1	1	0	0	0	0	0	1	1	1	1	1	0	0	0	0	0
t_8	1	1	1	1	1	0	0	0	0	0	1	1	1	1	1	0	0	0	0	0
t_9	1	1	1	1	1	1	1	0	0	0	1	1	1	1	1	1	0	0	0	0
t_{10}	1	1	1	1	1	1	1	1	0	0	1	1	1	1	1	1	1	1	0	0
t_{11}	1	1	1	1	1	1	1	1	1	0	1	1	1	1	1	1	1	1	1	0
t_{12}	1	1	1	1	1	1	1	1	1	1	1	1	1	1	1	1	1	1	1	1
t_{13}	1	1	1	1	1	1	1	1	0	0	1	1	1	1	1	1	1	1	0	0
t_{14}	1	1	1	1	1	1	1	0	0	0	1	1	1	1	1	1	0	0	0	0
t_{15}	1	1	1	1	1	0	0	0	0	0	1	1	1	1	1	0	0	0	0	0
t_{16}	1	1	1	1	1	0	0	0	0	0	1	1	1	1	1	0	0	0	0	0
t_{17}	1	1	1	1	1	0	0	0	0	0	1	1	1	1	1	0	0	0	0	0
t_{18}	1	1	1	1	1	0	0	0	0	0	1	1	1	1	1	0	0	0	0	0
t_{19}	1	1	1	1	1	0	0	0	0	0	1	1	1	1	1	0	0	0	0	0
t_{20}	1	1	1	1	1	1	1	1	0	0	1	1	1	1	1	1	1	1	0	0
t_{21}	1	1	1	1	1	1	1	0	0	0	1	1	1	1	1	1	1	0	0	0
t_{22}	1	1	0	0	1	1	1	0	0	0	1	1	1	0	0	1	1	0	0	0
t_{23}	1	1	0	0	1	0	0	0	0	0	1	1	0	0	0	0	0	0	0	0
t_{24}	1	1	0	0	0	0	0	0	0	0	1	1	0	0	0	0	0	0	0	0

Table 4.7: Scheduling of 20 Generation test unit system using CAOA algorithm for conventional thermal systems																						
Hour/ Units	**P_1**	**P_2**	**P_3**	**P_4**	**P_5**	**P_6**	**P_7**	**P_8**	**P_9**	**P_{10}**	**P_{11}**	**P_{12}**	**P_{13}**	**P_{14}**	**P_{15}**	**P_{16}**	**P_{17}**	**P_{18}**	**P_{19}**	**P_{20}**	**SUC ($)**	**FC ($)**
t_1	455	245	0	0	0	0	0	0	0	0	455	245	0	0	0	0	0	0	0	0	0	27366.3
t_2	455	295	0	0	0	0	0	0	0	0	455	295	0	0	0	0	0	0	0	0	2010	29109
t_3	455	330	0	130	0	0	0	0	0	0	455	330	0	0	0	0	0	0	0	0	900	33191.4
t_4	455	418	0	130	25	0	0	0	0	0	455	418	0	0	0	0	0	0	0	0	1110	37197.5
t_5	455	403	0	130	25	0	0	0	0	0	455	403	0	130	0	0	0	0	0	0	0	39532.7
t_6	455	455	0	130	55	0	0	0	0	0	455	455	0	130	55	0	0	0	0	10	0	44467.1
t_7	455	455	0	130	45	0	0	0	0	0	455	455	130	130	45	0	0	0	0	0	0	46008.8
t_8	455	455	130	130	30	0	0	0	0	0	455	455	130	130	30	0	0	0	0	0	860	48300.7
t_9	455	455	130	130	97.5	20	25	0	0	0	455	455	130	130	97.5	20	0	0	0	0	520	53838.8
t_{10}	455	455	130	130	162	33	25	10	0	0	455	455	130	130	162	33	25	10	0	0	460	60115.1
t_{11}	455	455	130	130	162	73	25	10	10	0	455	455	130	130	162	73	25	10	10	0	120	63832.1
t_{12}	455	455	130	130	162	80	25	43	10	10	455	455	130	130	162	80	25	43	10	10	120	67780.3
t_{13}	455	455	130	130	162	33	25	10	0	0	455	455	130	130	162	33	25	10	0	0	0	60115.1
t_{14}	455	455	130	130	97.5	20	25	0	0	0	455	455	130	130	97.5	20	0	0	0	0	0	53838.8
t_{15}	455	455	130	130	30	0	0	0	0	0	455	455	130	130	30	0	0	0	0	0	0	48300.7
t_{16}	455	310	130	130	25	0	0	0	0	0	455	310	130	130	25	0	0	0	0	0	0	43027.3
t_{17}	455	260	130	130	25	0	0	0	0	0	455	260	130	130	25	0	0	0	0	0	0	41283.6
t_{18}	455	360	130	130	25	0	0	0	0	0	455	360	130	130	25	0	0	0	0	0	0	44774.1
t_{19}	455	455	130	130	30	0	0	0	0	0	455	455	130	130	30	0	0	0	0	0	0	48300.7
t_{20}	455	455	130	130	162	33	25	10	0	0	455	455	130	130	162	33	25	10	0	0	1240	60115.1
t_{21}	455	455	130	130	85	20	25	0	0	0	455	455	130	130	85	20	25	0	0	0	0	54502.1
t_{22}	455	455	0	0	160	20	25	0	0	0	455	455	130	0	0	20	25	0	0	0	60	45286.4
t_{23}	455	433	0	0	25	0	0	0	0	0	455	433	0	0	0	0	0	0	0	0	0	34862.5
t_{24}	455	345	0	0	0	0	0	0	0	0	455	345	0	0	0	0	0	0	0	0	0	30854.8

Table 4.8: Individual fuel cost of a 20 Generating Unit System using the CAOA for conventional Thermal system

Hours/ Units	P_1	P_2	P_3	P_4	P_5	P_6	P_7	P_8	P_9	P_{10}	P_{11}	P_{12}	P_{13}	P_{14}	P_{15}	P_{16}	P_{17}	P_{18}	P_{19}	P_{20}	SUC ($)	FC ($)
t_1	8465.8	5217.3	0	0	0	0	0	0	0	0	8465.8	5217.3	0	0	0	0	0	0	0	0	0	27366.26
t_2	8465.8	6088.7	0	0	0	0	0	0	0	0	8465.8	6088.7	0	0	0	0	0	0	0	0	2010	29109
t_3	8465.8	6699.6	0	2860.7	0	0	0	0	0	0	8465.8	6699.6	0	0	0	0	0	0	0	0	900	33191.42
t_4	8465.8	8230.1	0	2860.7	944.99	0	0	0	0	0	8465.8	8230.1	0	0	0	0	0	0	0	0	1110	37197.46
t_5	8465.8	7967.4	0	2860.7	944.99	0	0	0	0	0	8465.8	7967.4	0	2860.7	0	0	0	0	0	0	0	39532.69
t_6	8465.8	8887.5	0	2860.7	1545.5	0	0	0	0	0	8465.8	8887.5	0	2860.7	1545.5	0	0	0	0	948.07	0	44467.07
t_7	8465.8	8887.5	0	2860.7	1344.6	0	0	0	0	0	8465.8	8887.5	2891.8	2860.7	1344.6	0	0	0	0	0	0	46008.84
t_8	8465.8	8887.5	2891.8	2860.7	1044.6	0	0	0	0	0	8465.8	8887.5	2891.8	2860.7	1044.6	0	0	0	0	0	860	48300.68
t_9	8465.8	8887.5	2891.8	2860.7	2408.6	818.05	1174	0	0	0	8465.8	8887.5	2891.8	2860.7	2408.6	818.05	0	0	0	0	520	53838.78
t_{10}	8465.8	8887.5	2891.8	2860.7	3745.9	1112.3	1174	919.61	0	0	8465.8	8887.5	2891.8	2860.7	3745.9	1112.3	1174	919.61	0	0	460	60115.1
t_{11}	8465.8	8887.5	2891.8	2860.7	3745.9	2032.9	1174	919.61	937.92	0	8465.8	8887.5	2891.8	2860.7	3745.9	2032.9	1174	919.61	937.92	0	120	63832.12
t_{12}	8465.8	8887.5	2891.8	2860.7	3745.9	2196.4	1174	1782.2	937.92	948.07	8465.8	8887.5	2891.8	2860.7	3745.9	2196.4	1174	1782.2	937.92	948.07	120	67780.33
t_{13}	8465.8	8887.5	2891.8	2860.7	3745.9	1112.3	1174	919.61	0	0	8465.8	8887.5	2891.8	2860.7	3745.9	1112.3	1174	919.61	0	0	0	60115.1
t_{14}	8465.8	8887.5	2891.8	2860.7	2408.6	818.05	1174	0	0	0	8465.8	8887.5	2891.8	2860.7	2408.6	818.05	0	0	0	0	0	53838.78
t_{15}	8465.8	8887.5	2891.8	2860.7	1044.6	0	0	0	0	0	8465.8	8887.5	2891.8	2860.7	1044.6	0	0	0	0	0	0	48300.68
t_{16}	8465.8	6350.4	2891.8	2860.7	944.99	0	0	0	0	0	8465.8	6350.4	2891.8	2860.7	944.99	0	0	0	0	0	0	43027.32
t_{17}	8465.8	5478.6	2891.8	2860.7	944.99	0	0	0	0	0	8465.8	5478.6	2891.8	2860.7	944.99	0	0	0	0	0	0	41283.65
t_{18}	8465.8	7223.8	2891.8	2860.7	944.99	0	0	0	0	0	8465.8	7223.8	2891.8	2860.7	944.99	0	0	0	0	0	0	44774.09
t_{19}	8465.8	8887.5	2891.8	2860.7	1044.6	0	0	0	0	0	8465.8	8887.5	2891.8	2860.7	1044.6	0	0	0	0	0	0	48300.68
t_{20}	8465.8	8887.5	2891.8	2860.7	3745.9	1112.3	1174	919.61	0	0	8465.8	8887.5	2891.8	2860.7	3745.9	1112.3	1174	919.61	0	0	1240	60115.1
t_{21}	8465.8	8887.5	2891.8	2860.7	2153.3	818.05	1174	0	0	0	8465.8	8887.5	2891.8	2860.7	2153.3	818.05	1174	0	0	0	0	54502.11
t_{22}	8465.8	8887.5	0	0	3703.9	818.05	1174	0	0	0	8465.8	8887.5	2891.8	0	0	818.05	1174	0	0	0	60	45286.37
t_{23}	8465.8	8492.9	0	0	944.99	0	0	0	0	0	8465.8	8492.9	0	0	0	0	0	0	0	0	0	34862.51
t_{24}	8465.8	6961.6	0	0	0	0	0	0	0	0	8465.8	6961.6	0	0	0	0	0	0	0	0	0	30854.84

Table 4.9: Commitment status using LFAOA algorithm with conventional Thermal system

Hours/Units	U_1	U_2	U_3	U_4	U_5	U_6	U_7	U_8	U_9	U_{10}	U_{11}	U_{12}	U_{13}	U_{14}	U_{15}	U_{16}	U_{17}	U_{18}	U_{19}	U_{20}
t_1	1	1	0	0	0	0	0	0	0	0	1	1	0	0	0	0	0	0	0	0
t_2	1	1	0	0	0	0	0	0	0	0	1	1	0	0	0	0	0	0	0	0
t_3	1	1	0	0	1	0	0	0	0	0	1	1	0	0	0	0	0	0	0	0
t_4	1	1	0	0	1	0	0	0	0	0	1	1	0	0	1	0	0	0	0	0
t_5	1	1	0	1	1	0	0	0	0	0	1	1	0	0	1	0	0	0	0	0
t_6	1	1	1	1	1	0	0	0	0	0	1	1	0	1	1	0	0	0	0	0
t_7	1	1	1	1	1	0	0	0	0	0	1	1	0	1	1	0	0	0	0	0
t_8	1	1	1	1	1	0	0	0	0	0	1	1	1	1	1	0	0	0	0	0
t_9	1	1	1	1	1	1	0	0	0	0	1	1	1	1	1	1	1	0	0	0
t_{10}	1	1	1	1	1	1	1	1	0	0	1	1	1	1	1	1	1	1	0	0
t_{11}	1	1	1	1	1	1	1	1	1	0	1	1	1	1	1	1	1	1	1	0
t_{12}	1	1	1	1	1	1	1	1	1	1	1	1	1	1	1	1	1	1	1	1
t_{13}	1	1	1	1	1	1	1	1	0	0	1	1	1	1	1	1	1	0	0	1
t_{14}	1	1	1	1	1	1	1	0	0	0	1	1	1	1	1	1	0	0	0	0
t_{15}	1	1	1	1	1	0	0	0	0	0	1	1	1	1	1	0	0	0	0	0
t_{16}	1	1	1	1	1	0	0	0	0	0	1	1	1	1	1	0	0	0	0	0
t_{17}	1	1	1	1	1	0	0	0	0	0	1	1	1	1	1	0	0	0	0	0
t_{18}	1	1	1	1	1	0	0	0	0	0	1	1	1	1	1	0	0	0	0	0
t_{19}	1	1	1	1	1	0	0	0	0	0	1	1	1	1	1	0	0	0	0	0
t_{20}	1	1	1	1	1	1	1	1	0	0	1	1	1	1	1	1	1	1	0	0
t_{21}	1	1	1	1	1	1	1	0	0	0	1	1	0	1	1	1	1	0	0	0
t_{22}	1	1	0	0	0	1	1	0	0	0	1	1	0	1	1	1	1	0	0	0
t_{23}	1	1	0	0	0	0	0	0	0	0	1	1	0	0	1	0	0	0	0	0
t_{24}	1	1	0	0	0	0	0	0	0	0	1	1	0	0	0	0	0	0	0	0

Table 4.10: Scheduling for a 20-Generating Unit System using the LFAOA Algorithm with a Conventional Thermal System

Hours/Units	P_1	P_2	P_3	P_4	P_5	P_6	P_7	P_8	P_9	P_{10}	P_{11}	P_{12}	P_{13}	P_{14}	P_{15}	P_{16}	P_{17}	P_{18}	P_{19}	P_{20}	Generated Power (MW)	SUC ($)	FC ($)
t_1	455	245	0	0	0	0	0	0	0	0	455	245	0	0	0	0	0	0	0	0	1400	930	27366.3
t_2	455	295	0	0	0	0	0	0	0	0	455	295	0	0	0	0	0	0	0	0	1500	430	29109
t_3	455	382	0	0	25	0	0	0	0	0	455	382	0	0	0	0	0	0	0	0	1700	820	33111.2
t_4	455	455	0	0	40	0	0	0	0	0	455	455	0	0	40	0	0	0	0	0	1900	0	37195.3
t_5	455	455	0	130	25	0	0	0	0	0	455	455	0	0	25	0	0	0	0	0	2000	2010	39457.2
t_6	455	425	130	130	25	0	0	0	0	0	455	425	0	130	25	0	0	0	0	0	2200	0	44157.7
t_7	455	455	130	130	45	0	0	0	0	0	455	455	0	130	45	0	0	0	0	0	2300	1100	46008.8
t_8	455	455	130	130	30	0	0	0	0	0	455	455	130	130	30	0	0	0	0	0	2400	0	48300.7
t_9	455	455	130	130	98	20	0	0	0	0	455	455	130	130	98	20	25	0	0	0	2600	770	53838.8
t_{10}	455	455	130	130	162	33	25	10	0	0	455	455	130	130	162	33	25	10	0	0	2800	380	60115.1
t_{11}	455	455	130	130	162	73	25	10	10	0	455	455	130	130	162	73	25	10	10	0	2900	120	63832.1
t_{12}	455	455	130	130	162	80	25	43	10	10	455	455	130	130	162	80	25	43	10	10	3000	120	67780.3
t_{13}	455	455	130	130	162	33	25	10	0	0	455	455	130	130	162	33	25	0	0	10	2800	0	60143.6
t_{14}	455	455	130	130	98	20	25	0	0	0	455	455	130	130	98	20	0	0	0	0	2600	0	53838.8
t_{15}	455	455	130	130	30	0	0	0	0	0	455	455	130	130	30	0	0	0	0	0	2400	0	48300.7
t_{16}	455	310	130	130	25	0	0	0	0	0	455	310	130	130	25	0	0	0	0	0	2100	0	43027.3
t_{17}	455	260	130	130	25	0	0	0	0	0	455	260	130	130	25	0	0	0	0	0	2000	0	41283.6
t_{18}	455	360	130	130	25	0	0	0	0	0	455	360	130	130	25	0	0	0	0	0	2200	170	44774.1
t_{19}	455	455	130	130	30	0	0	0	0	0	455	455	130	130	30	0	0	0	0	0	2400	260	48300.7
t_{20}	455	455	130	130	162	33	25	10	0	0	455	455	130	130	162	33	25	10	0	0	2800	550	60115.1
t_{21}	455	455	130	130	150	20	25	0	0	0	455	455	0	130	150	20	25	0	0	0	2600	0	54292.9
t_{22}	455	455	0	0	0	20	25	0	0	0	455	455	0	130	160	20	25	0	0	0	2200	0	45255.2
t_{23}	455	433	0	0	0	0	0	0	0	0	455	433	0	0	25	0	0	0	0	0	1800	0	34862.5
t_{24}	455	345	0	0	0	0	0	0	0	0	455	345	0	0	0	0	0	0	0	0	1600	0	30854.8

Table 4.11: Individual fuel costs for 20 Generating Unit systems using the LFAOA algorithm considering thermal systems

Hours/ Units	P_1	P_2	P_3	P_4	P_5	P_6	P_7	P_8	P_9	P_{10}	P_{11}	P_{12}	P_{13}	P_{14}	P_{15}	P_{16}	P_{17}	P_{18}	P_{19}	P_{20}	SUC ($)	FC ($)
t_1	8466	5217	0	0	0	0	0	0	0	0	8465.8	5217.3	0	0	0	0	0	0	0	0	930	27366.26
t_2	8466	6089	0	0	0	0	0	0	0	0	8465.8	6088.7	0	0	0	0	0	0	0	0	430	29109
t_3	8466	7617	0	0	945	0	0	0	0	0	8465.8	7617.3	0	0	0	0	0	0	0	0	820	33111.24
t_4	8466	8887	0	0	1244	0	0	0	0	0	8465.8	8887.5	0	0	1244	0	0	0	0	0	0	37195.34
t_5	8466	8887	0	2861	945	0	0	0	0	0	8465.8	8887.5	0	0	945	0	0	0	0	0	2010	39457.23
t_6	8466	8361	2892	2861	945	0	0	0	0	0	8465.8	8361.5	0	2861	945	0	0	0	0	0	0	44157.72
t_7	8466	8887	2892	2861	1345	0	0	0	0	0	8465.8	8887.5	0	2861	1345	0	0	0	0	0	1100	46008.84
t_8	8466	8887	2892	2861	1045	0	0	0	0	0	8465.8	8887.5	2892	2861	1045	0	0	0	0	0	0	48300.68
t_9	8466	8887	2892	2861	2409	818	0	0	0	0	8465.8	8887.5	2892	2861	2409	818	1174	0	0	0	770	53838.78
t_{10}	8466	8887	2892	2861	3746	1112	1174	919.6	0	0	8465.8	8887.5	2892	2861	3746	1112	1174	919.6	0	0	380	60115.1
t_{11}	8466	8887	2892	2861	3746	2033	1174	919.6	937.9	0	8465.8	8887.5	2892	2861	3746	2033	1174	919.6	937.9	0	120	63832.12
t_{12}	8466	8887	2892	2861	3746	2196	1174	1782	937.9	948.1	8465.8	8887.5	2892	2861	3746	2196	1174	1782	937.9	948.1	120	67780.33
t_{13}	8466	8887	2892	2861	3746	1112	1174	919.6	0	0	8465.8	8887.5	2892	2861	3746	1112	1174	0	0	948.1	0	60143.56
t_{14}	8466	8887	2892	2861	2409	818	1174	0	0	0	8465.8	8887.5	2892	2861	2409	818	0	0	0	0	0	53838.78
t_{15}	8466	8887	2892	2861	1045	0	0	0	0	0	8465.8	8887.5	2892	2861	1045	0	0	0	0	0	0	48300.68
t_{16}	8466	6350	2892	2861	945	0	0	0	0	0	8465.8	6350.4	2892	2861	945	0	0	0	0	0	0	43027.32
t_{17}	8466	5479	2892	2861	945	0	0	0	0	0	8465.8	5478.6	2892	2861	945	0	0	0	0	0	0	41283.65
t_{18}	8466	7224	2892	2861	945	0	0	0	0	0	8465.8	7223.8	2892	2861	945	0	0	0	0	0	170	44774.09
t_{19}	8466	8887	2892	2861	1045	0	0	0	0	0	8465.8	8887.5	2892	2861	1045	0	0	0	0	0	260	48300.68
t_{20}	8466	8887	2892	2861	3746	1112	1174	919.6	0	0	8465.8	8887.5	2892	2861	3746	1112	1174	919.6	0	0	550	60115.1
t_{21}	8466	8887	2892	2861	3495	818	1174	0	0	0	8465.8	8887.5	0	2861	3495	818	1174	0	0	0	0	54292.9
t_{22}	8466	8887	0	0	0	818	1174	0	0	0	8465.8	8887.5	0	2861	3704	818	1174	0	0	0	0	45255.23
t_{23}	8466	8493	0	0	0	0	0	0	0	0	8465.8	8492.9	0	0	945	0	0	0	0	0	0	34862.51
t_{24}	8466	6962	0	0	0	0	0	0	0	0	8465.8	6961.6	0	0	0	0	0	0	0	0	0	30854.84

The analysis of statistical results obtained from the optimization algorithms of CAOA for security constrained unit commitment problem is given in the table format. **Table 4.12** illustrates the statistical and hypothetical results of the 20-generating unit system using CAOA.

Table 4.12: The statistical and hypothetical results of the 20-generating unit system using the CAOA algorithm

Best value ($)	Average Value ($)	Worst Value ($)	STD	Median	Wilcoxon Test	T-Test		Best Time (sec.)	Average Time (sec.)	Worst Time (sec.)
					p-value	p-value	h-Value			
1123401	1125228	1126808	1014.409	1125441	1.73E-06	4.44E-90	1	0	0.021875	0.03125

Table 4.13 illustrates the statistical and hypothetical analysis of 20 Generating Unit System results for LFAOA optimization algorithms for thermal systems.

Table 4.13: Statistical and hypothetical analysis of 20 Generating Unit System results for LFAOA optimization algorithms for thermal systems

Best value ($)	Average Value ($)	Worst Value ($)	STD	Median	Wilcoxon Test	T-Test		Best Time (sec.)	Average Time (sec.)	Worst Time (sec.)
					p-value	p-value	h-Value			
1122982	1124992	1126145	837.827	1125285	1.734E-06	1.7E-92	1	0	0.0193	0.031

Table 4.14 illustrates the statistical analysis of the SCUC problem of CAOA optimization algorithms for 40 test unit systems.

Table 4.14: Statistical analysis of the SCUC problem of the CAOA optimization algorithms for 40 test unit systems

Best Value ($)	Avg. Value ($)	Worst Value ($)	STD	Median	Wilcoxon Test	T-Test		Best Time (Sec.)	Average Time (sec.)
					p-value	p-value	h-Value		
2245351	2249723	2254254	2056.49	2249815	1.73E-06	6.60E-90	1	0.01563	0.02969

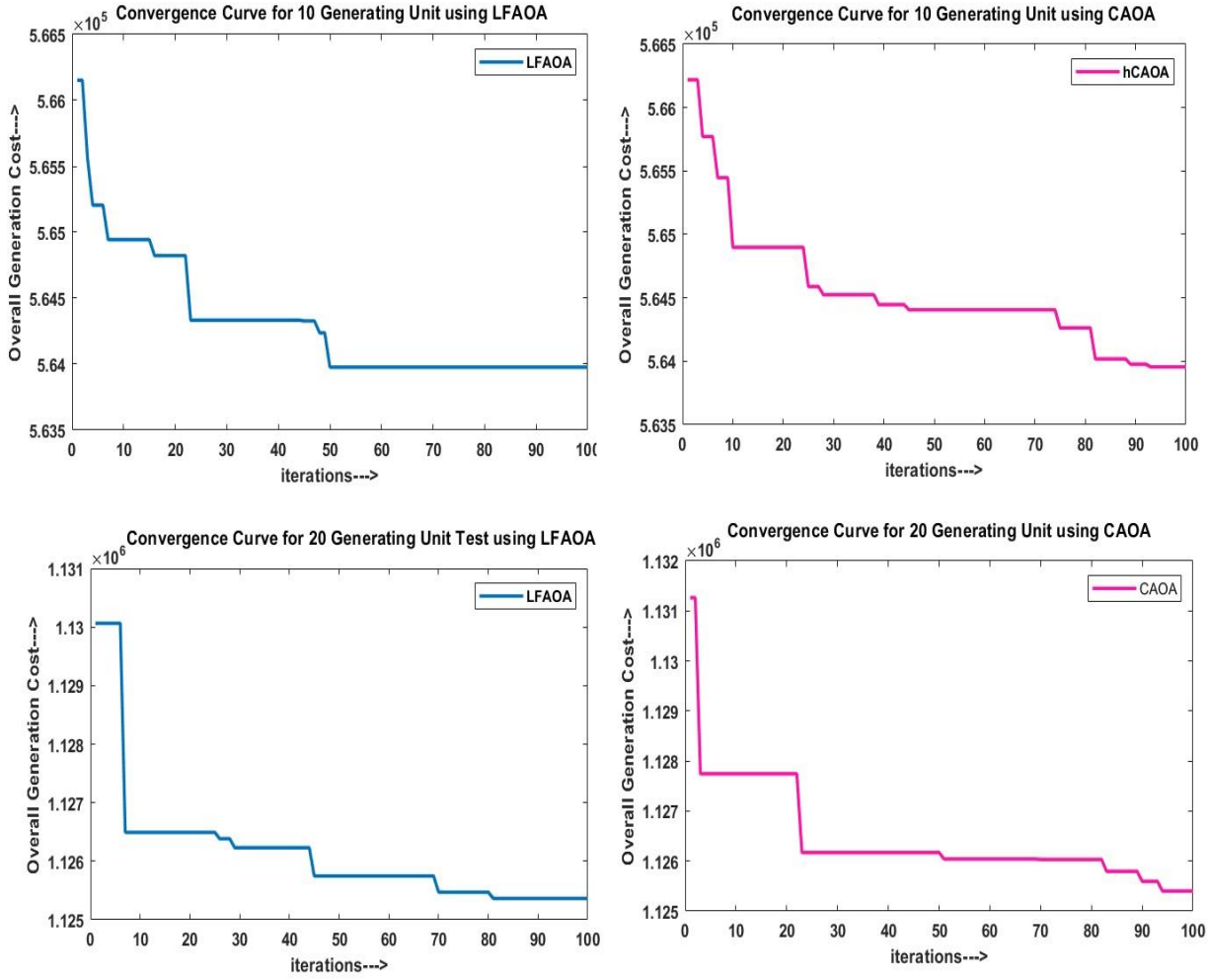

Figure 4.3: Convergence curve for the 10, 20-generating unit system (best value) using LFAOA and CAOA (10-unit test system with 10% SR)

Figure 4.3 illustrates the convergence curve for the best value of the 10 Generating Unit system using the levy flight arithmetic optimization algorithm and chaotic arithmetic optimization. Ten thermal-generating systems are being tested. After the simulation, the best-valued result is shown in the convergence curve.

4.6 CONCLUSIONS

This chapter presents the resolution of the security constraint unit commitment problem through the use of hybrid techniques. The successful scheduling of 10, 20, and 40-unit generating systems has been achieved through testing. The suggested hybrid optimizers can measure maximum profits. Simulated results indicate that the CAOA optimizer for fuel cost is superior to existing heuristics, meta-heuristics, and evolutionary search optimizers. The suggested optimizer can determine satisfactory profit values with commitment scheduling within a reasonable computation time. This powerful optimizer can be applied to obtain solutions for the SCUC problem in modern power sectors. The analysis includes the variation in profit value (best, average, and worst), standard deviation, and median value. Hypothesis testing methods such as the Wilcoxon rank sum method and t-test can determine the p-value and h-value. Computational times are also analyzed as the best, average, and worst times of simulations.

CHAPTER 5

SECURITY CONSTRAINT UNIT COMMITMENT PROBLEM WITH PEVs AND RENEWABLE ENERGY SOURCES

5.1 INTRODUCTION

The security constraint unit commitment problem is a crucial power sector optimization problem that aims to schedule the commitment of generating units to meet load demand while satisfying a number of constraints, including ramp rate limits, unit availability, and transmission network security. The SCUC problem has faced significant difficulties in recent years as a result of the uncertainties and variabilities associated with the integration of PEVs and renewable energy sources into power systems. The problem may become more complicated and challenging to solve when PEVs and RESs are integrated because they may bring stochasticity and nonlinearity into the equation.

This chapter focuses on the integration of PEVs and RESs into the SCUC problem and proposes various optimization techniques to address the challenges arising from this integration. The chapter begins by providing an overview of the SCUC problem and the challenges posed by the integration of PEVs and RESs. It then discusses the state-of-the-art optimization techniques used in solving the SCUC problem, with a focus on traditional methods and recent advances. Next, the chapter presents the proposed optimization techniques for integrating PEVs and RESs into the SCUC problem. In addition, the chapter emphasizes the significance of the proposed methods for enhancing power system reliability and economic efficiency. Numerical simulations based on data from real-world power systems are used to evaluate the proposed methods' efficacy. The outcomes show that incorporating PEVs and RESs effectively mitigates the effects of uncertainties and variabilities on the SCUC problem using the proposed methods. Initially, plug-in electric vehicles were only considered as dispatchable peak-level power plants for profit-based unit commitment planning. While electric vehicles have gained popularity in recent times, they have a surprising historical background. In 1834, Thomas Davenport created the first non-

rechargeable battery-operated EV in the form of a tricycle. After the invention of lead-acid batteries in 1874, David Salomon succeeded in developing an electric vehicle with a rechargeable battery. This development resulted in the construction of commercial EVs in the late 1886s by numerous companies. The current scenario of the electric vehicles is given in Table 5.1.

Table 5.1 Current electric vehicles scenario in India

Sr. No.	Manufacturing Company	Model	Power Consumption	Battery Range (Kwh)	Torque	Transmission	Maximum Speed
1	Tata Motors	Nexon EV	28.0 kWh/100 km	312 km	245 Nm	Automatic	120 km/h
2	Mahindra Electric	eKUV100	15.9 kWh/100 km	147 km	120 Nm	Automatic	80 km/h
3	MG Motors	ZS EV	18.6 kWh/100 km	419 km	353 Nm	Automatic	140 km/h
4	Hyundai Motors	Kona Electric	14.3 kWh/100 km	452 km	395 Nm	Automatic	167 km/h
5	Audi	e-tron	75kWh/100km	222 km	664 Nm	Automatic	200 km/h
6	Mercedes-Benz India	EQC	80 kWh	471 km	765 Nm	Automatic	180 km/h

Various initiatives have been taken by the Indian government to encourage the use of electric vehicles and renewable energy sources in the country. The Public Electric Versatility Mission Plan (NEMMP) 2020 was sent off in 2013 to empower the reception of EVs and to advance practical transportation. By 2030, the government intends to achieve a 30% PEV penetration rate.

The Faster Adoption and Manufacturing of Electric Vehicles (FAME) program is one of several initiatives and policies launched by the government to encourage the use of PEVs. This plan gives monetary motivating forces to purchasers of PEVs, as well as to makers and sellers to advance the turn of events and offers of PEVs. Additionally, the plan encourages the development of a nationwide charging infrastructure.

The Indian government unveiled Phase II of the Faster Adoption and Manufacturing of Hybrid and Electric Vehicles in India (FAME India) scheme in March 2021. The primary objective of this scheme is to facilitate the rapid adoption of electric vehicles and improve the charging infrastructure across the country. With a budget of INR 18,100 crore (equivalent to USD 2.4 billion) for a five-year period beginning April 2021, the scheme focuses on four core areas: (1) demand creation, (2) charging infrastructure, (3) supply-side incentives, and (4) skill development and awareness. To drive consumer demand, the government is providing purchase subsidies, interest-free loans for EV buyers, and tax incentives for manufacturers to boost local production of electric vehicles.

The Indian government has implemented numerous policies and initiatives to encourage the generation of renewable energy sources across the country. One such initiative is the National Solar Mission, introduced in 2010, which has set a target of achieving 100 GW of solar power capacity by 2022. Moreover, the government has established an objective of reaching 450 GW of renewable energy capacity by 2030.

The Ministry of New and Renewable Energy (MNRE) is responsible for carrying out various policies and programs related to renewable energy generation. The MNRE provides incentives and subsidies to support the development of renewable energy projects, including solar, wind, and bioenergy.

To encourage the installation of solar pumps for irrigation and grid-connected solar power projects, the government has introduced the Kisan Urja Suraksha evam Utthaan Mahaabhiyan (KUSUM) scheme. The scheme offers financial assistance to farmers to install solar pumps, which helps in reducing their reliance on diesel-based pumps and promoting the use of renewable energy sources.

Additionally, the Rooftop Solar Program is another scheme launched by the government to boost the adoption of solar power systems on the rooftops of residential and commercial buildings. Through various incentives and subsidies, the government provides financial assistance for the installation of rooftop solar power systems. In this chapter, the following cases are discussed and solved for the security constraints unit commitment problem.

Case 1: SCUC problem without considering PEV and RES.

Case 2: SCUC problem considering PEV.

Case 3: SCUC problem considering RES (Wind).

Case 4: SCUC problem considering RES (Solar).

Case 5: SCUC problem considering PEV and RES (Wind).

Case 6: SCUC problem considering PEV and RES (Solar).

Case 7: SCUC problem considering PEV and RES (Solar + Wind).

5.2 MATHEMATICAL PROBLEM FORMULATION OF SCUC PROBLEM CONSIDERING PEVs & RES

The optimization problem of SCUC is widely studied in the power systems field. Its objective is to determine the most cost-effective schedule for generators while considering operating and security constraints. However, when integrating PEVs and RES into the power system, the problem formulation becomes more intricate. In this scenario, the problem's objective is not only to minimize the operating cost but also to consider the PEVs' charging and discharging schedules and the intermittent nature of RES. The addition of PEVs provides a new source of demand response and energy storage, while RES provides clean energy.

To formulate the SCUC problem integrated with PEVs and RES, various mathematical models and constraints must be taken into account. The key variables include the unit commitment status, generators' power output, PEVs' charging and discharging schedules, and RES curtailment. The constraints encompass power balance, ramping, minimum and maximum generator output, voltage, and stability constraints.

5.2.1 Objective function of SCUC problem considering PEVs and RES

The main goal of the security constraint unit commitment problem is to determine the best schedule for running the available power generators in order to minimize the overall cost of generating and operating electricity. This cost includes factors such as the price of fuel, as well as the costs of starting up and shutting down generators. To calculate fuel costs, data on the characteristics of each generator k such as fuel prices, efficiency rates, and startup and shutdown times are used to solve a mathematical equation that represents the power output of each generator at a given hour time t. This equation is non-linear, non-smooth, and non-convex, and can be expressed in a quadratic form.

The equation that calculates the power output of each generator at a given t^{th} hour is a non-linear, non-smooth, and non-convex quadratic equation. The objective function of the security constraint unit commitment problem integrated with EVs and RES is shown in the equation (5.1).

$$\min F_{k,t} = \sum_{k=1}^{NG}\sum_{t=1}^{NH}\left[(a_k P_{k,t}^2 + b_k P_{k,t} + c_k) \times U_{k,t} + SUC_k \times \{U_{k,t} \times (1 - U_{k,(t-1)})\} + SDC_k \times U_{k,t-1}(1 - U_{k,t}) + \sum_{t=1}^{NH} C_{PEV} + \sum_{t=1}^{NH} C_{RES} \right]$$
$$\left(k = 1, 2, ..., NG(\text{Number of Generating Units}); \quad t = 1, 2, ..., \text{ Number of Hours}\right)$$

(5.1)

where, $F_{k,t}$ represent the cost associated with the k^{th} generating unit at the t^{th} hour and a_k, b_k, and c_k are its fuel and operational cost coefficients. $U_{k,t}$ and $(1 - U_{k,(t-1)})$ is the committed status of the k^{th} unit at t^{th} hour and $(t-1)^{th}$ hour respectively. SUC_k is the start-up cost of the k^{th} unit at t^{th} hour. The total cost ($F_{k,t}$) for all the generating units (NG) for a particular time at t^{th} hour is given by the equation (5.1). The cost of starting up a thermal generating unit is influenced by temperature. This type of cost refers to the expenses incurred during the process of bringing the unit online, and it is calculated based on the length of time the unit has been inactive. Conversely, shut down cost is a predetermined

amount for each unit that is shut down. To represent start-up cost mathematically, it can be denoted as (SUC_{tk}).

$$SUC_{kt} = \begin{cases} HSC_k; \text{ for } \mathrm{MDT}_k \le T_k^{OFF} \le (CSH_k + MDT_k) \\ CSC_k; \text{ for } T_i^{ON} \ge (MDT_k + CSH_k) \end{cases} \qquad (k = 1,2,...,NG;\ h = 1,2,3....H) \quad (5.2)$$

In this context, the terms CSC_k and HSC_k represent the cost of cold start-up and hot start-up for the k^{th} unit, respectively. Additionally, MDT_k refers to the minimum downtime for the k^{th} unit, while T_k^{OFF} denotes the duration of time that the k^{th} thermal unit has been offline continuously until the current hour t. CSC_k represents the hour at which cold start is initiated for the k^{th} unit. The start-up cost for a thermal unit is determined by its downtime. If the downtime exceeds the MDT plus the predetermined Cold-Start Hours, then a Cold-Start Cost is required to bring the unit back online. On the other hand, if the downtime is shorter than the specified duration, then a Hot-Start Cost is needed to restart the unit. Various constraints related to the security constraint unit commitment problem are elaborated below.

5.2.2 Constraints of SCUC problem for PEVs-RES

The security-constrained unit commitment problem Associated with RES and PEVs consists of a number of constraints that must be taken into consideration in order to guarantee an energy system that is both dependable and effective. One of the essential limitations is the power balance condition, which expects that the power supply from all sources should be equivalent to the power interest consistently. To ensure that each generating unit and transmission line operates within safe and stable parameters, it is also necessary to take into consideration the minimum and maximum operating limits.

The availability of renewable energy sources, which are affected by the weather and can change over time, is another significant constraint. To balance the intermittent nature of these sources, this necessitates the use of appropriate storage and demand response strategies as well as precise forecasting of RES output. Additionally, the SCUC problem's

inclusion of PEVs imposes unique constraints, such as the requirement to manage these vehicles' charging and discharging in order to avoid overburdening local distribution networks. In order to optimize charging schedules and minimize the impact on the power system, this necessitates modeling the charging behavior of PEVs and taking into account their interaction with the grid. Lastly, the issue must be resolved within security constraints by evaluating and mitigating potential system failures and contingencies to guarantee an energy system that is dependable and enduring. This includes looking at how generator and transmission line outages might affect things, as well as the possibility of cascading failures and unstable voltage.

5.2.2.1 Power Balance with PEVs

The mathematical formulation for power balance constraint in the presence of plug-in electric vehicles and renewable energy sources is given by the equation (5.3).

$$\sum_{k=G}^{t=NH} P_G^k + \sum_{k=RES}^{t=NH} P_{RES}^k \mp \sum_{k=PEV}^{t=NH} P_{PEV}^k = P_D^k \tag{5.3}$$

$$\begin{cases} P_{PEVs} = P_{PEVs} & \text{Discharing period of PEVs} \\ P_{PEVs} = -P_{PEVs} & \text{Charing Period of PEVs} \end{cases} \tag{5.3a}$$

Maintaining power balance or load balance is extremely important in the power system. P_G^k is the conventional power generation for the k[th] unit, $P_{RES}^k$is the renewable power generation for the k[th] unit, P_{EV}^k is the power from electric vehicle, where '+' indicate the discharging of power and '-' indicate the charging of the electric vehicle, P_D^k is the power demand of the system. Equation (5.3a) illustrates the charging and discharging nature of electric vehicle. This constraint ensures that the total power generated by all committed generating units during a specific time t (hour) is either greater than or equal to the power demand for that corresponding time period. Equation (5.3) outlines the power balance constraint that must be followed when charging electric vehicles.

$$\sum_{k=1}^{NG} P_{k,t} U_{k,t} = P_{D_t} + P_{D_T}^{PEVs} \tag{5.4}$$

The power system must ensure that the total power generated at a specific t^{th} hour and the power generated from renewable energy sources ($P_t^{\text{Re}newable}$) at the same time period meet the demand for electricity. This means that the combined electricity generated by the k^{th} unit at time t^{th} hour (h) must also meet the load demand P_{D_t} . The power balance constraints considering renewable sources is given by equation (5.5)

$$\sum_{k=1}^{NG} P_{k,t} U_{k,t} + P_t^{RES} = P_{D_t} \tag{5.5}$$

The mathematical modeling for power balance constraint considering PEVs and RES is given by equation (5.6)

$$\sum_{k=1}^{NG} P_{k(\max)} U_{k,t} + P_t^{\text{Re}newable} = P_{D_t} + P_{D_t}^{PEVs} \tag{5.6}$$

Here, $P_t^{\text{Re}newable}$ is the renewable power at t^{th} hour, P_{D_t} is the demand of power for t^{th} hour and $P_{D_t}^{PEVs}$ is the power demand from plug-in electric vehicles for time (t) hour.

5.2.2.2 Spinning reserve constraints of SCUC problem

The mathematical formulation for spinning reserve constraints considering PEVs and RES is given by equation (5.7)

$$\sum_{k=1}^{NG} P_{Gk}^{\max} \mp \sum_{k=1}^{NG} P_{PEV_k} + \sum_{k=1}^{NG} P_{\text{Re}newable_k} \geq P_{D_k} + SR_t \tag{5.7}$$

Where, $P_{Gk}^{\max}$ is the maximum power generation for k^{th} unit, P_{PEV_k} is the power of charging and discharging for the k^{th} unit, $P_{\text{Re}newable_k}$ is the renewable power generation for k^{th} unit, P_{D_k} is the power demand of the k^{th} , SR_t is the spinning reserve for the time t^{th} hour. In the equation (5.7), the '$\mp$' indicate the charging of PEVs (-) and '+' indicate the discharging of the PEVs.

In the spinning reserve process, when considering the charging of PEVs for the particular hour of to time (t) is given by equation (5.9) and for discharging in presence of renewable energy sources (RES) is given by the equation (5.10)

$$\sum_{k=1}^{NG} P_{k(\max)} U_{k,t} + P_t^{\text{Re}\,newable} \geq P_{D_t} + SR_t \tag{5.8}$$

The spinning reserve constraint for with RES and charging nature of PEVs is mathematical formulated as shown in equation (5.9).

$$\sum_{k=1}^{NG} P_{k(\max)} U_{k,t} + P_t^{\text{Re}\,newable} \geq P_{D_t} + P_{D_t}^{PEVs} + SR_t \tag{5.9}$$

The spinning reserve constraint for with RES and discharging nature of PEVs is mathematical formulated as shown in equation (5.9).

$$\sum_{k=1}^{NG} P_{k(\max)} U_{k,t} + P_t^{\text{Re}\,newable} \geq P_{D_t} - P_{D_t}^{PEVs} + SR_t \tag{5.10}$$

5.2.2.3 Minimum up and down time constraints for SCUC problem

In the SCUC problem process, the minimum up and down time constraint plays a significant role in regulating the amount of time that a generating unit must stay on or off before it can be turned on or off again. By carefully managing the use of generating units in adherence to these constraints, system operators can ensure the provision of dependable and cost-effective energy to fulfill the expected load, while also promoting the efficient use of resources.

$$T_{tk}^{ON} \geq MUT_k \qquad (\mathrm{k} = 1,2,...,NG;\ t = 1,2,...,Hour) \tag{5.11}$$

In this equation, the symbol T_{tk}^{ON} represents the time duration that a unit k^{th} remains continuously operational in t hours, while MUT_k refers to the minimum time that a particular unit must remain active before it can be shut down again, also measured in hours. Both of these parameters are relevant to the k units being considered. After a unit has been

turned off, it cannot be restarted until a certain minimum duration has elapsed, known as the "down-time" period. This constraint can be expressed mathematically as follows:

$$T_{tk}^{OFF} \geq MDT_k \qquad (\mathrm{k} = 1, 2, ..., NG;\ t = 1, 2, ..., Hour) \tag{5.12}$$

In this context, the variable "T_{tk}^{OFF}" represents the length of time that the k^{th} unit has been continuously inactive in hours. Additionally, the parameter "MDT_k" refers to the minimum duration of inactivity required for that specific unit k, also measured in hours t.

5.2.2.4 Thermal Constraints for SCUC problem

Thermal constraints are a security constraint that is crucial to consider in the operation of power systems. These constraints set limits on the maximum power output of thermal generators, including coal, gas, or nuclear power plants. Such limits exist due to the physical constraints of their equipment or cooling systems. Typically, thermal constraints are stated as inequality constraints, which restrict the maximum power generation capacity of thermal generators. For instance, the capacity limit of a thermal generator could be articulated as follows:

$$P_{Thermal,t} \leq P_{Max} \tag{5.13}$$

Where $P_{Thermal,t}$ is the thermal output of the generator at time t, and P_{Max} is the maximum allowable thermal output. The operational limit of a thermal generator can be expressed as:

$$P_{Thermal,t} \leq \alpha \times P_{Max} \tag{5.14}$$

Where α is a safety factor that accounts for the generator's operating conditions and typically ranges between 0.85 to 0.95.

5.2.2.5 Crew Constraints for SCUC problem

Crew constraints play a crucial role in ensuring the safe and efficient operation and maintenance of power systems. They establish a limit on the number of workers that can work on power system equipment, ensuring that maintenance and repair tasks are carried

out effectively while maintaining a reliable power system. Crew constraints are usually expressed as a maximum limit on the number of workers assigned to a specific piece of equipment or area.

5.2.2.6 Initial Operating Status of Generation Units

In order to ensure that every unit meets its minimum up/down time requirements, the initial operating status of each unit must consider the previous day's schedule. This means that the starting status of each unit is influenced by its previous operating state and the minimum duration it must remain in that state before it can transition to another state. By factoring in these considerations, the initial operating status of each unit can be determined in a way that promotes system reliability and efficiency.

5.2.2.7 Plug-in electric vehicles balance

In order to schedule a specified period according to the forecasts or registered PEVs, the total number of vehicles (N) should not be more than or equal to the maximum for which they have been authorized.

$$\sum_{t=1} N_{V2G}(t) = N_{V2G}^{max} \tag{5.15}$$

Total vehicles in parking lots shall be taken into account as a percentage of the maximum number of vehicles per hour.

$$N_{V2G}(t) = \beta\%\ N_{V2G}^{\max} \tag{5.16}$$

5.3 Methodologies for SCUC problem with PEVs & RES

To solve the SCUC problem, which involves physical constraints and thermal power units, RES, and EVs unit's, researchers have used the CAOA algorithm, a chaotic version of AOA. The study incorporates the impact of charging and discharging Plug-in Electric Vehicles with Renewable Energy Sources [32]. Using the CAOA algorithm, the research aims to optimize the operation of thermal units in an economically efficient way while meeting time-varying power demands and adhering to physical and system constraints. This includes accounting for the impact of RES in both summer and winter seasons.

In order to address different system constraints within the SCUC problem, including but not limited to the spinning reserve constraint, minimum up and down time constraint, and de-commitment of excessive power generators, a specific procedure has been established [127]. In the upcoming chapters, we will delve into the suggested hybrid optimizers that have been proposed to effectively solve the security constraint unit commitment problem [128].

5.3.1 Managing Spinning Reserve Constraint in SCUC problem with Charging and Discharging of PEVs

The reserve capacity requirement for various power units can be met by taking into account both the minimum up and down time of each unit, as well as the duration for which the ith unit remains in a continuously OFF state. To ensure compliance with the algorithm, reserve constraints must be adjusted accordingly, as demonstrated in the flowchart provided in Figure 5.1.

Step 1: Arrange the power generation in a decreasing order based on their maximum capacity to generate power

Step 2:

$$\textit{or } k = 1 \textit{ to } NG \textit{ if } u_{k,t} = 0 \quad \textit{then } u_{k,t} = 1$$
$$\textit{else if } \mathrm{T}_{k,t}^{OFF} \geq T_k^{MDT_k}$$
$$\textit{then } T_{k,t}^{ON} = T_{k,t-1}^{ON} + 1 \text{ and } T_{k,t}^{OFF} = 0$$

Step 3: Check the newly generated power output of the units for validation.

Step 4: if $\sum_{k=1}^{NG} P_{k(\max)} U_{k,t} \geq P_{D_t} + P_{D_t}^{PEVs} + SR_t$ belongs to charging,

$$\sum_{k=1}^{NG} P_{k(\max)} U_{k,t} \geq P_{D_t} - P_{D_t}^{PEVs} + SR_t \text{ belongs to discharging}$$

If the condition is not met, proceed to step 2, otherwise terminate the algorithm.

Step 5: if $T_{k,t}^{OFF} \le T_k^{MDT_k}$ then do $l = t - T_{k,t}^{OFF} + 1$ and set $u_{k,t} = 1$

Step 6: Find out $T_k^l = T_{k,l-1}^{ON} + 1$ and $T_{k,t}^{OFF} = 0$

Step 7: If $1 > t$, Check the power output $\sum_{k=1}^{NG} P_{k(\max)} U_{k,t} \ge P_{D_t} + P_{D_t}^{PEVs} + SR_t$ of the generator to ensure its accuracy for charging and $\sum_{k=1}^{NG} P_{k(\max)} U_{k,t} \ge P_{D_t} - P_{D_t}^{PEVs} + SR_t$, belongs to discharging of PEVs and then proceed to step 5.

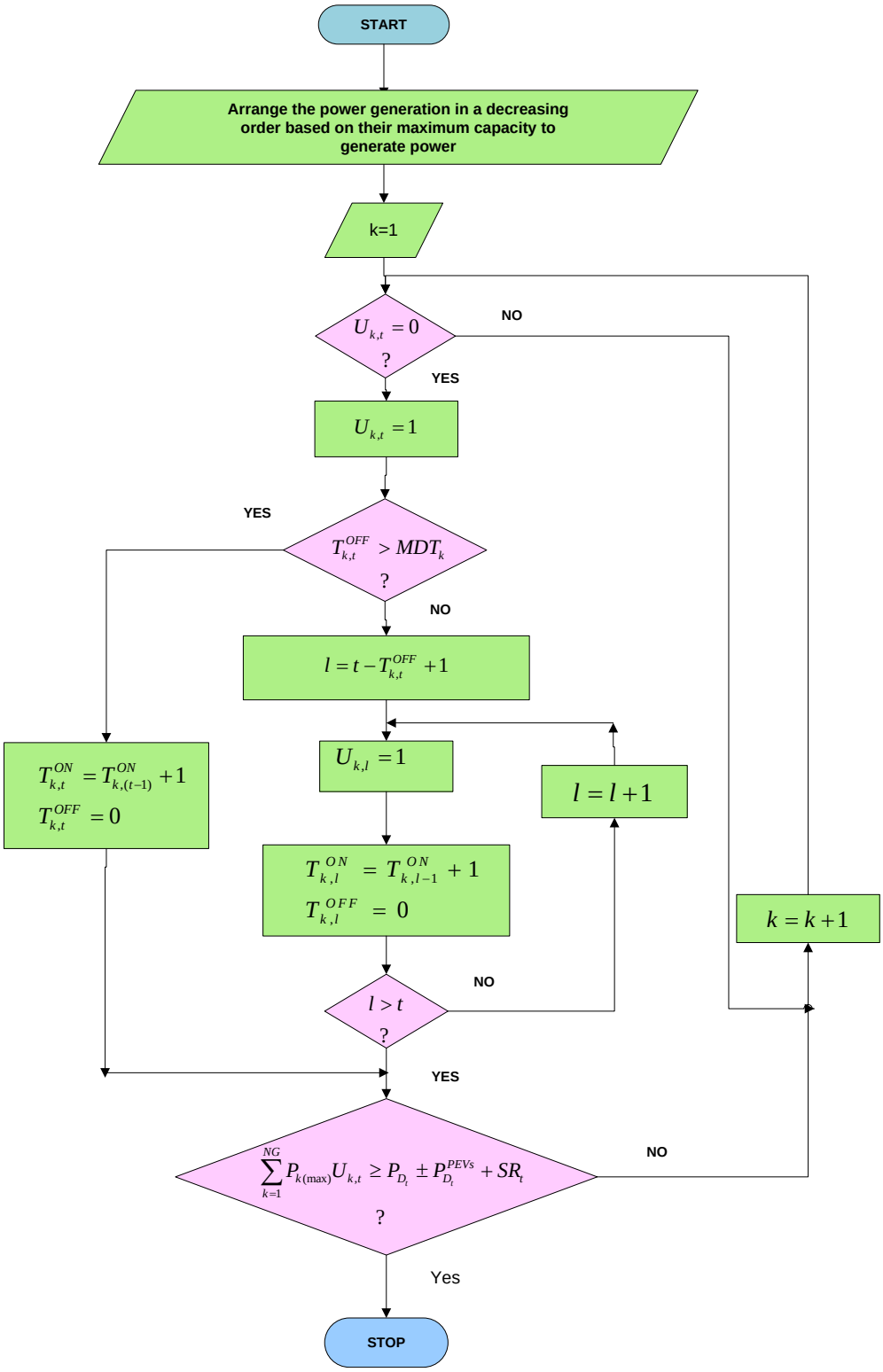

Figure 5.1: Flowchart for Spinning Reserve Constraints with PEVs

5.3.2 Spinning Reserve Constraint in SCUC problem with RES

In the SCUC problem with RES, spinning reserve constraint is an essential consideration. In the event of an unexpected outage or contingency, spinning reserves are the available generating capacity that can be quickly increased or decreased to meet demand. The stepwise procedure for spinning reserve constraint with RES for SCUC problem and flowchart is shown in the figure 5.2.

Step 1: Arrange the power generation in a decreasing order based on their maximum capacity to generate power

Step 2:

$$or\ k = 1\ to\ NG\ if\ u_{k,t} = 0 \quad then\ u_{k,t} = 1$$
$$else\ if\ \mathrm{T}_{k,t}^{OFF} \geq T_k^{MDT_k}$$
$$then\ T_{k,t}^{ON} = T_{k,t-1}^{ON} + 1 \text{ and } T_{k,t}^{OFF} = 0$$

Step 3: Check the newly generated power output of the units for validation.

Step 4: if $\sum_{k=1}^{NG} P_{k(\max)} U_{k,t} + P_k^{RES} \geq P_{D_t} + SR_t$ then break the process. If the condition is not met, proceed to step 2, otherwise terminate the algorithm.

Step 5: if $T_{k,t}^{OFF} < T_k^{MDT_k}$ then do $l = t - T_{k,t}^{OFF} + 1$ and set $u_{k,t} = 1$

Step 6: Find out $T_k^l = T_{k,l-1}^{ON} + 1$ and $T_{k,t}^{OFF} = 0$

Step 7: If $1 > t$, Check the power output $\sum_{k=1}^{NG} P_{k(\max)} U_{k,t} + P_t^{RES} \geq P_{D_t} + SR_t$ of the generator to ensure its accuracy for RES and then proceed to step 5.

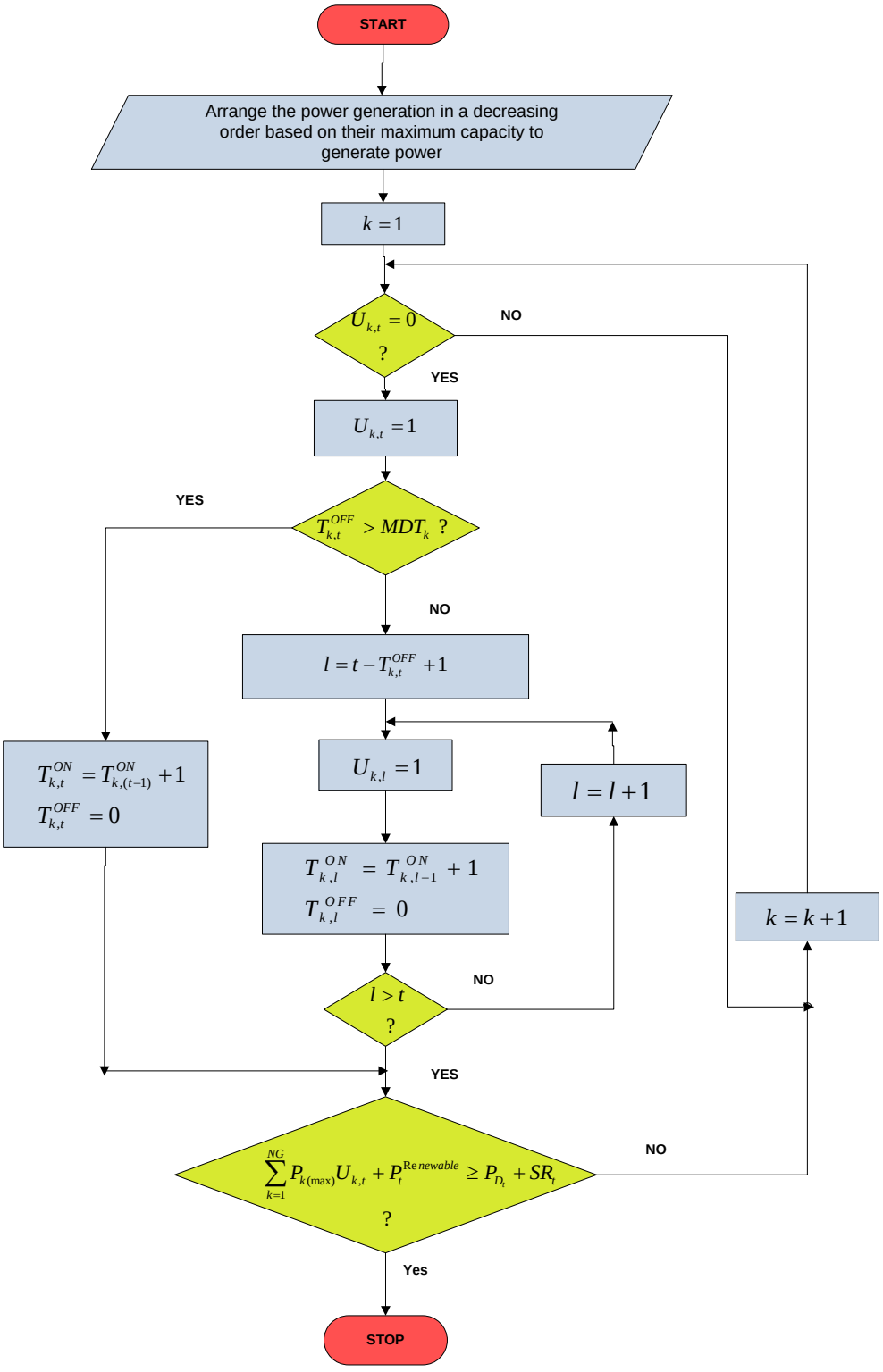

Figure 5.2: Flowchart for Spinning Reserve Constraints with RES

5.3.3 Spinning Reserve Constraint in SCUC problem with PEVs & RES

To meet the reserve capacity requirements of various power units, it is necessary to take into account the minimum up and down times for each unit, as well as the duration of time that the ith unit remains in a continuously OFF state [51]. The reserve constraints should be adjusted according to the algorithm outlined in the flowchart provided in Figure 5.3.

Step 1: Arrange the power generation in a decreasing order based on their maximum capacity to generate power

Step 2:

$or\ k = 1\ to\ NG\ if\ u_{k,t} = 0 \quad then\ u_{k,t} = 1$

$else\ if\ \mathrm{T}_{k,t}^{OFF} \geq T_k^{MDT_k}$

$then\ T_{k,t}^{ON} = T_{k,t-1}^{ON} + 1$ and $T_{k,t}^{OFF} = 0$

Step 3: Check the newly generated power output of the units for validation.

Step 4: if $\sum_{k=1}^{NG} P_{k(\max)} U_{k,t} + P_t^{RES} \geq P_{D_t} + P_{D_t}^{PEVs} + SR_t$ belongs to charging,

$\sum_{k=1}^{NG} P_{k(\max)} U_{k,t} + P_t^{RES} \geq P_{D_t} - P_{D_t}^{EVs} + SR_t$ belongs to discharging

If the condition is not met, proceed to step 2, otherwise terminate the algorithm.

Step 5: if $T_{k,t}^{OFF} \leq T_k^{MDT_k}$ then do $l = t - T_{k,t}^{OFF} + 1$ and set $u_{k,t} = 1$

Step 6: Find out $T_k^l = T_{k,l-1}^{ON} + 1$ and $T_{k,t}^{OFF} = 0$

Step 7: If $1 > t$, Check the power output $\sum_{k=1}^{NG} P_{k(\max)} U_{k,t} + P_t^{RES} \geq P_{D_t} + P_{D_t}^{PEVs} + SR_t$ of the generator to ensure its accuracy for charging and $\sum_{k=1}^{NG} P_{k(\max)} U_{k,t} P_t^{RES} \geq P_{D_t} - P_{D_t}^{PEVs} + SR_t$, belongs to discharging of PEVSs and then proceed to step 5.

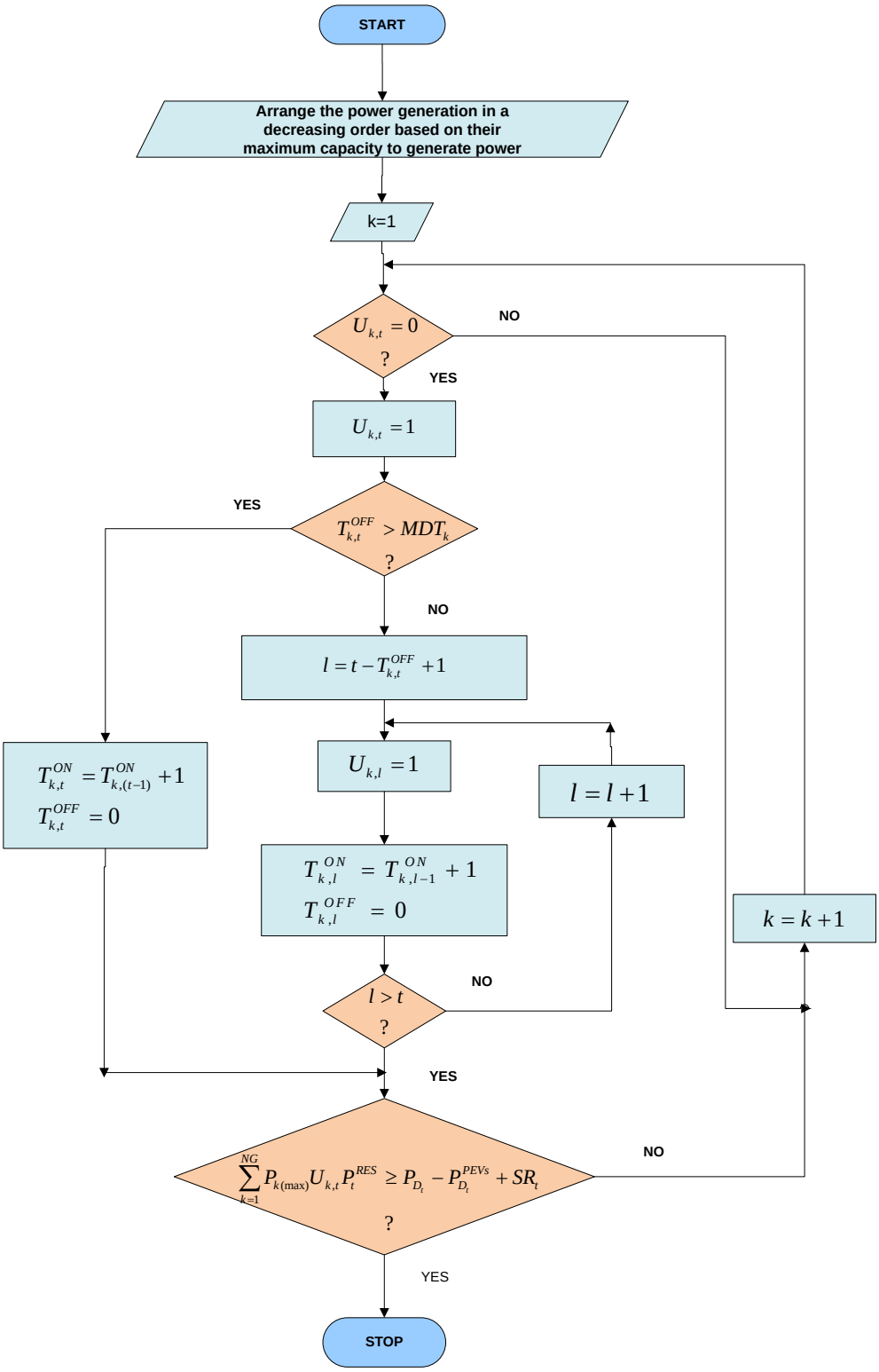

Figure 5.3: Flowchart of repairing for spinning reserve constraints with RES and PEVs

5.3.4 Addressing the Constraints related to Minimum up and Down time

The method utilized to meet the minimum downtime requirement of generating units involves the implementation of a particular repair mechanism.

Algorithm for MUT/MDT

Step 1: Arrange the power generation in a decreasing order based on their maximum capacity to generate power

Step 2: for $t=1$ to T and $k=1;NG$, then set $k=1$

Step 3: If $U_{k,t}=1$ then set $U_{k,(t-1)}=0$

Step 4: Check $T_{tk}^{ON} < MUT_k$ and set $U_{k,t}=0$ or else set $U_{k,t}=1$

Step 5: If $U_{k,(t-1)}=1$, then set $U_{k,t}=0$

Step 6: if $T_{k(t-1)}^{ON} < MUT_k$, then set $U_{k,t}=1$ and stop if.

Step 7: if $t+MDT_k-1 \le T$ and $T_{t+MDT_t-1}^{OFF} \le MDT_k$, then set $U_{k,t}=1$ and otherwise end if.

Step 8: if $t+MDT_k-1 > T$ and $\sum_{t=1}^{H} U_{k,t} > 0$, then set $U_{k,t}=1$ and end if or else proceeds to next step 5

Step 9: Modify the time period for both the committed and decommitted generation units of the k^{th} unit using the equations $T_{tk}^{ON} \ge MDT_k$ and $T_{tk}^{OFF} \ge MDT_k$.

5.3.5 De-commitment of the excessive unit with RES and PEVs

To meet the load demand and reserve requirements of all thermal units while minimizing downtime, it is necessary to decommit excessive thermal units [116]. The algorithm can address the constraint of maintaining minimum downtime and uptime for each unit, as well as the duration during which a particular power unit remains continuously turned off. A

flowchart for this process is presented in Figure 5.4. The steps for the de-commitment of excessive unit as follow.

Step 1: Arrange the power generation in a decreasing order based on their maximum capacity to generate power

Step 2: for $t = 1 \text{to } T$ and for $k = 1$ to NG, then $k = t(NG + 1 - k)$ and find out generated power, $P1 = P_{k(\max)} \times (U_{k,t})'$

or $k = 1$ *to NG if* $u_{k,t} = 0$ *then* $u_{k,t} = 1$

else if $\mathrm{T}_{k,t}^{OFF} \geq T_k^{MDT_k}$

then $T_{k,t}^{ON} = T_{k,t-1}^{ON} + 1$ and $T_{k,t}^{OFF} = 0$

$t = 1$

T

$k = 1$

NG

$k = t(NG + 1 - k)$

Step 3: Check the newly generated power output of the units for validation.

Step 4: if $\sum_{k=1}^{NG} P_{k(\max)} U_{k,t} + P_t^{RES} \geq P_{D_t} + P_{D_t}^{PEVs} + SR_t$ belongs to charging,

$\sum_{k=1}^{NG} P_{k(\max)} U_{k,t} + P_t^{RES} \geq P_{D_t} - P_{D_t}^{PEVs} + SR_t$ belongs to discharging

and $T_{k,l}^{ON} > MUT_k$ then do $U_{k,t} = 0$, else terminate the algorithm, or else if $T_{k,t}^{ON} = 1$, do $U_{k,t} = 0$, else do the increment 1 by 1 and proceeds to step 2.

Step 5: if $T_{k,t}^{ON} = 0$ and find out $T_{k,t}^{OFF} = T_{k,t_0}^{OFF} + 1$

Step 6: if $U_{k,t} = 1$, check the output power Find out

$\sum_{k=1}^{NG} P_{k(\max)} U_{k,t} + P_t^{RES} \geq P_{D_t} + P_{D_t}^{PEVs} + SR_t$ for charging &

$\sum_{k=1}^{NG} P_{k(\max)} U_{k,t} P_t^{RES} \geq P_{D_t} - P_{D_t}^{PEVs} + SR_t$ for discharging of PEVs, else OFF the generating unit and move to step 4.

The flowchart for de-commitment unit in presence of RES and charging-discharging nature of PEVs is shown in Figure 5.4.

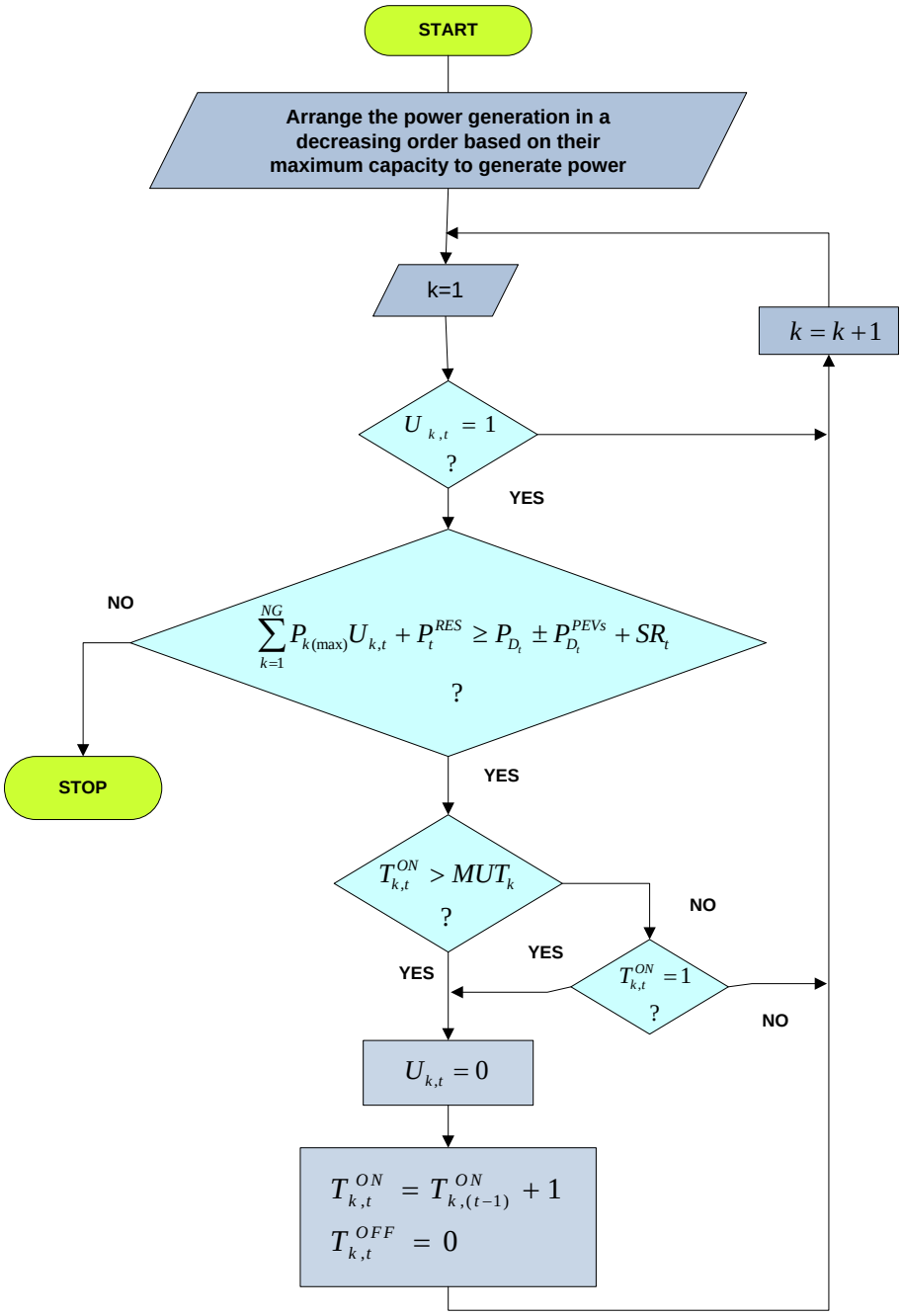

Figure 5.4: Flowchart of the de-commitment with RES and PEVs

Below is a different way of presenting the procedure to SCUC problem with the impact of charging and discharging nature of PEVs and RES in summer and winter days [7].

The SCUC problem parameters that are entered include the effects of the charging and discharging behavior of PEVs as well as the effects of renewable energy sources on both summer and winter days. These renewable sources include power from solar radiation, as well as power generated through G2V and V2G operations. Other factors that are taken into account include the maximum and minimum power levels, revenue and energy prices, minimum up time and minimum time, the initial status, and the hot start and cold start costs [129].

Step 1. Initialize the parameters for the proposed algorithm.

Step 2. Set the iteration counter K to 1.

Step 3. Randomize the search agent locations.

Step 4. Calculate the power for each search agent according to the priority list, considering the impact of charging and discharging nature of PEVs and the impact of RES in summer and winter days.

Step 5. Update the search agent position to satisfy the spinning reserve constraint, taking into account the impact of charging and discharging nature of PEVs and the impact of RES in summer and winter days.

Step 6. Repair each search agent position to ensure minimum up and down time violations are maintained.

Step 7. Decommit excessive generating units to reduce excessive spinning reserve, considering the impact of PEVs and RES in both summer and winter days.

Step 8. Calculate fuel cost using start-up cost and overall profit.

Step 9. Evaluate the individual cost for each generating unit.

Step 10. Compare the total power generation cost of each population and choose the best value for total fuel cost. Upgrade the generator scheduling using the proposed technique.

Step 11. Verify the value of I for the maximum number of iterations. If not reached, increase the iteration count by 1.

Step 12. Evaluate the actual power generation schedule and optimal cost for the committed unit.

Step 13. Record the power generation scheduling status, commitment unit status, and optimal cost, considering the impact of charging and discharging nature of PEVs and the impact of RES in summer and winter days $\sum_{k=1}^{NG} P_{k(\max)} U_{k,t} + P_t^{\text{Renewable}} \geq P_{D_t} \pm P_t^{PEVs} + SR_t$.

5.3.6 Photovoltaic system power output

The solar power plant in this research work is used to supply power. It consists of a set of photovoltaic panels covering an area of 150 hectares, with a capacity of 60 MW as the power base. The efficiency of the photovoltaic array is considered to be 0.3 due to the low efficiency of solar panels, which convert only a small fraction of solar radiation into power. To evaluate the problem completely, information about solar radiation and ambient temperature is collected for a summer day or a winter day. If the system works at the maximum output power point, the relationship between the output power and the photovoltaic system shall be described as follows:

$$P_{PV}^{max} = \eta A_{PV} S_{Radition} [1 - 0.005 (T_c - 25)] \quad (5.17)$$

where, η represents the photoelectric conversion efficiency of the PV array in percentage (%), A_{PV} denotes the total area of the array in square meters (m^2), $S_{Radition}$ indicates the incident solar radiation on the panels measured in kilowatts per square meter (kW/m^2), and T_c stands for the operational temperature of the panels in degrees Celsius (°C). Conversely, it's noteworthy that the majority of grid-connected PV inverters function in the Maximum

Power Point Tracking (MPPT) mode, maintaining a relatively consistent power conversion efficiency. Table 5.4 and 5.5 present data on temperature and solar radiation for a summer day and a winter day, respectively.

5.4 TEST SYSTEM

The SCUC problem was successfully solved by considering the limitations of power generation units and various system sizes, including small, medium, and large-scale systems. The test data for renewable energy sources has been discussed and illustrated in Table 5.2 to 5.6.

5.4.1 Data for renewable energy sources

To optimize the on and off units, charging and discharging of vehicles are also employed. The system assumes a fleet of 40,000 vehicles, of which only 20% are involved in charging and discharging. Each vehicle has a battery capacity of 15 kW, a departure state of charge (d) of 0.50%, and an efficiency (g) of 85%. In this system, 8000 vehicles can participate which is equivalent to 51 MW of electrical power [90].

Table 5.2 Transfer of power during V2G and G2V operations during summer [90]

Time	Number of PEVs	Pg2v	Pv2g
t_1	5094	32.4	--
t_2	3225	20.5	--
t_3	6984	44.5	--
t_4	7575	48.2	--
t_5	4480	28.5	--
t_6	4905	31.2	--
t_7	1128	7.18	--
t_8	235	1.4	--
t_9	7844	--	50
t_{10}	7033	--	44.8
t_{11}	6801	--	43.3
t_{12}	7558	--	48.1
t_{13}	7680	--	48.9
t_{14}	2505	--	15.9
t_{15}	4309	27.4	--
t_{16}	5759	36.7	--
t_{17}	2392	15.2	--
t_{18}	6955	44.3	--
t_{19}	2827	18.1	--
t_{20}	7844	--	50
t_{21}	5220	--	33.2
t_{22}	6130	--	39.7
t_{23}	2794	--	17.8
t_{24}	5043	--	32.1

Table 5.3 Transfer of power during V2G and G2V operations during winter [90]			
Time	**Number of PEVs**	**Pg2v**	**Pv2g**
t_1	6159	39.2	--
t_2	6588	41.9	--
t_3	7528	47.9	--
t_4	7394	47.1	--
t_5	6631	42.2	--
t_6	4230	26.9	--
t_7	93	0.58	--
t_8	3629	23.1	--
t_9	7535	--	48
t_{10}	7844	--	50
t_{11}	7325	--	46.6
t_{12}	6252	--	39.8
t_{13}	7681	--	48.9
t_{14}	5946	--	37.9
t_{15}	253	1.6	--
t_{16}	7844	50	--
t_{17}	6630	42.2	--
t_{18}	3657	23.3	--
t_{19}	734	4.6	--
t_{20}	4689	--	29.8
t_{21}	7481	--	47.6
t_{22}	2423	--	15.4
t_{23}	3193	--	20.3
t_{24}	273	--	1.73

The solar power plant in this research work is used to supply power. It consists of a set of photovoltaic panels covering an area of 150 hectares, with a capacity of 60 MW as the power base. The efficiency of the photovoltaic array is considered to be 0.3 due to the low efficiency of solar panels, which convert only a small fraction of solar radiation into power. Tables 5.4 and Table 5.5 present data on temperature and solar radiation for a summer and a winter day, respectively. The data on renewable energy sources belongs to the National Renewable Energy Laboratory, Texas (USA). The information presented is derived from a reference paper that relies on the findings of the published research paper [90].

Table 5.4 The hourly information on solar energy for a summer day [90]			
Time	**Radiation (W/m^2)**	**Temperature (^0C)**	**Output power (MW)**
t_1	0	37	0
t_2	0	37	0
t_3	0	37	0
t_4	0	37	0
t_5	0	37	0
t_6	0	37	0
t_7	0	37	0
t_8	80.67	37	4.55
t_9	277.98	37	15.67
t_{10}	484.89	37	27.34
t_{11}	659.06	37	37.17
t_{12}	816.76	37	46.06
t_{13}	919.5	37	51.86
t_{14}	965.79	37	54.47
t_{15}	790.64	37	44.59
t_{16}	866.43	37	48.86
t_{17}	670.97	37	37.84
t_{18}	595.89	37	33.6
t_{19}	346.83	37	19.59
t_{20}	115.42	37	6.51
t_{21}	2.97	37	0.16
t_{22}	0	37	0
t_{23}	0	37	0
t_{24}	0	37	0

Table 5.5 The hourly information on solar energy for a winter day [90]			
Time	**Radiation (W/m^2)**	**Temperature (^0C)**	**Output power (MW)**
t_1	0	22	0
t_2	0	22	0
t_3	0	22	0
t_4	0	22	0
t_5	0	22	0
t_6	0	22	0
t_7	0	22	0
t_8	0	22	0
t_9	9.4	22	0.5729
t_{10}	58.52	22	3.56
t_{11}	10.42	22	6.6
t_{12}	296.24	22	18.04
t_{13}	361.11	22	21.99
t_{14}	271.34	22	16.52
t_{15}	527.44	22	32.12
t_{16}	496.76	22	28.6
t_{17}	379.27	22	23.09
t_{18}	301.46	22	18.32
t_{19}	131.16	22	7.98
t_{20}	3.06	22	0.18
t_{21}	0	22	0
t_{22}	0	22	0
t_{23}	0	22	0
t_{24}	0	22	0

The assessment takes into consideration varying temperatures during summer and winter days. Specifically, a temperature of 37 degrees Celsius is considered for summer days, while a temperature of 22 degrees Celsius is taken into account for winter days. To ensure a comprehensive analysis, data pertaining to solar energy radiation and environmental temperature have been factored in for summer days and for winter days.

The power produced by wind turbine varies to cube of the rated speed. This however is applicable for certain range of speed. Indeed, for a small wind speed, there is not enough torque the turbine. The wind speed at which the rotor starts to rotate is called the cut-in-speed. Below cut-in-speed, no power is produced. The cut-in-speed is typically about 3 to 4 m/s. On the other hand, if the wind is strong, the rotor cannot produce large power because of mechanical constraints. Therefore, the so-called cut-out-speed is the maximum speed at which power can be safely produces. The cut-out-speed lies typically around 25m/s. Finally, electrical generator also imposes a limit on the power that can be produced as output power. Thus, beyond a certain wind speed, the power is limited to a constat value. This maximum output power is referred to as rated power and typically occurs for wind speed from 12 to 17 m/s. The Weibull distribution function developed by Swedish professor Waloddi Weibull in 1951 is the most widely used life time distribution in reliability engineering. It is a versatile distribution function, based on the value of shape parameter. The probability distribution function for the calculation of wind power can be mathematically represented as

$$pdf(v, g, \lambda) = \frac{g}{\lambda}\left(\frac{v}{\lambda}\right)^{g-1} exp\left[-\left(\frac{v}{g}\right)^{g}\right] \tag{5.18}$$

Where, $pdf(v, g, \lambda)$ is the probability density function of the wind speed, λ is the Weibull scale parameter, g is the dimensionless Weibull shape parameter, v is the velocity in m/s. The data for the wind power generation test system includes consideration of a shape factor of 2, a scale factor of 7, a cut-in speed set at 25 m/s, and a rated speed ranging from 11 to 15 m/s. The turbine data sheet specifies a capacity of 1.5 MW. The wind farm is sized at 25.5 MW, featuring 17 wind turbines, each with a capacity of 1.5 MW.

Table 5.6 Day-ahead forecasted wind power output [131]

Hour	1	2	3	4	5	6	7	8	9	10	11	12
Demand (MW)	177	171	158	145	142	137	120	109	116	116	117	115
Hour	13	14	15	16	17	18	19	20	21	22	23	24
Demand (MW)	114	109	107	111	103	90.5	99.6	120	127	137	160	175

The available wind power, denoted as P, that can be obtained within the cross-sectional area (A_C) (the circular area created by the wind turbine blades) perpendicular to the wind at a speed V (m/s), considering a given air density (K_g/m^3), is expressed by the following equation.

$$P = \frac{1}{2}\rho_{air}\, C_p A_C V^3 \tag{5.19}$$

where, P = Power Captured, ρ_{air} = Air density kg/m^3, A_C = Swept Area of the turbine, V^3 = Wind Velocity in m/s, C_p = Power Coefficient.

5.5 RESULT AND DISCUSSION

To determine the effectiveness of the proposed techniques for the SCUC problem, standard test systems were utilized. These test systems were classified into small-scale (10 units), medium-scale (20 generating units), and large-scale (40 generating units) systems. The performance of the proposed algorithms was evaluated using MATLAB 2021a (8.1.0.604) software on a 64-bit version of Windows 11 Home Basic, with a CPU operating at 2.10 GHz, 8 GB of RAM, and an Intel® CoreTM i5-2310M processor. According to statistical analysis, the CAOA algorithms proposed were found to be effective.

5.5.1 Hybrid Chaotic Arithmetic Optimization Algorithm and Levy Flight Arithmetic Optimization algorithm with plug-in electric vehicles and renewable energy sources

The CAOA and LFAOA are novel hybrid algorithms that combine chaotic maps and levy flight strategies with arithmetic optimization techniques. These algorithms are designed to address optimization problems by incorporating both exploratory and exploitative phases, which are stimulated using arithmetic operations such as division, multiplication, addition, and subtraction. CAOA and LFAOA are population-based algorithms that do not rely on gradients, which makes them suitable for a wide range of optimization problems.

The CAOA and LFAOA algorithms are effective in the exploratory phase, where they generate a diverse set of solutions using chaotic maps. It also has a strong ability to adapt from the exploratory phase to the exploitative phase, where it refines the solutions using arithmetic operations. Overall, CAOA and LFAOA are powerful optimizers that can be applied to a variety of optimization problems. Its ability to combine chaotic maps with arithmetic optimization techniques makes it a promising algorithm that can effectively address complex optimization issues.

5.5.1.1 System of Ten Generating Units

The efficiency of the proposed CAOA and LFAOA optimizers is tested using a specialized system comprising 10 power-generating units that operate for 24 hours. The CAOA and LFAOA techniques are subjected to evaluation through 100 iterations, while 30 trial runs

verify the effectiveness of the CAOA and LFAOA algorithms. Details of the commitment status, optimal scheduling, and costs of the 10 generating units for thermal units with PEVs are presented in **Tables 5.7** and **5.8**, respectively. **Table 5.7** illustrates the commitment status, while **Table 5.8** displays the optimal scheduling of power-generating units during the 24-hour period. P1 operates continuously, supplying 455 MW of power. When the unit is active (indicated as '1') and is off (indicated as '0') otherwise. The commitment status, optimal scheduling, and individual fuel costs of each of the 10 generating units for thermal units and solar units are presented in **Tables 5.9, 5.10,** and **5.11**, respectively. The commitment status, optimal scheduling, and individual fuel costs of each of the 10 generating units for thermal units and wind units are presented in **Tables 5.12, 5.13,** and **5.14**, respectively.

Table 5.13 illustrates the scheduling for a 10-generating unit system using the CAOA algorithm for the SCUC problem (Thermal System + Wind). **Table 5.14** illustrates the individual fuel cost for a 10-generating unit system using the CAOA algorithm for the SCUC problem (thermal system + wind). **Table 5.15** illustrates the committed status for a 10-generating unit system using the CAOA algorithm for the SCUC problem (thermal + solar + wind). **Table 5.16** illustrates the scheduling for a 10-generating unit system using the CAOA algorithm for the SCUC problem (thermal + solar + wind). **Table 5.17** illustrates the committed status for a 10-generating unit system using the CAOA algorithm for the SCUC problem (thermal + solar + PEVs). **Table 5.18** illustrates the scheduling for a 10-generating unit system using the CAOA algorithm for the SCUC problem (thermal + solar + PEVs). **Table 5.19** illustrates the individual fuel cost for 10 generating units using CAOA for the SCUC problem, considering the thermal, solar, and PEV systems. **Table 5.20** illustrates the committed status for a 10-generating unit system using the CAOA algorithm for the SCUC problem (thermal + solar + PEVs + wind). **Table 5.21** illustrates the scheduling for a 10-generating unit system using the CAOA algorithm for the SCUC problem (thermal + solar + PEVs + wind). **Table 5.22** illustrates the individual fuel cost for 10 generating unit systems using CAOA for the SCUC problem, considering the thermal + solar + PEV + wind systems. **Table 5.23** illustrates the committed status and

scheduling for a 10-generating unit system using the LFAOA algorithm with PEVs (thermal +PEVs). **Table 5.24** illustrates the individual fuel cost for 10 generating unit systems using the LFAOA algorithm with PEVs (thermal + PEVs). **Table 5.25** illustrates the committed status and scheduling for the 10-Generating Unit system using the LFAOA algorithm with wind power (thermal system + wind). **Table 5.26** illustrates the individual fuel cost for 10 generating unit systems using the LFAOA algorithm for wind power (thermal + wind). **Table 5.27** illustrates the committed status and scheduling for the 10-Generating Unit system using the LFAOA algorithm with solar and PEVs (thermal + solar + PEVs). **Table 5.28** illustrates the individual fuel cost for 10 generating unit systems using the LFAOA algorithm for solar and PEV systems (thermal + solar + PEVs). **Table 5.29** illustrates the committed status and scheduling for a 10-generation unit system using the LFAOA algorithm with wind power and PEVs (thermal + wind + PEVs). **Table 5.30** illustrates the individual fuel cost for 10 generating units using the LFAOA algorithm for wind power and PEVs (thermal + wind + PEVs). **Table 5.31** illustrates the committed status and scheduling for a 10-generating unit system using the LFAOA algorithm with solar, wind, and PEVs (thermal + solar + wind + PEVs). **Table 5.32** illustrates the individual fuel cost for 10 generating units using the LFAOA algorithm for solar and PEV power (thermal + solar + wind + PEVs). **Tables 5.33** and **5.34** illustrate the statistical analysis and hypothetical testing of 10 generating unit system results for the different cases using the CAOA optimization algorithms. The result shows the best value, worst value, rank test, and p-test. **Table 5.35** illustrates the statistical analysis and hypothetical testing of 10 generating unit system results for the different cases using the LFAOA optimization algorithms.

Table 5.7: Committed status for a 10-generating unit system using the CAOA algorithm with PEVs (Thermal System+PEVs)

Units/ Hour	t_1	t_2	t_3	t_4	t_5	t_6	t_7	t_8	t_9	t_{10}	t_{11}	t_{12}	t_{13}	t_{14}	t_{15}	t_{16}	t_{17}	t_{18}	t_{19}	t_{20}	t_{21}	t_{22}	t_{23}	t_{24}
U_1	1	1	1	1	1	1	1	1	1	1	1	1	1	1	1	1	1	1	1	1	1	1	1	1
U_2	1	1	1	1	1	1	1	1	1	1	1	1	1	1	1	1	1	1	1	1	1	1	1	1
U_3	0	0	0	0	0	1	1	1	1	1	1	1	1	1	1	1	1	1	1	1	1	0	0	0
U_4	0	0	1	1	1	1	1	1	1	1	1	1	1	1	1	1	1	1	1	1	1	1	0	0
U_5	0	0	0	1	1	1	1	1	1	1	1	1	1	1	1	1	1	1	1	1	1	1	1	0
U_6	0	0	0	0	0	0	0	0	1	1	1	1	1	1	1	0	0	0	1	1	1	0	0	0
U_7	0	0	0	0	0	0	0	0	0	1	1	1	1	1	0	0	0	0	0	0	0	0	0	0
U_8	0	0	0	0	0	0	0	0	0	0	1	1	0	0	0	0	0	0	0	1	0	0	0	0
U_9	0	0	0	0	0	0	0	0	0	0	1	1	0	0	0	0	0	0	0	1	0	0	0	0
U_{10}	0	0	0	0	0	0	0	0	0	0	0	0	0	0	0	0	0	0	0	0	0	0	0	0

Table 5.8: Scheduling of a 10-generating unit system using the CAOA algorithm with PEVs (Thermal System+PEVs) in summer															
Hours/Units	**P_1**	**P_2**	**P_3**	**P_4**	**P_5**	**P_6**	**P_7**	**P_8**	**P_9**	**P_{10}**	**Number of PEVs**	**P_{G2V}**	**P_{V2G}**	**Power Generated (MW)**	**Hourly Cost ($)**
t_1	455	277.4	0	0	0	0	0	0	0	0	5094	32.4	0	700	14247.6
t_2	455	316.5	0	0	0	0	0	0	0	0	3225	20.5	0	751	14929.7
t_3	455	286.2	0	130	0	0	0	0	0	0	6984	44.5	0	826.7	17262.4
t_4	455	382.3	0	130	25	0	0	0	0	0	7575	48.2	0	944.1	19886.2
t_5	455	413	0	130	25	0	0	0	0	0	4480	28.5	0	994.5	20422.6
t_6	455	399.2	130	130	25	0	0	0	0	0	4905	31.2	0	1108	23073.6
t_7	455	423.5	130	130	25	0	0	0	0	0	1128	7.18	0	1156.32	23499.2
t_8	455	455	130	130	33.67	0	0	0	0	0	235	1.4	0	1202.27	24223.6
t_9	455	455	130	130	63.24	20	0	0	0	0	7844	0	50	1303.24	25635.6
t_{10}	455	455	130	130	139.5	20	25	0	0	0	7033	0	44.8	1399.3	28373.8
t_{11}	455	455	130	130	162	39.77	25	10	10	0	6801	0	43.3	1460.07	31149.7
t_{12}	455	455	130	130	162	74.27	25	10	10	10	7558	0	48.1	1509.37	31945.7
t_{13}	455	455	130	130	138.3	20	25	0	0	0	7680	0	48.9	1402.2	28347.8
t_{14}	455	455	130	130	82.53	20	25	0	0	0	2505	0	15.9	1313.43	27200.8
t_{15}	455	455	130	130	39.02	20	0	0	0	0	4309	27.4	0	1201.62	25148.6
t_{16}	455	316.8	130	130	25	0	0	0	0	0	5759	36.7	0	1020.1	21632.5
t_{17}	455	294.8	130	130	25	0	0	0	0	0	2392	15.2	0	1019.6	21248.5
t_{18}	455	400.6	130	130	25	0	0	0	0	0	6955	44.3	0	1096.3	23096.7
t_{19}	455	455	130	130	51.21	20	0	0	0	0	2827	18.1	0	1223.11	25393.1
t_{20}	455	455	130	130	143	20	0	10	10	0	7844	0	50	1403	29130.7
t_{21}	455	455	130	130	93.42	20	0	0	0	0	5220	0	33.2	1316.62	26248.9
t_{22}	455	442.6	0	130	25	0	0	0	0	0	6130	0	39.7	1092.3	20940.8
t_{23}	455	384.1	0	0	25	0	0	0	0	0	2794	0	17.8	881.9	17055.8
t_{24}	455	300.6	0	0	0	0	0	0	0	0	5043	0	32.1	787.7	14652

Table 5.9: Committed status for a 10-generating unit system using the CAOA algorithm with Solar for SCUC problem (Thermal System + Solar)

Units/ Hour	t_1	t_2	t_3	t_4	t_5	t_6	t_7	t_8	t_9	t_{10}	t_{11}	t_{12}	t_{13}	t_{14}	t_{15}	t_{16}	t_{17}	t_{18}	t_{19}	t_{20}	t_{21}	t_{22}	t_{23}	t_{24}
U_1	1	1	1	1	1	1	1	1	1	1	1	1	1	1	1	1	1	1	1	1	1	1	1	1
U_2	1	1	1	1	1	1	1	1	1	1	1	1	1	1	1	1	1	1	1	1	1	1	1	1
U_3	0	0	0	0	0	1	1	1	1	1	1	1	1	1	1	1	1	1	1	1	1	1	0	0
U_4	0	0	0	1	1	1	1	1	1	1	1	1	1	1	1	1	1	1	1	1	1	1	1	0
U_5	0	0	1	1	1	1	1	1	1	1	1	1	1	1	1	1	1	1	1	1	1	0	0	0
U_6	0	0	0	0	0	0	0	0	1	1	1	1	1	1	1	1	1	1	1	1	1	0	0	0
U_7	0	0	0	0	0	0	0	0	0	1	1	1	1	0	0	0	0	0	0	0	0	0	0	0
U_8	0	0	0	0	0	0	0	0	0	0	1	1	0	0	0	0	0	0	0	1	0	0	0	0
U_9	0	0	0	0	0	0	0	0	0	0	0	0	0	0	0	0	0	0	0	0	0	0	0	0
U_{10}	0	0	0	0	0	0	0	0	0	0	0	0	0	0	0	0	0	0	0	1	0	0	0	0

Table 5.10: Scheduling for a 10-generating unit system using the CAOA algorithm with Solar for SCUC problem (Thermal + Solar)													
Hours/Units	**P_1**	**P_2**	**P_3**	**P_4**	**P_5**	**P_6**	**P_7**	**P_8**	**P_9**	**P_{10}**	**P_{solar} (MW)**	**Generated Power (MW)**	**Hourly Cost ($)**
t_1	455	277.4	0	0	0	0	0	0	0	0	0	732.4	14247.6
t_2	455	316.5	0	0	0	0	0	0	0	0	0	771.5	14929.7
t_3	455	391.24	0	0	25	0	0	0	0	0	0	871.24	17181.1
t_4	455	382.35	0	130	25	0	0	0	0	0	0	992.35	19886.2
t_5	455	412.99	0	130	25	0	0	0	0	0	0	1022.99	20422.6
t_6	455	399.24	130	130	25	0	0	0	0	0	0	1139.24	23073.6
t_7	455	423.54	130	130	25	0	0	0	0	0	0	1163.54	23499.2
t_8	455	455	130	130	29.12	0	0	0	0	0	4.55	1203.67	24132.8
t_9	455	455	130	130	47.57	20	0	0	0	0	15.67	1253.24	25319.9
t_{10}	455	455	130	130	112.18	20	25	0	0	0	27.34	1354.52	27807.8
t_{11}	455	455	130	130	154.6	20	25	10	0	0	37.17	1416.77	29608.2
t_{12}	455	455	130	130	162	38.21	25	10	0	0	46.06	1451.27	30176.2
t_{13}	455	455	130	130	86.41	20	25	0	0	0	51.86	1353.27	27279.8
t_{14}	455	455	130	130	53.06	20	0	0	0	0	54.47	1297.53	25430.3
t_{15}	455	444.43	130	130	25	0	0	0	0	0	44.59	1229.02	23865.4
t_{16}	455	267.95	130	130	25	0	0	0	0	0	48.86	1056.81	20780.3
t_{17}	455	256.96	130	130	25	0	0	0	0	0	37.84	1034.8	20588.9
t_{18}	455	366.96	130	130	25	0	0	0	0	0	33.6	1140.56	22508.7
t_{19}	455	455	130	130	31.62	20	0	0	0	0	19.59	1241.21	25000.7
t_{20}	455	455	130	130	136.53	20	0	10	0	10	6.51	1353.04	29005.3
t_{21}	455	455	130	130	93.26	20	0	0	0	0	0.16	1283.42	26245.6
t_{22}	455	337.56	130	130	0	0	0	0	0	0	0	1052.56	21049.9
t_{23}	455	279.08	0	130	0	0	0	0	0	0	0	864.08	17137.6
t_{24}	455	300.59	0	0	0	0	0	0	0	0	0	755.59	14652

Table 5.11: Individual fuel cost for a 10-generating unit system using the CAOA algorithm for SCUC problem with RES (Thermal + Solar)

Hours/ Units	P_1	P_2	P_3	P_4	P_5	P_6	P_7	P_8	P_9	P_{10}	SUC ($)	Hourly Cost ($)
t_1	8465.822	5781.779	0	0	0	0	0	0	0	0	0	14247.601
t_2	8465.822	6463.843	0	0	0	0	0	0	0	0	0	14929.665
t_3	8465.822	7770.254	0	0	944.9875	0	0	0	0	0	260	17181.063
t_4	8465.822	7614.68	0	2860.659	944.9875	0	0	0	0	0	560	19886.149
t_5	8465.822	8151.081	0	2860.659	944.9875	0	0	0	0	0	1910	20422.55
t_6	8465.822	7910.294	2891.8	2860.659	944.9875	0	0	0	0	0	0	23073.563
t_7	8465.822	8335.91	2891.8	2860.659	944.9875	0	0	0	0	0	0	23499.179
t_8	8465.822	8887.478	2891.8	2860.659	1027.039	0	0	0	0	0	0	24132.798
t_9	8465.822	8887.478	2891.8	2860.659	1396.135	818.048	0	0	0	0	60	25319.942
t_{10}	8465.822	8887.478	2891.8	2860.659	2710.032	818.048	1173.994	0	0	0	260	27807.832
t_{11}	8465.822	8887.478	2891.8	2860.659	3590.747	818.048	1173.994	919.613	0	0	90	29608.16
t_{12}	8465.822	8887.478	2891.8	2860.659	3745.851	1230.95	1173.994	919.613	0	0	0	30176.166
t_{13}	8465.822	8887.478	2891.8	2860.659	2181.994	818.048	1173.994	0	0	0	0	27279.795
t_{14}	8465.822	8887.478	2891.8	2860.659	1506.487	818.048	0	0	0	0	0	25430.294
t_{15}	8465.822	8702.092	2891.8	2860.659	944.9875	0	0	0	0	0	0	23865.361
t_{16}	8465.822	5617.074	2891.8	2860.659	944.9875	0	0	0	0	0	0	20780.343
t_{17}	8465.822	5425.598	2891.8	2860.659	944.9875	0	0	0	0	0	0	20588.867
t_{18}	8465.822	7345.474	2891.8	2860.659	944.9875	0	0	0	0	0	0	22508.743
t_{19}	8465.822	8887.478	2891.8	2860.659	1076.893	818.048	0	0	0	0	170	25000.7
t_{20}	8465.822	8887.478	2891.8	2860.659	3213.83	818.048	0	919.613	0	948.073	260	29005.323
t_{21}	8465.822	8887.478	2891.8	2860.659	2321.838	818.048	0	0	0	0	0	26245.645
t_{22}	8465.822	6831.609	2891.8	2860.659	0	0	0	0	0	0	0	21049.89
t_{23}	8465.822	5811.065	0	2860.659	0	0	0	0	0	0	0	17137.546
t_{24}	8465.822	6186.193	0	0	0	0	0	0	0	0	0	14652.015

Table 5.12: Committed status for a 10-generating unit system using the CAOA algorithm for SCUC problem (Thermal + Wind)

Hours/Units	U_1	U_2	U_3	U_4	U_5	U_6	U_7	U_8	U_9	U_{10}
t_1	1	1	0	0	0	0	0	0	0	0
t_2	1	1	0	0	0	0	0	0	0	0
t_3	1	1	0	0	0	0	0	0	0	0
t_4	1	1	0	0	0	0	0	0	0	0
t_5	1	1	0	0	1	0	0	0	0	0
t_6	1	1	0	0	1	0	0	0	0	0
t_7	1	1	0	1	1	0	0	0	0	0
t_8	1	1	0	1	1	0	0	0	0	0
t_9	1	1	1	1	1	0	0	0	0	0
t_{10}	1	1	1	1	1	0	1	0	0	0
t_{11}	1	1	1	1	1	1	1	0	0	0
t_{12}	1	1	1	1	1	1	1	1	0	0
t_{13}	1	1	1	1	1	1	1	0	0	0
t_{14}	1	1	1	1	1	0	0	0	0	0
t_{15}	1	1	1	1	1	0	0	0	0	0
t_{16}	1	1	1	1	1	0	0	0	0	0
t_{17}	1	1	1	1	1	0	0	0	0	0
t_{18}	1	1	1	1	1	0	0	0	0	0
t_{19}	1	1	1	1	1	0	0	0	0	0
t_{20}	1	1	1	1	1	1	0	0	0	0
t_{21}	1	1	1	1	1	1	0	0	0	0
t_{22}	1	1	1	0	0	1	0	0	0	0
t_{23}	1	1	0	0	0	0	0	0	0	0
t_{24}	1	1	0	0	0	0	0	0	0	0

Table 5.13: Scheduling for a 10-generating unit system using the CAOA algorithm for SCUC problem (Thermal System + Wind)													
Hour/Unit	**P_1**	**P_2**	**P_3**	**P_4**	**P_5**	**P_6**	**P_7**	**P_8**	**P_9**	**P_{10}**	**P_{wind} (MW)**	**Generated Power (MW)**	**Hourly Cost ($)**
t_1	373	150	0	0	0	0	0	0	0	0	177	700	10671.6
t_2	429	150	0	0	0	0	0	0	0	0	171	750	11599.8
t_3	455	237	0	0	0	0	0	0	0	0	158	850	13543.9
t_4	455	350	0	0	0	0	0	0	0	0	145	950	15514.8
t_5	455	378	0	0	25	0	0	0	0	0	142	1000	16949.4
t_6	455	455	0	0	53	0	0	0	0	0	137	1100	18858.6
t_7	455	420	0	130	25	0	0	0	0	0	120	1150	20545.4
t_8	455	455	0	130	51	0	0	0	0	0	109	1200	21679
t_9	455	444	130	130	25	0	0	0	0	0	116	1300	23857.8
t_{10}	455	455	130	130	89	0	25	0	0	0	116	1400	26514.6
t_{11}	455	455	130	130	118	20	25	0	0	0	117	1450	27927.8
t_{12}	455	455	130	130	160	20	25	10	0	0	115	1500	29721.3
t_{13}	455	455	130	130	71	20	25	0	0	0	114	1400	26966.6
t_{14}	455	451	130	130	25	0	0	0	0	0	109	1300	23980.6
t_{15}	455	353	130	130	25	0	0	0	0	0	107	1200	22264.7
t_{16}	455	199	130	130	25	0	0	0	0	0	111	1050	19580.3
t_{17}	455	157	130	130	25	0	0	0	0	0	103	1000	18850.7
t_{18}	455	269.5	130	130	25	0	0	0	0	0	90.5	1100	20807.4
t_{19}	455	360.4	130	130	25	0	0	0	0	0	99.6	1200	22394
t_{20}	455	455	130	130	90	20	0	0	0	0	120	1400	26179
t_{21}	455	413	130	130	25	20	0	0	0	0	127	1300	24132.6
t_{22}	455	358	130	0	0	20	0	0	0	0	137	1100	19364.5
t_{23}	455	285	0	0	0	0	0	0	0	0	160	900	14380.1
t_{24}	455	170	0	0	0	0	0	0	0	0	175	800	12379

Table 5.14: Individual fuel cost for a 10-generating unit system using the CAOA algorithm for SCUC problem (Thermal + Wind)												
Hours/Units	**P_1**	**P_2**	**P_3**	**P_4**	**P_5**	**P_6**	**P_7**	**P_8**	**P_9**	**P_{10}**	**SUC ($)**	**Hourly Cost ($)**
t_1	7105.65	3565.98	0	0	0	0	0	0	0	0	560	10671.63
t_2	8033.85	3565.98	0	0	0	0	0	0	0	0	170	11599.82
t_3	8465.82	5078.03	0	0	0	0	0	0	0	0	550	13543.85
t_4	8465.82	7048.98	0	0	0	0	0	0	0	0	900	15514.8
t_5	8465.82	7538.57	0	0	944.988	0	0	0	0	0	520	16949.38
t_6	8465.82	8887.48	0	0	1505.28	0	0	0	0	0	0	18858.58
t_7	8465.82	8273.88	0	2860.66	944.988	0	0	0	0	0	0	20545.35
t_8	8465.82	8887.48	0	2860.66	1465.05	0	0	0	0	0	0	21679.01
t_9	8465.82	8694.55	2891.8	2860.66	944.988	0	0	0	0	0	0	23857.82
t_{10}	8465.82	8887.48	2891.8	2860.66	2234.83	0	1173.99	0	0	0	170	26514.58
t_{11}	8465.82	8887.48	2891.8	2860.66	2830.02	818.048	1173.99	0	0	0	0	27927.82
t_{12}	8465.82	8887.48	2891.8	2860.66	3703.89	818.048	1173.99	919.613	0	0	60	29721.3
t_{13}	8465.82	8887.48	2891.8	2860.66	1868.76	818.048	1173.99	0	0	0	0	26966.56
t_{14}	8465.82	8817.31	2891.8	2860.66	944.988	0	0	0	0	0	0	23980.58
t_{15}	8465.82	7101.41	2891.8	2860.66	944.988	0	0	0	0	0	0	22264.68
t_{16}	8465.82	4417.02	2891.8	2860.66	944.988	0	0	0	0	0	0	19580.28
t_{17}	8465.82	3687.46	2891.8	2860.66	944.988	0	0	0	0	0	170	18850.73
t_{18}	8465.82	5644.09	2891.8	2860.66	944.988	0	0	0	0	0	0	20807.35
t_{19}	8465.82	7230.77	2891.8	2860.66	944.988	0	0	0	0	0	0	22394.04
t_{20}	8465.82	8887.48	2891.8	2860.66	2255.24	818.048	0	0	0	0	0	26179.04
t_{21}	8465.82	8151.26	2891.8	2860.66	944.988	818.048	0	0	0	0	0	24132.57
t_{22}	8465.82	7188.81	2891.8	0	0	818.048	0	0	0	0	0	19364.48
t_{23}	8465.82	5914.28	0	0	0	0	0	0	0	0	0	14380.1
t_{24}	8465.82	3913.16	0	0	0	0	0	0	0	0	0	12378.98

Table 5.15: Committed status for a 10-generating unit system using the CAOA algorithm for SCUC problem (Thermal +Solar + Wind)

Units/ Hour	t_1	t_2	t_3	t_4	t_5	t_6	t_7	t_8	t_9	t_{10}	t_{11}	t_{12}	t_{13}	t_{14}	t_{15}	t_{16}	t_{17}	t_{18}	t_{19}	t_{20}	t_{21}	t_{22}	t_{23}	t_{24}
U_1	1	1	1	1	1	1	1	1	1	1	1	1	1	1	1	1	1	1	1	1	1	1	1	1
U_2	1	1	1	1	1	1	1	1	1	1	1	1	1	1	1	1	1	1	1	1	1	1	1	1
U_3	0	0	0	0	0	0	0	0	1	1	1	1	1	1	1	1	1	1	1	1	1	1	0	0
U_4	0	0	0	0	0	0	1	1	1	1	1	1	1	1	1	1	1	1	1	1	1	0	0	0
U_5	0	0	0	0	1	1	1	1	1	1	1	1	1	1	1	1	1	1	1	1	1	0	0	0
U_6	0	0	0	0	0	0	0	0	0	0	1	1	1	0	0	0	0	0	0	1	1	1	0	0
U_7	0	0	0	0	0	0	0	0	0	1	1	1	1	0	0	0	0	0	0	0	0	0	0	0
U_8	0	0	0	0	0	0	0	0	0	0	0	1	0	0	0	0	0	0	0	0	0	0	0	0
U_9	0	0	0	0	0	0	0	0	0	0	0	0	0	0	0	0	0	0	0	0	0	0	0	0
U_{10}	0	0	0	0	0	0	0	0	0	0	0	0	0	0	0	0	0	0	0	0	0	0	0	0

Table 5.16: Scheduling for a 10-generating unit system using the CAOA algorithm for SCUC problem (Thermal +Solar + Wind)														
Hours/ Units	**P_1**	**P_2**	**P_3**	**P_4**	**P_5**	**P_6**	**P_7**	**P_8**	**P_9**	**P_{10}**	**P_{solar} (MW)**	**P_{wind} (MW)**	**Generated Power (MW)**	**Hourly Cost ($)**
t_1	373	150	0	0	0	0	0	0	0	0	0	177	700	10671.63
t_2	429	150	0	0	0	0	0	0	0	0	0	171	750	11599.82
t_3	455	237	0	0	0	0	0	0	0	0	0	158	850	13543.85
t_4	455	350	0	0	0	0	0	0	0	0	0	145	950	15514.8
t_5	455	378	0	0	25	0	0	0	0	0	0	142	1000	16949.38
t_6	455	455	0	0	53	0	0	0	0	0	0	137	1100	18858.58
t_7	455	420	0	130	25	0	0	0	0	0	0	120	1150	20545.35
t_8	455	455	0	130	51	0	0	0	0	0	4.55	109	1195.45	21679.01
t_9	455	444	130	130	25	0	0	0	0	0	15.67	116	1284.33	23857.82
t_{10}	455	455	130	130	89	0	25	0	0	0	27.34	116	1372.66	26514.58
t_{11}	455	455	130	130	118	20	25	0	0	0	37.17	117	1412.83	27927.82
t_{12}	455	455	130	130	160	20	25	10	0	0	46.06	115	1453.94	29721.3
t_{13}	455	455	130	130	71	20	25	0	0	0	51.86	114	1348.14	26966.56
t_{14}	455	451	130	130	25	0	0	0	0	0	54.47	109	1245.53	23980.58
t_{15}	455	353	130	130	25	0	0	0	0	0	44.59	107	1155.41	22264.68
t_{16}	455	199	130	130	25	0	0	0	0	0	48.86	111	1001.14	19580.28
t_{17}	455	157	130	130	25	0	0	0	0	0	37.84	103	962.16	18850.73
t_{18}	455	269.5	130	130	25	0	0	0	0	0	33.6	90.5	1066.4	20807.35
t_{19}	455	360.4	130	130	25	0	0	0	0	0	19.59	99.6	1180.41	22394.04
t_{20}	455	455	130	130	90	20	0	0	0	0	6.51	120	1393.49	26179.04
t_{21}	455	413	130	130	25	20	0	0	0	0	0.16	127	1299.84	24132.57
t_{22}	455	358	130	0	0	20	0	0	0	0	0	137	1100	19364.48
t_{23}	455	285	0	0	0	0	0	0	0	0	0	160	900	14380.1
t_{24}	455	170	0	0	0	0	0	0	0	0	0	175	800	12378.98

Table 5.17: Scheduling for a 10-generating unit system using the CAOA algorithm for SCUC problem (Thermal +Solar + PEVs)																								
Units/ Hour	**t_1**	**t_2**	**t_3**	**t_4**	**t_5**	**t_6**	**t_7**	**t_8**	**t_9**	**t_{10}**	**t_{11}**	**t_{12}**	**t_{13}**	**t_{14}**	**t_{15}**	**t_{16}**	**t_{17}**	**t_{18}**	**t_{19}**	**t_{20}**	**t_{21}**	**t_{22}**	**t_{23}**	**t_{24}**
U_1	1	1	1	1	1	1	1	1	1	1	1	1	1	1	1	1	1	1	1	1	1	1	1	1
U_2	1	1	1	1	1	1	1	1	1	1	1	1	1	1	1	1	1	1	1	1	1	1	1	1
U_3	0	0	0	0	0	1	1	1	1	1	1	1	1	1	1	1	1	1	1	1	1	1	0	0
U_4	0	0	1	1	1	1	1	1	1	1	1	1	1	1	1	1	1	1	1	1	1	1	1	0
U_5	0	0	0	1	1	1	1	1	1	1	1	1	1	1	1	1	1	1	1	1	1	0	0	0
U_6	0	0	0	0	0	0	0	0	1	1	1	1	1	1	0	0	0	0	1	1	1	0	0	0
U_7	0	0	0	0	0	0	0	0	0	1	1	1	1	0	0	0	0	0	0	0	0	0	0	0
U_8	0	0	0	0	0	0	0	0	0	0	1	1	0	0	0	0	0	0	0	1	0	0	0	0
U_9	0	0	0	0	0	0	0	0	0	0	0	0	0	0	0	0	0	0	0	1	0	0	0	0
U_{10}	0	0	0	0	0	0	0	0	0	0	0	0	0	0	0	0	0	0	0	0	0	0	0	0

Table 5.18: Scheduling for a 10-generating unit system using the CAOA algorithm for SCUC problem (Thermal +Solar + PEVs)															
Hours/Units	**P_1**	**P_2**	**P_3**	**P_4**	**P_5**	**P_6**	**P_7**	**P_8**	**P_9**	**P_{10}**	**Number of PEVs**	**P_{solar} (MW)**	**P_{PEVs} (MW)**	**Generated Power (MW)**	**Hourly Cost ($)**
t_1	455	277.4	0	0	0	0	0	0	0	0	5094	0	-32.4	700	14247.6
t_2	455	316.5	0	0	0	0	0	0	0	0	3225	0	-20.5	751	14929.7
t_3	455	286.24	0	130	0	0	0	0	0	0	6984	0	-44.5	826.74	17262.4
t_4	455	382.35	0	130	25	0	0	0	0	0	7575	0	-48.2	944.15	19886.2
t_5	455	412.99	0	130	25	0	0	0	0	0	4480	0	-28.5	994.49	20422.6
t_6	455	399.24	130	130	25	0	0	0	0	0	4905	0	-31.2	1108.04	23073.6
t_7	455	423.54	130	130	25	0	0	0	0	0	1128	0	-7.18	1156.36	23499.2
t_8	455	455	130	130	29.12	0	0	0	0	0	235	4.55	-1.4	1202.27	24132.8
t_9	455	455	130	130	47.57	20	0	0	0	0	7844	15.67	50	1303.24	25319.9
t_{10}	455	455	130	130	112.18	20	25	0	0	0	7033	27.34	44.8	1399.32	27807.8
t_{11}	455	455	130	130	154.6	20	25	10	0	0	6801	37.17	43.3	1460.07	29608.2
t_{12}	455	455	130	130	162	38.21	25	10	0	0	7558	46.06	48.1	1499.37	30176.2
t_{13}	455	455	130	130	86.41	20	25	0	0	0	7680	51.86	48.9	1402.17	27279.8
t_{14}	455	455	130	130	53.06	20	0	0	0	0	2505	54.47	15.9	1313.43	25430.3
t_{15}	455	444.43	130	130	25	0	0	0	0	0	4309	44.59	-27.4	1201.62	23865.4
t_{16}	455	267.95	130	130	25	0	0	0	0	0	5759	48.86	-36.7	1020.11	20780.3
t_{17}	455	256.96	130	130	25	0	0	0	0	0	2392	37.84	-15.2	1019.6	20588.9
t_{18}	455	366.96	130	130	25	0	0	0	0	0	6955	33.6	-44.3	1096.26	22508.7
t_{19}	455	455	130	130	31.62	20	0	0	0	0	2827	19.59	-18.1	1223.11	25000.7
t_{20}	455	455	130	130	136.53	20	0	10	10	0	7844	6.51	50	1403.04	28995.2
t_{21}	455	455	130	130	93.26	20	0	0	0	0	5220	0.16	33.2	1316.62	26245.6
t_{22}	455	337.56	130	130	0	0	0	0	0	0	6130	0	39.7	1092.26	21049.9
t_{23}	455	279.08	0	130	0	0	0	0	0	0	2794	0	17.8	881.88	17137.6
t_{24}	455	300.59	0	0	0	0	0	0	0	0	5043	0	32.1	787.69	14652

Table 5.19 Individual fuel cost for 10 generating unit using CAOA for SCUC problem considering (Thermal + SOLAR +PEVs) system												
Hour/ Units	**P_1**	**P_2**	**P_3**	**P_4**	**P_5**	**P_6**	**P_7**	**P_8**	**P_9**	**P_{10}**	**SUC ($)**	**Hourly Cost ($)**
t_1	8465.82	5782	0	0	0	0	0	0	0	0	0	14247.6007
t_2	8465.82	6464	0	0	0	0	0	0	0	0	0	14929.6654
t_3	8465.82	5936	0	2861	0	0	0	0	0	0	560	17262.3827
t_4	8465.82	7615	0	2861	945	0	0	0	0	0	1970	19886.1489
t_5	8465.82	8151	0	2861	945	0	0	0	0	0	0	20422.5497
t_6	8465.82	7910	2892	2861	945	0	0	0	0	0	0	23073.5626
t_7	8465.82	8336	2892	2861	945	0	0	0	0	0	0	23499.1786
t_8	8465.82	8887	2892	2861	1027	0	0	0	0	0	0	24132.7977
t_9	8465.82	8887	2892	2861	1396	818	0	0	0	0	0	25319.9421
t_{10}	8465.82	8887	2892	2861	2710	818	1174	0	0	0	60	27807.8322
t_{11}	8465.82	8887	2892	2861	3591	818	1174	920	0	0	580	29608.1601
t_{12}	8465.82	8887	2892	2861	3746	1231	1174	920	0	0	0	30176.1665
t_{13}	8465.82	8887	2892	2861	2182	818	1174	0	0	0	0	27279.7949
t_{14}	8465.82	8887	2892	2861	1506	818	0	0	0	0	0	25430.2939
t_{15}	8465.82	8702	2892	2861	945	0	0	0	0	0	0	23865.3609
t_{16}	8465.82	5617	2892	2861	945	0	0	0	0	0	0	20780.3426
t_{17}	8465.82	5426	2892	2861	945	0	0	0	0	0	0	20588.8669
t_{18}	8465.82	7345	2892	2861	945	0	0	0	0	0	260	22508.7426
t_{19}	8465.82	8887	2892	2861	1077	818	0	0	0	0	230	25000.7001
t_{20}	8465.82	8887	2892	2861	3214	818	0	920	938	0	0	28995.1717
t_{21}	8465.82	8887	2892	2861	2322	818	0	0	0	0	0	26245.6445
t_{22}	8465.82	6832	2892	2861	0	0	0	0	0	0	60	21049.8901
t_{23}	8465.82	5811	0	2861	0	0	0	0	0	0	0	17137.5464
t_{24}	8465.82	6186	0	0	0	0	0	0	0	0	0	14652.0153

Table 5.20: Committed status for a 10-generating unit system using the CAOA algorithm for SCUC problem (Thermal +Solar + PEVs +Wind)																								
Units/ Hour	**t_1**	**t_2**	**t_3**	**t_4**	**t_5**	**t_6**	**t_7**	**t_8**	**t_9**	**t_{10}**	**t_{11}**	**t_{12}**	**t_{13}**	**t_{14}**	**t_{15}**	**t_{16}**	**t_{17}**	**t_{18}**	**t_{19}**	**t_{20}**	**t_{21}**	**t_{22}**	**t_{23}**	**t_{24}**
U_1	1	1	1	1	1	1	1	1	1	1	1	1	1	1	1	1	1	1	1	1	1	1	1	1
U_2	1	1	1	1	1	1	1	1	1	1	1	1	1	1	1	1	1	1	1	1	1	1	1	1
U_3	0	0	0	0	0	0	0	0	0	1	1	1	1	1	0	0	0	0	0	1	1	1	1	1
U_4	0	0	0	0	0	1	1	1	1	1	1	1	1	1	1	1	1	1	1	1	1	0	0	0
U_5	0	0	0	1	1	1	1	1	1	1	1	1	1	1	1	1	1	1	1	1	1	0	0	0
U_6	0	0	0	0	0	0	0	0	1	1	1	1	0	0	0	0	0	0	1	1	1	0	0	0
U_7	0	0	0	0	0	0	0	0	0	0	0	0	0	0	0	0	0	0	0	0	0	0	0	0
U_8	0	0	0	0	0	0	0	0	0	0	0	0	0	0	0	0	0	0	0	0	0	0	0	0
U_9	0	0	0	0	0	0	0	0	0	0	0	0	0	0	0	0	0	0	0	0	0	0	0	0
U_{10}	0	0	0	0	0	0	0	0	0	0	0	1	0	0	0	0	0	0	0	0	0	0	0	0

Table 5.21: Scheduling for a 10-generating unit system using the CAOA algorithm (Thermal +Solar + PEVs + Wind)																	
Hours/Units	**P_1**	**P_2**	**P_3**	**P_4**	**P_5**	**P_6**	**P_7**	**P_8**	**P_9**	**P_{10}**	**Number of PEVs**	**P_{solar} (MW)**	**P_{PEVs} (MW)**	**P_{wind} (MW)**	**Generated Power (MW)**	**Load Demand (MW)**	**Hourly Cost ($)**
t_1	405.4	150	0	0	0	0	0	0	0	0	5094	0	-32.4	177	700	555.4	11208.3
t_2	450.5	150	0	0	0	0	0	0	0	0	3225	0	-20.5	171	751	600.5	11957
t_3	455	258.2	0	0	0	0	0	0	0	0	6984	0	-44.5	158	826.7	713.24	13913.7
t_4	455	367.4	0	0	25	0	0	0	0	0	7575	0	-48.2	145	944.2	847.35	16763.1
t_5	455	401	0	0	25	0	0	0	0	0	4480	0	-28.5	142	994.5	880.99	17351.7
t_6	455	392.2	0	130	25	0	0	0	0	0	4905	0	-31.2	137	1108	1002.24	20059.2
t_7	455	433.5	0	130	25	0	0	0	0	0	1128	0	-7.18	120	1156.32	1043.54	20782.6
t_8	455	455	0	130	50.12	0	0	0	0	0	235	4.55	-1.4	109	1202.27	1090.12	21661.3
t_9	455	455	0	130	61.57	20	0	0	0	0	7844	15.67	50	116	1303.24	1121.57	22710
t_{10}	455	451.2	130	130	25	20	0	0	0	0	7033	27.34	44.8	116	1399.34	1211.18	24801.8
t_{11}	455	455	130	130	72.6	20	0	0	0	0	6801	37.17	43.3	117	1460.07	1262.6	25825
t_{12}	455	455	130	130	90.21	20	0	0	0	10	7558	46.06	48.1	115	1499.37	1290.21	27131.4
t_{13}	455	447.4	130	130	25	0	0	0	0	0	7680	51.86	48.9	114	1402.16	1187.41	23917.6
t_{14}	455	394.1	130	130	25	0	0	0	0	0	2505	54.47	15.9	109	1313.47	1134.06	22982.9
t_{15}	455	455	0	130	37.43	0	0	0	0	0	4309	44.59	-27.4	107	1201.62	1077.43	21406.9
t_{16}	455	287	0	130	25	0	0	0	0	0	5759	48.86	-36.7	111	1020.16	896.95	18219.8
t_{17}	455	284	0	130	25	0	0	0	0	0	2392	37.84	-15.2	103	1019.64	893.96	18167.6
t_{18}	455	406.5	0	130	25	0	0	0	0	0	6955	33.6	-44.3	90.5	1096.3	1016.46	20308.2
t_{19}	455	455	0	130	62.02	20	0	0	0	0	2827	19.59	-18.1	99.6	1223.11	1122.02	22719.1
t_{20}	455	455	130	130	36.53	20	0	0	0	0	7844	6.51	50	120	1403.04	1226.53	25098.8
t_{21}	455	396.3	130	130	25	20	0	0	0	0	5220	0.16	33.2	127	1316.66	1156.26	23839.4
t_{22}	455	330.6	130	0	0	0	0	0	0	0	6130	0	39.7	137	1092.3	915.56	18067
t_{23}	455	150	99.08	0	0	0	0	0	0	0	2794	0	17.8	160	881.88	704.08	14396.2
t_{24}	410.6	150	20	0	0	0	0	0	0	0	5043	0	32.1	175	787.7	580.59	12327.2

Table 5.22 Individual fuel cost for 10 generating unit system using the CAOA for SCUC problem (Thermal + Solar + PEVs + Wind)												
Hours/ Units	**P_1**	**P_2**	**P_3**	**P_4**	**P_5**	**P_6**	**P_7**	**P_8**	**P_9**	**P_{10}**	**SUC ($)**	**Hourly Cost ($)**
t_1	7642.3136	3565.975	0	0	0	0	0	0	0	0	0	11208.289
t_2	8391.0111	3565.975	0	0	0	0	0	0	0	0	0	11956.986
t_3	8465.822	5447.8956	0	0	0	0	0	0	0	0	1370	13913.718
t_4	8465.822	7352.2943	0	0	944.9875	0	0	0	0	0	0	16763.104
t_5	8465.822	7940.9332	0	0	944.9875	0	0	0	0	0	1240	17351.743
t_6	8465.822	7787.7566	0	2860.659	944.9875	0	0	0	0	0	0	20059.225
t_7	8465.822	8511.167	0	2860.659	944.9875	0	0	0	0	0	0	20782.636
t_8	8465.822	8887.4777	0	2860.659	1447.3618	0	0	0	0	0	0	21661.321
t_9	8465.822	8887.4777	0	2860.659	1678.0166	818.048	0	0	0	0	0	22710.023
t_{10}	8465.822	8820.4715	2891.8	2860.659	944.9875	818.048	0	0	0	0	0	24801.788
t_{11}	8465.822	8887.4777	2891.8	2860.659	1901.1976	818.048	0	0	0	0	0	25825.004
t_{12}	8465.822	8887.4777	2891.8	2860.659	2259.5256	818.048	0	0	0	948.073	60	27131.405
t_{13}	8465.822	8754.3511	2891.8	2860.659	944.9875	0	0	0	0	0	0	23917.62
t_{14}	8465.822	7819.6134	2891.8	2860.659	944.9875	0	0	0	0	0	0	22982.882
t_{15}	8465.822	8887.4777	0	2860.659	1192.947	0	0	0	0	0	0	21406.906
t_{16}	8465.822	5948.2825	0	2860.659	944.9875	0	0	0	0	0	520	18219.751
t_{17}	8465.822	5896.1459	0	2860.659	944.9875	0	0	0	0	0	0	18167.614
t_{18}	8465.822	8036.7146	0	2860.659	944.9875	0	0	0	0	0	0	20308.183
t_{19}	8465.822	8887.4777	0	2860.659	1687.103	818.048	0	0	0	0	0	22719.11
t_{20}	8465.822	8887.4777	2891.8	2860.659	1174.9521	818.048	0	0	0	0	340	25098.759
t_{21}	8465.822	7858.1244	2891.8	2860.659	944.9875	818.048	0	0	0	0	60	23839.441
t_{22}	8465.822	6709.3393	2891.8	0	0	0	0	0	0	0	0	18066.961
t_{23}	8465.822	3565.975	2364.3617	0	0	0	0	0	0	0	0	14396.159
t_{24}	7728.3725	3565.975	1032.8	0	0	0	0	0	0	0	0	12327.147

Table 5.23: Committed status and scheduling for a 10-generating unit system using the LFAOA algorithm with PEVs (Thermal +PEVs)																								
Committed status for SCUC problem (Thermal + PEVs)											**Scheduling of the committed units for SCUC problem (Thermal + PEVs)**													
Hours/Units	**U_1**	**U_2**	**U_3**	**U_4**	**U_5**	**U_6**	**U_7**	**U_8**	**U_9**	**U_{10}**	**P_1**	**P_2**	**P_3**	**P_4**	**P_5**	**P_6**	**P_7**	**P_8**	**P_9**	**P_{10}**	**Number of PEVs**	**P_{PEVs} (MW)**	**Power Generated (MW)**	**Hourly Cost ($)**
t_1	1	1	0	0	0	0	0	0	0	0	455	277.4	0	0	0	0	0	0	0	0	5094	-32.4	700	14247.60074
t_2	1	1	0	0	0	0	0	0	0	0	455	316.5	0	0	0	0	0	0	0	0	3225	-20.5	751	14929.6654
t_3	1	1	0	0	1	0	0	0	0	0	455	391.2	0	0	25	0	0	0	0	0	6984	-44.5	826.7	17181.06321
t_4	1	1	0	1	1	0	0	0	0	0	455	382.3	0	130	25	0	0	0	0	0	7575	-48.2	944.1	19886.14887
t_5	1	1	0	1	1	0	0	0	0	0	455	413	0	130	25	0	0	0	0	0	4480	-28.5	994.5	20422.54973
t_6	1	1	1	1	1	0	0	0	0	0	455	399.2	130	130	25	0	0	0	0	0	4905	-31.2	1108	23073.5626
t_7	1	1	1	1	1	0	0	0	0	0	455	423.5	130	130	25	0	0	0	0	0	1128	-7.18	1156.32	23499.1786
t_8	1	1	1	1	1	0	0	0	0	0	455	455	130	130	33.67	0	0	0	0	0	235	-1.4	1202.27	24223.56975
t_9	1	1	1	1	1	1	0	0	0	0	455	455	130	130	63.24	20	0	0	0	0	7844	50	1303.24	25635.55195
t_{10}	1	1	1	1	1	1	1	0	0	0	455	455	130	130	139.5	20	25	0	0	0	7033	44.8	1399.3	28373.8185
t_{11}	1	1	1	1	1	1	1	1	10	0	455	455	130	130	162	39.77	25	10	10	0	6801	43.3	1460.07	31149.68019
t_{12}	1	1	1	1	1	1	1	1	10	0	455	455	130	130	162	74.27	25	10	10	0	7558	48.1	1499.37	31945.66297
t_{13}	1	1	1	1	1	1	1	0	0	0	455	455	130	130	138.3	20	25	0	0	0	7680	48.9	1402.2	28347.8115
t_{14}	1	1	1	1	1	1	1	0	0	0	455	455	130	130	82.53	20	25	0	0	0	2505	15.9	1313.43	27200.75008
t_{15}	1	1	1	1	1	1	0	0	0	0	455	455	130	130	39.02	20	0	0	0	0	4309	-27.4	1201.62	25148.56054
t_{16}	1	1	1	1	1	0	0	0	0	0	455	316.8	130	130	25	0	0	0	0	0	5759	-36.7	1020.1	21632.52336
t_{17}	1	1	1	1	1	0	0	0	0	0	455	294.8	130	130	25	0	0	0	0	0	2392	-15.2	1019.6	21248.45768
t_{18}	1	1	1	1	1	0	0	0	0	0	455	400.6	130	130	25	0	0	0	0	0	6955	-44.3	1096.3	23096.67308
t_{19}	1	1	1	1	1	1	0	0	0	0	455	455	130	130	51.21	20	0	0	0	0	2827	-18.1	1223.11	25393.08116
t_{20}	1	1	1	1	1	1	0	1	0	1	455	455	130	130	143	20	0	10	0	10	7844	50	1403	29140.81331
t_{21}	1	1	1	1	1	1	0	0	0	0	455	455	130	130	93.42	20	0	0	0	0	5220	33.2	1316.62	26248.91539
t_{22}	1	1	1	1	0	0	0	0	0	0	455	337.6	130	130	0	0	0	0	0	0	6130	39.7	1092.3	21049.89009
t_{23}	1	1	0	1	0	0	0	0	0	0	455	279.1	0	130	0	0	0	0	0	0	2794	17.8	881.9	17137.54635
t_{24}	1	1	0	0	0	0	0	0	0	0	455	300.6	0	0	0	0	0	0	0	0	5043	32.1	787.7	14652.01525

Table 5.24: Individual fuel cost for 10 generating unit system using LFAOA algorithm with PEVs (Thermal + PEVs)												
Hours/ Units	**P_1**	**P_2**	**P_3**	**P_4**	**P_5**	**P_6**	**P_7**	**P_8**	**P_9**	**P_{10}**	**SUC ($)**	**Hourly Cost ($)**
t_1	8465.822	5781.779	0	0	0	0	0	0	0	0	2010	14247.60074
t_2	8465.822	6463.843	0	0	0	0	0	0	0	0	0	14929.6654
t_3	8465.822	7770.254	0	0	944.9875	0	0	0	0	0	0	17181.06321
t_4	8465.822	7614.68	0	2860.659	944.9875	0	0	0	0	0	0	19886.14887
t_5	8465.822	8151.081	0	2860.659	944.9875	0	0	0	0	0	0	20422.54973
t_6	8465.822	7910.294	2891.8	2860.659	944.9875	0	0	0	0	0	60	23073.5626
t_7	8465.822	8335.91	2891.8	2860.659	944.9875	0	0	0	0	0	0	23499.1786
t_8	8465.822	8887.478	2891.8	2860.659	1117.811	0	0	0	0	0	860	24223.56975
t_9	8465.822	8887.478	2891.8	2860.659	1711.745	818.048	0	0	0	0	0	25635.55195
t_{10}	8465.822	8887.478	2891.8	2860.659	3276.018	818.048	1173.994	0	0	0	0	28373.8185
t_{11}	8465.822	8887.478	2891.8	2860.659	3745.851	1266.542	1173.994	919.613	937.922	0	120	31149.68019
t_{12}	8465.822	8887.478	2891.8	2860.659	3745.851	2062.524	1173.994	919.613	937.922	0	0	31945.66297
t_{13}	8465.822	8887.478	2891.8	2860.659	3250.011	818.048	1173.994	0	0	0	0	28347.8115
t_{14}	8465.822	8887.478	2891.8	2860.659	2102.95	818.048	1173.994	0	0	0	0	27200.75008
t_{15}	8465.822	8887.478	2891.8	2860.659	1224.754	818.048	0	0	0	0	0	25148.56054
t_{16}	8465.822	6469.255	2891.8	2860.659	944.9875	0	0	0	0	0	0	21632.52336
t_{17}	8465.822	6085.189	2891.8	2860.659	944.9875	0	0	0	0	0	0	21248.45768
t_{18}	8465.822	7933.405	2891.8	2860.659	944.9875	0	0	0	0	0	0	23096.67308
t_{19}	8465.822	8887.478	2891.8	2860.659	1469.274	818.048	0	0	0	0	170	25393.08116
t_{20}	8465.822	8887.478	2891.8	2860.659	3349.321	818.048	0	919.613	0	948.073	120	29140.81331
t_{21}	8465.822	8887.478	2891.8	2860.659	2325.109	818.048	0	0	0	0	0	26248.91539
t_{22}	8465.822	6831.609	2891.8	2860.659	0	0	0	0	0	0	0	21049.89009
t_{23}	8465.822	5811.065	0	2860.659	0	0	0	0	0	0	0	17137.54635
t_{24}	8465.822	6186.193	0	0	0	0	0	0	0	0	0	14652.01525

Table 5.25: Committed status and scheduling for 10-generating unit system using LFAOA algorithm with Wind Power (Thermal + Wind)																								
Committed Status											**Scheduling of the committed units for SCUC problem (Thermal + Wind)**													
Hours/Units	**U_1**	**U_2**	**U_3**	**U_4**	**U_5**	**U_6**	**U_7**	**U_8**	**U_9**	**U_{10}**	**P_1**	**P_2**	**P_3**	**P_4**	**P_5**	**P_6**	**P_7**	**P_8**	**P_9**	**P_{10}**	**P_{wind} (MW)**	**Power Generated (MW)**	**Hourly Cost ($)**
t_1	1	1	0	0	0	0	0	0	0	0	373	150	0	0	0	0	0	0	0	0	177	700	10671.6269
t_2	1	1	0	0	0	0	0	0	0	0	429	150	0	0	0	0	0	0	0	0	171	750	11599.8247
t_3	1	1	0	0	0	0	0	0	0	0	455	237	0	0	0	0	0	0	0	0	158	850	13543.8544
t_4	1	1	0	0	0	0	0	0	0	0	455	350	0	0	0	0	0	0	0	0	145	950	15514.797
t_5	1	1	0	0	1	0	0	0	0	0	455	378	0	0	25	0	0	0	0	0	142	1000	16949.3835
t_6	1	1	0	0	1	0	0	0	0	0	455	455	0	0	53	0	0	0	0	0	137	1100	18858.5796
t_7	1	1	1	0	1	0	0	0	0	0	455	420	130	0	25	0	0	0	0	0	120	1150	20576.4935
t_8	1	1	1	0	1	0	0	0	0	0	455	455	130	0	51	0	0	0	0	0	109	1200	21710.1517
t_9	1	1	1	1	1	0	0	0	0	0	455	444	130	130	25	0	0	0	0	0	116	1300	23857.8207
t_{10}	1	1	1	1	1	1	1	0	0	0	455	455	130	130	69	20	25	0	0	0	116	1400	26926.0493
t_{11}	1	1	1	1	1	1	1	0	0	0	455	455	130	130	118	20	25	0	0	0	117	1450	27927.818
t_{12}	1	1	1	1	1	1	1	1	0	0	455	455	130	130	160	20	25	10	0	0	115	1500	29721.3015
t_{13}	1	1	1	1	1	0	1	0	0	0	455	455	130	130	91	0	25	0	0	0	114	1400	26555.4109
t_{14}	1	1	1	1	1	0	0	0	0	0	455	451	130	130	25	0	0	0	0	0	109	1300	23980.5828
t_{15}	1	1	1	1	1	0	0	0	0	0	455	353	130	130	25	0	0	0	0	0	107	1200	22264.6773
t_{16}	1	1	1	1	1	0	0	0	0	0	455	199	130	130	25	0	0	0	0	0	111	1050	19580.2848
t_{17}	1	1	1	1	1	0	0	0	0	0	455	157	130	130	25	0	0	0	0	0	103	1000	18850.7297
t_{18}	1	1	1	1	1	0	0	0	0	0	455	269.5	130	130	25	0	0	0	0	0	90.5	1100	20807.3539
t_{19}	1	1	1	1	1	0	0	0	0	0	455	360.4	130	130	25	0	0	0	0	0	99.6	1200	22394.0378
t_{20}	1	1	1	1	1	1	0	0	0	0	455	455	130	130	90	20	0	0	0	0	120	1400	26179.0448
t_{21}	1	1	1	1	1	1	0	0	0	0	455	413	130	130	25	20	0	0	0	0	127	1300	24132.5729
t_{22}	1	1	0	1	0	1	0	0	0	0	455	358	0	130	0	20	0	0	0	0	137	1100	19333.3398
t_{23}	1	1	0	0	0	0	0	0	0	0	455	285	0	0	0	0	0	0	0	0	160	900	14380.1018
t_{24}	1	1	0	0	0	0	0	0	0	0	455	170	0	0	0	0	0	0	0	0	175	800	12378.981

Table 5.26: Individual fuel cost for 10 generating unit system using LFAOA algorithm for with Wind Power (Thermal + Wind)												
Hours/ Units	**P_1**	**P_2**	**P_3**	**P_4**	**P_5**	**P_6**	**P_7**	**P_8**	**P_9**	**P_{10}**	**SUC ($)**	**Hourly Cost ($)**
t_1	7105.652	3565.975	0	0	0	0	0	0	0	0	200	10671.63
t_2	8033.85	3565.975	0	0	0	0	0	0	0	0	0	11599.82
t_3	8465.822	5078.032	0	0	0	0	0	0	0	0	1450	13543.85
t_4	8465.822	7048.975	0	0	0	0	0	0	0	0	560	15514.8
t_5	8465.822	7538.574	0	0	944.9875	0	0	0	0	0	520	16949.38
t_6	8465.822	8887.478	0	0	1505.28	0	0	0	0	0	0	18858.58
t_7	8465.822	8273.884	2891.8	0	944.9875	0	0	0	0	0	0	20576.49
t_8	8465.822	8887.478	2891.8	0	1465.052	0	0	0	0	0	0	21710.15
t_9	8465.822	8694.552	2891.8	2860.659	944.9875	0	0	0	0	0	0	23857.82
t_{10}	8465.822	8887.478	2891.8	2860.659	1828.249	818.048	1173.994	0	0	0	170	26926.05
t_{11}	8465.822	8887.478	2891.8	2860.659	2830.018	818.048	1173.994	0	0	0	0	27927.82
t_{12}	8465.822	8887.478	2891.8	2860.659	3703.888	818.048	1173.994	919.613	0	0	60	29721.3
t_{13}	8465.822	8887.478	2891.8	2860.659	2275.658	0	1173.994	0	0	0	0	26555.41
t_{14}	8465.822	8817.314	2891.8	2860.659	944.9875	0	0	0	0	0	0	23980.58
t_{15}	8465.822	7101.409	2891.8	2860.659	944.9875	0	0	0	0	0	0	22264.68
t_{16}	8465.822	4417.016	2891.8	2860.659	944.9875	0	0	0	0	0	0	19580.28
t_{17}	8465.822	3687.461	2891.8	2860.659	944.9875	0	0	0	0	0	0	18850.73
t_{18}	8465.822	5644.085	2891.8	2860.659	944.9875	0	0	0	0	0	0	20807.35
t_{19}	8465.822	7230.769	2891.8	2860.659	944.9875	0	0	0	0	0	0	22394.04
t_{20}	8465.822	8887.478	2891.8	2860.659	2255.238	818.048	0	0	0	0	340	26179.04
t_{21}	8465.822	8151.256	2891.8	2860.659	944.9875	818.048	0	0	0	0	0	24132.57
t_{22}	8465.822	7188.811	0	2860.659	0	818.048	0	0	0	0	0	19333.34
t_{23}	8465.822	5914.28	0	0	0	0	0	0	0	0	0	14380.1
t_{24}	8465.822	3913.159	0	0	0	0	0	0	0	0	0	12378.98

Table 5.27: Committed status and scheduling for 10-Generating unit system using the LFAOA for SCUC problem (Thermal + Solar + PEVs)																									
Committed Status											**Scheduling of the committed units for (Thermal + Solar + PEVs) units**														
Hours/Units	**U_1**	**U_2**	**U_3**	**U_4**	**U_5**	**U_6**	**U_7**	**U_8**	**U_9**	**U_{10}**	**P_1**	**P_2**	**P_3**	**P_4**	**P_5**	**P_6**	**P_7**	**P_8**	**P_9**	**P_{10}**	**Number of PEVs**	**P_{PEVs} (MW)**	**P_{solar} (MW)**	**Power Generated ($)**	**Hourly Cost ($)**
t_1	1	1	0	0	0	0	0	0	0	0	455	277.4	0	0	0	0	0	0	0	0	5094	-32.4	0	732.4	14247.6
t_2	1	1	0	0	0	0	0	0	0	0	455	316.5	0	0	0	0	0	0	0	0	3225	-20.5	0	771.5	14929.67
t_3	1	1	0	0	1	0	0	0	0	0	455	391.2	0	0	25	0	0	0	0	0	6984	-44.5	0	871.24	17181.06
t_4	1	1	0	1	1	0	0	0	0	0	455	382.4	0	130	25	0	0	0	0	0	7575	-48.2	0	992.35	19886.15
t_5	1	1	0	1	1	0	0	0	0	0	455	413	0	130	25	0	0	0	0	0	4480	-28.5	0	1022.99	20422.55
t_6	1	1	1	1	1	0	0	0	0	0	455	399.2	130	130	25	0	0	0	0	0	4905	-31.2	0	1139.24	23073.56
t_7	1	1	1	1	1	0	0	0	0	0	455	423.5	130	130	25	0	0	0	0	0	1128	-7.18	0	1163.54	23499.18
t_8	1	1	1	1	1	0	0	0	0	0	455	455	130	130	29.12	0	0	0	0	0	235	-1.4	4.55	1199.12	24132.8
t_9	1	1	1	1	1	1	0	0	0	0	455	455	130	130	47.57	20	0	0	0	0	7844	50	15.67	1237.57	25319.94
t_{10}	1	1	1	1	1	1	1	0	0	0	455	455	130	130	112.2	20	25	0	0	0	7033	44.8	27.34	1327.18	27807.83
t_{11}	1	1	1	1	1	1	1	1	0	0	455	455	130	130	154.6	20	25	10	0	0	6801	43.3	37.17	1379.6	29608.16
t_{12}	1	1	1	1	1	1	1	1	0	0	455	455	130	130	162	38.21	25	10	0	0	7558	48.1	46.06	1405.21	30176.17
t_{13}	1	1	1	1	1	1	1	0	0	0	455	455	130	130	86.41	20	25	0	0	0	7680	48.9	51.86	1301.41	27279.79
t_{14}	1	1	1	1	1	1	0	0	0	0	455	455	130	130	53.06	20	0	0	0	0	2505	15.9	54.47	1243.06	25430.29
t_{15}	1	1	1	1	1	0	0	0	0	0	455	444.4	130	130	25	0	0	0	0	0	4309	-27.4	44.59	1184.43	23865.36
t_{16}	1	1	1	1	1	0	0	0	0	0	455	268	130	130	25	0	0	0	0	0	5759	-36.7	48.86	1007.95	20780.34
t_{17}	1	1	1	1	1	0	0	0	0	0	455	257	130	130	25	0	0	0	0	0	2392	-15.2	37.84	996.96	20588.87
t_{18}	1	1	1	1	1	0	0	0	0	0	455	367	130	130	25	0	0	0	0	0	6955	-44.3	33.6	1106.96	22508.74
t_{19}	1	1	1	1	1	1	0	0	0	0	455	455	130	130	31.62	20	0	0	0	0	2827	-18.1	19.59	1221.62	25000.7
t_{20}	1	1	1	1	1	1	0	1	0	1	455	455	130	130	136.5	20	0	10	0	10	7844	50	6.51	1346.53	29005.32
t_{21}	1	1	1	1	1	1	0	0	0	0	455	455	130	130	93.26	20	0	0	0	0	5220	33.2	0.16	1283.26	26245.64
t_{22}	1	1	0	1	1	0	0	0	0	0	455	442.6	0	130	25	0	0	0	0	0	6130	39.7	0	1052.56	20940.77
t_{23}	1	1	0	1	0	0	0	0	0	0	455	279.1	0	130	0	0	0	0	0	0	2794	17.8	0	864.08	17137.55
t_{24}	1	1	0	0	0	0	0	0	0	0	455	300.6	0	0	0	0	0	0	0	0	5043	32.1	0	755.59	14652.02

Table 5.28: Individual fuel cost for 10 generating unit system using LFAOA algorithm (Thermal +Solar + PEVs)

Hours/ Units	P_1	P_2	P_3	P_4	P_5	P_6	P_7	P_8	P_9	P_{10}	SUC ($)	Hourly Cost ($)
t_1	8465.822	5781.779	0	0	0	0	0	0	0	0	0	14247.6
t_2	8465.822	6463.843	0	0	0	0	0	0	0	0	2010	14929.67
t_3	8465.822	7770.254	0	0	944.9875	0	0	0	0	0	0	17181.06
t_4	8465.822	7614.68	0	2860.659	944.9875	0	0	0	0	0	0	19886.15
t_5	8465.822	8151.081	0	2860.659	944.9875	0	0	0	0	0	0	20422.55
t_6	8465.822	7910.294	2891.8	2860.659	944.9875	0	0	0	0	0	0	23073.56
t_7	8465.822	8335.91	2891.8	2860.659	944.9875	0	0	0	0	0	340	23499.18
t_8	8465.822	8887.478	2891.8	2860.659	1027.039	0	0	0	0	0	60	24132.8
t_9	8465.822	8887.478	2891.8	2860.659	1396.135	818.048	0	0	0	0	0	25319.94
t_{10}	8465.822	8887.478	2891.8	2860.659	2710.032	818.048	1173.994	0	0	0	520	27807.83
t_{11}	8465.822	8887.478	2891.8	2860.659	3590.747	818.048	1173.994	919.613	0	0	60	29608.16
t_{12}	8465.822	8887.478	2891.8	2860.659	3745.851	1230.95	1173.994	919.613	0	0	0	30176.17
t_{13}	8465.822	8887.478	2891.8	2860.659	2181.994	818.048	1173.994	0	0	0	0	27279.79
t_{14}	8465.822	8887.478	2891.8	2860.659	1506.487	818.048	0	0	0	0	0	25430.29
t_{15}	8465.822	8702.092	2891.8	2860.659	944.9875	0	0	0	0	0	0	23865.36
t_{16}	8465.822	5617.074	2891.8	2860.659	944.9875	0	0	0	0	0	0	20780.34
t_{17}	8465.822	5425.598	2891.8	2860.659	944.9875	0	0	0	0	0	260	20588.87
t_{18}	8465.822	7345.474	2891.8	2860.659	944.9875	0	0	0	0	0	0	22508.74
t_{19}	8465.822	8887.478	2891.8	2860.659	1076.893	818.048	0	0	0	0	0	25000.7
t_{20}	8465.822	8887.478	2891.8	2860.659	3213.83	818.048	0	919.613	0	948.073	170	29005.32
t_{21}	8465.822	8887.478	2891.8	2860.659	2321.838	818.048	0	0	0	0	0	26245.64
t_{22}	8465.822	8669.302	0	2860.659	944.9875	0	0	0	0	0	0	20940.77
t_{23}	8465.822	5811.065	0	2860.659	0	0	0	0	0	0	60	17137.55
t_{24}	8465.822	6186.193	0	0	0	0	0	0	0	0	0	14652.02

Table 5.29: Committed status and scheduling for a 10-Generating Unit system using the LFAOA algorithm with Wind Power and PEVs (Thermal + PEVs + Wind)

Committed Status											Scheduling of the committed units for (Thermal + Wind + PEVs)													
Hours/ Units	**U_1**	**U_2**	**U_3**	**U_4**	**U_5**	**U_6**	**U_7**	**U_8**	**U_9**	**U_{10}**	**P_1**	**P_2**	**P_3**	**P_4**	**P_5**	**P_6**	**P_7**	**P_8**	**P_9**	**P_{10}**	**Number of PEVs**	**P_{PEVs} (MW)**	**P_{wind} (MW)**	**Power Generated ($)**	**Hourly Cost ($)**
T1	1	1	0	0	0	0	0	0	0	0	405.4	150	0	0	0	0	0	0	0	0	5094	-32.4	177	555.4	11208.29
T2	1	1	0	0	0	0	0	0	0	0	450.5	150	0	0	0	0	0	0	0	0	3225	-20.5	171	600.5	11956.99
T3	1	1	0	0	0	0	0	0	0	0	455	258.2	0	0	0	0	0	0	0	0	6984	-44.5	158	713.24	13913.72
T4	1	1	0	0	1	0	0	0	0	0	455	367.4	0	0	25	0	0	0	0	0	7575	-48.2	145	847.35	16763.1
T5	1	1	0	0	1	0	0	0	0	0	455	401	0	0	25	0	0	0	0	0	4480	-28.5	142	880.99	17351.74
T6	1	1	0	1	1	0	0	0	0	0	455	392.2	0	130	25	0	0	0	0	0	4905	-31.2	137	1002.24	20059.23
T7	1	1	0	1	1	0	0	0	0	0	455	433.5	0	130	25	0	0	0	0	0	1128	-7.18	120	1043.54	20782.64
T8	1	1	1	1	1	0	0	0	0	0	455	354.7	130	130	25	0	0	0	0	0	235	-1.4	109	1094.67	22293.87
T9	1	1	1	1	1	0	0	0	0	0	455	397.2	130	130	25	0	0	0	0	0	7844	50	116	1137.24	23038.55
T10	1	1	1	1	1	1	0	0	0	0	455	455	130	130	48.52	20	0	0	0	0	7033	44.8	116	1238.52	25339.02
T11	1	1	1	1	1	1	1	0	0	0	455	455	130	130	84.77	20	25	0	0	0	6801	43.3	117	1299.77	27246.37
T12	1	1	1	1	1	1	1	0	0	0	455	455	130	130	121.3	20	25	0	0	0	7558	48.1	115	1336.27	27995.35
T13	1	1	1	1	1	0	1	0	0	0	455	455	130	130	44.27	0	25	0	0	0	7680	48.9	114	1239.27	25609.67
T14	1	1	1	1	1	0	0	0	0	0	455	448.5	130	130	25	0	0	0	0	0	2505	15.9	109	1188.53	23937.26
T15	1	1	1	1	1	0	0	0	0	0	455	382	130	130	25	0	0	0	0	0	4309	-27.4	107	1122.02	22772.17
T16	1	1	1	1	1	0	0	0	0	0	455	205.8	130	130	25	0	0	0	0	0	5759	-36.7	111	945.81	19698.68
T17	1	1	1	1	1	0	0	0	0	0	455	191.8	130	130	25	0	0	0	0	0	2392	-15.2	103	931.8	19455.14
T18	1	1	1	1	1	0	0	0	0	0	455	310.1	130	130	25	0	0	0	0	0	6955	-44.3	90.5	1050.06	21514.71
T19	1	1	1	1	1	0	0	0	0	0	455	401.6	130	130	25	0	0	0	0	0	2827	-18.1	99.6	1141.61	23115.06
T20	1	1	1	1	1	0	0	0	0	1	455	455	130	130	53.04	0	0	0	0	10	7844	50	120	1233.04	25559.92
T21	1	1	1	1	1	0	0	0	0	0	455	416.4	130	130	25	0	0	0	0	0	5220	33.2	127	1156.42	23374.43
T22	1	1	1	0	0	0	0	0	0	0	455	330.6	130	0	0	0	0	0	0	0	6130	39.7	137	915.56	18066.96
T23	1	1	0	0	0	0	0	0	0	0	455	249.1	0	0	0	0	0	0	0	0	2794	17.8	160	704.08	13754.18
T24	1	1	0	0	0	0	0	0	0	0	430.6	150	0	0	0	0	0	0	0	0	5043	32.1	175	580.59	11626.22

Table 5.30: Individual fuel cost for 10 Generating Unit system using the LFAOA algorithm (Thermal + Wind + PEVs)												
Hours/ Units	**P_1**	**P_2**	**P_3**	**P_4**	**P_5**	**P_6**	**P_7**	**P_8**	**P_9**	**P_{10}**	**SUC ($)**	**Hourly Cost ($)**
t_1	7642.314	3565.975	0	0	0	0	0	0	0	0	900	11208.29
t_2	8391.011	3565.975	0	0	0	0	0	0	0	0	550	11956.99
t_3	8465.822	5447.896	0	0	0	0	0	0	0	0	0	13913.72
t_4	8465.822	7352.294	0	0	944.9875	0	0	0	0	0	1080	16763.1
t_5	8465.822	7940.933	0	0	944.9875	0	0	0	0	0	0	17351.74
t_6	8465.822	7787.757	0	2860.659	944.9875	0	0	0	0	0	0	20059.23
t_7	8465.822	8511.167	0	2860.659	944.9875	0	0	0	0	0	0	20782.64
t_8	8465.822	7130.599	2891.8	2860.659	944.9875	0	0	0	0	0	0	22293.87
t_9	8465.822	7875.28	2891.8	2860.659	944.9875	0	0	0	0	0	0	23038.55
t_{10}	8465.822	8887.478	2891.8	2860.659	1415.214	818.048	0	0	0	0	260	25339.02
t_{11}	8465.822	8887.478	2891.8	2860.659	2148.569	818.048	1173.994	0	0	0	340	27246.37
t_{12}	8465.822	8887.478	2891.8	2860.659	2897.551	818.048	1173.994	0	0	0	0	27995.35
t_{13}	8465.822	8887.478	2891.8	2860.659	1329.919	0	1173.994	0	0	0	0	25609.67
t_{14}	8465.822	8773.993	2891.8	2860.659	944.9875	0	0	0	0	0	0	23937.26
t_{15}	8465.822	7608.906	2891.8	2860.659	944.9875	0	0	0	0	0	0	22772.17
t_{16}	8465.822	4535.412	2891.8	2860.659	944.9875	0	0	0	0	0	0	19698.68
t_{17}	8465.822	4291.872	2891.8	2860.659	944.9875	0	0	0	0	0	0	19455.14
t_{18}	8465.822	6351.438	2891.8	2860.659	944.9875	0	0	0	0	0	0	21514.71
t_{19}	8465.822	7951.789	2891.8	2860.659	944.9875	0	0	0	0	0	0	23115.06
t_{20}	8465.822	8887.478	2891.8	2860.659	1506.085	0	0	0	0	948.073	60	25559.92
t_{21}	8465.822	8211.165	2891.8	2860.659	944.9875	0	0	0	0	0	0	23374.43
t_{22}	8465.822	6709.339	2891.8	0	0	0	0	0	0	0	0	18066.96
t_{23}	8465.822	5288.353	0	0	0	0	0	0	0	0	0	13754.18
t_{24}	8060.248	3565.975	0	0	0	0	0	0	0	0	0	11626.22

Table 5.31: Committed status and scheduling for a 10-Generating unit system using the LFAOA algorithm (Thermal + Solar + Wind + PEVs)

Committed Status											Scheduling of the committed units (Thermal + PEVs + Solar + Wind)														
Hours/Units	U_1	U_2	U_3	U_4	U_5	U_6	U_7	U_8	U_9	U_{10}	P_1	P_2	P_3	P_4	P_5	P_6	P_7	P_8	P_9	P_{10}	**Number of PEVs**	P_{PEVs} **(MW)**	P_{solar} **(MW)**	P_{wind} **(MW)**	**Power Generated (MW)**	**Hourly Cost ($)**
t_1	1	1	0	0	0	0	0	0	0	0	405.4	150	0	0	0	0	0	0	0	0	5094	-32.4	0	177	700	11208.29
t_2	1	1	0	0	0	0	0	0	0	0	450.5	150	0	0	0	0	0	0	0	0	3225	-20.5	0	171	751	11956.99
t_3	1	1	0	0	0	0	0	0	0	0	455	258.24	0	0	0	0	0	0	0	0	6984	-44.5	0	158	826.74	13913.72
t_4	1	1	0	0	1	0	0	0	0	0	455	367.35	0	0	25	0	0	0	0	0	7575	-48.2	0	145	944.15	16763.1
t_5	1	1	0	0	1	0	0	0	0	0	455	400.99	0	0	25	0	0	0	0	0	4480	-28.5	0	142	994.49	17351.74
t_6	1	1	0	1	1	0	0	0	0	0	455	392.24	0	130	25	0	0	0	0	0	4905	-31.2	0	137	1108.04	20059.23
t_7	1	1	0	1	1	0	0	0	0	0	455	433.54	0	130	25	0	0	0	0	0	1128	-7.18	0	120	1156.36	20782.64
t_8	1	1	0	1	1	0	0	0	0	0	455	455	0	130	50.12	0	0	0	0	0	235	-1.4	4.55	109	1202.27	21661.32
t_9	1	1	1	1	1	0	0	0	0	0	455	381.57	130	130	25	0	0	0	0	0	7844	50	15.67	116	1303.24	22764.3
t_{10}	1	1	1	1	1	1	0	0	0	0	455	451.18	130	130	25	20	0	0	0	0	7033	44.8	27.34	116	1399.32	24801.79
t_{11}	1	1	1	1	1	1	0	0	0	0	455	455	130	130	72.6	20	0	0	0	0	6801	43.3	37.17	117	1460.07	25825
t_{12}	1	1	1	1	1	1	1	0	0	0	455	455	130	130	75.21	20	25	0	0	0	7558	48.1	46.06	115	1499.37	27051.95
t_{13}	1	1	1	1	1	0	1	0	0	0	455	422.41	130	130	25	0	25	0	0	0	7680	48.9	51.86	114	1402.17	24653.37
t_{14}	1	1	0	1	1	0	1	0	0	0	455	455	0	130	69.06	0	25	0	0	0	2505	15.9	54.47	109	1313.43	23217.42
t_{15}	1	1	0	1	1	0	0	0	0	0	455	455	0	130	37.43	0	0	0	0	0	4309	-27.4	44.59	107	1201.62	21406.91
t_{16}	1	1	0	1	1	0	0	0	0	0	455	286.95	0	130	25	0	0	0	0	0	5759	-36.7	48.86	111	1020.11	18219.75
t_{17}	1	1	0	1	1	0	0	0	0	0	455	283.96	0	130	25	0	0	0	0	0	2392	-15.2	37.84	103	1019.6	18167.61
t_{18}	1	1	0	1	1	1	0	0	0	0	455	386.46	0	130	25	20	0	0	0	0	6955	-44.3	33.6	90.5	1096.26	20776.12
t_{19}	1	1	1	1	1	1	0	0	0	0	455	362.02	130	130	25	20	0	0	0	0	2827	-18.1	19.59	99.6	1223.11	23240.41
t_{20}	1	1	1	1	1	1	0	0	0	0	455	455	130	130	36.53	20	0	0	0	0	7844	50	6.51	120	1403.04	25098.76
t_{21}	1	1	1	1	1	0	0	0	0	0	455	416.26	130	130	25	0	0	0	0	0	5220	33.2	0.16	127	1316.62	23371.63
t_{22}	1	1	1	0	0	0	0	0	0	0	455	330.56	130	0	0	0	0	0	0	0	6130	39.7	0	137	1092.26	18066.96
t_{23}	1	1	1	0	0	0	0	0	0	0	455	150	99.08	0	0	0	0	0	0	0	2794	17.8	0	160	881.88	14396.16
t_{24}	1	1	0	0	0	0	0	0	0	0	430.6	150	0	0	0	0	0	0	0	0	5043	32.1	0	175	787.69	11626.22

Table 5.32: Individual fuel cost for 10 Generating unit system using LFAOA algorithm for with solar and PEVs Power (Thermal +Solar +Wind+ PEVs)

Hours	P_1	P_2	P_3	P_4	P_5	P_6	P_7	P_8	P_9	P_{10}	SUC ($)	Hourly Cost ($)
t_1	7642.314	3565.975	0	0	0	0	0	0	0	0	0	11208.29
t_2	8391.011	3565.975	0	0	0	0	0	0	0	0	820	11956.99
t_3	8465.822	5447.896	0	0	0	0	0	0	0	0	900	13913.72
t_4	8465.822	7352.294	0	0	944.9875	0	0	0	0	0	550	16763.1
t_5	8465.822	7940.933	0	0	944.9875	0	0	0	0	0	0	17351.74
t_6	8465.822	7787.757	0	2860.659	944.9875	0	0	0	0	0	0	20059.23
t_7	8465.822	8511.167	0	2860.659	944.9875	0	0	0	0	0	0	20782.64
t_8	8465.822	8887.478	0	2860.659	1447.362	0	0	0	0	0	0	21661.32
t_9	8465.822	7601.033	2891.8	2860.659	944.9875	0	0	0	0	0	380	22764.3
t_{10}	8465.822	8820.471	2891.8	2860.659	944.9875	818.048	0	0	0	0	340	24801.79
t_{11}	8465.822	8887.478	2891.8	2860.659	1901.198	818.048	0	0	0	0	30	25825
t_{12}	8465.822	8887.478	2891.8	2860.659	1954.15	818.048	1173.99	0	0	0	0	27051.95
t_{13}	8465.822	8316.11	2891.8	2860.659	944.9875	0	1173.99	0	0	0	0	24653.37
t_{14}	8465.822	8887.478	0	2860.659	1829.464	0	1173.99	0	0	0	60	23217.42
t_{15}	8465.822	8887.478	0	2860.659	1192.947	0	0	0	0	0	0	21406.91
t_{16}	8465.822	5948.282	0	2860.659	944.9875	0	0	0	0	0	0	18219.75
t_{17}	8465.822	5896.146	0	2860.659	944.9875	0	0	0	0	0	0	18167.61
t_{18}	8465.822	7686.599	0	2860.659	944.9875	818.048	0	0	0	0	170	20776.12
t_{19}	8465.822	7259.093	2891.8	2860.659	944.9875	818.048	0	0	0	0	0	23240.41
t_{20}	8465.822	8887.478	2891.8	2860.659	1174.952	818.048	0	0	0	0	0	25098.76
t_{21}	8465.822	8208.362	2891.8	2860.659	944.9875	0	0	0	0	0	0	23371.63
t_{22}	8465.822	6709.339	2891.8	0	0	0	0	0	0	0	0	18066.96
t_{23}	8465.822	3565.975	2364.362	0	0	0	0	0	0	0	0	14396.16
t_{24}	8060.248	3565.975	0	0	0	0	0	0	0	0	0	11626.22

Table 5.33: Statistical analysis and hypothetical testing of 10 Generating Unit system results for CAOA optimization algorithms with different cases

Test Cases	Best ($)	Average ($)	Worst ($)	STD	Median	Wilcoxon Test	T-Test		Best Time (sec.)	Average Time (sec.)	Worst Time (sec.)
						p-value	p-value	h-Value			
Conventional Thermal System	563427.8	564297	565017.7	387.2645	564327	1.73E-06	1.63E-93	1	0	0.02083	0.0313
Thermal+ PEVs	558645.4	559191.3	559914	290.0386	559151.6	1.73E-06	4.85E-97	1	0.0156	0.02083	0.0625
Thermal+ Solar	547399.2	548219.2	549022.3	377.9526	548147	1.73E-06	1.86E-93	1	0.0156	0.02031	0.0313
Thermal + Wind	491763.4	493505.5	494666.4	695.5368	493729.6	1.73E-06	1.89E-84	1	0.0156	0.0224	0.0469
Thermal+ PEVs + Solar	547620.4	548275	549291.5	411.3319	548258.5	1.73E-06	2.16E-92	1	0	0.01927	0.0313
Thermal+ PEVs +Wind	489870	490994.5	492368.4	624.9831	491057	1.73E-06	9.83E-86	1	0.0156	0.01875	0.0313
Thermal+ Solar+ +Wind + PEVs	479205.8	481668.3	483869.4	981.2449	481767	1.73E-06	8.23E-80	1	0	0.02083	0.0469

TABLE 5.34 Comparison of 10 Generating Unit system for CAOA optimization algorithms (Winter)

Test Case	Best ($)	Average ($)	Worst ($)	STD	Median	Wilcoxon Test	T-Test		Best Time (Sec.)	Average Time (Sec.)	Worst Time (Sec.)
						p-value	p-value	h-Value			
Thermal System	563427.8	564297	565017.7	387.2645	564327	1.73E-06	1.63E-93	1	0	0.02083	0.0313
Thermal+ PEVs	558645.4	559191.3	559914	290.0386	559151.6	1.73E-06	4.85E-97	1	0.0156	0.02083	0.0625
Thermal + Wind	491763.4	493505.5	494666.4	695.5368	493729.6	1.73E-06	1.89E-84	1	0.0156	0.0224	0.0469
Thermal +Solar	547789	548330.9	549188.4	378.468	548220.2	1.73E-06	1.92E-93	1	0.015625	0.019792	0.03125
Thermal+ PEVs +Wind	489870	490994.5	492368.4	624.9831	491057	1.73E-06	9.83E-86	1	0.0156	0.01875	0.0313
Thermal + Solar + PEVs	553388	553938.1	555209.3	383.4611	553878	1.73E-06	2.09E-93	1	0.015625	0.01875	0.03125
Thermal + Solar + Wind + PEVs	485784.2	487554.7	489141.7	958.405	487786.9	1.73E-06	2.92E-80	1	0.015625	0.019792	0.03125

Table 5.35: Statistical and hypothetical analysis of the results for the10 Generating Units system with LFAOA optimization algorithms with different cases.

Test Cases	Best ($)	Average ($)	Worst ($)	STD	Median	Wilcoxon Test	T-Test		Best Time (sec.)	Average Time (sec.)	Worst Time (sec.)
						p-value	p-value	h-Value			
Conventional Thermal Generation	563487.02	564299.59	565246	381.6837	564228.26	1.732E-06	1.069E-93	1	0	0.01875	0.04688
Thermal+ PEVs	558205.09	559064.62	559897.14	298.26935	559040.88	1.734E-06	1.098E-96	1	0.015625	0.01667	0.03125
Thermal + Wind	491994.82	493305.74	494286.28	681.52612	493490.26	1.733E-06	1.057E-84	1	0	0.01823	0.03125
Thermal + Solar	206605.64	208154.42	209405.26	757.34891	208063.64	1.734E-06	1.659E-72	1	0.015625	0.02604	0.125
Thermal + Solar + PEVs	547200.07	548207.69	549019.05	425.70341	548231.3	1.734E-06	5.864E-92	1	0	0.01719	0.04688
Thermal + Wind + PEVs	489623.26	491058.22	492493.66	723.71075	491115.49	1.734E-06	6.887E-84	1	0	0.02865	0.0625
Thermal + Solar + Wind + PEVs	479631.38	481418.43	483227.22	982.28388	481428.78	1.734E-06	8.614E-80	1	0	0.0151	0.03125

5.5.1.2 System of 20 Generating Units

The efficiency of the proposed CAOA and LFAOA optimizers is tested using a specialized system comprising 20 power-generating units that operate for 24 hours. The CAOA and LFAOA techniques are subjected to evaluation through 100 iterations, while 30 trial runs verify the effectiveness of the CAOA and LFAOA algorithms. Details of the commitment status, optimal scheduling, and individual fuel costs of each of the 20 generating units for thermal unit with PEVs are presented in **Tables 5.36**, **5.37**, and **5.38**, respectively. The commitment status, optimal scheduling, and individual fuel costs of each of the 20 generating units for the thermal unit with Solar unit are presented in **Tables 5.39**, **5.40**, and **5.41**, respectively. The commitment status, optimal scheduling, and individual fuel costs of each of the 20 generating units for thermal unit with wind units are presented in **Tables 5.42**, **5.43**, and **5.44**, respectively. The commitment status, optimal scheduling, and individual fuel costs of each of the 20 generating units for thermal, solar, and PEVs units are presented in **Tables 5.45**, **5.46**, and **5.47**, respectively. **Table 5.48** illustrates the committed status for a 20-generating unit using CAOA with a (Thermal + Solar + PEVs) system. **Table 5.44** illustrates the scheduling for a 20-generating unit using CAOA with solar and PEVs (Thermal + Solar + PEVs) systems. **Table 5.45** illustrates the committed status for 20 generating units using CAOA, considering (Thermal + Solar + PEVs) systems. **Table 5.46** illustrates the scheduling for a 20-generating unit using CAOA with wind and PEVs in a power generation (Thermal +Wind +PEVs) system. **Table 5.47** illustrates the individual fuel costs for a 20-generating unit using the CAOA, algorithm with a (Thermal + Solar + PEVs) system. **Table 5.48** illustrates the committed status for 20 generating units with the help of CAOA for the SCUC problem considering thermal, wind, and PEVs systems. **Table 5.49** illustrates the scheduling status for a 20-generating unit with the help of the CAOA algorithm. **Table 5.50** illustrates the individual fuel cost for a 20-generating unit with the help of the CAOA algorithm with a thermal, solar, wind and PEVs system. **Table 5.51** illustrates the committed status for 20 generating units with the help of the CAOA for the SCUC problem considering the thermal, solar, wind, and PEV systems. **Table 5.52** illustrates the scheduling status for a 20-generating unit system with the help of the LFAOA

algorithm with PEVs (thermal +PEVs) system. **Table 5.53** illustrates the individual fuel cost for a 20-generating unit system with the help of the LFAOA algorithm with a thermal + PEV system. **Table 5.54** illustrates the committed status for 20 generating units with the help of the LFAOA algorithm with the PEVs (thermal +PEVs) system. **Table 5.55** illustrates the scheduling for a 20-generation unit with the help of the LFAOA algorithm with a thermal and solar system. **Table 5.56** illustrates the individual fuel cost for a 20-generating unit with the help of the LFAOA algorithm with a thermal and solar system. **Table 5.57** illustrates the committed status for a 20-generating unit with the help of the LFAOA algorithm with a solar (thermal + solar) system. **Table 5.58** illustrates the scheduling for a 20-generating unit with the help of the LFAOA algorithm with a thermal and solar system. **Table 5.59** illustrates the individual fuel cost for a 20-generating unit with the help of the LFAOA algorithm with a thermal and solar system. **Table 5.60** illustrates the committed status for a 20-generating unit with the help of the LFAOA algorithm with the thermal + wind system. **Table 5.61** illustrates the scheduling for a 20-generating unit with the help of the LFAOA algorithm with the thermal + wind system. **Table 5.62** illustrates the individual fuel cost for a 20-generating unit system using the LFAOA algorithm with a thermal + wind system. **Table 5.63** illustrates the committed status for a 20-generating unit with the help of the solar and PEVs (thermal + solar + PEVs) systems. **Table 5.64** illustrates the scheduling for a 20-generating unit system using the LFAOA algorithm with a thermal, solar, and PEV system. **Table 5.65** illustrates the individual fuel cost for 20 generating unit systems using the LFAOA algorithm with the thermal, solar, and PEV systems. **Table 5.66** illustrates the committed status for a 20-generating unit system using the LFAOA algorithm with a wind and PEVs (thermal + wind +PEVs) system. **Table 5.67** illustrates the scheduling for a 20-generating unit system using the LFAOA algorithm with a thermal + wind + PEVs system. **Table 5.68** illustrates the individual fuel cost for 20 generating unit systems using the LFAOA algorithm with wind and PEVs (thermal + wind + PEVs) systems. **Table 5.69** illustrates the committed status for a 20-generating unit using the LFAOA algorithm with a thermal, solar, wind, and PEV system. **Table 5.70** Scheduling for a 20-generating unit system using the LFAOA algorithm

with a thermal, solar, wind, and PEV system. **Table 5.71** illustrates the individual fuel cost for 20 generating unit systems using the LFAOA algorithm with solar, wind, and PEVs (thermal + wind + PEVs) systems. **Table 5.72** illustrates the statistical and hypothetical analysis of 20 generating unit systems using CAOA optimization algorithms with different cases. **Table 5.73** illustrates the comparison of 20 generating unit systems for CAOA with different cases (Winter). **Table 5.74** illustrates the comparison of 20 generating unit systems using the LFAOA optimization algorithms with different cases (Summer). **Table 5.75** illustrates the comparison of 20 generating unit systems using the LFAOA algorithms in different cases (Winter).

Table 5.36: Committed status for a 20-generating unit system using the CAOA algorithm with PEVs (Thermal System+PEVs)

Units/ Hour	t_1	t_2	t_3	t_4	t_5	t_6	t_7	t_8	t_9	t_{10}	t_{11}	t_{12}	t_{13}	t_{14}	t_{15}	t_{16}	t_{17}	t_{18}	t_{19}	t_{20}	t_{21}	t_{22}	t_{23}	t_{24}
U_1	1	1	1	1	1	1	1	1	1	1	1	1	1	1	1	1	1	1	1	1	1	1	1	1
U_2	1	1	1	1	1	1	1	1	1	1	1	1	1	1	1	1	1	1	1	1	1	1	1	1
U_3	0	0	0	0	0	0	0	1	1	1	1	1	1	1	1	1	1	1	1	1	1	1	0	0
U_4	0	0	0	0	0	1	1	1	1	1	1	1	1	1	1	1	1	1	1	1	1	1	1	0
U_5	0	0	0	0	1	1	1	1	1	1	1	1	1	1	1	1	1	1	1	1	1	0	0	0
U_6	0	0	0	0	0	0	0	0	1	1	1	1	1	1	0	0	0	0	0	1	1	1	1	0
U_7	0	0	0	0	0	0	0	0	1	1	1	1	1	0	0	0	0	0	0	1	1	1	0	0
U_8	0	0	0	0	0	0	0	0	0	1	1	1	1	1	0	0	0	0	0	1	0	0	0	0
U_9	0	0	0	0	0	0	0	0	0	1	1	1	1	0	0	0	0	0	0	1	0	0	0	0
U_{10}	0	0	0	0	0	0	0	0	0	0	1	1	0	0	0	0	0	0	0	0	0	0	0	0
U_{11}	1	1	1	1	1	1	1	1	1	1	1	1	1	1	1	1	1	1	1	1	1	1	1	1
U_{22}	1	1	1	1	1	1	1	1	1	1	1	1	1	1	1	1	1	1	1	1	1	1	1	1
U_{13}	0	0	1	1	1	1	1	1	1	1	1	1	1	1	1	1	1	1	1	1	1	1	0	0
U_{14}	0	0	0	0	0	0	1	1	1	1	1	1	1	1	1	1	1	1	1	1	1	0	0	0
U_{15}	0	0	0	1	1	1	1	1	1	1	1	1	1	1	1	1	1	1	1	1	1	0	0	0
U_{16}	0	0	0	0	0	0	0	0	0	1	1	1	1	1	0	0	0	0	0	1	1	1	0	0
U_{17}	0	0	0	0	0	0	0	0	1	1	1	1	1	0	0	0	0	0	0	1	1	1	0	0
U_{18}	0	0	0	0	0	0	0	0	0	1	1	1	1	0	0	0	0	0	0	1	0	0	0	0
U_{19}	0	0	0	0	0	0	0	0	0	0	0	1	0	0	0	0	0	0	0	0	0	0	0	0
U_{20}	0	0	0	0	0	0	0	0	0	0	1	1	0	0	0	0	0	0	0	0	0	0	0	0

Table 5.37: Scheduling for a 20-generating unit system using the CAOA algorithm with PEVs (Thermal + PEVs)

Hour/Units	P_1	P_2	P_3	P_4	P_5	P_6	P_7	P_8	P_9	P_{10}	P_{11}	P_{12}	P_{13}	P_{14}	P_{15}	P_{16}	P_{17}	P_{18}	P_{19}	P_{20}	Number of PEVs	P_{PEVs} (MW)	Generated Power (MW)	Hourly Cost ($)
t_1	455	229	0	0	0	0	0	0	0	0	455	229	0	0	0	0	0	0	0	0	5094	-32.4	1335.6	26802.28
t_2	455	284	0	0	0	0	0	0	0	0	455	284	0	0	0	0	0	0	0	0	3225	-20.5	1457.5	28734.05
t_3	455	319	0	0	0	0	0	0	0	0	455	319	130	0	0	0	0	0	0	0	6984	-44.5	1633.5	32851.68
t_4	455	396	0	0	0	0	0	0	0	0	455	396	130	0	25	0	0	0	0	0	7575	-48.2	1808.8	36486.96
t_5	455	444	0	0	25	0	0	0	0	0	455	444	130	0	25	0	0	0	0	0	4480	-28.5	1949.5	39085.16
t_6	455	455	0	130	40	0	0	0	0	0	455	455	130	0	40	0	0	0	0	0	4905	-31.2	2128.8	42963.01
t_7	455	455	0	130	38	0	0	0	0	0	455	455	130	130	38	0	0	0	0	0	1128	-7.18	2278.82	45737.61
t_8	455	455	130	130	28	0	0	0	0	0	455	455	130	130	28	0	0	0	0	0	235	-1.4	2394.6	48227.53
t_9	455	455	130	130	118	20	25	0	0	0	455	455	130	130	118	0	25	0	0	0	7844	50	2696	55053.28
t_{10}	455	455	130	130	162	51	25	10	10	0	455	455	130	130	162	51	25	10	0	0	7033	44.8	2890.8	61863.96
t_{11}	455	455	130	130	162	80	25	15	10	10	455	455	130	130	162	80	25	15	0	10	6801	43.3	2977.3	65357.42
t_{12}	455	455	130	130	162	80	25	55	22	10	455	455	130	130	162	80	25	55	22	10	7558	48.1	3096.1	69088.28
t_{13}	455	455	130	130	162	51	25	10	10	0	455	455	130	130	162	51	25	10	0	0	7680	48.9	2894.9	61892.7
t_{14}	455	455	130	130	106	20	0	10	0	0	455	455	130	130	106	20	0	0	0	0	2505	15.9	2617.9	53942.72
t_{15}	455	445	130	130	25	0	0	0	0	0	455	445	130	130	25	0	0	0	0	0	4309	-27.4	2342.6	47767.9
t_{16}	455	307	130	130	25	0	0	0	0	0	455	307	130	130	25	0	0	0	0	0	5759	-36.7	2057.3	42908.48
t_{17}	455	243	130	130	25	0	0	0	0	0	455	243	130	130	25	0	0	0	0	0	2392	-15.2	1950.8	40677.58
t_{18}	455	340	130	130	25	0	0	0	0	0	455	340	130	130	25	0	0	0	0	0	6955	-44.3	2115.7	44065.23
t_{19}	455	439	130	130	25	0	0	0	0	0	455	439	130	130	25	0	0	0	0	0	2827	-18.1	2339.9	47554.15
t_{20}	455	455	130	130	162	51	25	10	10	0	455	455	130	130	162	51	25	10	0	0	7844	50	2896	61897.98
t_{21}	455	455	130	130	93	20	25	0	0	0	455	455	130	130	93	20	25	0	0	0	5220	33.2	2649.2	54840.5
t_{22}	455	429	130	130	0	20	25	0	0	0	455	429	130	0	0	20	25	0	0	0	6130	39.7	2287.7	46413.36
t_{23}	455	388	0	130	0	20	0	0	0	0	455	388	0	0	0	0	0	0	0	0	2794	17.8	1853.8	36036.05
t_{24}	455	367	0	0	0	0	0	0	0	0	455	367	0	0	0	0	0	0	0	0	5043	32.1	1676.1	31631.16

Table 5.38: Individual fuel cost for 20 generating unit system using the CAOA for SCUC problem considering (Thermal + PEVs) system

Hours/ Units	P_1	P_2	P_3	P_4	P_5	P_6	P_7	P_8	P_9	P_{10}	P_{11}	P_{12}	P_{13}	P_{14}	P_{15}	P_{16}	P_{17}	P_{18}	P_{19}	P_{20}	SUC	Hourly Cost ($)
t_1	8465.82	4935.32	0	0	0	0	0	0	0	0	8465.82	4935.32	0	0	0	0	0	0	0	0	0	26802.28
t_2	8465.82	5901.2	0	0	0	0	0	0	0	0	8465.82	5901.2	0	0	0	0	0	0	0	0	890	28734.05
t_3	8465.82	6514.12	0	0	0	0	0	0	0	0	8465.82	6514.12	2891.8	0	0	0	0	0	0	0	1120	32851.68
t_4	8465.82	7859.26	0	0	0	0	0	0	0	0	8465.82	7859.26	2891.8	0	944.988	0	0	0	0	0	580	36486.96
t_5	8465.82	8685.87	0	0	944.988	0	0	0	0	0	8465.82	8685.87	2891.8	0	944.988	0	0	0	0	0	2350	39085.16
t_6	8465.82	8887.48	0	2860.66	1251.98	0	0	0	0	0	8465.82	8887.48	2891.8	0	1251.98	0	0	0	0	0	120	42963.01
t_7	8465.82	8887.48	0	2860.66	1208.95	0	0	0	0	0	8465.82	8887.48	2891.8	2860.66	1208.95	0	0	0	0	0	0	45737.61
t_8	8465.82	8887.48	2891.8	2860.66	1008.01	0	0	0	0	0	8465.82	8887.48	2891.8	2860.66	1008.01	0	0	0	0	0	690	48227.53
t_9	8465.82	8887.48	2891.8	2860.66	2837.86	818.048	1173.99	0	0	0	8465.82	8887.48	2891.8	2860.66	2837.86	0	1174	0	0	0	230	55053.28
t_{10}	8465.82	8887.48	2891.8	2860.66	3745.85	1517.8	1173.99	919.6	937.9	0	8465.82	8887.48	2891.8	2860.66	3745.85	1517.8	1174	919.6	0	0	380	61863.96
t_{11}	8465.82	8887.48	2891.8	2860.66	3745.85	2196.37	1173.99	1040	937.9	948.1	8465.82	8887.48	2891.8	2860.66	3745.85	2196.37	1174	1040	0	948.1	120	65357.42
t_{12}	8465.82	8887.48	2891.8	2860.66	3745.85	2196.37	1173.99	2098	1276	948.1	8465.82	8887.48	2891.8	2860.66	3745.85	2196.37	1174	2098	1276	948.1	60	69088.28
t_{13}	8465.82	8887.48	2891.8	2860.66	3745.85	1532.17	1173.99	919.6	937.9	0	8465.82	8887.48	2891.8	2860.66	3745.85	1532.17	1174	919.6	0	0	0	61892.7
t_{14}	8465.82	8887.48	2891.8	2860.66	2587.75	818.048	0	919.6	0	0	8465.82	8887.48	2891.8	2860.66	2587.75	818.048	0	0	0	0	30	53942.72
t_{15}	8465.82	8720.68	2891.8	2860.66	944.988	0	0	0	0	0	8465.82	8720.68	2891.8	2860.66	944.988	0	0	0	0	0	0	47767.9
t_{16}	8465.82	6290.97	2891.8	2860.66	944.988	0	0	0	0	0	8465.82	6290.97	2891.8	2860.66	944.988	0	0	0	0	0	0	42908.48
t_{17}	8465.82	5175.52	2891.8	2860.66	944.988	0	0	0	0	0	8465.82	5175.52	2891.8	2860.66	944.988	0	0	0	0	0	0	40677.58
t_{18}	8465.82	6869.34	2891.8	2860.66	944.988	0	0	0	0	0	8465.82	6869.34	2891.8	2860.66	944.988	0	0	0	0	0	320	44065.23
t_{19}	8465.82	8613.81	2891.8	2860.66	944.988	0	0	0	0	0	8465.82	8613.81	2891.8	2860.66	944.988	0	0	0	0	0	0	47554.15
t_{20}	8465.82	8887.48	2891.8	2860.66	3745.85	1534.81	1173.99	919.6	937.9	0	8465.82	8887.48	2891.8	2860.66	3745.85	1534.81	1174	919.6	0	0	1010	61897.98
t_{21}	8465.82	8887.48	2891.8	2860.66	2322.45	818.048	1173.99	0	0	0	8465.82	8887.48	2891.8	2860.66	2322.45	818.048	1174	0	0	0	0	54840.5
t_{22}	8465.82	8426.69	2891.8	2860.66	0	818.048	1173.99	0	0	0	8465.82	8426.69	2891.8	0	0	818.048	1174	0	0	0	0	46413.36
t_{23}	8465.82	7712.85	0	2860.66	0	818.048	0	0	0	0	8465.82	7712.85	0	0	0	0	0	0	0	0	0	36036.05
t_{24}	8465.82	7349.76	0	0	0	0	0	0	0	0	8465.82	7349.76	0	0	0	0	0	0	0	0	0	31631.16

Table 5.39: Committed status for a 20-generating unit system using the CAOA algorithm (Thermal System + Solar)

Units/Hours	t_1	t_2	t_3	t_4	t_5	t_6	t_7	t_8	t_9	t_{10}	t_{11}	t_{12}	t_{13}	t_{14}	t_{15}	t_{16}	t_{17}	t_{18}	t_{19}	t_{20}	t_{21}	t_{22}	t_{23}	t_{24}
U_1	1	1	1	1	1	1	1	1	1	1	1	1	1	1	1	1	1	1	1	1	1	1	1	1
U_2	1	1	1	1	1	1	1	1	1	1	1	1	1	1	1	1	1	1	1	1	1	1	1	0
U_3	0	0	0	0	0	0	0	0	0	0	0	0	0	0	0	0	0	0	0	0	0	0	0	0
U_4	0	0	0	0	0	0	0	0	0	0	0	0	0	0	0	0	0	0	0	0	0	0	0	0
U_5	0	0	0	0	0	0	0	0	0	0	0	0	0	0	0	0	0	0	0	0	0	0	0	0
U_6	0	0	0	0	0	0	0	0	0	0	0	0	0	0	0	0	0	0	0	0	0	0	0	0
U_7	0	0	0	0	0	0	0	0	0	0	0	0	0	0	0	0	0	0	0	0	0	0	0	0
U_8	0	0	0	0	0	0	0	0	0	0	0	0	0	0	0	0	0	0	0	0	0	0	0	0
U_9	0	0	0	0	0	0	0	0	0	0	0	0	0	0	0	0	0	0	0	0	0	0	0	0
U_{10}	0	0	0	0	0	0	0	0	0	0	0	0	0	0	0	0	0	0	0	0	0	0	0	0
U_{11}	1	1	1	1	1	1	1	1	1	1	1	1	1	1	1	1	1	1	1	1	1	1	1	1
U_{22}	0	0	0	0	0	0	0	0	0	1	1	1	1	1	1	1	1	1	1	1	1	0	0	0
U_{13}	0	0	0	0	0	0	0	0	0	0	0	0	0	0	0	0	0	0	0	0	0	0	0	0
U_{14}	0	0	0	0	0	0	0	0	0	0	0	0	0	0	0	0	0	0	0	0	0	0	0	0
U_{15}	0	0	0	0	0	0	0	0	0	0	0	0	0	0	0	0	0	0	0	0	0	0	0	0
U_{16}	0	0	0	0	0	0	0	0	0	0	0	0	0	0	0	0	0	0	0	0	0	0	0	0
U_{17}	0	0	0	0	0	0	0	0	0	0	0	0	0	0	0	0	0	0	0	0	0	0	0	0
U_{18}	0	0	0	0	0	0	0	0	0	0	0	0	0	0	0	0	0	0	0	0	0	0	0	0
U_{19}	0	0	0	0	0	0	0	0	0	0	0	0	0	0	0	0	0	0	0	0	0	0	0	0
U_{20}	0	0	0	0	0	0	0	0	0	0	0	0	0	0	0	0	0	0	0	0	0	0	0	0

Table 5.40: Scheduling for a 20-generating unit system using the CAOA algorithm (Thermal + Solar)

Hour/Units	P_1	P_2	P_3	P_4	P_5	P_6	P_7	P_8	P_9	P_{10}	P_{11}	P_{12}	P_{13}	P_{14}	P_{15}	P_{16}	P_{17}	P_{18}	P_{19}	P_{20}	P_{solar} (MW)	Generated Power (MW)	Hourly Cost ($)
t_1	291.2	150	0	0	0	0	0	0	0	0	291.2	0	0	0	0	0	0	0	0	0	0	732.4	15076.44
t_2	310.75	150	0	0	0	0	0	0	0	0	310.75	0	0	0	0	0	0	0	0	0	0	771.5	15720.76
t_3	360.62	150	0	0	0	0	0	0	0	0	360.62	0	0	0	0	0	0	0	0	0	0	871.24	17367.7
t_4	421.17	150	0	0	0	0	0	0	0	0	421.17	0	0	0	0	0	0	0	0	0	0	992.35	19373.91
t_5	436.49	150	0	0	0	0	0	0	0	0	436.49	0	0	0	0	0	0	0	0	0	0	1022.99	19882.59
t_6	455	229.24	0	0	0	0	0	0	0	0	455	0	0	0	0	0	0	0	0	0	0	1139.24	21874.62
t_7	455	253.54	0	0	0	0	0	0	0	0	455	0	0	0	0	0	0	0	0	0	0	1163.54	22297.67
t_8	455	289.12	0	0	0	0	0	0	0	0	455	0	0	0	0	0	0	0	0	0	4.55	1199.12	22917.77
t_9	455	327.57	0	0	0	0	0	0	0	0	455	0	0	0	0	0	0	0	0	0	15.67	1237.57	23588.77
t_{10}	455	208.59	0	0	0	0	0	0	0	0	455	208.59	0	0	0	0	0	0	0	0	27.34	1327.18	26099.15
t_{11}	455	234.8	0	0	0	0	0	0	0	0	455	234.8	0	0	0	0	0	0	0	0	37.17	1379.6	27011.12
t_{12}	455	247.61	0	0	0	0	0	0	0	0	455	247.61	0	0	0	0	0	0	0	0	46.06	1405.21	27456.98
t_{13}	455	195.71	0	0	0	0	0	0	0	0	455	195.71	0	0	0	0	0	0	0	0	51.86	1301.41	25651.13
t_{14}	455	166.53	0	0	0	0	0	0	0	0	455	166.53	0	0	0	0	0	0	0	0	54.47	1243.06	24637.45
t_{15}	442.21	150	0	0	0	0	0	0	0	0	442.21	150	0	0	0	0	0	0	0	0	44.59	1184.43	23638.6
t_{16}	353.97	150	0	0	0	0	0	0	0	0	353.97	150	0	0	0	0	0	0	0	0	48.86	1007.95	20713.95
t_{17}	348.48	150	0	0	0	0	0	0	0	0	348.48	150	0	0	0	0	0	0	0	0	37.84	996.96	20532.31
t_{18}	403.48	150	0	0	0	0	0	0	0	0	403.48	150	0	0	0	0	0	0	0	0	33.6	1106.96	22352.92
t_{19}	455	155.81	0	0	0	0	0	0	0	0	455	155.81	0	0	0	0	0	0	0	0	19.59	1221.62	24265.26
t_{20}	455	218.27	0	0	0	0	0	0	0	0	455	218.27	0	0	0	0	0	0	0	0	6.51	1346.53	26435.69
t_{21}	455	186.63	0	0	0	0	0	0	0	0	455	186.63	0	0	0	0	0	0	0	0	0.16	1283.26	25335.71
t_{22}	451.28	150	0	0	0	0	0	0	0	0	451.28	0	0	0	0	0	0	0	0	0	0	1052.56	20373.93
t_{23}	357.04	150	0	0	0	0	0	0	0	0	357.04	0	0	0	0	0	0	0	0	0	0	864.08	17249.31
t_{24}	377.8	0	0	0	0	0	0	0	0	0	377.8	0	0	0	0	0	0	0	0	0	0	755.59	14370.02

Table 5.41: Individual fuel cost for 20 generating unit system using CAOA for SCUC problem considering (Thermal + Solar) system

Hours/ Units	P_1	P_2	P_3	P_4	P_5	P_6	P_7	P_8	P_9	P_{10}	P_{11}	P_{12}	P_{13}	P_{14}	P_{15}	P_{16}	P_{17}	P_{18}	P_{19}	P_{20}	SUC ($)	Hourly Cost ($)
t_1	5755	3566	0	0	0	0	0	0	0	0	5755	0	0	0	0	0	0	0	0	0	0	15076
t_2	6077	3566	0	0	0	0	0	0	0	0	6077	0	0	0	0	0	0	0	0	0	0	15721
t_3	6901	3566	0	0	0	0	0	0	0	0	6901	0	0	0	0	0	0	0	0	0	170	17368
t_4	7904	3566	0	0	0	0	0	0	0	0	7904	0	0	0	0	0	0	0	0	0	0	19374
t_5	8158	3566	0	0	0	0	0	0	0	0	8158	0	0	0	0	0	0	0	0	0	1110	19883
t_6	8466	4943	0	0	0	0	0	0	0	0	8466	0	0	0	0	0	0	0	0	0	4880	21875
t_7	8466	5366	0	0	0	0	0	0	0	0	8466	0	0	0	0	0	0	0	0	0	0	22298
t_8	8466	5986	0	0	0	0	0	0	0	0	8466	0	0	0	0	0	0	0	0	0	1800	22918
t_9	8466	6657	0	0	0	0	0	0	0	0	8466	0	0	0	0	0	0	0	0	0	170	23589
t_{10}	8466	4584	0	0	0	0	0	0	0	0	8466	4584	0	0	0	0	0	0	0	0	0	26099
t_{11}	8466	5040	0	0	0	0	0	0	0	0	8466	5040	0	0	0	0	0	0	0	0	520	27011
t_{12}	8466	5263	0	0	0	0	0	0	0	0	8466	5263	0	0	0	0	0	0	0	0	5000	27457
t_{13}	8466	4360	0	0	0	0	0	0	0	0	8466	4360	0	0	0	0	0	0	0	0	5000	25651
t_{14}	8466	3853	0	0	0	0	0	0	0	0	8466	3853	0	0	0	0	0	0	0	0	0	24637
t_{15}	8253	3566	0	0	0	0	0	0	0	0	8253	3566	0	0	0	0	0	0	0	0	0	23639
t_{16}	6791	3566	0	0	0	0	0	0	0	0	6791	3566	0	0	0	0	0	0	0	0	1110	20714
t_{17}	6700	3566	0	0	0	0	0	0	0	0	6700	3566	0	0	0	0	0	0	0	0	0	20532
t_{18}	7610	3566	0	0	0	0	0	0	0	0	7610	3566	0	0	0	0	0	0	0	0	0	22353
t_{19}	8466	3667	0	0	0	0	0	0	0	0	8466	3667	0	0	0	0	0	0	0	0	0	24265
t_{20}	8466	4752	0	0	0	0	0	0	0	0	8466	4752	0	0	0	0	0	0	0	0	0	26436
t_{21}	8466	4202	0	0	0	0	0	0	0	0	8466	4202	0	0	0	0	0	0	0	0	4500	25336
t_{22}	8404	3566	0	0	0	0	0	0	0	0	8404	0	0	0	0	0	0	0	0	0	2220	20374
t_{23}	6842	3566	0	0	0	0	0	0	0	0	6842	0	0	0	0	0	0	0	0	0	2140	17249
t_{24}	7185	0	0	0	0	0	0	0	0	0	7185	0	0	0	0	0	0	0	0	0	0	14370

Table 5.42: Committed status for a 20-generating unit system using the CAOA algorithm with Solar power generation (Thermal System + Wind)

Units/Hour	t_1	t_2	t_3	t_4	t_5	t_6	t_7	t_8	t_9	t_{10}	t_{11}	t_{12}	t_{13}	t_{14}	t_{15}	t_{16}	t_{17}	t_{18}	t_{19}	t_{20}	t_{21}	t_{22}	t_{23}	t_{24}
U_1	1	1	1	1	1	1	1	1	1	1	1	1	1	1	1	1	1	1	1	1	1	1	1	1
U_2	1	1	1	1	1	1	1	1	1	1	1	1	1	1	1	1	1	1	1	1	1	1	1	1
U_3	0	0	0	0	0	0	0	0	1	1	1	1	1	1	1	1	1	1	1	1	1	0	0	0
U_4	0	0	0	1	1	1	1	1	1	1	1	1	1	1	1	1	1	1	1	1	1	0	0	0
U_5	0	0	0	0	0	1	1	1	1	1	1	1	1	1	1	1	1	1	1	1	1	0	0	0
U_6	0	0	0	0	0	0	0	0	0	1	1	1	1	1	0	0	0	0	0	1	1	1	0	0
U_7	0	0	0	0	0	0	0	0	0	1	1	1	1	0	0	0	0	0	0	1	1	1	0	0
U_8	0	0	0	0	0	0	0	0	0	0	1	1	0	0	0	0	0	0	0	0	0	0	0	1
U_9	0	0	0	0	0	0	0	0	0	0	0	1	0	0	0	0	0	0	0	0	0	0	0	0
U_{10}	0	0	0	0	0	0	0	0	0	0	0	0	0	0	0	0	0	0	0	0	0	0	0	0
U_{11}	1	1	1	1	1	1	1	1	1	1	1	1	1	1	1	1	1	1	1	1	1	1	1	1
U_{22}	1	1	1	1	1	1	1	1	1	1	1	1	1	1	1	1	1	1	1	1	1	1	1	0
U_{13}	0	0	0	0	0	0	0	1	1	1	1	1	1	1	0	0	0	0	0	1	1	1	1	1
U_{14}	0	0	0	0	0	0	1	1	1	1	1	1	1	1	1	1	1	1	1	1	1	1	0	0
U_{15}	0	0	0	0	1	1	1	1	1	1	1	1	1	1	1	1	1	1	1	1	0	0	0	0
U_{16}	0	0	0	0	0	0	0	0	0	1	1	1	1	0	0	0	0	0	0	1	1	1	0	0
U_{17}	0	0	0	0	0	0	0	0	1	1	1	1	1	0	0	0	0	0	0	0	0	0	0	0
U_{18}	0	0	0	0	0	0	0	0	0	0	1	1	0	0	0	0	0	0	0	1	0	0	0	1
U_{19}	0	0	0	0	0	0	0	0	0	0	0	1	0	0	0	0	0	0	0	0	0	0	0	0
U_{20}	0	0	0	0	0	0	0	0	0	0	0	0	0	0	0	0	0	0	0	0	0	0	0	0

Table 5.43: Scheduling for a 20-generating unit system using the CAOA algorithm (Thermal System + Wind)

Hour/Units	P_1	P_2	P_3	P_4	P_5	P_6	P_7	P_8	P_9	P_{10}	P_{11}	P_{12}	P_{13}	P_{14}	P_{15}	P_{16}	P_{17}	P_{18}	P_{19}	P_{20}	P_{wind} (MW)	Generated Power (MW)	Hourly Cost ($)
t_1	455	156.5	0	0	0	0	0	0	0	0	455	156.5	0	0	0	0	0	0	0	0	177	1400	24289.2
t_2	455	209.5	0	0	0	0	0	0	0	0	455	209.5	0	0	0	0	0	0	0	0	171	1500	26130.8
t_3	455	316	0	0	0	0	0	0	0	0	455	316	0	0	0	0	0	0	0	0	158	1700	29841.9
t_4	455	357.5	0	130	0	0	0	0	0	0	455	357.5	0	0	0	0	0	0	0	0	145	1900	34152.4
t_5	455	396.5	0	130	0	0	0	0	0	0	455	396.5	0	0	25	0	0	0	0	0	142	2000	36461.9
t_6	455	455	0	130	56.5	0	0	0	0	0	455	455	0	0	56.5	0	0	0	0	0	137	2200	40718.8
t_7	455	455	0	130	50	0	0	0	0	0	455	455	0	130	50	0	0	0	0	0	120	2300	43317.8
t_8	455	455	0	130	40.5	0	0	0	0	0	455	455	130	130	40.5	0	0	0	0	0	109	2400	45828.5
t_9	455	455	130	130	59.5	0	0	0	0	0	455	455	130	130	59.5	0	25	0	0	0	116	2600	50658
t_{10}	455	455	130	130	127	20	25	0	0	0	455	455	130	130	127	20	25	0	0	0	116	2800	56227.8
t_{11}	455	455	130	130	162	24.5	25	10	0	0	455	455	130	130	162	24.5	25	10	0	0	117	2900	59729.7
t_{12}	455	455	130	130	162	65.5	25	10	10	0	455	455	130	130	162	65.5	25	10	10	0	115	3000	63483.4
t_{13}	455	455	130	130	128	20	25	0	0	0	455	455	130	130	128	20	25	0	0	0	114	2800	56269.2
t_{14}	455	455	130	130	65.5	20	0	0	0	0	455	455	130	130	65.5	0	0	0	0	0	109	2600	50544.4
t_{15}	455	455	130	130	41.5	0	0	0	0	0	455	455	0	130	41.5	0	0	0	0	0	107	2400	45868.5
t_{16}	455	319.5	130	130	25	0	0	0	0	0	455	319.5	0	130	25	0	0	0	0	0	111	2100	40467.2
t_{17}	455	273.5	130	130	25	0	0	0	0	0	455	273.5	0	130	25	0	0	0	0	0	103	2000	38862.3
t_{18}	455	379.7	130	130	25	0	0	0	0	0	455	379.7	0	130	25	0	0	0	0	0	90.5	2199.9	42573.1
t_{19}	455	455	130	130	45.2	0	0	0	0	0	455	455	0	130	45.2	0	0	0	0	0	99.6	2400	46016.9
t_{20}	455	455	130	130	132.5	20	25	0	0	0	455	455	130	130	132.5	20	0	10	0	0	120	2800	56201.5
t_{21}	455	455	130	130	68	20	25	0	0	0	455	455	130	130	0	20	0	0	0	0	127	2600	50829.6
t_{22}	455	414	0	0	0	20	25	0	0	0	455	414	130	130	0	20	0	0	0	0	137	2200	41831.7
t_{23}	455	300	0	0	0	0	0	0	0	0	455	300	130	0	0	0	0	0	0	0	160	1800	32175.2
t_{24}	455	365	0	0	0	0	0	10	0	0	455	0	130	0	0	0	0	10	0	0	175	1600	28973.9

Table 5.44: Individual fuel cost for 20 generating unit system using the CAOA for SCUC problem considering (Thermal + Wind) system

Hours/ Units	P_1	P_2	P_3	P_4	P_5	P_6	P_7	P_8	P_9	P_{10}	P_{11}	P_{12}	P_{13}	P_{14}	P_{15}	P_{16}	P_{17}	P_{18}	P_{19}	P_{20}	SUC ($)	Hourly Cost ($)
t_1	8465.8	3678.8	0	0	0	0	0	0	0	0	8465.8	3678.8	0	0	0	0	0	0	0	0	0	24289.209
t_2	8465.8	4599.6	0	0	0	0	0	0	0	0	8465.8	4599.6	0	0	0	0	0	0	0	0	0	26130.796
t_3	8465.8	6455.1	0	0	0	0	0	0	0	0	8465.8	6455.1	0	0	0	0	0	0	0	0	1620	29841.875
t_4	8465.8	7180.1	0	2860.7	0	0	0	0	0	0	8465.8	7180.1	0	0	0	0	0	0	0	0	0	34152.443
t_5	8465.8	7862.3	0	2860.7	0	0	0	0	0	0	8465.8	7862.3	0	0	944.99	0	0	0	0	0	1450	36461.942
t_6	8465.8	8887.5	0	2860.7	1575.8	0	0	0	0	0	8465.8	8887.5	0	0	1575.8	0	0	0	0	0	0	40718.769
t_7	8465.8	8887.5	0	2860.7	1445	0	0	0	0	0	8465.8	8887.5	0	2860.7	1445	0	0	0	0	0	0	43317.818
t_8	8465.8	8887.5	0	2860.7	1254.4	0	0	0	0	0	8465.8	8887.5	2891.8	2860.7	1254.4	0	0	0	0	0	2920	45828.474
t_9	8465.8	8887.5	2891.8	2860.7	1636.2	0	0	0	0	0	8465.8	8887.5	2891.8	2860.7	1636.2	0	1174	0	0	0	520	50657.992
t_{10}	8465.8	8887.5	2891.8	2860.7	3016.1	818.05	1174	0	0	0	8465.8	8887.5	2891.8	2860.7	3016.1	818.05	1174	0	0	0	690	56227.788
t_{11}	8465.8	8887.5	2891.8	2860.7	3745.9	919.64	1174	919.61	0	0	8465.8	8887.5	2891.8	2860.7	3745.9	919.64	1174	920	0	0	120	59729.721
t_{12}	8465.8	8887.5	2891.8	2860.7	3745.9	1858.6	1174	919.61	937.92	0	8465.8	8887.5	2891.8	2860.7	3745.9	1858.6	1174	920	938	0	120	63483.43
t_{13}	8465.8	8887.5	2891.8	2860.7	3036.8	818.05	1174	0	0	0	8465.8	8887.5	2891.8	2860.7	3036.8	818.05	1174	0	0	0	60	56269.218
t_{14}	8465.8	8887.5	2891.8	2860.7	1757.4	818.05	0	0	0	0	8465.8	8887.5	2891.8	2860.7	1757.4	0	0	0	0	0	0	50544.416
t_{15}	8465.8	8887.5	2891.8	2860.7	1274.4	0	0	0	0	0	8465.8	8887.5	0	2860.7	1274.4	0	0	0	0	0	60	45868.527
t_{16}	8465.8	6516.2	2891.8	2860.7	944.99	0	0	0	0	0	8465.8	6516.2	0	2860.7	944.99	0	0	0	0	0	120	40467.167
t_{17}	8465.8	5713.8	2891.8	2860.7	944.99	0	0	0	0	0	8465.8	5713.8	0	2860.7	944.99	0	0	0	0	0	0	38862.334
t_{18}	8465.8	7569.2	2891.8	2860.7	944.99	0	0	0	0	0	8465.8	7569.2	0	2860.7	944.99	0	0	0	0	0	0	42573.117
t_{19}	8465.8	8887.5	2891.8	2860.7	1348.6	0	0	0	0	0	8465.8	8887.5	0	2860.7	1348.6	0	0	0	0	0	170	46016.86
t_{20}	8465.8	8887.5	2891.8	2860.7	3130.1	818.05	1174	0	0	0	8465.8	8887.5	2891.8	2860.7	3130.1	818.05	0	920	0	0	1380	56201.468
t_{21}	8465.8	8887.5	2891.8	2860.7	1808	818.05	1174	0	0	0	8465.8	8887.5	2891.8	2860.7	0	818.05	0	0	0	0	0	50829.611
t_{22}	8465.8	8168.8	0	0	0	818.05	1174	0	0	0	8465.8	8168.8	2891.8	2860.7	0	818.05	0	0	0	0	0	41831.738
t_{23}	8465.8	6175.9	0	0	0	0	0	0	0	0	8465.8	6175.9	2891.8	0	0	0	0	0	0	0	0	32175.244
t_{24}	8465.8	7311.2	0	0	0	0	0	919.61	0	0	8465.8	0	2891.8	0	0	0	0	920	0	0	0	28973.87

Table 5.45: Committed status for a 20-generating unit system using the CAOA algorithm with (Thermal +Solar+ PEVs) system

Units/Hour	t_1	t_2	t_3	t_4	t_5	t_6	t_7	t_8	t_9	t_{10}	t_{11}	t_{12}	t_{13}	t_{14}	t_{15}	t_{16}	t_{17}	t_{18}	t_{19}	t_{20}	t_{21}	t_{22}	t_{23}	t_{24}
U_1	1	1	1	1	1	1	1	1	1	1	1	1	1	1	1	1	1	1	1	1	1	1	1	1
U_2	1	1	1	1	1	1	1	1	1	1	1	1	1	1	1	1	1	1	1	1	1	1	1	0
U_3	0	0	0	0	0	0	0	0	0	0	0	0	0	0	0	0	0	0	0	0	0	0	0	0
U_4	0	0	0	0	0	0	0	0	0	0	0	0	0	0	0	0	0	0	0	0	0	0	0	0
U_5	0	0	0	0	0	0	0	0	0	0	0	0	0	0	0	0	0	0	0	0	0	0	0	0
U_6	0	0	0	0	0	0	0	0	0	0	0	0	0	0	0	0	0	0	0	0	0	0	0	0
U_7	0	0	0	0	0	0	0	0	0	0	0	0	0	0	0	0	0	0	0	0	0	0	0	0
U_8	0	0	0	0	0	0	0	0	0	0	0	0	0	0	0	0	0	0	0	0	0	0	0	0
U_9	0	0	0	0	0	0	0	0	0	0	0	0	0	0	0	0	0	0	0	0	0	0	0	0
U_{10}	0	0	0	0	0	0	0	0	0	0	0	0	0	0	0	0	0	0	0	0	0	0	0	0
U_{11}	1	1	1	1	1	1	1	1	1	1	1	1	1	1	1	1	1	1	1	1	1	1	1	1
U_{22}	0	0	0	0	0	0	0	0	0	1	1	1	1	1	1	1	1	1	1	1	1	0	0	0
U_{13}	0	0	0	0	0	0	0	0	0	0	0	0	0	0	0	0	0	0	0	0	0	0	0	0
U_{14}	0	0	0	0	0	0	0	0	0	0	0	0	0	0	0	0	0	0	0	0	0	0	0	0
U_{15}	0	0	0	0	0	0	0	0	0	0	0	0	0	0	0	0	0	0	0	0	0	0	0	0
U_{16}	0	0	0	0	0	0	0	0	0	0	0	0	0	0	0	0	0	0	0	0	0	0	0	0
U_{17}	0	0	0	0	0	0	0	0	0	0	0	0	0	0	0	0	0	0	0	0	0	0	0	0
U_{18}	0	0	0	0	0	0	0	0	0	0	0	0	0	0	0	0	0	0	0	0	0	0	0	0
U_{19}	0	0	0	0	0	0	0	0	0	0	0	0	0	0	0	0	0	0	0	0	0	0	0	0
U_{20}	0	0	0	0	0	0	0	0	0	0	0	0	0	0	0	0	0	0	0	0	0	0	0	0

Table 5.46: Scheduling for a 20-generating unit system using the CAOA algorithm with Solar and PEVs (Thermal + Solar + PEVs)

Hour/Units	P_1	P_2	P_3	P_4	P_5	P_6	P_7	P_8	P_9	P_{10}	P_{11}	P_{12}	P_{13}	P_{14}	P_{15}	P_{16}	P_{17}	P_{18}	P_{19}	P_{20}	Number of PEVs	P_{PEVs} (MW)	P_{solar} (MW)	Generated Power (MW)	Hourly Cost ($)
t_1	291.2	150	0	0	0	0	0	0	0	0	291.2	0	0	0	0	0	0	0	0	0	5094	-32.4	0	700	15076.4
t_2	310.75	150	0	0	0	0	0	0	0	0	310.75	0	0	0	0	0	0	0	0	0	3225	-20.5	0	751	15720.8
t_3	360.62	150	0	0	0	0	0	0	0	0	360.62	0	0	0	0	0	0	0	0	0	6984	-44.5	0	826.74	17367.7
t_4	421.18	150	0	0	0	0	0	0	0	0	421.18	0	0	0	0	0	0	0	0	0	7575	-48.2	0	944.15	19373.9
t_5	436.5	150	0	0	0	0	0	0	0	0	436.5	0	0	0	0	0	0	0	0	0	4480	-28.5	0	994.49	19882.6
t_6	455	229.24	0	0	0	0	0	0	0	0	455	0	0	0	0	0	0	0	0	0	4905	-31.2	0	1108.04	21874.6
t_7	455	253.54	0	0	0	0	0	0	0	0	455	0	0	0	0	0	0	0	0	0	1128	-7.18	0	1156.36	22297.7
t_8	455	289.12	0	0	0	0	0	0	0	0	455	0	0	0	0	0	0	0	0	0	235	-1.4	4.55	1202.27	22917.8
t_9	455	327.57	0	0	0	0	0	0	0	0	455	0	0	0	0	0	0	0	0	0	7844	50	15.67	1303.24	23588.8
t_{10}	455	208.59	0	0	0	0	0	0	0	0	455	208.59	0	0	0	0	0	0	0	0	7033	44.8	27.34	1399.32	26099.1
t_{11}	455	234.8	0	0	0	0	0	0	0	0	455	234.8	0	0	0	0	0	0	0	0	6801	43.3	37.17	1460.07	27011.1
t_{12}	455	247.61	0	0	0	0	0	0	0	0	455	247.61	0	0	0	0	0	0	0	0	7558	48.1	46.06	1499.37	27457
t_{13}	455	195.71	0	0	0	0	0	0	0	0	455	195.71	0	0	0	0	0	0	0	0	7680	48.9	51.86	1402.17	25651.1
t_{14}	455	166.53	0	0	0	0	0	0	0	0	455	166.53	0	0	0	0	0	0	0	0	2505	15.9	54.47	1313.43	24637.5
t_{15}	442.22	150	0	0	0	0	0	0	0	0	442.22	150	0	0	0	0	0	0	0	0	4309	-27.4	44.59	1201.62	23638.6
t_{16}	353.98	150	0	0	0	0	0	0	0	0	353.98	150	0	0	0	0	0	0	0	0	5759	-36.7	48.86	1020.11	20713.9
t_{17}	348.48	150	0	0	0	0	0	0	0	0	348.48	150	0	0	0	0	0	0	0	0	2392	-15.2	37.84	1019.6	20532.3
t_{18}	403.48	150	0	0	0	0	0	0	0	0	403.48	150	0	0	0	0	0	0	0	0	6955	-44.3	33.6	1096.26	22352.9
t_{19}	455	155.81	0	0	0	0	0	0	0	0	455	155.81	0	0	0	0	0	0	0	0	2827	-18.1	19.59	1223.11	24265.3
t_{20}	455	218.27	0	0	0	0	0	0	0	0	455	218.27	0	0	0	0	0	0	0	0	7844	50	6.51	1403.04	26435.7
t_{21}	455	186.63	0	0	0	0	0	0	0	0	455	186.63	0	0	0	0	0	0	0	0	5220	33.2	0.16	1316.62	25335.7
t_{22}	451.28	150	0	0	0	0	0	0	0	0	451.28	0	0	0	0	0	0	0	0	0	6130	39.7	0	1092.26	20373.9
t_{23}	357.04	150	0	0	0	0	0	0	0	0	357.04	0	0	0	0	0	0	0	0	0	2794	17.8	0	881.88	17249.3
t_{24}	377.8	0	0	0	0	0	0	0	0	0	377.8	0	0	0	0	0	0	0	0	0	5043	32.1	0	787.69	14370

Table 5.47: Individual fuel cost for 20 generating unit system using the CAOA considering (Thermal + Solar + PEVs) system

Hours/ Units	P_1	P_2	P_3	P_4	P_5	P_6	P_7	P_8	P_9	P_{10}	P_{11}	P_{12}	P_{13}	P_{14}	P_{15}	P_{16}	P_{17}	P_{18}	P_{19}	P_{20}	SUC ($)	Hourly Cost ($)
t_1	5755.231	3565.975	0	0	0	0	0	0	0	0	5755.231	0	0	0	0	0	0	0	0	0	0	15076.44
t_2	6077.394	3565.975	0	0	0	0	0	0	0	0	6077.394	0	0	0	0	0	0	0	0	0	0	15720.76
t_3	6900.86	3565.975	0	0	0	0	0	0	0	0	6900.86	0	0	0	0	0	0	0	0	0	0	17367.7
t_4	7903.97	3565.975	0	0	0	0	0	0	0	0	7903.97	0	0	0	0	0	0	0	0	0	0	19373.91
t_5	8158.307	3565.975	0	0	0	0	0	0	0	0	8158.307	0	0	0	0	0	0	0	0	0	0	19882.59
t_6	8465.822	4942.973	0	0	0	0	0	0	0	0	8465.822	0	0	0	0	0	0	0	0	0	0	21874.62
t_7	8465.822	5366.028	0	0	0	0	0	0	0	0	8465.822	0	0	0	0	0	0	0	0	0	0	22297.67
t_8	8465.822	5986.124	0	0	0	0	0	0	0	0	8465.822	0	0	0	0	0	0	0	0	0	0	22917.77
t_9	8465.822	6657.122	0	0	0	0	0	0	0	0	8465.822	0	0	0	0	0	0	0	0	0	0	23588.77
t_{10}	8465.822	4583.751	0	0	0	0	0	0	0	0	8465.822	4583.751	0	0	0	0	0	0	0	0	5000	26099.15
t_{11}	8465.822	5039.739	0	0	0	0	0	0	0	0	8465.822	5039.739	0	0	0	0	0	0	0	0	0	27011.12
t_{12}	8465.822	5262.668	0	0	0	0	0	0	0	0	8465.822	5262.668	0	0	0	0	0	0	0	0	0	27456.98
t_{13}	8465.822	4359.741	0	0	0	0	0	0	0	0	8465.822	4359.741	0	0	0	0	0	0	0	0	0	25651.13
t_{14}	8465.822	3852.905	0	0	0	0	0	0	0	0	8465.822	3852.905	0	0	0	0	0	0	0	0	0	24637.45
t_{15}	8253.327	3565.975	0	0	0	0	0	0	0	0	8253.327	3565.975	0	0	0	0	0	0	0	0	0	23638.6
t_{16}	6790.998	3565.975	0	0	0	0	0	0	0	0	6790.998	3565.975	0	0	0	0	0	0	0	0	0	20713.95
t_{17}	6700.182	3565.975	0	0	0	0	0	0	0	0	6700.182	3565.975	0	0	0	0	0	0	0	0	0	20532.31
t_{18}	7610.483	3565.975	0	0	0	0	0	0	0	0	7610.483	3565.975	0	0	0	0	0	0	0	0	0	22352.92
t_{19}	8465.822	3666.806	0	0	0	0	0	0	0	0	8465.822	3666.806	0	0	0	0	0	0	0	0	0	24265.26
t_{20}	8465.822	4752.022	0	0	0	0	0	0	0	0	8465.822	4752.022	0	0	0	0	0	0	0	0	0	26435.69
t_{21}	8465.822	4202.031	0	0	0	0	0	0	0	0	8465.822	4202.031	0	0	0	0	0	0	0	0	0	25335.71
t_{22}	8403.977	3565.975	0	0	0	0	0	0	0	0	8403.977	0	0	0	0	0	0	0	0	0	0	20373.93
t_{23}	6841.667	3565.975	0	0	0	0	0	0	0	0	6841.667	0	0	0	0	0	0	0	0	0	0	17249.31
t_{24}	7185.011	0	0	0	0	0	0	0	0	0	7185.011	0	0	0	0	0	0	0	0	0	0	14370.02

Table 5.48: Committed status for a 20-generating unit system using the CAOA algorithm with Solar power generation (Thermal +Wind +PEVs)																								
Units/Hour	t_1	t_2	t_3	t_4	t_5	t_6	t_7	t_8	t_9	t_{10}	t_{11}	t_{12}	t_{13}	t_{14}	t_{15}	t_{16}	t_{17}	t_{18}	t_{19}	t_{20}	t_{21}	t_{22}	t_{23}	t_{24}
U_1	1	1	1	1	1	1	1	1	1	1	1	1	1	1	1	1	1	1	1	1	1	1	1	1
U_2	1	1	1	1	1	1	1	1	1	1	1	1	1	1	1	1	1	1	1	1	1	1	1	1
U_3	0	0	0	0	0	0	0	1	1	1	1	1	1	1	1	1	1	1	1	1	1	0	0	0
U_4	0	0	0	0	1	1	1	1	1	1	1	1	1	1	1	1	1	1	1	1	1	1	0	0
U_5	0	0	0	1	1	1	1	1	1	1	1	1	1	1	1	1	1	1	1	1	1	0	0	0
U_6	0	0	0	0	0	0	0	0	1	1	1	1	1	1	0	0	0	0	0	1	1	1	0	0
U_7	0	0	0	0	0	0	0	0	0	1	1	1	1	0	0	0	0	0	0	0	0	0	0	0
U_8	0	0	0	0	0	0	0	0	0	0	1	1	0	0	0	0	0	0	0	0	0	0	0	0
U_9	0	0	0	0	0	0	0	0	0	0	0	1	0	0	0	0	0	0	0	0	0	0	0	0
U_{10}	0	0	0	0	0	0	0	0	0	0	0	0	1	0	0	0	0	0	0	1	0	0	0	0
U_{11}	1	1	1	1	1	1	1	1	1	1	1	1	1	1	1	1	1	1	1	1	1	1	1	0
U_{22}	1	1	1	1	1	1	1	1	1	1	1	1	1	1	1	1	1	1	1	1	1	1	1	1
U_{13}	0	0	0	0	0	0	0	0	1	1	1	1	1	1	0	0	0	0	0	1	1	1	1	1
U_{14}	0	0	0	0	0	1	1	1	1	1	1	1	1	1	1	1	1	1	1	1	1	1	0	0
U_{15}	0	0	0	0	0	1	1	1	1	1	1	1	1	1	1	1	1	1	1	1	1	0	0	0
U_{16}	0	0	0	0	0	0	0	0	0	1	1	1	1	0	0	0	0	1	1	1	0	0	0	1
U_{17}	0	0	0	0	0	0	0	0	0	1	1	1	0	0	0	0	0	0	1	1	1	0	0	0
U_{18}	0	0	0	0	0	0	0	0	0	0	1	1	0	0	0	0	0	0	0	0	0	0	0	0
U_{19}	0	0	0	0	0	0	0	0	0	0	0	1	0	0	0	0	0	0	0	0	0	0	0	0
U_{20}	0	0	0	0	0	0	0	0	0	0	0	0	0	0	0	0	0	0	0	0	0	0	0	0

Table 5.49: Scheduling for a 20-generating unit system using the CAOA algorithm with (Thermal + Wind + PEVs) system																									
Hour/Units	**P_1**	**P_2**	**P_3**	**P_4**	**P_5**	**P_6**	**P_7**	**P_8**	**P_9**	**P_{10}**	**P_{11}**	**P_{12}**	**P_{13}**	**P_{14}**	**P_{15}**	**P_{16}**	**P_{17}**	**P_{18}**	**P_{19}**	**P_{20}**	**P_{wind} (MW)**	**Number of PEVs**	**P_{PEVs} (MW)**	**Generated Power (MW)**	**Hourly Cost ($)**
t_1	455	157	0	0	0	0	0	0	0	0	455	157	0	0	0	0	0	0	0	0	177	5094	-32.4	1368.6	24289.21
t_2	455	210	0	0	0	0	0	0	0	0	455	210	0	0	0	0	0	0	0	0	171	3225	-20.5	1480.5	26130.8
t_3	455	316	0	0	0	0	0	0	0	0	455	316	0	0	0	0	0	0	0	0	158	6984	-44.5	1655.5	29841.87
t_4	455	410	0	0	25	0	0	0	0	0	455	410	0	0	0	0	0	0	0	0	145	7575	-48.2	1851.8	34074.05
t_5	455	396	0	130	25	0	0	0	0	0	455	396	0	0	0	0	0	0	0	0	142	4480	-28.5	1970.5	36461.94
t_6	455	422	0	130	25	0	0	0	0	0	455	422	0	130	25	0	0	0	0	0	137	4905	-31.2	2169.8	41143.27
t_7	455	455	0	130	50	0	0	0	0	0	455	455	0	130	50	0	0	0	0	0	120	1128	-7.18	2292.82	43317.82
t_8	455	455	130	130	40.5	0	0	0	0	0	455	455	0	130	40.5	0	0	0	0	0	109	235	-1.4	2398.6	45828.47
t_9	455	455	130	130	62	20	0	0	0	0	455	455	130	130	62	0	0	0	0	0	116	7844	50	2650	50402.96
t_{10}	455	455	130	130	127	20	25	0	0	0	455	455	130	130	127	20	25	0	0	0	116	7033	44.8	2844.8	56227.79
t_{11}	455	455	130	130	162	24.5	25	10	0	0	455	455	130	130	162	24.5	25	10	0	0	117	6801	43.3	2943.3	59729.72
t_{12}	455	455	130	130	162	65.5	25	10	10	0	455	455	130	130	162	65.5	25	10	10	0	115	7558	48.1	3048.1	63483.43
t_{13}	455	455	130	130	135	20	25	0	0	10	455	455	130	130	135	20	0	0	0	0	114	7680	48.9	2847.9	56354.53
t_{14}	455	455	130	130	65.5	20	0	0	0	0	455	455	130	130	65.5	0	0	0	0	0	109	2505	15.9	2615.9	50544.42
t_{15}	455	455	130	130	41.5	0	0	0	0	0	455	455	0	130	41.5	0	0	0	0	0	107	4309	-27.4	2372.6	45868.53
t_{16}	455	320	130	130	25	0	0	0	0	0	455	320	0	130	25	0	0	0	0	0	111	5759	-36.7	2064.3	40467.17
t_{17}	455	274	130	130	25	0	0	0	0	0	455	274	0	130	25	0	0	0	0	0	103	2392	-15.2	1985.8	38862.33
t_{18}	455	370	130	130	25	0	0	0	0	0	455	370	0	130	25	20	0	0	0	0	90.5	6955	-44.3	2156.2	43041.32
t_{19}	455	453	130	130	25	0	0	0	0	0	455	453	0	130	25	20	25	0	0	0	99.6	2827	-18.1	2382.5	47121.04
t_{20}	455	455	130	130	132	20	0	0	0	10	455	455	130	130	132	20	25	0	0	0	120	7844	50	2849	56229.93
t_{21}	455	455	130	130	44	20	0	0	0	0	455	455	130	130	44	0	25	0	0	0	127	5220	33.2	2633.2	50852.57
t_{22}	455	372	0	130	0	20	0	0	0	0	455	372	130	130	0	0	0	0	0	0	137	6130	39.7	2240.7	41212.56
t_{23}	455	300	0	0	0	0	0	0	0	0	455	300	130	0	0	0	0	0	0	0	160	2794	17.8	1817.8	32175.24
t_{24}	455	410	0	0	0	0	0	0	0	0	0	410	130	0	0	20	0	0	0	0	175	5043	32.1	1632.1	28373.09

Table 5.50: Individual fuel cost for 20 generating unit system using the CAOA for SCUC problem considering (Thermal + Wind + PEVs) system

Hours/ Units	P_1	P_2	P_3	P_4	P_5	P_6	P_7	P_8	P_9	P_{10}	P_{11}	P_{12}	P_{13}	P_{14}	P_{15}	P_{16}	P_{17}	P_{18}	P_{19}	P_{20}	SUC ($)	Hourly Cost ($)
t_1	8465.82	3678.78	0	0	0	0	0	0	0	0	8465.82	3678.78	0	0	0	0	0	0	0	0	0	24289.209
t_2	8465.82	4599.58	0	0	0	0	0	0	0	0	8465.82	4599.58	0	0	0	0	0	0	0	0	550	26130.796
t_3	8465.82	6455.12	0	0	0	0	0	0	0	0	8465.82	6455.12	0	0	0	0	0	0	0	0	1120	29841.875
t_4	8465.82	8098.71	0	0	944.988	0	0	0	0	0	8465.82	8098.71	0	0	0	0	0	0	0	0	1450	34074.054
t_5	8465.82	7862.33	0	2860.66	944.988	0	0	0	0	0	8465.82	7862.33	0	0	0	0	0	0	0	0	0	36461.942
t_6	8465.82	8300.17	0	2860.66	944.988	0	0	0	0	0	8465.82	8300.17	0	2861	945	0	0	0	0	0	0	41143.268
t_7	8465.82	8887.48	0	2860.66	1444.95	0	0	0	0	0	8465.82	8887.48	0	2861	1445	0	0	0	0	0	0	43317.818
t_8	8465.82	8887.48	2891.8	2860.66	1254.38	0	0	0	0	0	8465.82	8887.48	0	2861	1254	0	0	0	0	0	520	45828.474
t_9	8465.82	8887.48	2891.8	2860.66	1686.7	818.05	0	0	0	0	8465.82	8887.48	2892	2861	1687	0	0	0	0	0	180	50402.964
t_{10}	8465.82	8887.48	2891.8	2860.66	3016.09	818.05	1174	0	0	0	8465.82	8887.48	2892	2861	3016	818	1174	0	0	0	3000	56227.788
t_{11}	8465.82	8887.48	2891.8	2860.66	3745.85	919.64	1174	919.61	0	0	8465.82	8887.48	2892	2861	3746	920	1174	920	0	0	60	59729.721
t_{12}	8465.82	8887.48	2891.8	2860.66	3745.85	1858.6	1174	919.61	937.92	0	8465.82	8887.48	2892	2861	3746	1859	1174	920	938	0	180	63483.43
t_{13}	8465.82	8887.48	2891.8	2860.66	3192.42	818.05	1174	0	0	948.07	8465.82	8887.48	2892	2861	3192	818	0	0	0	0	0	56354.528
t_{14}	8465.82	8887.48	2891.8	2860.66	1757.43	818.05	0	0	0	0	8465.82	8887.48	2892	2861	1757	0	0	0	0	0	0	50544.416
t_{15}	8465.82	8887.48	2891.8	2860.66	1274.4	0	0	0	0	0	8465.82	8887.48	0	2861	1274	0	0	0	0	0	0	45868.527
t_{16}	8465.82	6516.21	2891.8	2860.66	944.988	0	0	0	0	0	8465.82	6516.21	0	2861	945	0	0	0	0	0	0	40467.167
t_{17}	8465.82	5713.8	2891.8	2860.66	944.988	0	0	0	0	0	8465.82	5713.8	0	2861	945	0	0	0	0	0	60	38862.334
t_{18}	8465.82	7394.27	2891.8	2860.66	944.988	0	0	0	0	0	8465.82	7394.27	0	2861	945	818	0	0	0	0	430	43041.318
t_{19}	8465.82	8847.13	2891.8	2860.66	944.988	0	0	0	0	0	8465.82	8847.13	0	2861	945	818	1174	0	0	0	0	47121.044
t_{20}	8465.82	8887.48	2891.8	2860.66	3130.12	818.05	0	0	0	948.07	8465.82	8887.48	2892	2861	3130	818	1174	0	0	0	690	56229.928
t_{21}	8465.82	8887.48	2891.8	2860.66	1324.51	818.05	0	0	0	0	8465.82	8887.48	2892	2861	1325	0	1174	0	0	0	0	50852.57
t_{22}	8465.82	7424.87	0	2860.66	0	818.05	0	0	0	0	8465.82	7424.87	2892	2861	0	0	0	0	0	0	0	41212.558
t_{23}	8465.82	6175.9	0	0	0	0	0	0	0	0	8465.82	6175.9	2892	0	0	0	0	0	0	0	0	32175.244
t_{24}	8465.82	8098.71	0	0	0	0	0	0	0	0	0	8098.71	2892	0	0	818	0	0	0	0	0	28373.092

Table 5.51: Committed status for a 20-generating unit system using the CAOA algorithm (Thermal + Solar + Wind + PEVs)

Units/Hour	t_1	t_2	t_3	t_4	t_5	t_6	t_7	t_8	t_9	t_{10}	t_{11}	t_{12}	t_{13}	t_{14}	t_{15}	t_{16}	t_{17}	t_{18}	t_{19}	t_{20}	t_{21}	t_{22}	t_{23}	t_{24}
U_1	1	1	1	1	1	1	1	1	1	1	1	1	1	1	1	1	1	1	1	1	1	1	1	1
U_2	1	1	1	1	1	1	1	1	1	1	1	1	1	1	1	1	1	1	1	1	1	1	1	0
U_3	0	0	0	0	0	0	0	0	0	0	0	0	0	0	0	0	0	0	0	0	0	0	0	0
U_4	0	0	0	0	0	0	0	0	0	0	0	0	0	0	0	0	0	0	0	0	0	0	0	0
U_5	0	0	0	0	0	0	0	0	0	0	0	0	0	0	0	0	0	0	0	0	0	0	0	0
U_6	0	0	0	0	0	0	0	0	0	0	0	0	0	0	0	0	0	0	0	0	0	0	0	0
U_7	0	0	0	0	0	0	0	0	0	0	0	0	0	0	0	0	0	0	0	0	0	0	0	0
U_8	0	0	0	0	0	0	0	0	0	0	0	0	0	0	0	0	0	0	0	0	0	0	0	0
U_9	0	0	0	0	0	0	0	0	0	0	0	0	0	0	0	0	0	0	0	0	0	0	0	0
U_{10}	0	0	0	0	0	0	0	0	0	0	0	0	0	0	0	0	0	0	0	0	0	0	0	0
U_{11}	1	1	1	1	1	1	1	1	1	1	1	1	1	1	1	1	1	1	1	1	1	1	1	1
U_{22}	0	0	0	0	0	0	0	0	0	1	1	1	1	1	1	1	1	1	1	1	1	0	0	0
U_{13}	0	0	0	0	0	0	0	0	0	0	0	0	0	0	0	0	0	0	0	0	0	0	0	0
U_{14}	0	0	0	0	0	0	0	0	0	0	0	0	0	0	0	0	0	0	0	0	0	0	0	0
U_{15}	0	0	0	0	0	0	0	0	0	0	0	0	0	0	0	0	0	0	0	0	0	0	0	0
U_{16}	0	0	0	0	0	0	0	0	0	0	0	0	0	0	0	0	0	0	0	0	0	0	0	0
U_{17}	0	0	0	0	0	0	0	0	0	0	0	0	0	0	0	0	0	0	0	0	0	0	0	0
U_{18}	0	0	0	0	0	0	0	0	0	0	0	0	0	0	0	0	0	0	0	0	0	0	0	0
U_{19}	0	0	0	0	0	0	0	0	0	0	0	0	0	0	0	0	0	0	0	0	0	0	0	0
U_{20}	0	0	0	0	0	0	0	0	0	0	0	0	0	0	0	0	0	0	0	0	0	0	0	0

Table 5.52: Scheduling for a 20-generating unit system using the CAOA algorithm with (Thermal +Solar +Wind +PEVs) system

Hour/Units	P_1	P_2	P_3	P_4	P_5	P_6	P_7	P_8	P_9	P_{10}	P_{11}	P_{12}	P_{13}	P_{14}	P_{15}	P_{16}	P_{17}	P_{18}	P_{19}	P_{20}	Number of PEVs	P_{PEVs} (MW)	P_{solar} (MW)	P_{wind} (MW)	Generated Power (MW)	Hourly Cost ($)
t_1	291.2	150	0	0	0	0	0	0	0	0	291.2	0	0	0	0	0	0	0	0	0	5094	-32.4	0	177	732.4	15076.44
t_2	310.75	150	0	0	0	0	0	0	0	0	310.75	0	0	0	0	0	0	0	0	0	3225	-20.5	0	171	771.5	15720.76
t_3	360.62	150	0	0	0	0	0	0	0	0	360.62	0	0	0	0	0	0	0	0	0	6984	-44.5	0	158	871.24	17367.7
t_4	421.17	150	0	0	0	0	0	0	0	0	421.17	0	0	0	0	0	0	0	0	0	7575	-48.2	0	145	992.35	19373.91
t_5	436.49	150	0	0	0	0	0	0	0	0	436.49	0	0	0	0	0	0	0	0	0	4480	-28.5	0	142	1022.99	19882.59
t_6	455	229.24	0	0	0	0	0	0	0	0	455	0	0	0	0	0	0	0	0	0	4905	-31.2	0	137	1139.24	21874.62
t_7	455	253.54	0	0	0	0	0	0	0	0	455	0	0	0	0	0	0	0	0	0	1128	-7.18	0	120	1163.54	22297.67
t_8	455	289.12	0	0	0	0	0	0	0	0	455	0	0	0	0	0	0	0	0	0	235	-1.4	4.55	109	1199.12	22917.77
t_9	455	327.57	0	0	0	0	0	0	0	0	455	0	0	0	0	0	0	0	0	0	7844	50	15.67	116	1237.57	23588.77
t_{10}	455	208.59	0	0	0	0	0	0	0	0	455	208.59	0	0	0	0	0	0	0	0	7033	44.8	27.34	116	1327.18	26099.15
t_{11}	455	234.8	0	0	0	0	0	0	0	0	455	234.8	0	0	0	0	0	0	0	0	6801	43.3	37.17	117	1379.6	27011.12
t_{12}	455	247.61	0	0	0	0	0	0	0	0	455	247.61	0	0	0	0	0	0	0	0	7558	48.1	46.06	115	1405.21	27456.98
t_{13}	455	195.71	0	0	0	0	0	0	0	0	455	195.71	0	0	0	0	0	0	0	0	7680	48.9	51.86	114	1301.41	25651.13
t_{14}	455	166.53	0	0	0	0	0	0	0	0	455	166.53	0	0	0	0	0	0	0	0	2505	15.9	54.47	109	1243.06	24637.45
t_{15}	442.21	150	0	0	0	0	0	0	0	0	442.21	150	0	0	0	0	0	0	0	0	4309	-27.4	44.59	107	1184.43	23638.6
t_{16}	353.97	150	0	0	0	0	0	0	0	0	353.97	150	0	0	0	0	0	0	0	0	5759	-36.7	48.86	111	1007.95	20713.95
t_{17}	348.48	150	0	0	0	0	0	0	0	0	348.48	150	0	0	0	0	0	0	0	0	2392	-15.2	37.84	103	996.96	20532.31
t_{18}	403.48	150	0	0	0	0	0	0	0	0	403.48	150	0	0	0	0	0	0	0	0	6955	-44.3	33.6	90.5	1106.96	22352.92
t_{19}	455	155.81	0	0	0	0	0	0	0	0	455	155.81	0	0	0	0	0	0	0	0	2827	-18.1	19.59	99.6	1221.62	24265.26
t_{20}	455	218.27	0	0	0	0	0	0	0	0	455	218.27	0	0	0	0	0	0	0	0	7844	50	6.51	120	1346.53	26435.69
t_{21}	455	186.63	0	0	0	0	0	0	0	0	455	186.63	0	0	0	0	0	0	0	0	5220	33.2	0.16	127	1283.26	25335.71
t_{22}	451.28	150	0	0	0	0	0	0	0	0	451.28	0	0	0	0	0	0	0	0	0	6130	39.7	0	137	1052.56	20373.93
t_{23}	357.04	150	0	0	0	0	0	0	0	0	357.04	0	0	0	0	0	0	0	0	0	2794	17.8	0	160	864.08	17249.31
t_{24}	377.8	0	0	0	0	0	0	0	0	0	377.8	0	0	0	0	0	0	0	0	0	5043	32.1	0	175	755.59	14370.02

Table 5.53: Individual fuel cost for 20 generating unit system using the CAOA for SCUC problem considering (Thermal + Solar + Wind+ PEVs) system

Hours/ Units	P_1	P_2	P_3	P_4	P_5	P_6	P_7	P_8	P_9	P_{10}	P_{11}	P_{12}	P_{13}	P_{14}	P_{15}	P_{16}	P_{17}	P_{18}	P_{19}	P_{20}	SUC ($)	Hourly Cost ($)
t_1	5755.231	3565.975	0	0	0	0	0	0	0	0	5755.231	0	0	0	0	0	0	0	0	0	0	15076.44
t_2	6077.394	3565.975	0	0	0	0	0	0	0	0	6077.394	0	0	0	0	0	0	0	0	0	0	15720.76
t_3	6900.86	3565.975	0	0	0	0	0	0	0	0	6900.86	0	0	0	0	0	0	0	0	0	170	17367.7
t_4	7903.97	3565.975	0	0	0	0	0	0	0	0	7903.97	0	0	0	0	0	0	0	0	0	0	19373.91
t_5	8158.307	3565.975	0	0	0	0	0	0	0	0	8158.307	0	0	0	0	0	0	0	0	0	1110	19882.59
t_6	8465.822	4942.973	0	0	0	0	0	0	0	0	8465.822	0	0	0	0	0	0	0	0	0	4880	21874.62
t_7	8465.822	5366.028	0	0	0	0	0	0	0	0	8465.822	0	0	0	0	0	0	0	0	0	0	22297.67
t_8	8465.822	5986.124	0	0	0	0	0	0	0	0	8465.822	0	0	0	0	0	0	0	0	0	1800	22917.77
t_9	8465.822	6657.122	0	0	0	0	0	0	0	0	8465.822	0	0	0	0	0	0	0	0	0	170	23588.77
t_{10}	8465.822	4583.751	0	0	0	0	0	0	0	0	8465.822	4583.751	0	0	0	0	0	0	0	0	0	26099.15
t_{11}	8465.822	5039.739	0	0	0	0	0	0	0	0	8465.822	5039.739	0	0	0	0	0	0	0	0	520	27011.12
t_{12}	8465.822	5262.668	0	0	0	0	0	0	0	0	8465.822	5262.668	0	0	0	0	0	0	0	0	5000	27456.98
t_{13}	8465.822	4359.741	0	0	0	0	0	0	0	0	8465.822	4359.741	0	0	0	0	0	0	0	0	5000	25651.13
t_{14}	8465.822	3852.905	0	0	0	0	0	0	0	0	8465.822	3852.905	0	0	0	0	0	0	0	0	0	24637.45
t_{15}	8253.327	3565.975	0	0	0	0	0	0	0	0	8253.327	3565.975	0	0	0	0	0	0	0	0	0	23638.6
t_{16}	6790.998	3565.975	0	0	0	0	0	0	0	0	6790.998	3565.975	0	0	0	0	0	0	0	0	1110	20713.95
t_{17}	6700.182	3565.975	0	0	0	0	0	0	0	0	6700.182	3565.975	0	0	0	0	0	0	0	0	0	20532.31
t_{18}	7610.483	3565.975	0	0	0	0	0	0	0	0	7610.483	3565.975	0	0	0	0	0	0	0	0	0	22352.92
t_{19}	8465.822	3666.806	0	0	0	0	0	0	0	0	8465.822	3666.806	0	0	0	0	0	0	0	0	0	24265.26
t_{20}	8465.822	4752.022	0	0	0	0	0	0	0	0	8465.822	4752.022	0	0	0	0	0	0	0	0	0	26435.69
t_{21}	8465.822	4202.031	0	0	0	0	0	0	0	0	8465.822	4202.031	0	0	0	0	0	0	0	0	4500	25335.71
t_{22}	8403.977	3565.975	0	0	0	0	0	0	0	0	8403.977	0	0	0	0	0	0	0	0	0	2220	20373.93
t_{23}	6841.667	3565.975	0	0	0	0	0	0	0	0	6841.667	0	0	0	0	0	0	0	0	0	2140	17249.31
t_{24}	7185.011	0	0	0	0	0	0	0	0	0	7185.011	0	0	0	0	0	0	0	0	0	0	14370.02

Table 5.54: Committed status for a 20-generating unit system using the LFAOA algorithm with PEVs (Thermal +PEVs) system

Units/Hours	t_1	t_2	t_3	t_4	t_5	t_6	t_7	t_8	t_9	t_{10}	t_{11}	t_{12}	t_{13}	t_{14}	t_{15}	t_{16}	t_{17}	t_{18}	t_{19}	t_{20}	t_{21}	t_{22}	t_{23}	t_{24}
U_1	1	1	1	1	1	1	1	1	1	1	1	1	1	1	1	1	1	1	1	1	1	1	1	1
U_2	1	1	1	1	1	1	1	1	1	1	1	1	1	1	1	1	1	1	1	1	1	1	1	1
U_3	0	0	0	0	1	1	1	1	1	1	1	1	1	1	1	1	1	1	1	1	1	0	0	0
U_4	0	0	1	1	1	1	1	1	1	1	1	1	1	1	1	1	1	1	1	1	1	1	1	0
U_5	0	0	0	1	1	1	1	1	1	1	1	1	1	1	1	1	1	1	1	1	1	1	0	0
U_6	0	0	0	0	0	0	0	0	1	1	1	1	1	1	0	0	0	0	1	1	1	0	0	0
U_7	0	0	0	0	0	0	0	0	1	1	1	1	1	1	0	0	0	0	0	1	1	1	0	0
U_8	0	0	0	0	0	0	0	0	0	1	1	1	1	0	0	0	0	0	0	1	0	0	0	0
U_9	0	0	0	0	0	0	0	0	0	1	1	1	1	0	0	0	0	0	0	1	0	0	0	0
U_{10}	0	0	0	0	0	0	0	0	0	0	1	1	0	0	0	0	0	0	0	0	0	0	0	0
U_{11}	1	1	1	1	1	1	1	1	1	1	1	1	1	1	1	1	1	1	1	1	1	1	1	1
U_{22}	1	1	1	1	1	1	1	1	1	1	1	1	1	1	1	1	1	1	1	1	1	1	1	1
U_{13}	0	0	0	0	0	0	0	1	1	1	1	1	1	1	0	0	0	0	0	1	1	1	1	1
U_{14}	0	0	0	0	0	0	1	1	1	1	1	1	1	1	1	1	1	1	1	1	0	0	0	0
U_{15}	0	0	0	0	0	1	1	1	1	1	1	1	1	1	1	1	1	1	1	1	1	0	0	0
U_{16}	0	0	0	0	0	0	0	0	1	1	1	1	1	1	1	0	0	0	0	1	1	1	0	0
U_{17}	0	0	0	0	0	0	0	0	1	1	1	1	1	0	0	0	0	0	0	1	1	1	0	0
U_{18}	0	0	0	0	0	0	0	0	0	1	1	1	1	0	0	0	0	0	0	1	1	0	0	0
U_{19}	0	0	0	0	0	0	0	0	0	0	1	1	0	0	0	0	0	0	0	0	0	0	0	0
U_{20}	0	0	0	0	0	0	0	0	0	0	0	1	0	0	0	0	0	0	0	0	0	0	0	0

Table 5.55: Scheduling for a 20-generating unit system using the LFAOA algorithm with (Thermal + PEVs) system

Hour/ Units	P_1	P_2	P_3	P_4	P_5	P_6	P_7	P_8	P_9	P_{10}	P_{11}	P_{12}	P_{13}	P_{14}	P_{15}	P_{16}	P_{17}	P_{18}	P_{19}	P_{20}	Power Generated (MW)	SUC ($)	Hourly Cost ($)
t_1	455	228.8	0	0	0	0	0	0	0	0	455	228.8	0	0	0	0	0	0	0	0	1367.6	0	26802.277
t_2	455	284.3	0	0	0	0	0	0	0	0	455	284.3	0	0	0	0	0	0	0	0	1478.5	0	28734.049
t_3	455	319.4	0	130	0	0	0	0	0	0	455	319.4	0	0	0	0	0	0	0	0	1678.76	2910	32820.543
t_4	455	396.3	0	130	25	0	0	0	0	0	455	396.3	0	0	0	0	0	0	0	0	1857.65	560	36455.815
t_5	455	391	130	130	25	0	0	0	0	0	455	391	0	0	0	0	0	0	0	0	1977.01	550	39161.372
t_6	455	455	130	130	40.38	0	0	0	0	0	455	455	0	0	40.38	0	0	0	0	0	2160.76	1380	42963.01
t_7	455	455	130	130	38.23	0	0	0	0	0	455	455	0	130	38.23	0	0	0	0	0	2286.46	0	45737.613
t_8	455	455	130	130	28.17	0	0	0	0	0	455	455	130	130	28.17	0	0	0	0	0	2396.33	0	48227.533
t_9	455	455	130	130	108.4	20	25	0	0	0	455	455	130	130	108.4	20	25	0	0	0	2646.76	340	55459.273
t_{10}	455	455	130	130	162	50.74	25	10	10	0	455	455	130	130	162	50.74	25	10	0	0	2845.48	180	61863.962
t_{11}	455	455	130	130	162	80	25	14.62	10	10	455	455	130	130	162	80	25	14.62	10	0	2933.23	120	65347.266
t_{12}	455	455	130	130	162	80	25	55	22.36	10	455	455	130	130	162	80	25	55	22.36	10	3048.73	60	69088.284
t_{13}	455	455	130	130	162	51.37	25	10	10	0	455	455	130	130	162	51.37	25	10	0	0	2846.73	0	61892.695
t_{14}	455	455	130	130	98.73	20	25	0	0	0	455	455	130	130	98.73	20	0	0	0	0	2602.47	0	53889.365
t_{15}	455	455	130	130	70.49	0	0	0	0	0	455	455	0	130	70.49	20	0	0	0	0	2370.98	0	47854.623
t_{16}	455	371.6	130	130	25	0	0	0	0	0	455	371.6	0	130	25	0	0	0	0	0	2093.19	120	42287.808
t_{17}	455	307.6	130	130	25	0	0	0	0	0	455	307.6	0	130	25	0	0	0	0	0	1965.2	260	40051.752
t_{18}	455	404.7	130	130	25	0	0	0	0	0	455	404.7	0	130	25	0	0	0	0	0	2159.44	170	43447.226
t_{19}	455	455	130	130	64.39	20	0	0	0	0	455	455	0	130	64.39	0	0	0	0	0	2358.79	0	47607.936
t_{20}	455	455	130	130	162	51.48	25	10	10	0	455	455	130	130	162	51.48	25	10	0	0	2846.96	610	61897.984
t_{21}	455	455	130	130	153.3	20	25	0	0	0	455	455	130	0	153.3	20	25	10	0	0	2616.58	0	55381.224
t_{22}	455	455	0	130	97.44	0	25	0	0	0	455	455	130	0	0	20	25	0	0	0	2247.44	0	46032.45
t_{23}	455	333	0	130	0	0	0	0	0	0	455	333	130	0	0	0	0	0	0	0	1835.92	0	36186.617
t_{24}	455	302.2	0	0	0	0	0	0	0	0	455	302.2	130	0	0	0	0	0	0	0	1644.41	0	32252.184

Table 5.56: Individual fuel cost for 20 generating unit system using the LFAOA algorithm with PEVs (Thermal +PEVs) system

Hours/ Units	P_1	P_2	P_3	P_4	P_5	P_6	P_7	P_8	P_9	P_{10}	P_{11}	P_{12}	P_{13}	P_{14}	P_{15}	P_{16}	P_{17}	P_{18}	P_{19}	P_{20}	SUC	Hourly Cost ($)
t_1	8465.82	4935.32	0	0	0	0	0	0	0	0	8465.82	4935.32	0	0	0	0	0	0	0	0	0	26802.2767
t_2	8465.82	5901.2	0	0	0	0	0	0	0	0	8465.82	5901.2	0	0	0	0	0	0	0	0	0	28734.0488
t_3	8465.82	6514.12	0	2860.66	0	0	0	0	0	0	8465.82	6514.12	0	0	0	0	0	0	0	0	2910	32820.5428
t_4	8465.82	7859.26	0	2860.66	944.988	0	0	0	0	0	8465.82	7859.26	0	0	0	0	0	0	0	0	560	36455.8151
t_5	8465.82	7766.14	2891.8	2860.66	944.988	0	0	0	0	0	8465.82	7766.14	0	0	0	0	0	0	0	0	550	39161.3717
t_6	8465.82	8887.48	2891.8	2860.66	1251.98	0	0	0	0	0	8465.82	8887.48	0	0	1251.98	0	0	0	0	0	1380	42963.0096
t_7	8465.82	8887.48	2891.8	2860.66	1208.95	0	0	0	0	0	8465.82	8887.48	0	2860.66	1208.95	0	0	0	0	0	0	45737.6133
t_8	8465.82	8887.48	2891.8	2860.66	1008.01	0	0	0	0	0	8465.82	8887.48	2891.8	2860.66	1008.01	0	0	0	0	0	0	48227.5329
t_9	8465.82	8887.48	2891.8	2860.66	2631.84	818.048	1173.99	0	0	0	8465.82	8887.48	2891.8	2860.66	2631.84	818.048	1173.99	0	0	0	340	55459.2729
t_{10}	8465.82	8887.48	2891.8	2860.66	3745.85	1517.8	1173.99	919.613	937.922	0	8465.82	8887.48	2891.8	2860.66	3745.85	1517.8	1173.99	919.613	0	0	180	61863.9616
t_{11}	8465.82	8887.48	2891.8	2860.66	3745.85	2196.37	1173.99	1039.7	937.922	948.073	8465.82	8887.48	2891.8	2860.66	3745.85	2196.37	1173.99	1039.7	937.922	0	120	65347.2662
t_{12}	8465.82	8887.48	2891.8	2860.66	3745.85	2196.37	1173.99	2098.09	1276	948.073	8465.82	8887.48	2891.8	2860.66	3745.85	2196.37	1173.99	2098.09	1276	948.073	60	69088.2837
t_{13}	8465.82	8887.48	2891.8	2860.66	3745.85	1532.17	1173.99	919.613	937.922	0	8465.82	8887.48	2891.8	2860.66	3745.85	1532.17	1173.99	919.613	0	0	0	61892.6953
t_{14}	8465.82	8887.48	2891.8	2860.66	2433.88	818.048	1173.99	0	0	0	8465.82	8887.48	2891.8	2860.66	2433.88	818.048	0	0	0	0	0	53889.3651
t_{15}	8465.82	8887.48	2891.8	2860.66	1858.43	0	0	0	0	0	8465.82	8887.48	0	2860.66	1858.43	818.048	0	0	0	0	0	47854.6235
t_{16}	8465.82	7426.54	2891.8	2860.66	944.988	0	0	0	0	0	8465.82	7426.54	0	2860.66	944.988	0	0	0	0	0	120	42287.8078
t_{17}	8465.82	6308.51	2891.8	2860.66	944.988	0	0	0	0	0	8465.82	6308.51	0	2860.66	944.988	0	0	0	0	0	260	40051.752
t_{18}	8465.82	8006.24	2891.8	2860.66	944.988	0	0	0	0	0	8465.82	8006.24	0	2860.66	944.988	0	0	0	0	0	170	43447.2263
t_{19}	8465.82	8887.48	2891.8	2860.66	1735.09	818.048	0	0	0	0	8465.82	8887.48	0	2860.66	1735.09	0	0	0	0	0	0	47607.9364
t_{20}	8465.82	8887.48	2891.8	2860.66	3745.85	1534.81	1173.99	919.613	937.922	0	8465.82	8887.48	2891.8	2860.66	3745.85	1534.81	1173.99	919.613	0	0	610	61897.9836
t_{21}	8465.82	8887.48	2891.8	2860.66	3563.33	818.048	1173.99	0	0	0	8465.82	8887.48	2891.8	0	3563.33	818.048	1173.99	919.613	0	0	0	55381.2237
t_{22}	8465.82	8887.48	0	2860.66	2407.36	0	1173.99	0	0	0	8465.82	8887.48	2891.8	0	0	818.048	1173.99	0	0	0	0	46032.4503
t_{23}	8465.82	6751.26	0	2860.66	0	0	0	0	0	0	8465.82	6751.26	2891.8	0	0	0	0	0	0	0	0	36186.6169
t_{24}	8465.82	6214.37	0	0	0	0	0	0	0	0	8465.82	6214.37	2891.8	0	0	0	0	0	0	0	0	32252.1839

Table 5.57: Committed Status for a 20-generating unit system using the LFAOA algorithm with (Thermal + Solar)																								
Units/Hour	**t_1**	**t_2**	**t_3**	**t_4**	**t_5**	**t_6**	**t_7**	**t_8**	**t_9**	**t_{10}**	**t_{11}**	**t_{12}**	**t_{13}**	**t_{14}**	**t_{15}**	**t_{16}**	**t_{17}**	**t_{18}**	**t_{19}**	**t_{20}**	**t_{21}**	**t_{22}**	**t_{23}**	**t_{24}**
U_1	1	1	1	1	1	1	1	1	1	1	1	1	1	1	1	1	1	1	1	1	1	1	1	0
U_2	1	1	1	1	1	1	1	1	1	1	1	1	1	1	1	1	1	1	1	1	1	1	1	1
U_3	1	1	1	1	1	1	1	1	1	1	1	1	1	1	1	1	1	1	1	1	1	1	1	1
U_4	0	0	0	0	0	0	0	1	1	1	1	1	1	1	0	0	0	0	0	1	1	1	1	1
U_5	0	0	0	1	1	1	1	1	1	1	1	1	0	0	0	0	0	0	0	0	0	0	0	1
U_6	0	0	0	0	0	0	0	0	0	0	0	0	0	0	0	0	0	0	0	1	1	1	0	0
U_7	0	0	0	0	0	0	0	0	0	0	0	0	0	0	0	0	0	0	0	0	0	0	0	0
U_8	0	0	0	0	0	0	0	0	0	0	0	0	0	0	0	0	0	0	0	0	0	0	0	0
U_9	0	0	0	0	0	0	0	0	0	0	0	0	0	0	0	0	0	0	0	0	0	0	0	0
U_{10}	0	0	0	0	0	0	0	0	0	0	0	0	0	0	0	0	0	0	0	0	0	0	0	0
U_{11}	1	1	1	1	1	1	1	1	1	1	1	1	1	1	1	1	1	1	1	1	1	1	1	1
U_{22}	0	0	0	0	0	0	0	0	0	1	1	1	1	1	1	1	1	1	1	1	0	0	0	0
U_{13}	0	0	0	0	1	1	1	1	1	1	1	1	1	1	1	1	1	1	1	1	1	0	0	0
U_{14}	0	0	0	0	0	0	0	0	1	1	1	1	1	0	0	0	0	0	0	0	0	0	0	0
U_{15}	0	0	1	1	1	1	1	1	1	1	1	1	1	0	0	0	0	0	0	1	1	1	1	1
U_{16}	0	0	0	0	0	0	0	0	0	0	0	0	0	0	0	0	0	0	0	0	0	0	0	0
U_{17}	0	0	0	0	0	0	0	0	0	0	0	0	0	0	0	0	0	0	0	0	0	0	0	0
U_{18}	0	0	0	0	0	0	0	0	0	0	0	0	0	0	0	0	0	0	0	0	0	0	0	0
U_{19}	0	0	0	0	0	0	0	0	0	0	0	0	0	0	0	0	0	0	0	0	0	0	0	0
U_{20}	0	0	0	0	0	0	0	0	0	0	0	0	0	0	0	0	0	0	0	0	0	0	0	0

Table 5.58: Scheduling for a 20-generating unit system using the LFAOA algorithm with (Thermal + Solar) system

Hours/ Units	P_1	P_2	P_3	P_4	P_5	P_6	P_7	P_8	P_9	P_{10}	P_{11}	P_{12}	P_{13}	P_{14}	P_{15}	P_{16}	P_{17}	P_{18}	P_{19}	P_{20}	Power Generated (MW)	SUC ($)	Hourly Cost ($)
t_1	455	245	245	0	0	0	0	0	0	0	455	0	0	0	0	0	0	0	0	0	1400	0	27366.26
t_2	455	295	295	0	0	0	0	0	0	0	455	0	0	0	0	0	0	0	0	0	1500	0	29109
t_3	455	382.5	382.5	0	0	0	0	0	0	0	455	0	0	0	25	0	0	0	0	0	1700	560	33111.241
t_4	455	455	455	0	40	0	0	0	0	0	455	0	0	0	40	0	0	0	0	0	1900	900	37195.336
t_5	455	346.66667	346.66667	0	25	0	0	0	0	0	455	0	346.66667	0	25	0	0	0	0	0	2000	560	39793.784
t_6	455	413.33333	413.33333	0	25	0	0	0	0	0	455	0	413.33333	0	25	0	0	0	0	0	2200	920	43292.904
t_7	455	446.66667	446.66667	0	25	0	0	0	0	0	455	0	446.66667	0	25	0	0	0	0	0	2300	0	45045.564
t_8	455	435.15	435.15	130	25	0	0	0	0	0	455	0	435.15	0	25	0	0	0	0	0	2395.45	5000	47300.446
t_9	455	454.77667	454.77667	130	25	0	0	0	0	0	455	0	454.77667	130	25	0	0	0	0	0	2584.33	1860	51193.617
t_{10}	455	388.165	388.165	130	25	0	0	0	0	0	455	388.165	388.165	130	25	0	0	0	0	0	2772.66	0	55408.682
t_{11}	455	410.7075	410.7075	130	25	0	0	0	0	0	455	410.7075	410.7075	130	25	0	0	0	0	0	2862.83	0	56987.347
t_{12}	455	433.485	433.485	130	25	0	0	0	0	0	455	433.485	433.485	130	25	0	0	0	0	0	2953.94	0	58583.749
t_{13}	455	388.285	388.285	130	0	0	0	0	0	0	455	388.285	388.285	130	25	0	0	0	0	0	2748.14	600	54472.095
t_{14}	455	376.3825	376.3825	130	0	0	0	0	0	0	455	376.3825	376.3825	0	0	0	0	0	0	0	2545.53	0	49833.414
t_{15}	455	361.3525	361.3525	0	0	0	0	0	0	0	455	361.3525	361.3525	0	0	0	0	0	0	0	2355.41	0	45921.334
t_{16}	455	285.285	285.285	0	0	0	0	0	0	0	455	285.285	285.285	0	0	0	0	0	0	0	2051.14	0	40608.641
t_{17}	455	263.04	263.04	0	0	0	0	0	0	0	455	263.04	263.04	0	0	0	0	0	0	0	1962.16	0	39057.721
t_{18}	455	314.1	314.1	0	0	0	0	0	0	0	455	314.1	314.1	0	0	0	0	0	0	0	2166.4	0	42619.445
t_{19}	455	367.6025	367.6025	0	0	0	0	0	0	0	455	367.6025	367.6025	0	0	0	0	0	0	0	2380.41	1980	46358.484
t_{20}	455	427.1225	427.1225	130	0	20	0	0	0	0	455	427.1225	427.1225	0	25	0	0	0	0	0	2793.49	0	55150.046
t_{21}	455	378.71	378.71	130	0	20	0	0	0	0	455	378.71	378.71	0	25	0	0	0	0	0	2599.84	770	51759.271
t_{22}	455	371.66667	371.66667	130	0	20	0	0	0	0	455	0	371.66667	0	25	0	0	0	0	0	2200	560	43838.657
t_{23}	455	367.5	367.5	130	0	0	0	0	0	0	455	0	0	0	25	0	0	0	0	0	1800	0	35447.125
t_{24}	0	455	455	130	52.5	0	0	0	0	0	455	0	0	0	52.5	0	0	0	0	0	1600	900	32091.876

Table 5.59: Individual fuel cost for 20 generating unit system using the LFAOA algorithm with Solar (Thermal +Solar)

Hours/ Units	P_1	P_2	P_3	P_4	P_5	P_6	P_7	P_8	P_9	P_{10}	P_{11}	P_{12}	P_{13}	P_{14}	P_{15}	P_{16}	P_{17}	P_{18}	P_{19}	P_{20}	SUC	Hourly Cost ($)
t_1	8465.822	5217.308	5217.308	0	0	0	0	0	0	0	8465.822	0	0	0	0	0	0	0	0	0	0	27366.2595
t_2	8465.822	6088.678	6088.678	0	0	0	0	0	0	0	8465.822	0	0	0	0	0	0	0	0	0	0	29108.9995
t_3	8465.822	7617.305	7617.305	0	0	0	0	0	0	0	8465.822	0	0	0	944.9875	0	0	0	0	0	560	33111.2414
t_4	8465.822	8887.478	8887.478	0	1244.368	0	0	0	0	0	8465.822	0	0	0	1244.368	0	0	0	0	0	900	37195.3355
t_5	8465.822	6990.722	6990.722	0	944.9875	0	0	0	0	0	8465.822	0	6990.72	0	944.9875	0	0	0	0	0	560	39793.7843
t_6	8465.822	8157.095	8157.095	0	944.9875	0	0	0	0	0	8465.822	0	8157.1	0	944.9875	0	0	0	0	0	920	43292.9043
t_7	8465.822	8741.315	8741.315	0	944.9875	0	0	0	0	0	8465.822	0	8741.32	0	944.9875	0	0	0	0	0	0	45045.5643
t_8	8465.822	8539.389	8539.389	2860.659	944.9875	0	0	0	0	0	8465.822	0	8539.39	0	944.9875	0	0	0	0	0	5000	47300.4456
t_9	8465.822	8883.56	8883.56	2860.659	944.9875	0	0	0	0	0	8465.822	0	8883.56	2860.659	944.9875	0	0	0	0	0	1860	51193.6171
t_{10}	8465.822	7716.436	7716.436	2860.659	944.9875	0	0	0	0	0	8465.822	7716.44	7716.44	2860.659	944.9875	0	0	0	0	0	0	55408.682
t_{11}	8465.822	8111.102	8111.102	2860.659	944.9875	0	0	0	0	0	8465.822	8111.1	8111.1	2860.659	944.9875	0	0	0	0	0	0	56987.3468
t_{12}	8465.822	8510.203	8510.203	2860.659	944.9875	0	0	0	0	0	8465.822	8510.2	8510.2	2860.659	944.9875	0	0	0	0	0	0	58583.7489
t_{13}	8465.822	7718.536	7718.536	2860.659	0	0	0	0	0	0	8465.822	7718.54	7718.54	2860.659	944.9875	0	0	0	0	0	600	54472.0948
t_{14}	8465.822	7510.278	7510.278	2860.659	0	0	0	0	0	0	8465.822	7510.28	7510.28	0	0	0	0	0	0	0	0	49833.4139
t_{15}	8465.822	7247.423	7247.423	0	0	0	0	0	0	0	8465.822	7247.42	7247.42	0	0	0	0	0	0	0	0	45921.3344
t_{16}	8465.822	5919.249	5919.249	0	0	0	0	0	0	0	8465.822	5919.25	5919.25	0	0	0	0	0	0	0	0	40608.6409
t_{17}	8465.822	5531.519	5531.519	0	0	0	0	0	0	0	8465.822	5531.52	5531.52	0	0	0	0	0	0	0	0	39057.7213
t_{18}	8465.822	6421.95	6421.95	0	0	0	0	0	0	0	8465.822	6421.95	6421.95	0	0	0	0	0	0	0	0	42619.4449
t_{19}	8465.822	7356.71	7356.71	0	0	0	0	0	0	0	8465.822	7356.71	7356.71	0	0	0	0	0	0	0	1980	46358.4838
t_{20}	8465.822	8398.689	8398.689	2860.659	0	818	0	0	0	0	8465.822	8398.69	8398.69	0	944.9875	0	0	0	0	0	0	55150.0456
t_{21}	8465.822	7550.995	7550.995	2860.659	0	818	0	0	0	0	8465.822	7551	7551	0	944.9875	0	0	0	0	0	770	51759.2713
t_{22}	8465.822	7427.789	7427.789	2860.659	0	818	0	0	0	0	8465.822	0	7427.79	0	944.9875	0	0	0	0	0	560	43838.6571
t_{23}	8465.822	7354.917	7354.917	2860.659	0	0	0	0	0	0	8465.822	0	0	0	944.9875	0	0	0	0	0	0	35447.1254
t_{24}	0	8887.478	8887.478	2860.659	1495.22	0	0	0	0	0	8465.822	0	0	0	1495.21988	0	0	0	0	0	900	32091.8763

Table 5.60: Committed status for a 20-generating unit system using the LFAOA algorithm with Wind (Thermal +Wind)																								
Units/Hour	**t_1**	**t_2**	**t_3**	**t_4**	**t_5**	**t_6**	**t_7**	**t_8**	**t_9**	**t_{10}**	**t_{11}**	**t_{12}**	**t_{13}**	**t_{14}**	**t_{15}**	**t_{16}**	**t_{17}**	**t_{18}**	**t_{19}**	**t_{20}**	**t_{21}**	**t_{22}**	**t_{23}**	**t_{24}**
U_1	1	1	1	1	1	1	1	1	1	1	1	1	1	1	1	1	1	1	1	1	1	1	1	1
U_2	1	1	1	1	1	1	1	1	1	1	1	1	1	1	1	1	1	1	1	1	1	1	1	1
U_3	0	0	0	0	0	0	0	0	1	1	1	1	1	1	1	1	1	1	1	1	1	1	0	0
U_4	0	0	0	0	0	0	1	1	1	1	1	1	1	1	1	1	1	1	1	1	1	1	0	0
U_5	0	0	0	0	1	1	1	1	1	1	1	1	1	1	1	1	1	1	1	1	0	0	0	0
U_6	0	0	0	0	0	0	0	0	1	1	1	1	1	1	0	0	0	0	1	1	1	0	0	0
U_7	0	0	0	0	0	0	0	0	0	1	1	1	1	0	0	0	0	0	0	0	0	0	0	0
U_8	0	0	0	0	0	0	0	0	0	0	1	1	0	0	0	0	0	0	0	0	0	0	0	0
U_9	0	0	0	0	0	0	0	0	0	0	0	1	0	0	0	0	0	0	0	1	0	0	0	0
U_{10}	0	0	0	0	0	0	0	0	0	0	0	0	0	0	0	0	0	0	0	0	0	0	0	0
U_{11}	1	1	1	1	1	1	1	1	1	1	1	1	1	1	1	1	1	1	1	1	1	1	1	1
U_{22}	1	1	1	1	1	1	1	1	1	1	1	1	1	1	1	1	1	1	1	1	1	1	1	1
U_{13}	0	0	0	0	0	0	0	1	1	1	1	1	1	1	1	1	1	1	1	1	0	0	0	0
U_{14}	0	0	0	1	1	1	1	1	1	1	1	1	1	1	1	1	1	1	1	1	1	0	0	0
U_{15}	0	0	0	0	0	1	1	1	1	1	1	1	1	1	1	1	1	1	1	1	0	0	0	0
U_{16}	0	0	0	0	0	0	0	0	0	1	1	1	1	0	0	0	0	0	0	1	1	1	0	0
U_{17}	0	0	0	0	0	0	0	0	0	1	1	1	1	0	0	0	0	0	0	1	1	1	0	0
U_{18}	0	0	0	0	0	0	0	0	0	0	1	1	0	0	0	0	0	0	0	0	0	0	0	0
U_{19}	0	0	0	0	0	0	0	0	0	0	0	1	0	0	0	0	0	0	0	0	0	0	0	0
U_{20}	0	0	0	0	0	0	0	0	0	0	0	0	0	0	0	0	0	0	0	0	0	0	0	0

Table 5.61: Scheduling for a 20-generating unit system using the LFAOA algorithm with (Thermal + Wind) system

Hours/ Units	P_1	P_2	P_3	P_4	P_5	P_6	P_7	P_8	P_9	P_{10}	P_{11}	P_{12}	P_{13}	P_{14}	P_{15}	P_{16}	P_{17}	P_{18}	P_{19}	P_{20}	Power Generated (MW)	SUC	Hourly Cost ($)
t_1	455	157	0	0	0	0	0	0	0	0	455	157	0	0	0	0	0	0	0	0	1223	0	24289.21
t_2	455	210	0	0	0	0	0	0	0	0	455	210	0	0	0	0	0	0	0	0	1329	560	26130.8
t_3	455	316	0	0	0	0	0	0	0	0	455	316	0	0	0	0	0	0	0	0	1542	0	29841.87
t_4	455	358	0	0	0	0	0	0	0	0	455	358	0	130	0	0	0	0	0	0	1755	2070	34152.44
t_5	455	396	0	0	25	0	0	0	0	0	455	396	0	130	0	0	0	0	0	0	1858	900	36461.94
t_6	455	455	0	0	56.5	0	0	0	0	0	455	455	0	130	56.5	0	0	0	0	0	2063	0	40718.77
t_7	455	455	0	130	50	0	0	0	0	0	455	455	0	130	50	0	0	0	0	0	2180	2020	43317.82
t_8	455	455	0	130	40.5	0	0	0	0	0	455	455	130	130	40.5	0	0	0	0	0	2291	0	45828.47
t_9	455	455	130	130	62	20	0	0	0	0	455	455	130	130	62	0	0	0	0	0	2484	0	50402.96
t_{10}	455	455	130	130	127	20	25	0	0	0	455	455	130	130	127	20	25	0	0	0	2684	860	56227.79
t_{11}	455	455	130	130	162	24.5	25	10	0	0	455	455	130	130	162	24.5	25	10	0	0	2783	120	59729.72
t_{12}	455	455	130	130	162	65.5	25	10	10	0	455	455	130	130	162	65.5	25	10	10	0	2885	120	63483.43
t_{13}	455	455	130	130	128	20	25	0	0	0	455	455	130	130	128	20	25	0	0	0	2686	0	56269.22
t_{14}	455	455	130	130	65.5	20	0	0	0	0	455	455	130	130	65.5	0	0	0	0	0	2491	0	50544.42
t_{15}	455	407	130	130	25	0	0	0	0	0	455	407	130	130	25	0	0	0	0	0	2293	60	46401.37
t_{16}	455	254	130	130	25	0	0	0	0	0	455	254	130	130	25	0	0	0	0	0	1989	0	41092.03
t_{17}	455	209	130	130	25	0	0	0	0	0	455	209	130	130	25	0	0	0	0	0	1897	60	39490.91
t_{18}	455	315	130	130	25	0	0	0	0	0	455	315	130	130	25	0	0	0	0	0	2109.5	0	43193.13
t_{19}	455	400	130	130	25	20	0	0	0	0	455	400	130	130	25	0	0	0	0	0	2300.4	60	46998.79
t_{20}	455	455	130	130	132	20	0	0	10	0	455	455	130	130	132	20	25	0	0	0	2680	1090	56219.78
t_{21}	455	455	130	130	0	20	0	0	0	0	455	455	130	130	68	20	25	0	0	0	2473	0	50829.61
t_{22}	455	359	130	130	0	0	0	0	0	0	455	359	0	130	0	20	25	0	0	0	2063	0	41949.39
t_{23}	455	365	0	0	0	0	0	0	0	0	455	365	0	0	0	0	0	0	0	0	1640	0	31554.04
t_{24}	455	258	0	0	0	0	0	0	0	0	455	258	0	0	0	0	0	0	0	0	1425	0	27801.65

Table 5.62: Individual fuel cost for 20 generating unit system using the LFAOA algorithm with Wind (Thermal +Wind) system

Hours/ Units	P_1	P_2	P_3	P_4	P_5	P_6	P_7	P_8	P_9	P_{10}	P_{11}	P_{12}	P_{13}	P_{14}	P_{15}	P_{16}	P_{17}	P_{18}	P_{19}	P_{20}	SUC	Hourly Cost ($)
t_1	8465.8	3678.8	0	0	0	0	0	0	0	0	8465.8	3678.8	0	0	0	0	0	0	0	0	0	24289
t_2	8465.8	4599.6	0	0	0	0	0	0	0	0	8465.8	4599.6	0	0	0	0	0	0	0	0	560	26131
t_3	8465.8	6455.1	0	0	0	0	0	0	0	0	8465.8	6455.1	0	0	0	0	0	0	0	0	0	29842
t_4	8465.8	7180.1	0	0	0	0	0	0	0	0	8465.8	7180.1	0	2860.7	0	0	0	0	0	0	2070	34152
t_5	8465.8	7862.3	0	0	944.99	0	0	0	0	0	8465.8	7862.3	0	2860.7	0	0	0	0	0	0	900	36462
t_6	8465.8	8887.5	0	0	1575.8	0	0	0	0	0	8465.8	8887.5	0	2860.7	1575.8	0	0	0	0	0	0	40719
t_7	8465.8	8887.5	0	2860.7	1445	0	0	0	0	0	8465.8	8887.5	0	2860.7	1445	0	0	0	0	0	2020	43318
t_8	8465.8	8887.5	0	2860.7	1254.4	0	0	0	0	0	8465.8	8887.5	2891.8	2860.7	1254.4	0	0	0	0	0	0	45828
t_9	8465.8	8887.5	2891.8	2860.7	1686.7	818.05	0	0	0	0	8465.8	8887.5	2891.8	2860.7	1686.7	0	0	0	0	0	0	50403
t_{10}	8465.8	8887.5	2891.8	2860.7	3016.1	818.05	1174	0	0	0	8465.8	8887.5	2891.8	2860.7	3016.1	818.05	1174	0	0	0	860	56228
t_{11}	8465.8	8887.5	2891.8	2860.7	3745.9	919.64	1174	919.61	0	0	8465.8	8887.5	2891.8	2860.7	3745.9	919.64	1174	919.61	0	0	120	59730
t_{12}	8465.8	8887.5	2891.8	2860.7	3745.9	1858.6	1174	919.61	937.92	0	8465.8	8887.5	2891.8	2860.7	3745.9	1858.6	1174	919.61	937.92	0	120	63483
t_{13}	8465.8	8887.5	2891.8	2860.7	3036.8	818.05	1174	0	0	0	8465.8	8887.5	2891.8	2860.7	3036.8	818.05	1174	0	0	0	0	56269
t_{14}	8465.8	8887.5	2891.8	2860.7	1757.4	818.05	0	0	0	0	8465.8	8887.5	2891.8	2860.7	1757.4	0	0	0	0	0	0	50544
t_{15}	8465.8	8037.4	2891.8	2860.7	944.99	0	0	0	0	0	8465.8	8037.4	2891.8	2860.7	944.99	0	0	0	0	0	60	46401
t_{16}	8465.8	5382.7	2891.8	2860.7	944.99	0	0	0	0	0	8465.8	5382.7	2891.8	2860.7	944.99	0	0	0	0	0	0	41092
t_{17}	8465.8	4582.2	2891.8	2860.7	944.99	0	0	0	0	0	8465.8	4582.2	2891.8	2860.7	944.99	0	0	0	0	0	60	39491
t_{18}	8465.8	6433.3	2891.8	2860.7	944.99	0	0	0	0	0	8465.8	6433.3	2891.8	2860.7	944.99	0	0	0	0	0	0	43193
t_{19}	8465.8	7927.1	2891.8	2860.7	944.99	818.05	0	0	0	0	8465.8	7927.1	2891.8	2860.7	944.99	0	0	0	0	0	60	46999
t_{20}	8465.8	8887.5	2891.8	2860.7	3130.1	818.05	0	0	937.92	0	8465.8	8887.5	2891.8	2860.7	3130.1	818.05	1174	0	0	0	1090	56220
t_{21}	8465.8	8887.5	2891.8	2860.7	0	818.05	0	0	0	0	8465.8	8887.5	2891.8	2860.7	1808	818.05	1174	0	0	0	0	50830
t_{22}	8465.8	7206.3	2891.8	2860.7	0	0	0	0	0	0	8465.8	7206.3	0	2860.7	0	818.05	1174	0	0	0	0	41949
t_{23}	8465.8	7311.2	0	0	0	0	0	0	0	0	8465.8	7311.2	0	0	0	0	0	0	0	0	0	31554
t_{24}	8465.8	5435	0	0	0	0	0	0	0	0	8465.8	5435	0	0	0	0	0	0	0	0	0	27802

Table 5.63: Committed status for a 20-generating unit system using the LFAOA algorithm with solar and PEVs (Thermal +Solar + PEVs) system																								
Hours/ Units	**t_1**	**t_2**	**t_3**	**t_4**	**t_5**	**t_6**	**t_7**	**t_8**	**t_9**	**t_{10}**	**t_{11}**	**t_{12}**	**t_{13}**	**t_{14}**	**t_{15}**	**t_{16}**	**t_{17}**	**t_{18}**	**t_{19}**	**t_{20}**	**t_{21}**	**t_{22}**	**t_{23}**	**t_{24}**
U_1	1	1	1	1	1	1	1	1	1	1	1	1	1	1	1	1	1	1	1	1	1	1	1	1
U_2	1	0	0	0	0	0	0	0	1	1	1	1	1	1	1	1	1	1	1	1	1	0	0	0
U_3	0	0	0	0	0	1	1	1	1	1	0	0	0	0	0	0	0	0	0	0	0	0	0	0
U_4	0	0	1	1	1	1	1	1	0	0	0	0	0	0	0	0	0	0	0	0	1	1	1	1
U_5	0	0	0	0	0	0	0	1	1	1	1	1	1	0	0	0	0	0	0	0	0	0	0	0
U_6	0	0	0	0	0	0	0	0	0	0	0	1	1	1	0	0	0	0	0	0	0	0	0	0
U_7	0	0	0	0	0	0	0	0	0	0	0	0	0	0	0	0	0	0	0	0	0	0	0	0
U_8	0	0	0	0	0	0	0	0	0	0	0	0	0	0	0	0	0	0	0	0	0	0	0	0
U_9	0	0	0	0	0	0	0	0	0	0	0	0	0	0	0	0	0	0	0	0	0	0	0	0
U_{10}	0	0	0	0	0	0	0	0	0	0	0	0	0	0	0	0	0	0	0	0	0	0	0	0
U_{11}	1	1	1	1	1	1	1	1	1	1	1	1	1	1	1	1	1	1	1	1	0	0	0	0
U_{22}	0	0	0	0	0	0	0	0	0	0	0	0	0	0	0	0	0	0	0	1	1	1	1	1
U_{13}	0	0	0	0	0	0	0	0	0	0	0	0	0	0	0	0	0	0	0	0	0	0	0	0
U_{14}	0	0	0	1	1	1	1	1	0	0	0	0	0	0	0	0	0	0	0	0	0	1	1	1
U_{15}	0	0	0	0	0	0	0	0	0	0	0	0	0	0	0	0	0	0	0	0	0	0	0	0
U_{16}	0	0	0	0	0	0	0	0	0	0	0	0	0	0	0	0	0	0	0	0	0	0	0	0
U_{17}	0	0	0	0	0	0	0	0	0	0	0	0	0	0	0	0	0	0	0	0	0	0	0	0
U_{18}	0	0	0	0	0	0	0	0	0	0	0	0	0	0	0	0	0	0	0	0	0	0	0	0
U_{19}	0	0	0	0	0	0	0	0	0	0	0	0	0	0	0	0	0	0	0	0	0	0	0	0
U_{20}	0	0	0	0	0	0	0	0	0	0	0	0	0	0	0	0	0	0	0	0	0	0	0	0

Table 5.64: Scheduling for a 20-generating unit system using the LFAOA algorithm with (Thermal+ Solar + PEVs) system

Hours/ Units	P_1	P_2	P_3	P_4	P_5	P_6	P_7	P_8	P_9	P_{10}	P_{11}	P_{12}	P_{13}	P_{14}	P_{15}	P_{16}	P_{17}	P_{18}	P_{19}	P_{20}	Power Generated (MW)	SUC	Hourly Cost ($)
t_1	366.2	0	0	0	0	0	0	0	0	0	366.2	0	0	0	0	0	0	0	0	0	732.4	0	13986.29
t_2	385.8	0	0	0	0	0	0	0	0	0	385.8	0	0	0	0	0	0	0	0	0	771.5	0	14633.44
t_3	424.1	0	0	23.02	0	0	0	0	0	0	424.1	0	0	0	0	0	0	0	0	0	871.24	560	16966.3
t_4	455	0	0	41.18	0	0	0	0	0	0	455	0	0	41.18	0	0	0	0	0	0	992.35	560	19657.57
t_5	455	0	0	56.5	0	0	0	0	0	0	455	0	0	56.5	0	0	0	0	0	0	1022.99	0	20169.45
t_6	455	0	62.8	83.22	0	0	0	0	0	0	455	0	0	83.22	0	0	0	0	0	0	1139.24	4620	22817.5
t_7	455	0	71.19	91.18	0	0	0	0	0	0	455	0	0	91.18	0	0	0	0	0	0	1163.54	0	23227.39
t_8	455	0	74.84	94.64	25	0	0	0	0	0	455	0	0	94.64	0	0	0	0	0	0	1199.12	1100	24351.09
t_9	455	172.6	130	0	25	0	0	0	0	0	455	0	0	0	0	0	0	0	0	0	1237.57	0	24726.22
t_{10}	455	262.2	130	0	25	0	0	0	0	0	455	0	0	0	0	0	0	0	0	0	1327.18	5000	26284.97
t_{11}	455	444.6	0	0	25	0	0	0	0	0	455	0	0	0	0	0	0	0	0	0	1379.6	0	26581.7
t_{12}	455	450.2	0	0	25	20	0	0	0	0	455	0	0	0	0	0	0	0	0	0	1405.21	5000	27498.14
t_{13}	455	346.4	0	0	25	20	0	0	0	0	455	0	0	0	0	0	0	0	0	0	1301.41	0	25680.92
t_{14}	455	313.1	0	0	0	20	0	0	0	0	455	0	0	0	0	0	0	0	0	0	1243.06	0	24153.49
t_{15}	455	274.4	0	0	0	0	0	0	0	0	455	0	0	0	0	0	0	0	0	0	1184.43	0	22661.65
t_{16}	429	150	0	0	0	0	0	0	0	0	429	0	0	0	0	0	0	0	0	0	1007.95	0	19632.84
t_{17}	423.5	150	0	0	0	0	0	0	0	0	423.5	0	0	0	0	0	0	0	0	0	996.96	0	19450.42
t_{18}	455	197	0	0	0	0	0	0	0	0	455	0	0	0	0	0	0	0	0	0	1106.96	0	21313.2
t_{19}	455	311.6	0	0	0	0	0	0	0	0	455	0	0	0	0	0	0	0	0	0	1221.62	0	23310.31
t_{20}	455	218.3	0	0	0	0	0	0	0	0	455	218.3	0	0	0	0	0	0	0	0	1346.53	1120	26435.69
t_{21}	455	349.1	0	130	0	0	0	0	0	0	0	349.1	0	0	0	0	0	0	0	0	1283.26	0	25394.02
t_{22}	455	0	0	130	0	0	0	0	0	0	0	337.6	0	130	0	0	0	0	0	0	1052.56	1120	21018.75
t_{23}	455	0	0	129.5	0	0	0	0	0	0	0	150	0	129.5	0	0	0	0	0	0	864.08	1650	17737.43
t_{24}	455	0	0	75.3	0	0	0	0	0	0	0	150	0	75.29	0	0	0	0	0	0	755.59	2480	15900.46

Table 5.65: Individual fuel cost for 20 generating Unit system using the LFAOA algorithm with (Thermal + Solar + PEVs) system

Hours/ Units	P_1	P_2	P_3	P_4	P_5	P_6	P_7	P_8	P_9	P_{10}	P_{11}	P_{12}	P_{13}	P_{14}	P_{15}	P_{16}	P_{17}	P_{18}	P_{19}	P_{20}	SUC	Hourly Cost ($)
t_1	6993.1	0	0	0	0	0	0	0	0	0	6993.147	0	0	0	0	0	0	0	0	0	0	13986.29
t_2	7316.7	0	0	0	0	0	0	0	0	0	7316.718	0	0	0	0	0	0	0	0	0	0	14633.44
t_3	7952.7	0	0	1061	0	0	0	0	0	0	7952.676	0	0	0	0	0	0	0	0	0	560	16966.3
t_4	8465.8	0	0	1363	0	0	0	0	0	0	8465.822	0	0	1362.965	0	0	0	0	0	0	560	19657.57
t_5	8465.8	0	0	1618.9	0	0	0	0	0	0	8465.822	0	0	1618.902	0	0	0	0	0	0	0	20169.45
t_6	8465.8	0	1750.3	2067.8	0	0	0	0	0	0	8465.822	0	0	2067.759	0	0	0	0	0	0	4620	22817.5
t_7	8465.8	0	1891.9	2201.9	0	0	0	0	0	0	8465.822	0	0	2201.93	0	0	0	0	0	0	0	23227.39
t_8	8465.8	0	1953.6	2260.4	944.99	0	0	0	0	0	8465.822	0	0	2260.43	0	0	0	0	0	0	1100	24351.09
t_9	8465.8	3957.8	2891.8	0	944.99	0	0	0	0	0	8465.822	0	0	0	0	0	0	0	0	0	0	24726.22
t_{10}	8465.8	5516.5	2891.8	0	944.99	0	0	0	0	0	8465.822	0	0	0	0	0	0	0	0	0	5000	26284.97
t_{11}	8465.8	8705.1	0	0	944.99	0	0	0	0	0	8465.822	0	0	0	0	0	0	0	0	0	0	26581.7
t_{12}	8465.8	8803.5	0	0	944.99	818.05	0	0	0	0	8465.822	0	0	0	0	0	0	0	0	0	5000	27498.14
t_{13}	8465.8	6986.2	0	0	944.99	818.05	0	0	0	0	8465.822	0	0	0	0	0	0	0	0	0	0	25680.92
t_{14}	8465.8	6403.8	0	0	0	818.05	0	0	0	0	8465.822	0	0	0	0	0	0	0	0	0	0	24153.49
t_{15}	8465.8	5730	0	0	0	0	0	0	0	0	8465.822	0	0	0	0	0	0	0	0	0	0	22661.65
t_{16}	8033.4	3566	0	0	0	0	0	0	0	0	8033.435	0	0	0	0	0	0	0	0	0	0	19632.84
t_{17}	7942.2	3566	0	0	0	0	0	0	0	0	7942.222	0	0	0	0	0	0	0	0	0	0	19450.42
t_{18}	8465.8	4381.6	0	0	0	0	0	0	0	0	8465.822	0	0	0	0	0	0	0	0	0	0	21313.2
t_{19}	8465.8	6378.7	0	0	0	0	0	0	0	0	8465.822	0	0	0	0	0	0	0	0	0	0	23310.31
t_{20}	8465.8	4752	0	0	0	0	0	0	0	0	8465.822	4752.022	0	0	0	0	0	0	0	0	1120	26435.69
t_{21}	8465.8	7033.8	0	2860.7	0	0	0	0	0	0	0	7033.77	0	0	0	0	0	0	0	0	0	25394.02
t_{22}	8465.8	0	0	2860.7	0	0	0	0	0	0	0	6831.609	0	2860.659	0	0	0	0	0	0	1120	21018.75
t_{23}	8465.8	0	0	2852.8	0	0	0	0	0	0	0	3565.975	0	2852.817	0	0	0	0	0	0	1650	17737.43
t_{24}	8465.8	0	0	1934.3	0	0	0	0	0	0	0	3565.975	0	1934.33	0	0	0	0	0	0	2480	15900.46

Table 5.66: Committed status for a 20-generating unit system using the LFAOA algorithm with Wind and PEVs (Thermal + Wind +PEVs) system

Hours/ Units	U_1	U_2	U_3	U_4	U_5	U_6	U_7	U_8	U_9	U_{10}	U_{11}	U_{12}	U_{13}	U_{14}	U_{15}	U_{16}	U_{17}	U_{18}	U_{19}	U_{20}
t_1	1	1	0	0	0	0	0	0	0	0	1	1	0	0	0	0	0	0	0	0
t_2	1	1	0	0	0	0	0	0	0	0	1	1	0	0	0	0	0	0	0	0
t_3	1	1	0	0	0	0	0	0	0	0	1	1	0	0	0	0	0	0	0	0
t_4	1	1	0	0	0	0	0	0	0	0	1	1	0	1	0	0	0	0	0	0
t_5	1	1	0	0	0	0	0	0	0	0	1	1	0	1	1	0	0	0	0	0
t_6	1	1	0	1	0	0	0	0	0	0	1	1	1	1	1	0	0	0	0	0
t_7	1	1	1	1	0	0	0	0	0	0	1	1	1	1	1	0	0	0	0	0
t_8	1	1	1	1	1	0	0	0	0	0	1	1	1	1	1	0	0	0	0	0
t_9	1	1	1	1	1	1	0	0	0	0	1	1	1	1	1	0	0	0	0	0
t_{10}	1	1	1	1	1	1	1	0	0	0	1	1	1	1	1	1	1	0	0	0
t_{11}	1	1	1	1	1	1	1	1	0	0	1	1	1	1	1	1	1	1	0	0
t_{12}	1	1	1	1	1	1	1	1	1	0	1	1	1	1	1	1	1	1	1	0
t_{13}	1	1	1	1	1	1	1	0	0	0	1	1	1	1	1	1	1	0	0	0
t_{14}	1	1	1	1	1	1	0	0	0	0	1	1	1	1	1	0	0	0	0	0
t_{15}	1	1	1	1	1	1	0	0	0	0	1	1	0	1	1	0	0	0	0	0
t_{16}	1	1	1	1	1	1	0	0	0	0	1	1	0	1	1	0	0	0	0	0
t_{17}	1	1	1	1	1	1	0	0	0	0	1	1	0	1	1	0	0	0	0	0
t_{18}	1	1	1	1	1	1	0	0	0	0	1	1	0	1	1	0	0	0	0	0
t_{19}	1	1	1	1	1	1	1	0	0	0	1	1	0	1	1	0	0	0	0	0
t_{20}	1	1	1	1	1	1	1	1	0	0	1	1	1	1	1	1	0	0	0	0
t_{21}	1	1	1	1	1	0	1	0	0	0	1	1	1	1	1	1	0	0	0	0
t_{22}	1	1	0	1	0	0	0	0	0	0	1	1	1	1	0	1	0	0	0	0
t_{23}	1	1	0	0	0	0	0	0	0	0	1	1	1	0	0	0	0	0	0	0
t_{24}	1	1	0	0	0	1	0	0	0	0	1	0	1	0	0	0	0	0	0	0

Table 5.67: Scheduling for a 20-generating unit system using the LFAOA algorithm with (Thermal+ Wind + PEVs) system

Hours / Units	P_1	P_2	P_3	P_4	P_5	P_6	P_7	P_8	P_9	P_{10}	P_{11}	P_{12}	P_{13}	P_{14}	P_{15}	P_{16}	P_{17}	P_{18}	P_{19}	P_{20}	Power Generated (MW)	SUC	Hourly Cost ($)
t_1	455	157	0	0	0	0	0	0	0	0	455	156.5	0	0	0	0	0	0	0	0	1223	0	24289.21
t_2	455	210	0	0	0	0	0	0	0	0	455	209.5	0	0	0	0	0	0	0	0	1329	430	26130.8
t_3	455	316	0	0	0	0	0	0	0	0	455	316	0	0	0	0	0	0	0	0	1542	1460	29841.87
t_4	455	358	0	0	0	0	0	0	0	0	455	357.5	0	130	0	0	0	0	0	0	1755	560	34152.44
t_5	455	396	0	0	0	0	0	0	0	0	455	396.5	0	130	25	0	0	0	0	0	1858	1450	36461.94
t_6	455	369	0	130	0	0	0	0	0	0	455	369	130	130	25	0	0	0	0	0	2063	0	41252.05
t_7	455	363	130	130	0	0	0	0	0	0	455	362.5	130	130	25	0	0	0	0	0	2180	0	43916.52
t_8	455	406	130	130	25	0	0	0	0	0	455	405.5	130	130	25	0	0	0	0	0	2291	1100	46366.34
t_9	455	455	130	130	62	20	0	0	0	0	455	455	130	130	62	0	0	0	0	0	2484	170	50402.96
t_{10}	455	455	130	130	127	20	25	0	0	0	455	455	130	130	127	20	25	0	0	0	2684	1120	56227.79
t_{11}	455	455	130	130	162	24.5	25	10	0	0	455	455	130	130	162	24.5	25	10	0	0	2783	120	59729.72
t_{12}	455	455	130	130	162	65.5	25	10	10	0	455	455	130	130	162	65.5	25	10	10	0	2885	120	63483.43
t_{13}	455	455	130	130	128	20	25	0	0	0	455	455	130	130	128	20	25	0	0	0	2686	0	56269.22
t_{14}	455	455	130	130	65.5	20	0	0	0	0	455	455	130	130	65.5	0	0	0	0	0	2491	0	50544.42
t_{15}	455	455	130	130	41.5	0	0	0	0	0	455	455	0	130	41.5	0	0	0	0	0	2293	60	45868.53
t_{16}	455	320	130	130	25	0	0	0	0	0	455	319.5	0	130	25	0	0	0	0	0	1989	0	40467.17
t_{17}	455	274	130	130	25	0	0	0	0	0	455	273.5	0	130	25	0	0	0	0	0	1897	0	38862.33
t_{18}	455	370	130	130	25	20	0	0	0	0	455	369.8	0	130	25	0	0	0	0	0	2109.5	0	43041.32
t_{19}	455	453	130	130	25	20	25	0	0	0	455	452.7	0	130	25	0	0	0	0	0	2300.4	400	47121.04
t_{20}	455	455	130	130	132.5	20	25	10	0	0	455	455	130	130	132.5	20	0	0	0	0	2680	580	56201.47
t_{21}	455	455	130	130	44	0	25	0	0	0	455	455	130	130	44	20	0	0	0	0	2473	0	50852.57
t_{22}	455	372	0	130	0	0	0	0	0	0	455	371.5	130	130	0	20	0	0	0	0	2063	0	41212.56
t_{23}	455	300	0	0	0	0	0	0	0	0	455	300	130	0	0	0	0	0	0	0	1640	0	32175.24
t_{24}	455	365	0	0	0	20	0	0	0	0	455	0	130	0	0	0	0	0	0	0	1425	0	27952.69

Table 5.68: Individual fuel cost for 20 generating unit system using the LFAOA algorithm with Wind and PEVs (Thermal + Wind + PEVs) system

Hours/ Units	P_1	P_2	P_3	P_4	P_5	P_6	P_7	P_8	P_9	P_{10}	P_{11}	P_{12}	P_{13}	P_{14}	P_{15}	P_{16}	P_{17}	P_{18}	P_{19}	P_{20}	SUC	Hourly Cost ($)
t_1	8465.8	3678.78	0	0	0	0	0	0	0	0	8465.822	3678.783	0	0	0	0	0	0	0	0	0	24289.21
t_2	8465.8	4599.58	0	0	0	0	0	0	0	0	8465.822	4599.576	0	0	0	0	0	0	0	0	430	26130.8
t_3	8465.8	6455.12	0	0	0	0	0	0	0	0	8465.822	6455.115	0	0	0	0	0	0	0	0	1460	29841.87
t_4	8465.8	7180.07	0	0	0	0	0	0	0	0	8465.822	7180.07	0	2860.659	0	0	0	0	0	0	560	34152.44
t_5	8465.8	7862.33	0	0	0	0	0	0	0	0	8465.822	7862.326	0	2860.659	944.988	0	0	0	0	0	1450	36461.94
t_6	8465.8	7381.15	0	2860.7	0	0	0	0	0	0	8465.822	7381.15	2891.8	2860.659	944.988	0	0	0	0	0	0	41252.05
t_7	8465.8	7267.49	2891.8	2860.7	0	0	0	0	0	0	8465.822	7267.486	2891.8	2860.659	944.988	0	0	0	0	0	0	43916.52
t_8	8465.8	8019.9	2891.8	2860.7	944.99	0	0	0	0	0	8465.822	8019.903	2891.8	2860.659	944.988	0	0	0	0	0	1100	46366.34
t_9	8465.8	8887.48	2891.8	2860.7	1686.7	818.05	0	0	0	0	8465.822	8887.478	2891.8	2860.659	1686.7	0	0	0	0	0	170	50402.96
t_{10}	8465.8	8887.48	2891.8	2860.7	3016.1	818.05	1174	0	0	0	8465.822	8887.478	2891.8	2860.659	3016.09	818.05	1174	0	0	0	1120	56227.79
t_{11}	8465.8	8887.48	2891.8	2860.7	3745.9	919.64	1174	919.61	0	0	8465.822	8887.478	2891.8	2860.659	3745.85	919.64	1174	919.61	0	0	120	59729.72
t_{12}	8465.8	8887.48	2891.8	2860.7	3745.9	1858.6	1174	919.61	937.9	0	8465.822	8887.478	2891.8	2860.659	3745.85	1858.6	1174	919.61	937.92	0	120	63483.43
t_{13}	8465.8	8887.48	2891.8	2860.7	3036.8	818.05	1174	0	0	0	8465.822	8887.478	2891.8	2860.659	3036.81	818.05	1174	0	0	0	0	56269.22
t_{14}	8465.8	8887.48	2891.8	2860.7	1757.4	818.05	0	0	0	0	8465.822	8887.478	2891.8	2860.659	1757.43	0	0	0	0	0	0	50544.42
t_{15}	8465.8	8887.48	2891.8	2860.7	1274.4	0	0	0	0	0	8465.822	8887.478	0	2860.659	1274.4	0	0	0	0	0	60	45868.53
t_{16}	8465.8	6516.21	2891.8	2860.7	944.99	0	0	0	0	0	8465.822	6516.215	0	2860.659	944.988	0	0	0	0	0	0	40467.17
t_{17}	8465.8	5713.8	2891.8	2860.7	944.99	0	0	0	0	0	8465.822	5713.799	0	2860.659	944.988	0	0	0	0	0	0	38862.33
t_{18}	8465.8	7394.27	2891.8	2860.7	944.99	818.05	0	0	0	0	8465.822	7394.267	0	2860.659	944.988	0	0	0	0	0	0	43041.32
t_{19}	8465.8	8847.13	2891.8	2860.7	944.99	818.05	1174	0	0	0	8465.822	8847.133	0	2860.659	944.988	0	0	0	0	0	400	47121.04
t_{20}	8465.8	8887.48	2891.8	2860.7	3130.1	818.05	1174	919.61	0	0	8465.822	8887.478	2891.8	2860.659	3130.12	818.05	0	0	0	0	580	56201.47
t_{21}	8465.8	8887.48	2891.8	2860.7	1324.5	0	1174	0	0	0	8465.822	8887.478	2891.8	2860.659	1324.51	818.05	0	0	0	0	0	50852.57
t_{22}	8465.8	7424.87	0	2860.7	0	0	0	0	0	0	8465.822	7424.874	2891.8	2860.659	0	818.05	0	0	0	0	0	41212.56
t_{23}	8465.8	6175.9	0	0	0	0	0	0	0	0	8465.822	6175.9	2891.8	0	0	0	0	0	0	0	0	32175.24
t_{24}	8465.8	7311.2	0	0	0	818.05	0	0	0	0	8465.822	0	2891.8	0	0	0	0	0	0	0	0	27952.69

Table 5.69: Committed status for a 20-generating unit using the LFAOA algorithm with Solar, Wind, and PEVs (Thermal + Solar + PEVs) system

Hours/Units	U_1	U_2	U_3	U_4	U_5	U_6	U_7	U_8	U_9	U_{10}	U_{11}	U_{12}	U_{13}	U_{14}	U_{15}	U_{16}	U_{17}	U_{18}	U_{19}	U_{20}
t_1	1	0	0	0	0	0	0	0	0	0	1	0	0	0	0	0	0	0	0	0
t_2	1	0	0	0	0	0	0	0	0	0	1	0	0	0	0	0	0	0	0	0
t_3	1	0	0	1	0	0	0	0	0	0	1	0	0	0	0	0	0	0	0	0
t_4	1	0	0	1	0	0	0	0	0	0	1	0	0	1	0	0	0	0	0	0
t_5	1	0	0	1	0	0	0	0	0	0	1	0	0	1	0	0	0	0	0	0
t_6	1	0	1	1	0	0	0	0	0	0	1	0	0	1	0	0	0	0	0	0
t_7	1	0	1	1	0	0	0	0	0	0	1	0	0	1	0	0	0	0	0	0
t_8	1	0	1	0	1	0	0	0	0	0	1	0	0	1	0	0	0	0	0	0
t_9	1	1	1	0	1	0	0	0	0	0	1	0	0	0	0	0	0	0	0	0
t_{10}	1	1	1	0	1	0	0	0	0	0	0	1	0	0	0	0	0	0	0	0
t_{11}	1	1	0	0	1	0	0	0	0	0	0	1	0	0	0	0	0	0	0	0
t_{12}	1	1	0	0	1	0	0	0	0	0	0	1	1	0	0	0	0	0	0	0
t_{13}	1	1	0	0	1	0	0	0	0	0	0	1	1	0	0	0	0	0	0	0
t_{14}	1	1	0	0	0	0	0	0	0	0	0	1	1	0	0	0	0	0	0	0
t_{15}	1	1	0	0	0	0	0	0	0	0	0	1	1	0	0	0	0	0	0	0
t_{16}	1	1	0	0	0	0	0	0	0	0	0	1	1	0	0	0	0	0	0	0
t_{17}	1	1	0	0	0	0	0	0	0	0	0	1	0	0	0	0	0	0	0	0
t_{18}	1	1	0	0	0	0	0	0	0	0	1	0	0	0	0	0	0	0	0	0
t_{19}	1	1	0	0	0	0	0	0	0	0	1	0	0	0	0	0	0	0	0	0
t_{20}	1	1	0	0	1	0	0	0	0	0	1	0	0	0	0	0	0	0	0	0
t_{21}	1	1	0	0	1	0	0	0	0	0	1	0	0	0	0	0	0	0	0	0
t_{22}	1	1	0	0	1	0	0	0	0	0	1	0	0	0	0	0	0	0	0	0
t_{23}	1	0	0	0	1	0	0	0	0	0	1	0	0	0	0	0	0	0	0	0
t_{24}	1	0	0	0	1	0	0	0	0	0	1	0	0	0	0	0	0	0	0	0

Table 5.70: Scheduling for a 20-generating unit system using the LFAOA algorithm with (Thermal + Solar + Wind + PEVs) system

Hours/Units	P_1	P_2	P_3	P_4	P_5	P_6	P_7	P_8	P_9	P_{10}	P_{11}	P_{12}	P_{13}	P_{14}	P_{15}	P_{16}	P_{17}	P_{18}	P_{19}	P_{20}	Power Generated (MW)	SUC ($)	Hourly Cost ($)
t_1	366.2	0	0	0	0	0	0	0	0	0	366.2	0	0	0	0	0	0	0	0	0	732.4	0	13986.29
t_2	385.8	0	0	0	0	0	0	0	0	0	385.8	0	0	0	0	0	0	0	0	0	771.5	1690	14633.44
t_3	424.1	0	0	23.02	0	0	0	0	0	0	424.1	0	0	0	0	0	0	0	0	0	871.24	1450	16966.3
t_4	455	0	0	41.18	0	0	0	0	0	0	455	0	0	41.18	0	0	0	0	0	0	992.35	560	19657.57
t_5	455	0	0	56.5	0	0	0	0	0	0	455	0	0	56.5	0	0	0	0	0	0	1022.99	0	20169.45
t_6	455	0	62.8	83.22	0	0	0	0	0	0	455	0	0	83.22	0	0	0	0	0	0	1139.24	1100	22817.5
t_7	455	0	71.19	91.18	0	0	0	0	0	0	455	0	0	91.18	0	0	0	0	0	0	1163.54	860	23227.39
t_8	455	0	130	0	29.12	0	0	0	0	0	455	0	0	130	0	0	0	0	0	0	1199.12	230	23711.14
t_9	455	172.6	130	0	25	0	0	0	0	0	455	0	0	0	0	0	0	0	0	0	1237.57	0	24726.22
t_{10}	455	358.6	130	0	25	0	0	0	0	0	0	358.6	0	0	0	0	0	0	0	0	1327.18	5000	26700.86
t_{11}	455	449.8	0	0	25	0	0	0	0	0	0	449.8	0	0	0	0	0	0	0	0	1379.6	5000	27003.34
t_{12}	455	397.6	0	0	25	0	0	0	0	0	0	397.6	130	0	0	0	0	0	0	0	1405.21	0	28065.95
t_{13}	455	345.7	0	0	25	0	0	0	0	0	0	345.7	130	0	0	0	0	0	0	0	1301.41	0	26250.44
t_{14}	455	329	0	0	0	0	0	0	0	0	0	329	130	0	0	0	0	0	0	0	1243.06	0	24722.86
t_{15}	455	299.7	0	0	0	0	0	0	0	0	0	299.7	130	0	0	0	0	0	0	0	1184.43	2570	23699.48
t_{16}	455	211.5	0	0	0	0	0	0	0	0	0	211.5	130	0	0	0	0	0	0	0	1007.95	0	20625.47
t_{17}	455	271	0	0	0	0	0	0	0	0	0	271	0	0	0	0	0	0	0	0	996.96	0	19805.58
t_{18}	455	197	0	0	0	0	0	0	0	0	455	0	0	0	0	0	0	0	0	0	1106.96	0	21313.2
t_{19}	455	311.6	0	0	0	0	0	0	0	0	455	0	0	0	0	0	0	0	0	0	1221.62	0	23310.31
t_{20}	455	411.5	0	0	25	0	0	0	0	0	455	0	0	0	0	0	0	0	0	0	1346.53	1800	26002.14
t_{21}	455	348.3	0	0	25	0	0	0	0	0	455	0	0	0	0	0	0	0	0	0	1283.26	0	24895.2
t_{22}	438.8	150	0	0	25	0	0	0	0	0	438.8	0	0	0	0	0	0	0	0	0	1052.56	0	20903.49
t_{23}	419.5	0	0	0	25	0	0	0	0	0	419.5	0	0	0	0	0	0	0	0	0	864.08	0	16698.67
t_{24}	365.3	0	0	0	25	0	0	0	0	0	365.3	0	0	0	0	0	0	0	0	0	755.59	0	14901.34

Table 5.71: Individual fuel cost for 20 Generating Unit system using LFAOA algorithm with Solar, Wind, and PEVs (Thermal + Wind + PEVs) system

Hours /Units	P_1	P_2	P_3	P_4	P_5	P_6	P_7	P_8	P_9	P_{10}	P_{11}	P_{12}	P_{13}	P_{14}	P_{15}	P_{16}	P_{17}	P_{18}	P_{19}	P_{20}	SUC	Hourly Cost ($)
t_1	6993.1	0	0	0	0	0	0	0	0	0	6993.15	0	0	0	0	0	0	0	0	0	0	13986.3
t_2	7316.7	0	0	0	0	0	0	0	0	0	7316.72	0	0	0	0	0	0	0	0	0	1690	14633.4
t_3	7952.7	0	0	1060.95	0	0	0	0	0	0	7952.68	0	0	0	0	0	0	0	0	0	1450	16966.3
t_4	8465.8	0	0	1362.96	0	0	0	0	0	0	8465.82	0	0	1362.96	0	0	0	0	0	0	560	19657.6
t_5	8465.8	0	0	1618.9	0	0	0	0	0	0	8465.82	0	0	1618.9	0	0	0	0	0	0	0	20169.4
t_6	8465.8	0	1750.34	2067.76	0	0	0	0	0	0	8465.82	0	0	2067.76	0	0	0	0	0	0	1100	22817.5
t_7	8465.8	0	1891.89	2201.93	0	0	0	0	0	0	8465.82	0	0	2201.93	0	0	0	0	0	0	860	23227.4
t_8	8465.8	0	2891.8	0	1027	0	0	0	0	0	8465.82	0	0	2860.66	0	0	0	0	0	0	230	23711.1
t_9	8465.8	3957.8	2891.8	0	944.99	0	0	0	0	0	8465.82	0	0	0	0	0	0	0	0	0	0	24726.2
t_{10}	8465.8	7199.1	2891.8	0	944.99	0	0	0	0	0	0	7199.1	0	0	0	0	0	0	0	0	5000	26700.9
t_{11}	8465.8	8796.3	0	0	944.99	0	0	0	0	0	0	8796.3	0	0	0	0	0	0	0	0	5000	27003.3
t_{12}	8465.8	7881.7	0	0	944.99	0	0	0	0	0	0	7881.7	2891.8	0	0	0	0	0	0	0	0	28065.9
t_{13}	8465.8	6973.9	0	0	944.99	0	0	0	0	0	0	6973.9	2891.8	0	0	0	0	0	0	0	0	26250.4
t_{14}	8465.8	6682.6	0	0	0	0	0	0	0	0	0	6682.6	2891.8	0	0	0	0	0	0	0	0	24722.9
t_{15}	8465.8	6170.9	0	0	0	0	0	0	0	0	0	6170.9	2891.8	0	0	0	0	0	0	0	2570	23699.5
t_{16}	8465.8	4633.9	0	0	0	0	0	0	0	0	0	4633.9	2891.8	0	0	0	0	0	0	0	0	20625.5
t_{17}	8465.8	5669.9	0	0	0	0	0	0	0	0	0	5669.9	0	0	0	0	0	0	0	0	0	19805.6
t_{18}	8465.8	4381.6	0	0	0	0	0	0	0	0	8465.82	0	0	0	0	0	0	0	0	0	0	21313.2
t_{19}	8465.8	6378.7	0	0	0	0	0	0	0	0	8465.82	0	0	0	0	0	0	0	0	0	0	23310.3
t_{20}	8465.8	8125.5	0	0	944.99	0	0	0	0	0	8465.82	0	0	0	0	0	0	0	0	0	1800	26002.1
t_{21}	8465.8	7018.6	0	0	944.99	0	0	0	0	0	8465.82	0	0	0	0	0	0	0	0	0	0	24895.2
t_{22}	8196.3	3566	0	0	944.99	0	0	0	0	0	8196.26	0	0	0	0	0	0	0	0	0	0	20903.5
t_{23}	7876.8	0	0	0	944.99	0	0	0	0	0	7876.84	0	0	0	0	0	0	0	0	0	0	16698.7
t_{24}	6978.2	0	0	0	944.99	0	0	0	0	0	6978.18	0	0	0	0	0	0	0	0	0	0	14901.3

Table 5.72: Statistical and hypothetical analysis of 20 Generating Unit System using the CAOA optimization algorithms with different cases.

Case No.	Test Case of Generation	Best ($)	Average ($)	Worst ($)	STD	Median	Wilcoxon Test	T-Test		Best Time	Average Time	Worst Time
							p-value	p-value	h-Value			
1	Conventional Thermal	1123401	1125228	1126808	1014.409	1125441	1.73E-06	4.44E-90	1	0	0.021875	0.03125
2	Thermal + Wind	1050684	1053318	1055245	1163.608	1053319	1.7344E-06	1.61315E-87	1	0	0.022396	0.03125
3	Thermal + PEVs	1129779	1131449	1132469	737.6434	1131661	1.7344E-06	3.67822E-94	1	0	0.017708	0.03125
4	Thermal + Solar	529223.7	544274.1	552843.7	8771.543	547948.7	1.67312E-06	9.17219E-54	1	0	0.017188	0.03125
5	Thermal + Wind + PEVs	1050274	1053285	1055320	1275.875	1053348	1.7344E-06	2.334E-86	1	0	0.020833	0.046875
6	Thermal + Solar + PEVs	529223.7	543445.7	552733.7	9131.463	547333.7	1.64473E-06	3.07601E-53	1	0	0.017708	0.03125
7	Thermal + Solar + Wind + PEVs	529223.7	544274.1	552843.7	8771.543	547948.7	1.67312E-06	9.17219E-54	1	0.015625	0.022396	0.03125

Table 5.73: Comparison of 20 Generating Unit Systems for CAOA algorithms with different cases (Winter)

Case No.	Test Case	Best ($)	Average ($)	Worst ($)	STD	Median	Wilcoxon Test	T-Test		Best Time	Average Time	Worst Time
							p-value	p-value	h-Value			
1	Conventional Thermal	1123401	1125228	1126808	1014.409	1125441	1.73E-06	4.44E-90	1	0	0.021875	0.03125
2	Thermal + Wind	1050684	1053318	1055245	1163.608	1053319	1.73E-06	1.61E-87	1	0	0.022396	0.03125
3	Thermal + PEVs	1129779	1131449	1132469	737.6434	1131661	1.73E-06	3.68E-94	1	0	0.017708	0.03125
4	Thermal + Solar	1081457	1084709	1089977	3158.419	1083792	1.61E-06	2.59E-75	1	0.015625	0.025521	0.03125
5	Thermal + Wind + PEVs	1050274	1053285	1055320	1275.875	1053348	1.73E-06	2.33E-86	1	0	0.020833	0.046875
6	Thermal + Solar + PEVs	1081739	1087956	1092831	3162.8	1087356	1.71E-06	2.48E-75	1	0.015625	0.023958	0.03125
7	Thermal +Solar + Wind +PEVs	534484.8	549968.8	561424.8	9842.716	554364.8	1.64E-06	1.91E-52	1	0.015625	0.016667	0.03125

Table 5.74: Comparison of 20 Generating Unit System using the LFAOA optimization algorithms with different cases (Summer)												
Case No.	**Test Case**	**Best ($)**	**Average ($)**	**Worst ($)**	**STD**	**Median**	**Wilcoxon Test**	**T-Test**		**Best Time**	**Average Time**	**Worst Time**
							p-value	**p-value**	**h-Value**			
1	Thermal System	1122982	1124992	1126145	837.8267	1125285	1.7E-06	1.7E-92	1	0	0.01927	0.03125
2	Thermal + PEVs	1128703	1131281	1133609	1058.88	1131489	1.7E-06	1.3E-89	1	0.01563	0.02448	0.0625
3	Thermal + Solar	1076156	1083411	1095504	4015.361	1083092	1.7E-06	2.8E-72	1	0	0.025	0.0625
4	Thermal + Wind	1050850	1052872	1054691	965.2989	1052869	1.7E-06	7.2E-90	1	0	0.02188	0.09375
5	Thermal + Wind + PEVs	1050394	1052750	1054823	1128.034	1052733	1.7E-06	6.7E-88	1	0	0.01771	0.03125
6	Thermal + Solar + PEVs	546799.2	552509.3	560623.6	3602.025	553141.5	1.7E-06	3.7E-65	1	0	0.02083	0.04688
7	Thermal + Solar +Wind + PEVs	545053.6	553022.2	560081.8	3475.161	553387.9	1.7E-06	1.3E-65	1	0	0.01927	0.04688

Table 5.75: Comparison of 20 Generating Unit Systems using the LFAOA algorithms with different cases (Winter)												
Case No.	Test Case	Best **($)**	Average **($)**	Worst **($)**	STD	Median	Wilcoxon Test	T-Test		Best Time	Average Time	Worst Time
							p-value	p-value	h-Value			
1	Thermal System	1122982	1124992	1126145	837.8267	1125285	1.70E-06	1.70E-92	1	0	0.01927	0.03125
2	Thermal + PEVs	1128703	1131281	1133609	1058.88	1131489	1.70E-06	1.30E-89	1	0.01563	0.02448	0.0625
3	Thermal + Wind	1050850	1052872	1054691	965.2989	1052869	1.70E-06	7.20E-90	1	0	0.02188	0.09375
4	UCP + Solar	1078056	1088209	1095322	3705.538	1088664	1.73E-06	2.43E-73	1	0.015625	0.015625	0.015625
5	Thermal + Wind + PEVs	1050394	1052750	1054823	1128.034	1052733	1.70E-06	6.70E-88	1	0	0.01771	0.03125
6	UCP + Solar+ PEVs	550849	555713.5	564662.7	3313.068	554672.7	1.73E-06	2.75E-66	1	0.015625	0.016146	0.03125
7	UCP +Solar +Wind + PEVs	1040688	1043229	1045202	1033.534	1043367	1.73E-06	6.85E-89	1	0.015625	0.01875	0.03125

5.5.1.3 System of 40 Generating Units

The efficiency of the proposed CAOA and LFAOA optimizers is tested using a specialized system comprising 40 power-generating units that operate for 24 hours. The CAOA and LFAOA techniques are subjected to evaluation through 100 iterations, while 30 trial runs verify the effectiveness of the CAOA and LFAOA algorithms. Details of the commitment status, optimal scheduling, and individual fuel costs of each of the 40 generating units for thermal units with solar, PEVs, and wind are presented in **Table 5.76**, which illustrates the statistical and hypothetical analysis of the 40 generating unit system using CAOA optimization algorithms with different cases. **Table 5.77** illustrates the statistical and hypothetical analysis of 40 generating units with the help of LFAOA optimization algorithms in different cases. **Table 5.78** illustrates the statistical and hypothetical analysis of 40 generating unit systems using CAOA optimization algorithms with different cases for the summer season. **Table 5.79** illustrates the statistical and hypothetical analysis of 40 generating unit systems using LFAOA optimizations algorithms with different cases for the winter season. **Table 5.80** illustrates the comparison of different generating unit systems for CAOA with different cases. **Table 5.81** illustrates the comparison of the generating unit system for the LFAOA algorithm with different cases. **Table 5.82** illustrates the cost comparison for the 10-unit system with other methods. **Figure 5.5** illustrates the cost comparison chart for the 10, 20, and 40-unit systems with CAOA. **Figure 5.6** illustrates the cost comparison chart for 10, 20, and 40-unit systems with the LFAOA algorithm. **Figure 5.7** illustrates the convergence curve for the 10-, 20-, and 40-unit systems using CAOA and LFAOA with the combined effects of thermal, solar, wind, and plug-in electric vehicles.

Table 5.76: Comparison of 40 Generating Unit Systems for the CAOA algorithms with different cases (Summer)

Test Case	Best ($)	Average ($)	Worst ($)	STD	Median	Wilcoxon Test	T-Test		Best Time	Average Time	Worst Time
						p-value	p-value	h-Value			
Thermal System	2246014	2250002	2252619	1578.101	2250432	1.73E-06	3.06E-93	1	0.015625	0.043229	0.09375
Thermal + PEV	2253149	2255037	2256230	859.5718	2255440	1.21E-06	6.40E-101	1	0.015625	0.047917	0.09375
Thermal + SOLAR	2161119	2169874	2182779	8420.975	2171364	1.37E-06	1.08E-71	1	0.015625	0.038021	0.078125
Thermal + WIND	2171041	2174544	2178548	1812.338	2175304	1.56E-06	4.56E-91	1	0	0.042188	0.09375
Thermal + WIND + PEV	2166287	2169067	2171629	1345.898	2169687	1.29E-06	8.77E-95	1	0.015625	0.039583	0.09375
Thermal + WIND + PEV + SOLAR	2155661	2158631	2163295	1577.27	2159496	1.51E-06	1.00E-92	1	0.015625	0.034375	0.0625

Table 5.77: Comparison of 40 Generating Unit Systems for the LFAOA algorithms with different cases (Summer)

Test Case	Best ($)	Average ($)	Worst ($)	STD	Median	Wilcoxon Test	T-Test		Best Time	Average Time	Worst Time
						p-value	p-value	h-Value			
Thermal System	2246537	2249809	2253202	1783.155	2249661	1.73E-06	1.06E-91	1	0.015625	0.04375	0.25
Thermal + PEV	2253445	2256169	2263766	1821.746	2255990	1.73E-06	1.82E-91	1	0.015625	0.040625	0.109375
Thermal + SOLAR	2170009	2182187	2197718	5673.393	2180770	1.73E-06	9.71E-77	1	0.01568	0.047917	0.109375
Thermal + WIND	2171968	2176212	2180380	2031.965	2176154	1.73E-06	1.23E-89	1	0.015625	0.038021	0.078125
Thermal + WIND + PEV	2167600	2170761	2172976	1694.269	2170961	1.73E-06	6.80E-92	1	0.015625	0.047396	0.078125
Thermal + WIND + PEV + SOLAR	2154973	2159186	2163594	2056.203	2159285	1.73E-06	2.18E-89	1	0.015623	0.03125	0.0625

Table 5.78: Comparison of 40 Generating Unit Systems for the CAOA algorithms with different cases (Winter)											
Test Case	**Best ($)**	**Average ($)**	**Worst ($)**	**STD**	**Median**	**Wilcoxon Test**	**T-Test**		**Best Time**	**Average Time**	**Worst Time**
						p-value	**p-value**	**h-Value**			
Thermal System	2246014	2250002	2252619	1578.101	2250432	1.73E-06	3.06E-93	1	0.015625	0.043229	0.09375
UCP+PEV	2253149	2255037	2256230	859.5718	2255440	1.21E-06	6.40E-101	1	0.015625	0.047917	0.09375
UCP+WIND	2171041	2174544	2178548	1812.338	2175304	1.56E-06	4.56E-91	1	0	0.042188	0.09375
UCP + Solar	2166011	2175905	2188591	9066.083	2177111	1.44E-06	8.45E-71	1	0.015625	0.038021	0.09375
UCP + Wind + PEV	2166287	2169067	2171629	1345.898	2169687	1.29E-06	8.77E-95	1	0.015625	0.039583	0.09375
UCP +Solar +PEV	2236352	2239549	2241407	1104.089	2239697	1.70E-06	1.11E-97	1	0.015625	0.041667	0.09375
UCP + Solar + Wind + PEVs	2162466	2164587	2168066	1369.87	2164498	1.56E-06	1.55E-94	1	0.015625	0.030729	0.046875

Table 5.79: Comparison of 40 Generating Unit Systems for the LFAOA algorithms with different cases (Winter)											
Test Case	**Best ($)**	**Average ($)**	**Worst ($)**	**STD**	**Median**	**Wilcoxon Test**	**T-Test**		**Best Time**	**Average Time**	**Worst Time**
						p-value	**p-value**	**h-Value**			
Thermal System	2246537	2249809	2253202	1783.155	2249661	1.73E-06	1.06E-91	1	0.015625	0.04375	0.25
Thermal + PEVs	2253445	2256169	2263766	1821.746	2255990	1.73E-06	1.82E-91	1	0.015625	0.040625	0.109375
Thermal + WIND	2171968	2176212	2180380	2031.965	2176154	1.73E-06	1.23E-89	1	0.015625	0.038021	0.078125
Thermal + SOLAR	2173390	2185194	2194906	5115.037	2185255	1.73E-06	4.62E-78	1	0.015625	0.040104	0.078125
Thermal + WIND + PEVs	2167600	2170761	2172976	1694.269	2170961	1.73E-06	6.80E-92	1	0.015625	0.047396	0.078125
Thermal + Solar + PEVs	2236865	2240862	2245808	2114.782	2241234	1.73E-06	1.68E-89	1	0.015625	0.044792	0.078125
Thermal + Solar + Wind + PEVs	2162821	2165482	2171353	1867.384	2165250	1.73E-06	1.23E-90	1	0.015625	0.035938	0.078125

Table 5.80: Comparison of Generating Unit Systems for the CAOA algorithms with different cases												
Test Units	**Test Case**	**Best ($)**	**Average ($)**	**Worst ($)**	**STD**	**Median**	**Wilcoxon Test**	**T-Test**		**Best Time**	**Average Time**	**Worst Time**
							p-value	**p-value**	**h-Value**			
10 Unit	Conventional Thermal System	563427.8	564297	565017.7	387.2645	564327	1.73E-06	1.63E-93	1	0	0.02083	0.0313
	Thermal+ PEVs	558645.4	559191.3	559914	290.0386	559151.6	1.73E-06	4.85E-97	1	0.0156	0.02083	0.0625
	Thermal+ Solar	547399.2	548219.2	549022.3	377.9526	548147	1.73E-06	1.86E-93	1	0.0156	0.02031	0.0313
	Thermal + Wind	491763.4	493505.5	494666.4	695.5368	493729.6	1.73E-06	1.89E-84	1	0.0156	0.0224	0.0469
	Thermal+ PEVs + Solar	547620.4	548275	549291.5	411.3319	548258.5	1.73E-06	2.16E-92	1	0	0.01927	0.0313
	Thermal+ PEVs +Wind	489870	490994.5	492368.4	624.9831	491057	1.73E-06	9.83E-86	1	0.0156	0.01875	0.0313
	Thermal+ Solar+ +Wind + PEVs	479205.8	481668.3	483869.4	981.2449	481767	1.73E-06	8.23E-80	1	0	0.02083	0.0469
20 Unit	Conventional Thermal	1123401	1125228	1126808	1014.409	1125441	1.73E-06	4.44E-90	1	0	0.021875	0.03125
	Thermal + Wind	1050684	1053318	1055245	1163.608	1053319	1.73E-06	1.61E-87	1	0	0.022396	0.03125
	Thermal + PEVs	1129779	1131449	1132469	737.6434	1131661	1.73E-06	3.68E-94	1	0	0.017708	0.03125
	Thermal + Solar	529223.7	544274.1	552843.7	8771.543	547948.7	1.67E-06	9.17E-54	1	0	0.017188	0.03125
	Thermal + Wind + PEVs	1050274	1053285	1055320	1275.875	1053348	1.73E-06	2.33E-86	1	0	0.020833	0.046875
	Thermal + Solar + PEVs	529223.7	543445.7	552733.7	9131.463	547333.7	1.64E-06	3.08E-53	1	0	0.017708	0.03125
	Thermal + Solar + Wind + PEVs	529223.7	544274.1	552843.7	8771.543	547948.7	1.67E-06	9.17E-54	1	0.015625	0.022396	0.03125
40 Unit	Thermal System	2246014	2250002	2252619	1578.101	2250432	1.73E-06	3.06E-93	1	0.015625	0.043229	0.09375
	Thermal + PEV	2253149	2255037	2256230	859.5718	2255440	1.21E-06	6.40E-101	1	0.015625	0.047917	0.09375
	Thermal + SOLAR	2161119	2169874	2182779	8420.975	2171364	1.37E-06	1.08E-71	1	0.015625	0.038021	0.078125
	Thermal + WIND	2171041	2174544	2178548	1812.338	2175304	1.56E-06	4.56E-91	1	0	0.042188	0.09375
	Thermal + WIND + PEV	2166287	2169067	2171629	1345.898	2169687	1.29E-06	8.77E-95	1	0.015625	0.039583	0.09375
	Thermal + WIND + PEV + SOLAR	2155661	2158631	2163295	1577.27	2159496	1.51E-06	1.00E-92	1	0.015625	0.034375	0.0625

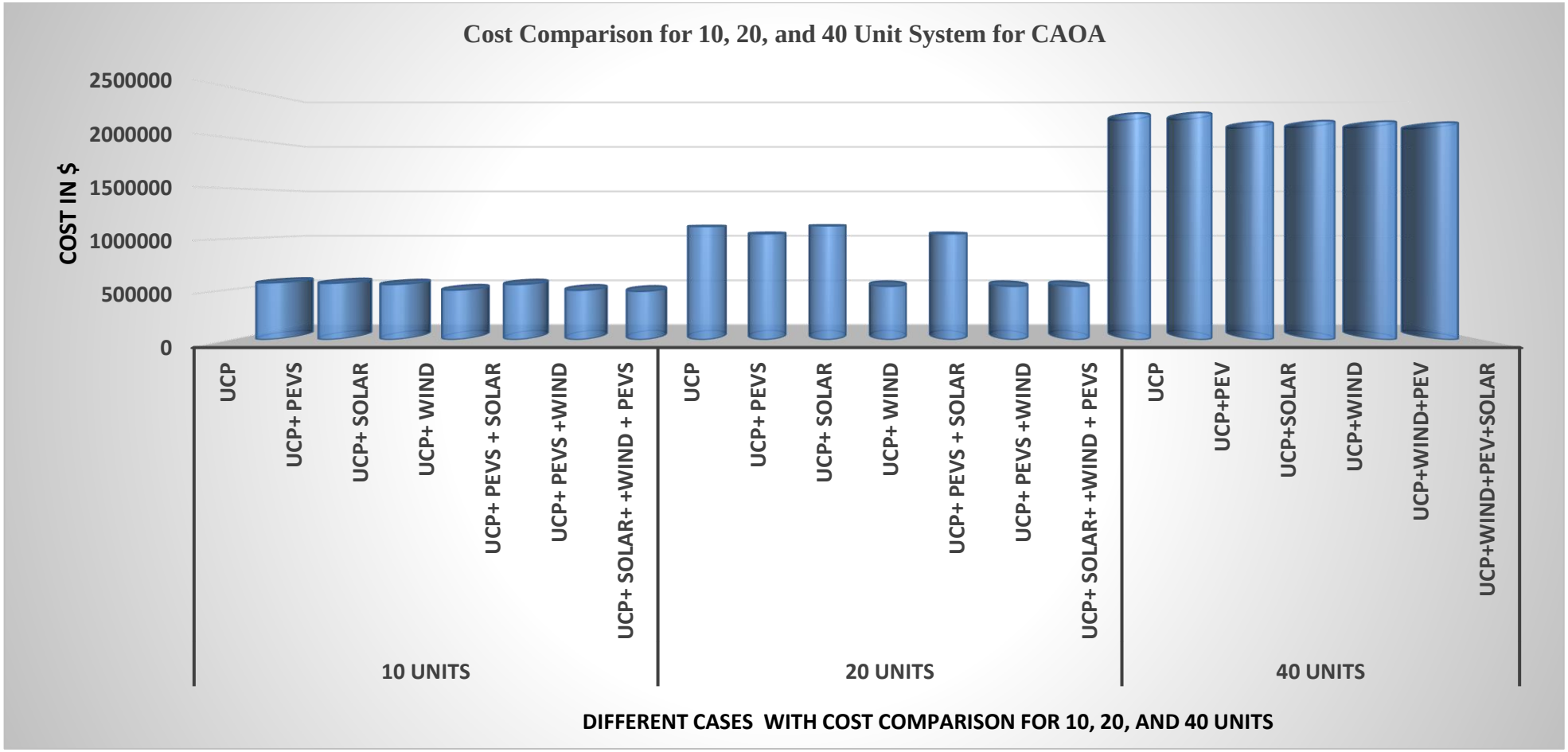

Figure 5.5 Cost Comparison of 10, 20 and 40 units using the CAOA

Table 5.81: Comparison of Generating Unit System results for the LFAOA optimization algorithms with different cases

Units	Test Case	Best ($)	Average ($)	Worst ($)	STD	Median	Wilcoxon Test	T-Test		Best Time	Average Time	Worst Time
							p-value	p-value	h-Value			
10 Unit	Conventional Thermal Generation	563487	564299.6	565246	381.6837	564228.3	1.73E-06	1.07E-93	1	0	0.01875	0.04688
	Thermal+ PEVs	558205.1	559064.6	559897.1	298.2694	559040.9	1.73E-06	1.10E-96	1	0.015625	0.01667	0.03125
	Thermal + Wind	491994.8	493305.7	494286.3	681.5261	493490.3	1.73E-06	1.06E-84	1	0	0.01823	0.03125
	Thermal + Solar	206605.6	208154.4	209405.3	757.3489	208063.6	1.73E-06	1.66E-72	1	0.015625	0.02604	0.125
	Thermal + Solar + PEVs	547200.1	548207.7	549019.1	425.7034	548231.3	1.73E-06	5.86E-92	1	0	0.01719	0.04688
	Thermal + Wind + PEVs	489623.3	491058.2	492493.7	723.7108	491115.5	1.73E-06	6.89E-84	1	0	0.02865	0.0625
	Thermal + Solar + Wind + PEVs	479631.4	481418.4	483227.2	982.2839	481428.8	1.73E-06	8.61E-80	1	0	0.0151	0.03125
20 Unit	Thermal System	1122982	1124992	1126145	837.8267	1125285	1.70E-06	1.70E-92	1	0	0.01927	0.03125
	Thermal + PEVs	1128703	1131281	1133609	1058.88	1131489	1.70E-06	1.30E-89	1	0.01563	0.02448	0.0625
	Thermal + Solar	1076156	1083411	1095504	4015.361	1083092	1.70E-06	2.80E-72	1	0	0.025	0.0625
	Thermal + Wind	1050850	1052872	1054691	965.2989	1052869	1.70E-06	7.20E-90	1	0	0.02188	0.09375
	Thermal + Wind + PEVs	1050394	1052750	1054823	1128.034	1052733	1.70E-06	6.70E-88	1	0	0.01771	0.03125
	Thermal + Solar + PEVs	546799.2	552509.3	560623.6	3602.025	553141.5	1.70E-06	3.70E-65	1	0	0.02083	0.04688
	Thermal + Solar +Wind + PEVs	545053.6	553022.2	560081.8	3475.161	553387.9	1.70E-06	1.30E-65	1	0	0.01927	0.04688
40 Unit	Thermal System	2246537	2249809	2253202	1783.155	2249661	1.73E-06	1.06E-91	1	0.015625	0.04375	0.25
	Thermal + PEV	2253445	2256169	2263766	1821.746	2255990	1.73E-06	1.82E-91	1	0.015625	0.040625	0.109375
	Thermal + SOLAR	2170009	2182187	2197718	5673.393	2180770	1.73E-06	9.71E-77	1	0.01568	0.047917	0.109375
	Thermal + WIND	2171968	2176212	2180380	2031.965	2176154	1.73E-06	1.23E-89	1	0.015625	0.038021	0.078125
	Thermal + WIND + PEV	2167600	2170761	2172976	1694.269	2170961	1.73E-06	6.80E-92	1	0.015625	0.047396	0.078125
	Thermal + WIND + PEV + SOLAR	2154973	2159186	2163594	2056.203	2159285	1.73E-06	2.18E-89	1	0.015623	0.03125	0.0625

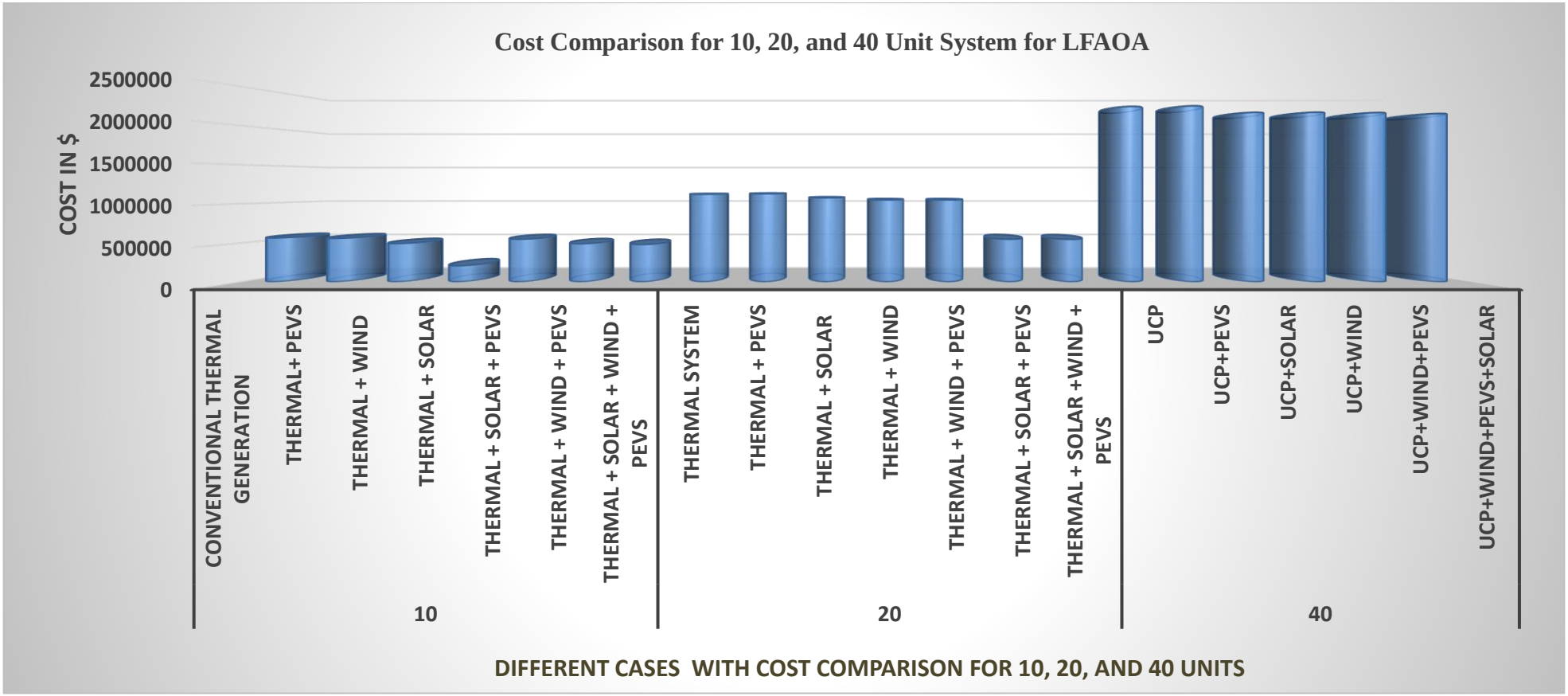

Figure 5.6 Cost Comparison of 10, 20 and 40 units using the LFAOA

Table 5.82: Cost Comparison for 10 Unit system with other methods				
Method	**Best ($)**	**Average**	**Worst**	**Average Time (Sec.)**
BAT[130]	564255.7	-	-	-
BAT-GA[130]	563917.8	-	-	-
CAOA Proposed method	563427.8	564297	565017.7	0.02083
LFAOA Proposed Method	563487.02	564299.59	565246	0.0151

In Table 5.82, a cost comparison is presented for a 10-unit system. The result clearly indicates that the proposed chaotic arithmetic optimization algorithm and levy flight arithmetic optimization algorithm have delivered outstanding results in comparison to the existing system. Specifically, the best cost for the proposed system is $563,428.8. In contrast, the BAT method records its best value at $564,255.7, and the Bat Genetic Algorithm (BAT-GA) at $563,917.8. Additionally, the proposed system exhibits a relatively shorter average time requirement. Table 5.80 and Table 5.81 present a comprehensive comparative study and analysis for systems with 10, 20, and 40 units, utilizing CAOA and LFAOA. Concurrently, a comparative analysis is provided by Tables 5.80 and 5.81. Visual representations of the results for the 10, 20, and 40-unit systems are depicted in Figures 5.5 and 5.6. The observations from these figures highlight that the integration of conventional power systems with freely available renewable energy sources can significantly reduce both fuel and generation costs. Tables 5.80 and 5.81 further elaborate on the results for the 10, 20, and 40-unit systems using CAOA and LFAOA. The parameters considered include best value, average value, worst value, standard deviation, Wilcoxon test, p-test, best time, average time, and worst time. In the global pursuit of carbon-zero policies, the proposed system proves to be particularly beneficial in minimizing carbon emissions and generation costs. For the 10, 20, and 40-unit systems, the best values using CAOA for thermal, wind, solar, and PEVs combinations are $479,205.8, $529,223.7, and $2,155,661, respectively, as illustrated in Table 5.80. Similarly, the best values for the same configurations using LFAOA are $479,205.8, $529,223.7, and $2,155,661, as presented in Table 5.81. Figure 5.7 illustrates the convergence curve for the proposed system. The percentage cost savings are 0.1467% and 0.0861%, in comparison to the BAT and

BAT-GA, methods using the CAOA algorithm. Similarly, the percentage cost savings are 0.1363% and 0.076390% in comparison to the BAT and BAT-GA algorithms, respectively, using the LFAOA method.

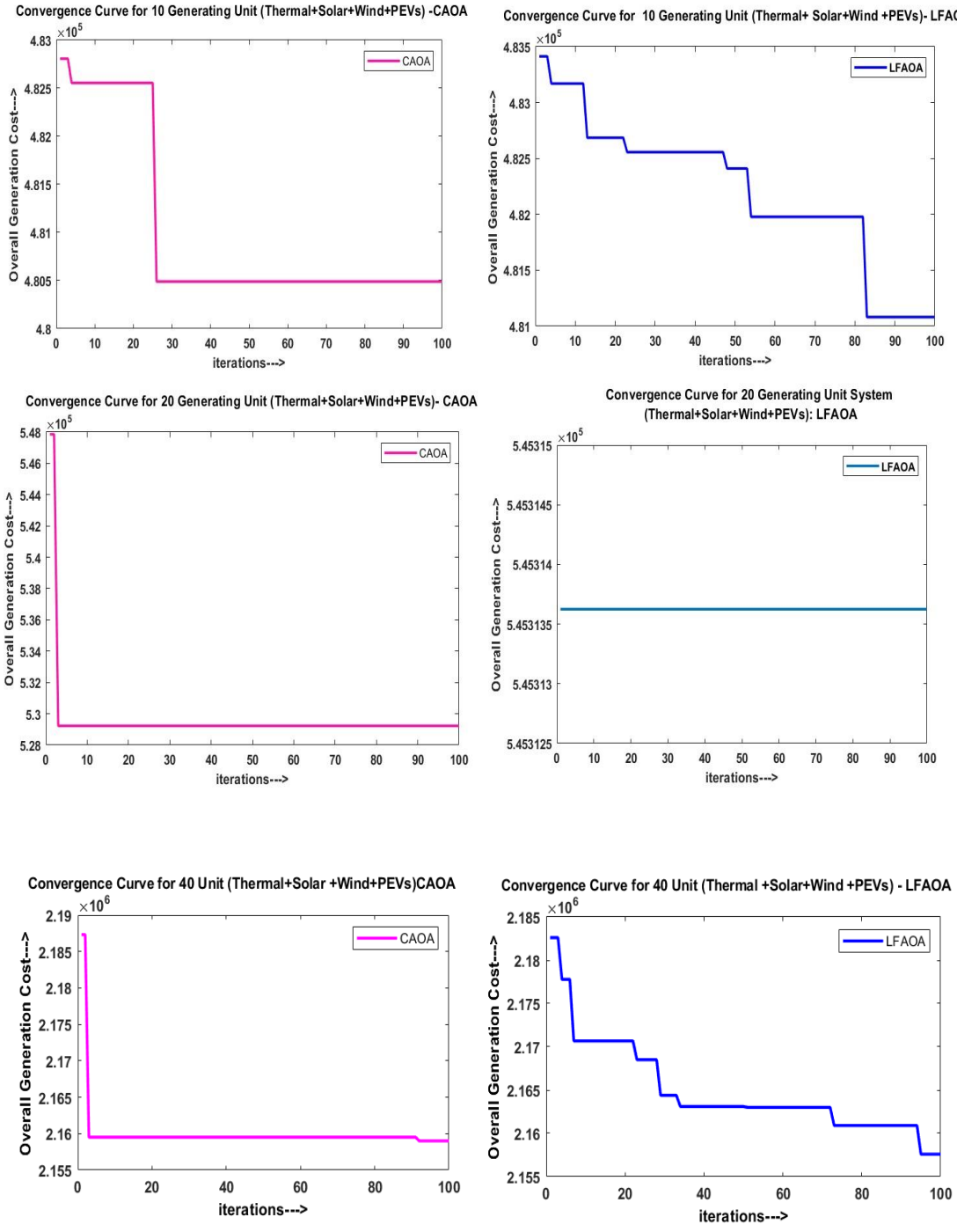

Figure 5.7 Convergence curve for 10, 20, 40 Generating Unit using CAOA and LFAOA

5.6 CONCLUSIONS

The problem of security constraint unit commitment has been solved using CAOA and LFAOA in this chapter. The test units, which are systems with 10, 20, and 40generating units, have been scheduled successfully and utilized the recommended hybrid optimizers to minimize the cost. The performances of the simulated results of the CAOA and LFAOA optimizer are compared to those of existing and newly developed heuristics, meta-heuristics, and evolutionary search optimizer. According to the simulation results, the recommended optimizer computes the satisfactory profit value with commitment scheduling in a reasonable amount of time.

A powerful optimizer like this can be used to find a solution for modern power sector security constraint unit commitment. The analysis takes into account the standard deviation and median values of the profit variation's best, average, and worst values. The Wilcoxon rank sum method and the t-test are two examples of hypothesis testing that can be used to determine the p-value and h-value. The best, average, and worst simulation times are also analyzed for the computational times. The effectiveness of the hybrid CAOA and LFAOA optimization technique to solve SCUC problem with the impact of PEVs and RES in summer and winter days has been successfully presented. The standard test system, which consists of thermal units for the small, medium, and large power sectors, has been evaluated for its performance. The suggested algorithm's efficacy was evaluated for systems with 10, 20, and 40 generating units, respectively. After a successful experiment, it was discovered that the proposed optimizer outperforms other existing optimizers in solving continuous, discrete, and non-linear optimization issues.

CHAPTER 6
CONCLUSION AND FUTURE SCOPE

6.1 INTRODUCTION

This section summarizes the major accomplishments of the research presented in the thesis and provides some recommendations for future research. It explains the important finding made by the study, focusing on improving analysis methods to address challenges in security constrained unit commitment to plug-in electric vehicles and unpredictable renewable energy sources like solar and wind energy. The research was also tested on different types of test systems, ranging from small to large systems. To ensure that the security constraints unit commitment problem was optimally solved, three types hybrid optimization strategies were used. Standard benchmark functions and engineering design problems served as tests for these optimization techniques. By testing it on various, varying-sized test systems, the suggested method's viability was evaluated. In examining the proposed system, we utilized data on renewable energy sources from the National Renewable Energy Laboratory, Texas, USA. This information is derived from the findings presented in research paper [90].

6.2 A NOTEWORTHY CONTRIBUTION

This study aims to develop a novel optimization strategy that takes system constraints into account while simultaneously increasing reliability. For the purpose of resolving difficult design issues, various current optimization techniques are discussed, with a focus on solar power and other RES. In the Security Constraint Unit Commitment Problem maintaining generator scheduling to meet power demand and boost profit is a crucial task. Renewable energy sources are an appealing alternative because they are more environmentally friendly and less expensive to operate than conventional fossil fuels. However, for optimal utilization, control engineering and power storage devices are required because solar power output varies with environmental conditions. A valuable asset in the power grid, electric vehicles represent a potential solution for storing and returning energy to the grid during peak load conditions.

The high operational costs associated with conventional fossil fuels necessitate the exploration of alternative energy sources. Additionally, the emissions from thermal power plants and transportation vehicles have a harmful impact on the environment. Therefore, renewable energy sources are being investigated as a viable solution to this problem. In this particular study, solar energy has been identified as a potential renewable energy source. However, solar energy cannot provide a constant power output since it depends on environmental conditions. Nevertheless, with the advancement of control engineering and power storage devices, solar energy can be effectively stored for future use. In addition, electric vehicles can be utilized to draw power from the grid and they possess various types of power storage systems. These stored energies can be fed back into the grid, and there are ample charging and discharging facilities available for plug-in electric vehicles. During peak load conditions, a significant amount of energy can be fed back into the power grid, thereby conserving energy.

The aim of this study is to improve the optimizer's ability to explore and exploit by incorporating different techniques, including Levy flight, random walk, and chaotic map. To achieve this, three different hybrid algorithms have been designed using recent metaheuristic techniques, including the Chaotic Arithmetic Optimization algorithm, Random Walk based Arithmetic Optimization Algorithm, and Levy flight strategies based Arithmetic Optimization Algorithm. The objective of this research is to develop hybrid algorithms that can effectively solve the SCUC problem while considering the integration of battery electric vehicles, plug-in electric vehicles, and renewable energy sources during both the summer and winter seasons. These hybrid algorithms incorporate modern techniques like the Arithmetic Optimization algorithm to enhance the optimization process and achieve better results. The research project aims to introduce three novel hybrid algorithms, which have been developed in the following approach:

1. The combination of Arithmetic Optimization Algorithm with chaotic map leads to the creation of a new hybrid algorithm, abbreviated as hybrid CAOA.
2. The combination of Arithmetic Optimization Algorithm with Random Walk based strategies results in the creation of another new hybrid algorithm, abbreviated as RWAOA.

3. The combination of Arithmetic Optimization Algorithm with Levy Flight based strategies leads to the creation of the third hybrid algorithm, abbreviated as LF-AOA

To validate the efficacy of the proposed hybrid methodologies, an extensive evaluation process was conducted, which involved applying them to 23 standard benchmark functions. The feasibility of the research was further confirmed by solving 10 multidisciplinary engineering design problems, including truss design, pressure vessel design, welded beam design, and rolling element problem, with successful outcomes. To validate the results, a comparative analysis of the performance of the proposed methods was conducted against other stochastic, heuristics, and meta-heuristic algorithms. Furthermore, the proposed methods were applied to security-constrained unit commitment problems for different test systems comprising 10, 20 and 40 units, and the results were discussed in detail to highlight their significant contributions.

A comprehensive performance evaluation of the proposed hybrid metaheuristic algorithms, namely CAOA, RWAOA, and LFAOA, was carried out using 23 standard benchmark functions. The benchmark functions were classified into three categories, namely unimodal, multi-modal, and fixed-dimension functions. The unimodal functions ranged from F1 to F7, the multi-modal functions ranged from F8 to F13, and the fixed dimension functions ranged from F14 to F23. The results of the testing indicated that the incorporation of chaotic tent function, random walk strategies, and levy flight strategies effectively enhanced the exploitation and exploration phases of the AOA optimizer. Furthermore, the newly designed algorithms demonstrated promising performance when tested on standard benchmark problems of varying complexities.

To strengthen the credibility of the proposed research, 11 diverse types of multidisciplinary engineering design problems were carefully examined. These problems encompassed various areas of engineering, including pressure vessel problems, truss design problems, welded beam design problems, rolling element problems, I-beam design problems, and others. The effectiveness of the proposed hybrid metaheuristic algorithms was assessed by testing them on these problems, with the aim of evaluating their suitability and efficacy in solving complex real-world engineering design problems.

The objective of this study was to solve a security constraint unit commitment problem with the aim of minimizing overall operating costs while satisfying technological and physical constraints and hourly power demand variations. Due to the problem's non-linearity, mixed integer nature and non-convexity, hybrid metaheuristic methods were utilized, specifically the combination of chaotic maps and Arithmetic Optimization Algorithm in developing CAOA and RWAOA, as well as LFAOA optimizers. The metaheuristic process was employed to handle a range of operational and system constraints, including unit constraints of the SCUC problem. The effectiveness of these techniques was demonstrated through successful implementation on various test systems comprising 10, 20, and more power units.

The proposed algorithms have been shown to be highly effective in addressing the SCUC problem across a wide range of power system sizes, from small to large scale. Their ability to provide efficient solutions to this problem has been clearly demonstrated through a rigorous testing process. The performance of the algorithms has been evaluated using standard test systems consisting of thermal generating units. The proposed CAOA algorithm has shown to be more efficient in solving continuous, discrete, and non-linear optimization problems compared to existing optimizers. The experiments conducted on 10, and 20 generating systems have shown that CAOA and LFAOA optimizers outperformed other existing methods by achieving lower minimum costs. The impact of PEVs and RES during summer and winter days has been considered while solving SCUC problem using CAOA and LFAOA optimizers. The test system included thermal generating units of small, medium, and large-scale power sectors. The effectiveness of the proposed algorithm was tested for 10, 20 and 40 generating systems. The results of the CAOA optimizer have shown better performance than other existing and recently developed heuristics, meta-heuristics, and evolutionary search optimizers. Additionally, the proposed optimizer has shown the ability to determine optimal solutions for SCUC problem with commitment scheduling in a reasonable amount of computational time, resulting in satisfactory minimum fuel cost values. Therefore, this powerful optimizer can be effectively applied in solving security constrained unit commitment problems in modern power sectors. To perform statistical analysis, various metrics including the best value, average value, worst value, standard deviation, and median value were taken into consideration. Moreover, hypothesis testing was conducted using the Wilcoxon rank sum method and t-test, with recorded p-values and h-values.

6.3 PROSPECTS FOR FUTURE RESEARCH

Some potential research studies for future scope based on the proposed work are:

- Investigating the impact of a deregulated market scenario in security constraint unit commitment problem using the proposed methodologies.
- Considering multi-objective optimization in security constraint unit commitment problem and exploring various cases.
- The proposed methodology has been expanded to tackle the security constraint unit commitment problem in multi-area power systems. Through this extension, the methodology can address the complexities and challenges associated with power systems that span multiple areas, providing effective solutions to this critical problem.
- Investigating novel metaheuristic search algorithm variations to address the problem of future security constraint unit commitment.

6.4 LIMITATIONS

The SCUC problem, a complex optimization problem in power system operations, presents several limitations despite extensive research and the development of various solution techniques. Here are some specific limitations of SCUC problem:

Computational Complexity: SCUC problem involves numerous decision variables and constraints, making it computationally demanding. As the power system size and the number of scenarios considered increase, solving SCUC problem for large-scale systems becomes time-consuming. Specialized algorithms and high-performance computing resources are often required.

Simplified Modelling Assumptions: SCUC problem simplifies the power system dynamics and operational constraints to make the problem tractable. However, these simplifications can lead to approximations of the real system behaviour. For instance, some SCUC problem models assume ideal transmission network conditions, disregarding losses, reactive power limits, and voltage constraints.

Uncertainty Modelling: SCUC problem incorporates uncertainties related to load demand, renewable generation, and other factors. However, accurately capturing and

modeling these uncertainties is challenging. The accuracy of obtained solutions depends on the quality of uncertainty modelling.

Data Availability and Accuracy: SCUC problem heavily relies on accurate and up-to-date data regarding the power system, including demand forecasts, generator characteristics, transmission network parameters, and market prices. However, obtaining reliable data can be challenging in practice. Data errors, incomplete information, or delays in data availability can impact the accuracy of SCUC problem solutions.

Computational Time Horizon: SCUC problem typically operates on an hourly or sub-hourly time horizon, suitable for day-ahead or intraday operations. However, it may not capture rapid changes or contingencies that occur in real-time operations.

These limitations underscore the challenges faced in solving SCUC problem. Ongoing efforts by researchers and practitioners focus on developing more sophisticated algorithms, incorporating realistic models, and addressing these limitations to enhance the accuracy and efficiency of SCUC problem solutions.

REFERENCES

[1] A. Gopi, P. Sharma, K. Sudhakar, W. K. Ngui, I. Kirpichnikova, and E. Cuce, "Weather Impact on Solar Farm Performance: A Comparative Analysis of Machine Learning Techniques," *Sustain.*, vol. 15, no. 1, 2023, doi: 10.3390/su15010439.

[2] L. Abualigah, A. Diabat, S. Mirjalili, M. Abd Elaziz, and A. H. Gandomi, "The Arithmetic Optimization Algorithm," *Comput. Methods Appl. Mech. Eng.*, vol. 376, p. 113609, 2021, doi: 10.1016/j.cma.2020.113609.

[3] E. Talebizadeh, M. Rashidinejad, and A. Abdollahi, "Evaluation of plug-in electric vehicles impact on cost-based unit commitment," *J. Power Sources*, vol. 248, pp. 545–552, 2014, doi: 10.1016/j.jpowsour.2013.09.009.

[4] Central Electricity Report (CEA), Govt. of India, 2023. doi:https://cea.nic.in/installed-capacity-report/?lang=en

[5] D. Dhawale, V. K. Kamboj, and P. Anand, "An optimal solution to unit commitment problem of realistic integrated power system involving wind and electric vehicles using chaotic slime mould optimizer," *J. Electr. Syst. Inf. Technol.*, vol. 2, 2023, doi: 10.1186/s43067-023-00069-2.

[6] V. K. Kamboj, S. K. Bath, and J. S. Dhillon, "Hybrid HS–random search algorithm considering ensemble and pitch violation for unit commitment problem," *Neural Comput. Appl.*, vol. 28, no. 5, pp. 1123–1148, 2017, doi: 10.1007/s00521-015-2114-6.

[7] G. Haddadian, N. Khalili, M. Khodayar, and M. Shahiedehpour, "Security-constrained power generation scheduling with thermal generating units, variable energy resources, and electric vehicle storage for V2G deployment," *International Journal of Electrical Power and Energy Systems*, vol. 73. pp. 498–507, 2015. doi: 10.1016/j.ijepes.2015.05.020.

[8] M. Hosseini Imani, M. Jabbari Ghadi, S. Shamshirband, and M. Balas, "Impact Evaluation of Electric Vehicle Parking on Solving Security-Constrained Unit Commitment Problem," *Math. Comput. Appl.*, vol. 23, no. 1, p. 13, Mar. 2018, doi: 10.3390/mca23010013.

[9] A. Nandi, V. Kumar Kamboj, and M. Khatri, "Hybrid chaotic approaches to solve profit based unit commitment with plug-in electric vehicle and renewable energy sources in winter and summer," *Mater. Today Proc.*, vol. 60, pp. 1865–1873, 2022, doi: 10.1016/j.matpr.2021.12.525.

[10] F. Mohamad, J. Teh, and H. Abunima, "Multi-Objective Optimization of Solar/Wind Penetration in Power Generation Systems," *IEEE Access*, vol. 7, pp. 169094–169106, 2019, doi: 10.1109/ACCESS.2019.2955112.

[11] G. E. Alvarez, M. G. Marcovecchio, and P. A. Aguirre, "Security-Constrained Unit Commitment Problem including thermal and pumped storage units: An MILP formulation by the application of linear approximations techniques," *Electr. Power Syst. Res.*, vol. 154, pp. 67–74, 2018, doi: 10.1016/j.epsr.2017.07.027.

[12] Z. Yang, K. Li, Q. Niu, and Y. Xue, "A comprehensive study of economic unit commitment of power systems integrating various renewable generations and plug-in electric vehicles," *Energy Convers. Manag.*, vol. 132, pp. 460–481, 2017, doi: 10.1016/j.enconman.2016.11.050.

[13] Y. Wang, Z. Yang, M. Mourshed, Y. Guo, Q. Niu, and X. Zhu, "Demand side management of plug-in electric vehicles and coordinated unit commitment: A novel parallel competitive swarm optimization method," *Energy Convers. Manag.*, vol. 196, no. March, pp. 935–949, 2019, doi: 10.1016/j.enconman.2019.06.012.

[14] M. H. Imani, K. Yousefpour, M. J. Ghadi, and M. T. Andani, "Simultaneous presence of wind farm and V2G in security constrained unit commitment problem considering uncertainty of wind generation," *2018 IEEE Texas Power Energy Conf. TPEC 2018*, vol. 2018-Febru, pp. 1–6, 2018, doi: 10.1109/TPEC.2018.8312082.

[15] N. Muralikrishnan, L. Jebaraj, and C. C. A. Rajan, “A comprehensive Review on Evolutionary Optimization Techniques applied for Unit Commitment Problem,” *IEEE Access*, 2020, doi: 10.1109/access.2020.3010275.

[16] S. Y. Abujarad, M. W. Mustafa, and J. J. Jamian, “Recent approaches of unit commitment in the presence of intermittent renewable energy resources: A review,” *Renew. Sustain. Energy Rev.*, vol. 70, no. October 2015, pp. 215–223, 2017, doi: 10.1016/j.rser.2016.11.246.

[17] V. K. Kamboj, S. K. Bath, and J. S. Dhillon, “A novel hybrid DE–random search approach for unit commitment problem,” *Neural Comput. Appl.*, vol. 28, no. 7, pp. 1559–1581, 2017, doi: 10.1007/s00521-015-2124-4.

[18] E. Nasrolahpour and H. Ghasemi, “A stochastic security constrained unit commitment model for reconfigurable networks with high wind power penetration,” *Electr. Power Syst. Res.*, vol. 121, pp. 341–350, 2015, doi: 10.1016/j.epsr.2014.10.014.

[19] T. Zhu, H. Zheng, and Z. Ma, “A chaotic particle swarm optimization algorithm for solving optimal power system problem of electric vehicle,” *Adv. Mech. Eng.*, vol. 11, no. 3, pp. 1–9, 2019, doi: 10.1177/1687814019833500.

[20] Q. Cai, Z. Xu, F. Wen, L. L. Lai, and K. P. Wong, “Security constrained unit commitment-based power system dispatching with plug-in hybrid electric vehicles,” *Proceeding - 2015 IEEE Int. Conf. Ind. Informatics, INDIN 2015*, pp. 1014–1021, 2015, doi: 10.1109/INDIN.2015.7281874.

[21] P. Nikolaidis and S. Chatzis, “Gaussian process-based Bayesian optimization for data-driven unit commitment,” *Int. J. Electr. Power Energy Syst.*, vol. 130, no. February, p. 106930, 2021, doi: 10.1016/j.ijepes.2021.106930.

[22] P. Nikolaidis, S. Chatzis, and A. Poullikkas, “Renewable energy integration through optimal unit commitment and electricity storage in weak power networks,” *Int. J. Sustain. Energy*, vol. 38, no. 4, pp. 398–414, 2019, doi: 10.1080/14786451.2018.1516669.

[23] P. Adraktas and A. Dagoumas, “Integration of electric vehicles in the unit commitment problem with uncertain renewable electricity generation,” *Int. J. Energy Econ. Policy*, vol. 9, no. 2, pp. 315–333, 2019, doi: 10.32479/ijeep.7125.

[24] S. Jiang *et al.*, “A novel robust security constrained unit commitment model considering HVDC regulation,” *Appl. Energy*, vol. 278, no. 2, p. 115652, 2020, doi: 10.1016/j.apenergy.2020.115652.

[25] M. Mehrtash, M. J. Kouhanjani, A. Pourjafar, and S. Beladi, “An Interior Point Optimization Method for Stochastic Security-constrained Unit Commitment in the Presence of Plug-in Electric Vehicles,” *J. Appl. Sci.*, vol. 16, no. 5, pp. 189–200, 2016, doi: 10.3923/jas.2016.189.200.

[26] D. Bertsimas, E. Litvinov, X. A. Sun, J. Zhao, and T. Zheng, “Adaptive robust optimization for the security constrained unit commitment problem,” *IEEE Trans. Power Syst.*, vol. 28, no. 1, pp. 52–63, 2013, doi: 10.1109/TPWRS.2012.2205021.

[27] C. Dai, W. Chen, L. Ran, Y. Zhang, and Y. Du, “Human Group Optimizer with Local Search,” pp. 310–320, 2011.

[28] H. Wu, Q. Zhai, X. Guan, F. Gao, and H. Ye, “Security-constrained unit commitment based on a realizable energy delivery formulation,” *Math. Probl. Eng.*, vol. 2012, 2012, doi: 10.1155/2012/178193.

[29] Q. Cheng *et al.*, "Solving hydro unit commitment problems with multiple hydraulic heads based on a two-layer nested optimization method". Elsevier Ltd, 2021. doi: 10.1016/j.renene.2021.02.126.

[30] R. H. Wuijts, M. van den Akker, and M. van den Broek, “An improved algorithm for single-unit commitment with ramping limits,” *Electr. Power Syst. Res.*, vol. 190, no. September 2020, p. 106720, 2021, doi: 10.1016/j.epsr.2020.106720.

[31] W. Zhang and L. Fu, “Faster identification of redundant security constraints in SCUC,” *Energy*

Reports, vol. 8, pp. 14144–14153, 2022, doi: 10.1016/j.egyr.2022.10.301.

[32] M. R. Elkadeem, M. Abd Elaziz, Z. Ullah, S. Wang, and S. W. Sharshir, "Optimal Planning of Renewable Energy-Integrated Distribution System Considering Uncertainties," *IEEE Access*, vol. 7, pp. 164887–164907, 2019, doi: 10.1109/ACCESS.2019.2947308.

[33] Y. Y. Hong, G. F. D. Apolinario, T. K. Lu, and C. C. Chu, "Chance-constrained unit commitment with energy storage systems in electric power systems," *Energy Reports*, vol. 8, pp. 1067–1090, Nov. 2022, doi: 10.1016/j.egyr.2021.12.035.

[34] H. Quan, D. Srinivasan, and A. Khosravi, "Integration of renewable generation uncertainties into stochastic unit commitment considering reserve and risk: A comparative study," *Energy*, vol. 103, pp. 735–745, 2016, doi: 10.1016/j.energy.2016.03.007.

[35] L. Baringo, L. Boffino, and G. Oggioni, "Robust expansion planning of a distribution system with electric vehicles, storage and renewable units," *Appl. Energy*, vol. 265, no. November 2019, p. 114679, 2020, doi: 10.1016/j.apenergy.2020.114679.

[36] A. Khandelwal, A. Bhargava, A. Sharma, and N. Sharma, "Security constrained transmission network expansion planning using grey wolf optimization algorithm," *J. Stat. Manag. Syst.*, vol. 22, no. 7, pp. 1239–1249, 2019, doi: 10.1080/09720510.2019.1609561.

[37] M. R. Mozafar, M. H. Moradi, and M. H. Amini, "A simultaneous approach for optimal allocation of renewable energy sources and electric vehicle charging stations in smart grids based on improved GA-PSO algorithm," *Sustain. Cities Soc.*, vol. 32, pp. 627–637, 2017, doi: 10.1016/j.scs.2017.05.007.

[38] X. Han, J. Su, Y. Hong, P. Gong, and D. Zhu, "Mid-to Long-Term Electric Load Forecasting Based on the EMD–Isomap–Adaboost Model," *Sustain.*, vol. 14, no. 13, 2022, doi: 10.3390/su14137608.

[39] P. Prebeg, G. Gasparovic, G. Krajacic, and N. Duic, "Long-term energy planning of Croatian power system using multi-objective optimization with focus on renewable energy and integration of electric vehicles," *Appl. Energy*, vol. 184, pp. 1493–1507, 2016, doi: 10.1016/j.apenergy.2016.03.086.

[40] H. Wertani, J. Ben Salem, and M. N. Lakhoua, "Analysis and supervision of a smart grid system with a systemic tool," *Electr. J.*, vol. 33, no. 6, p. 106784, 2020, doi: 10.1016/j.tej.2020.106784.

[41] S. Jiang *et al.*, "A novel robust frequency-constrained unit commitment model with emergency control of HVDC," *Energy Reports*, vol. 8, pp. 15729–15739, 2022, doi: 10.1016/j.egyr.2022.12.069.

[42] P. P. Vergara, J. C. López, L. C. P. da Silva, and M. J. Rider, "Security-constrained optimal energy management system for three-phase residential microgrids," *Electr. Power Syst. Res.*, vol. 146, pp. 371–382, 2017, doi: 10.1016/j.epsr.2017.02.012.

[43] Y. Ji, Q. Xu, J. Zhao, Y. Yang, and L. Sun, "Day-ahead and intra-day optimization for energy and reserve scheduling under wind uncertainty and generation outages," *Electr. Power Syst. Res.*, vol. 195, no. September 2020, p. 107133, 2021, doi: 10.1016/j.epsr.2021.107133.

[44] Y. Yang and L. Wu, "Machine learning approaches to the unit commitment problem: Current trends, emerging challenges, and new strategies," *Electr. J.*, vol. 34, no. 1, p. 106889, 2021, doi: 10.1016/j.tej.2020.106889.

[45] A. E. Labrador Rivas and T. Abrão, "Faults in smart grid systems: Monitoring, detection and classification," *Electr. Power Syst. Res.*, vol. 189, no. July, p. 106602, 2020, doi: 10.1016/j.epsr.2020.106602.

[46] B. Jimada-Ojuolape and J. Teh, "Surveys on the reliability impacts of power system cyber–physical layers," *Sustain. Cities Soc.*, vol. 62, no. July, p. 102384, 2020, doi: 10.1016/j.scs.2020.102384.

[47] M. A. Ferrag, M. Babaghayou, and M. A. Yazici, "Cyber security for fog-based smart grid

SCADA systems: Solutions and challenges," *J. Inf. Secur. Appl.*, vol. 52, 2020, doi: 10.1016/j.jisa.2020.102500.

[48] P. Matoušek, O. Ryšavý, M. Grégr, and V. Havlena, "Flow based monitoring of ICS communication in the smart grid," *J. Inf. Secur. Appl.*, vol. 54, 2020, doi: 10.1016/j.jisa.2020.102535.

[49] H. Quan, D. Srinivasan, A. M. Khambadkone, and A. Khosravi, "A computational framework for uncertainty integration in stochastic unit commitment with intermittent renewable energy sources," *Appl. Energy*, vol. 152, pp. 71–82, 2015, doi: 10.1016/j.apenergy.2015.04.103.

[50] M. E. Khodayar, L. Wu, and M. Shahidehpour, "Hourly coordination of electric vehicle operation and volatile wind power generation in SCUC," *IEEE Trans. Smart Grid*, vol. 3, no. 3, pp. 1271–1279, 2012, doi: 10.1109/TSG.2012.2186642.

[51] A. Nandi and V. K. Kamboj, "A meliorated Harris Hawks optimizer for combinatorial unit commitment problem with photovoltaic applications," *J. Electr. Syst. Inf. Technol.*, vol. 8, no. 1, 2021, doi: 10.1186/s43067-020-00026-3.

[52] M. Rahmani, S. Hossein Hosseinian, and M. Abedi, "Optimal integration of Demand Response Programs and electric vehicles into the SCUC," *Sustain. Energy, Grids Networks*, vol. 26, p. 100414, 2021, doi: 10.1016/j.segan.2020.100414.

[53] F. H. Aghdam and M. T. Hagh, "Security Constrained Unit Commitment (SCUC)formulation and its solving with Modified Imperialist Competitive Algorithm (MICA)," *J. King Saud Univ. - Eng. Sci.*, vol. 31, no. 3, pp. 253–261, 2019, doi: 10.1016/j.jksues.2017.08.003.

[54] Q. Cheng *et al.*, "Solving hydro unit commitment problems with multiple hydraulic heads based on a two-layer nested optimization method," *Renew. Energy*, vol. 172, pp. 317–326, 2021, doi: 10.1016/j.renene.2021.02.126.

[55] Q. Niu, L. Zhang, and H. Zhang, "Impact of wind power penetration on unit commitment," *Commun. Comput. Inf. Sci.*, vol. 463, pp. 388–397, 2014, doi: 10.1007/978-3-662-45286-8_41.

[56] Y. Wang, Z. Yang, M. Mourshed, Y. Guo, Q. Niu, and X. Zhu, "Demand side management of plug-in electric vehicles and coordinated unit commitment: A novel parallel competitive swarm optimization method," *Energy Convers. Manag.*, vol. 196, pp. 935–949, 2019, doi: 10.1016/j.enconman.2019.06.012.

[57] A. Ahmadi, A. Esmaeel Nezhad, P. Siano, B. Hredzak, and S. Saha, "Information-Gap Decision Theory for Robust Security-Constrained Unit Commitment of Joint Renewable Energy and Gridable Vehicles," *IEEE Trans. Ind. Informatics*, vol. 16, no. 5, pp. 3064–3075, 2020, doi: 10.1109/TII.2019.2908834.

[58] J. Zhang, J. Zhang, F. Zhang, M. Chi, and L. Wan, "An Improved Symbiosis Particle Swarm Optimization for Solving Economic Load Dispatch Problem," *J. Electr. Comput. Eng.*, vol. 2021, 2021, doi: 10.1155/2021/8869477.

[59] A. Y. Saber and G. K. Venayagamoorthy, "Intelligent unit commitment with vehicle-to-grid -A cost-emission optimization," *J. Power Sources*, vol. 195, no. 3, pp. 898–911, 2010, doi: 10.1016/j.jpowsour.2009.08.035.

[60] Z. Ding, Y. Lu, K. Lai, M. Yang, and W. J. Lee, "Optimal coordinated operation scheduling for electric vehicle aggregator and charging stations in an integrated electricity-transportation system," *Int. J. Electr. Power Energy Syst.*, vol. 121, no. March, p. 106040, 2020, doi: 10.1016/j.ijepes.2020.106040.

[61] G. Haddadian, N. Khalili, M. Khodayar, and M. Shahiedehpour, "Security-constrained power generation scheduling with thermal generating units, variable energy resources, and electric vehicle storage for V2G deployment," *Int. J. Electr. Power Energy Syst.*, vol. 73, pp. 498–507, 2015, doi: 10.1016/j.ijepes.2015.05.020.

[62] Y. Sun, Z. Chen, Z. Li, W. Tian, and M. Shahidehpour, "EV Charging Schedule in Coupled Constrained Networks of Transportation and Power System," *IEEE Trans. Smart Grid*, vol. PP,

no. c, p. 1, 2018, doi: 10.1109/TSG.2018.2864258.

[63] H. Chen, S. Jiao, M. Wang, A. A. Heidari, and X. Zhao, “Parameters identification of photovoltaic cells and modules using diversification-enriched Harris hawks optimization with chaotic drifts,” *J. Clean. Prod.*, vol. 244, p. 118778, 2020, doi: 10.1016/j.jclepro.2019.118778.

[64] M. Ghasemi, S. Ghavidel, E. Akbari, and A. A. Vahed, “Solving non-linear, non-smooth and non-convex optimal power flow problems using chaotic invasive weed optimization algorithms based on chaos,” *Energy*, vol. 73, pp. 340–353, 2014, doi: 10.1016/j.energy.2014.06.026.

[65] J. Han, J. Park, and K. Lee, “Optimal scheduling for electric vehicle charging under variable maximum charging power,” *Energies*, vol. 10, no. 7, pp. 1–15, 2017, doi: 10.3390/en10070933.

[66] H. Rezaie, M. H. Kazemi-Rahbar, B. Vahidi, and H. Rastegar, “Solution of combined economic and emission dispatch problem using a novel chaotic improved harmony search algorithm,” *J. Comput. Des. Eng.*, vol. 6, no. 3, pp. 447–467, 2019, doi: 10.1016/j.jcde.2018.08.001.

[67] E. Nycander, G. Morales-España, and L. Söder, “Security constrained unit commitment with continuous time-varying reserves,” *Electr. Power Syst. Res.*, vol. 199, no. March, 2021, doi: 10.1016/j.epsr.2021.107276.

[68] A. Bhadoria and V. K. Kamboj, “Optimal generation scheduling and dispatch of thermal generating units considering impact of wind penetration using hGWO-RES algorithm,” *Appl. Intell.*, vol. 49, no. 4, pp. 1517–1547, 2019, doi: 10.1007/s10489-018-1325-9.

[69] C. Sjc, “Investigation of wind characteristics and wind energy assessment in Sao,” 2009.

[70] H. Ye and Z. Li, “Robust security-constrained unit commitment and dispatch with recourse cost requirement,” *IEEE Trans. Power Syst.*, vol. 31, no. 5, pp. 3527–3536, 2016, doi: 10.1109/TPWRS.2015.2493162.

[71] A. Nandi and V. K. Kamboj, “A New Solution to Profit Based Unit Commitment Problem Considering PEVs / BEVs and Renewable Energy Sources,” vol. 01070, pp. 1–8, 2020.

[72] M. Abdelateef Mostafa, E. A. El-Hay, and M. M. ELkholy, *Recent Trends in Wind Energy Conversion System with Grid Integration Based on Soft Computing Methods: Comprehensive Review, Comparisons and Insights*, no. 0123456789. Springer Netherlands, 2022. doi: 10.1007/s11831-022-09842-4.

[73] V. K. Kamboj, S. K. Bath, and J. S. Dhillon, “Implementation of hybrid harmony/random search algorithm considering ensemble and pitch violation for unit commitment problem,” *Int. J. Electr. Power Energy Syst.*, vol. 77, pp. 228–249, 2016, doi: 10.1016/j.ijepes.2015.11.045.

[74] D. Karaboga and B. Akay, “A comparative study of Artificial Bee Colony algorithm,” *Appl. Math. Comput.*, vol. 214, no. 1, pp. 108–132, 2009, doi: 10.1016/j.amc.2009.03.090.

[75] X. Yang, S. Deb, and A. C. B. Behaviour, “Cuckoo Search via L ´ evy Flights,” pp. 210–214, 2009.

[76] A. Yang X-s., “new metaheuristic bat-inspired algorithm,” in *Nature inspired cooperative strategies for optimization (NICSO 2010)*, ; p. 65-74: Springer, 2010.

[77] X. S. Yang, “Firefly algorithm,” *Eng. Optim. pp*, vol. 221, 2010.

[78] D. Karaboga, B. Gorkemli, C. Ozturk, and N. Karaboga, “A comprehensive survey: Artificial bee colony (ABC) algorithm and applications,” *Artif. Intell. Rev.*, vol. 42, no. 1, 2014, doi: 10.1007/s10462-012-9328-0.

[79] A. H. Gandomi and A. H. Alavi, *Krill herd: A new bio-inspired optimization algorithm*, vol. 17, no. 12. Elsevier B.V., 2012. doi: 10.1016/j.cnsns.2012.05.010.

[80] Y. X-s., “Flower pollination algorithm for global optimization,” in *Unconventional computation and natural computation*, ; p. 240-249: Springer, 2012.

[81] S. Mirjalili, S. M. Mirjalili, and A. Lewis, *Grey Wolf Optimizer*, vol. 69. Elsevier Ltd, 2014. doi: 10.1016/j.advengsoft.2013.12.007.

[82] S. C. Satapathy, A. Naik, and K. Parvathi, "A teaching learning based optimization based on orthogonal design for solving global optimization problems," pp. 1–12, 2013.

[83] S. Mirjalili, "Knowledge-Based Systems Moth-flame optimization algorithm : A novel nature-inspired heuristic paradigm," *Knowledge-Based Syst.*, vol. 89, pp. 228–249, 2015, doi: 10.1016/j.knosys.2015.07.006.

[84] S. Mirjalili and A. Lewis, *The Whale Optimization Algorithm*, vol. 95. Elsevier Ltd, 2016. doi: 10.1016/j.advengsoft.2016.01.008.

[85] S. Saremi, S. Mirjalili, and A. Lewis, *Grasshopper Optimisation Algorithm: Theory and application*, vol. 105. Elsevier Ltd, 2017. doi: 10.1016/j.advengsoft.2017.01.004.

[86] W. L. Lim, A. Wibowo, M. I. Desa, and H. Haron, "A biogeography-based optimization algorithm hybridized with tabu search for the quadratic assignment problem," *Comput. Intell. Neurosci.*, vol. 2016, 2016, doi: 10.1155/2016/5803893.

[87] V. Ariables, "T HE B UTTERFLY -P ARTICLE S WARM O PTIMIZATION (B UTTERFLY -PSO / BF-PSO) T ECHNIQUE AND I TS," vol. 4, no. 3, pp. 23–39, 2015.

[88] M. Dorigo, M. Birattari, and T. Stutzle, "Ant colony optimization," *IEEE Comput. Intell. Mag.*, vol. 1, no. 4, pp. 28–39, 2006, doi: 10.1109/MCI.2006.329691.

[89] L. Abualigah, A. Diabat, P. Sumari, and A. H. Gandomi, "A Novel Evolutionary Arithmetic Optimization Algorithm for Multilevel Thresholding Segmentation of COVID-19 CT Images," 2021.

[90] S. Maghsudlu and S. Mohammadi, "Optimal scheduled unit commitment considering suitable power of electric vehicle and photovoltaic uncertainty," *J. Renew. Sustain. Energy*, vol. 10, no. 4, 2018, doi: 10.1063/1.5009247.

[91] J. Xie, Y. Q. Zhou, and H. Chen, "A bat algorithm based on Lévy flights trajectory," *Moshi Shibie yu Rengong Zhineng/Pattern Recognit. Artif. Intell.*, vol. 26, no. 9, pp. 829–837, 2013.

[92] S. Mirjalili, *Dragonfly algorithm: a new meta-heuristic optimization technique for solving single-objective, discrete, and multi-objective problems*, vol. 27, no. 4. Springer London, 2016. doi: 10.1007/s00521-015-1920-1.

[93] A. Sadollah, H. Eskandar, A. Bahreininejad, and J. H. Kim, "Water cycle algorithm with evaporation rate for solving constrained and unconstrained optimization problems," *Appl. Soft Comput. J.*, vol. 30, pp. 58–71, 2015, doi: 10.1016/j.asoc.2015.01.050.

[94] G. G. Wang, S. Deb, and L. D. S. Coelho, "Elephant Herding Optimization," *Proc. - 2015 3rd Int. Symp. Comput. Bus. Intell. ISCBI 2015*, pp. 1–5, 2016, doi: 10.1109/ISCBI.2015.8.

[95] S. Li, H. Chen, M. Wang, A. Asghar, and S. Mirjalili, "Slime mould algorithm : A new method for stochastic optimization," vol. 111, pp. 300–323, 2020, doi: 10.1016/j.future.2020.03.055.

[96] A. R. Yildiz and P. Mehta, "Manta ray foraging optimization algorithm and hybrid Taguchi salp swarm-Nelder-Mead algorithm for the structural design of engineering components," *Mater. Test.*, vol. 64, no. 5, pp. 706–713, 2022, doi: 10.1515/mt-2022-0012.

[97] A. J. Lockett, "No free lunch theorems," *Nat. Comput. Ser.*, vol. 1, no. 1, pp. 287–322, 2020, doi: 10.1007/978-3-662-62007-6_12.

[98] P. G. Dhawale, V. K. Kamboj, and S. K. Bath, "A levy flight based strategy to improve the exploitation capability of arithmetic optimization algorithm for engineering global optimization problems," *Trans. Emerg. Telecommun. Technol.*, no. September 2022, pp. 1–65, 2023, doi: 10.1002/ett.4739.

[99] G. Kaur and S. Arora, "Chaotic whale optimization algorithm," *J. Comput. Des. Eng.*, vol. 5, no.

3, pp. 275–284, 2018, doi: 10.1016/j.jcde.2017.12.006.

[100] S. Gupta and K. Deep, “A novel Random Walk Grey Wolf Optimizer,” *Swarm Evol. Comput.*, Jan. 2018, doi: 10.1016/j.swevo.2018.01.001.

[101] S. Katoch, S. S. Chauhan, and V. Kumar, *A review on genetic algorithm: past, present, and future*, vol. 80, no. 5. Multimedia Tools and Applications, 2021. doi: 10.1007/s11042-020-10139-6.

[102] M. A. Quddus, M. Kabli, and M. Marufuzzaman, “Modeling electric vehicle charging station expansion with an integration of renewable energy and Vehicle-to-Grid sources,” *Transp. Res. Part E Logist. Transp. Rev.*, vol. 128, no. June, pp. 251–279, 2019, doi: 10.1016/j.tre.2019.06.006.

[103] A. Slowik and H. Kwasnicka, “Evolutionary algorithms and their applications to engineering problems,” *Neural Comput. Appl.*, vol. 32, no. 16, pp. 12363–12379, 2020, doi: 10.1007/s00521-020-04832-8.

[104] E. Rashedi, H. Nezamabadi-pour, and S. Saryazdi, “GSA: A Gravitational Search Algorithm,” *Inf. Sci. (Ny).*, vol. 179, no. 13, pp. 2232–2248, 2009, doi: 10.1016/j.ins.2009.03.004.

[105] D. Simon, “Biogeography-Based Optimization,” *IEEE Trans. Evol. Comput.*, vol. 12, no. 6, pp. 702–713, Dec. 2008.

[106] A. Bhadoria, S. Marwaha, and V. K. Kamboj, *BMFO-SIG: A Novel Binary Moth Flame Optimizer Algorithm with Sigmoidal Transformation for Combinatorial Unit Commitment and Numerical Optimization Problems*. Springer Singapore, 2020. doi: 10.1007/s41403-020-00185-9.

[107] P. Snaselova and F. Zboril, “Genetic algorithm using theory of chaos,” *Procedia Comput. Sci.*, vol. 51, no. 1, pp. 316–325, 2015, doi: 10.1016/j.procs.2015.05.248.

[108] J. Wang and D. Wang, “Particle swarm optimization with a leader and followers,” *Prog. Nat. Sci.*, vol. 18, no. 11, pp. 1437–1443, 2008, doi: 10.1016/j.pnsc.2008.03.029.

[109] A. Nandi and V. K. Kamboj, “Hgwo-RES : A Hybrid Algorithm with Improved Exploitation Capability For Profit Based Unit Commitment Problem,” no. 16, pp. 4731–4741, 2019.

[110] A. Nandi and V. K. Kamboj, “A Canis lupus inspired upgraded Harris hawks optimizer for nonlinear, constrained, continuous, and discrete engineering design problem,” *Int. J. Numer. Methods Eng.*, vol. 122, no. 4, pp. 1051–1088, 2021, doi: 10.1002/nme.6573.

[111] V. K. Kamboj, A. Nandi, A. Bhadoria, and S. Sehgal, “An intensify Harris Hawks optimizer for numerical and engineering optimization problems,” *Appl. Soft Comput. J.*, vol. 89, p. 106018, 2020, doi: 10.1016/j.asoc.2019.106018.

[112] D. Dhawale, V. K. Kamboj, and P. Anand, *An improved Chaotic Harris Hawks Optimizer for solving numerical and engineering optimization problems*, no. 0123456789. Springer London, 2021. doi: 10.1007/s00366-021-01487-4.

[113] D. Dhawale, V. K. Kamboj, and P. Anand, *An effective solution to numerical and multi-disciplinary design optimization problems using chaotic slime mold algorithm*, no. Ml. Springer London, 2021. doi: 10.1007/s00366-021-01409-4.

[114] H. Zhu, Y. Hu, and W. Zhu, “A dynamic adaptive particle swarm optimization and genetic algorithm for different constrained engineering design optimization problems,” *Adv. Mech. Eng.*, vol. 11, no. 3, pp. 1–27, 2019, doi: 10.1177/1687814018824930.

[115] W. Liu *et al.*, “Efficacy and safety of Qing-Feng-Gan-Ke Granules in patients with postinfectious cough: Study protocol of a novel-design phase III placebo-controlled, double-blind randomized trial,” *BMC Complement. Altern. Med.*, vol. 15, no. 1, pp. 1–11, 2015, doi: 10.1186/s12906-015-0812-3.

[116] P. Anand, M. Rizwan, S. Kaur, B. Gulnar, P. Vikram, and K. Kamboj, “Optimal Sizing of Hybrid

Renewable Energy System for Electricity Production for Remote Areas," *Iran. J. Sci. Technol. Trans. Electr. Eng.*, vol. 46, no. 4, pp. 1149–1174, 2022, doi: 10.1007/s40998-022-00524-2.

[117] A. Hossein and G. X. Yang, "Cuckoo search algorithm : a metaheuristic approach to solve structural optimization problems," pp. 17–35, 2013, doi: 10.1007/s00366-011-0241-y.

[118] S. Mirjalili and A. Lewis, "Adaptive gbest-guided gravitational search algorithm," *Neural Comput. Appl.*, vol. 25, no. 7–8, pp. 1569–1584, 2014, doi: 10.1007/s00521-014-1640-y.

[119] A. K. Qin, V. L. Huang, and P. N. Suganthan, "Adaptation for Global Numerical Optimization," vol. 13, no. 2, pp. 398–417, 2009.

[120] J. Kennedy and (1995) Eberhart R. C., "Particle Swarm Optimization," in *Proceedings of the IEEE International Conference on Neural Networks*, pp. 1942–1948.

[121] R. Y. M. Nakamura, L. A. M. Pereira, K. A. Costa, D. Rodrigues, J. P. Papa, and X. S. Yang, *BBA: A binary bat algorithm for feature selection*. 2012. doi: 10.1109/SIBGRAPI.2012.47.

[122] J. Zhao and Z. M. Gao, "The Chaotic Slime Mould Algorithm with Chebyshev Map," *J. Phys. Conf. Ser.*, vol. 1631, no. 1, 2020, doi: 10.1088/1742-6596/1631/1/012071.

[123] D. Dhawale and V. K. Kamboj, "Scope of Intelligence Approcahes for Unit Commitment Under Uncertain Sustainable Energy Environment For Effective Vehicle To Grid Operations-A Comprehensive Review," vol. 01034, 2020.

[124] S. Prashar, V. K. Kamboj, and K. D. Singh, "A Cost Effective Solution to Security Constrained Unit Commitment and Dispatch Problem using Hybrid Search Algorithm," *E3S Web Conf.*, vol. 184, 2020, doi: 10.1051/e3sconf/202018401071.

[125] V. K. Kamboj, A. Bhadoria, and S. K. Bath, "Solution of non-convex economic load dispatch problem for small-scale power systems using ant lion optimizer," *Neural Comput. Appl.*, vol. 28, no. 8, pp. 2181–2192, 2017, doi: 10.1007/s00521-015-2148-9.

[126] T. Venkatesan and M. Y. Sanavullah, "Electrical Power and Energy Systems SFLA approach to solve PBUC problem with emission limitation," *Int. J. Electr. POWER ENERGY Syst.*, vol. 46, pp. 1–9, 2013, doi: 10.1016/j.ijepes.2012.09.006.

[127] A. Y. Saber and G. K. Venayagamoorthy, *V2G scheduling - A modern approach to unit commitment with Vehicle-to-Grid using particle swarm optimization*, vol. 42, no. 9. IFAC, 2009. doi: 10.3182/20090705-4-SF-2005.00047.

[128] J. Liang and W. Tang, "Interval based transmission contingency-constrained unit commitment for integrated energy systems with high renewable penetration," *Int. J. Electr. Power Energy Syst.*, vol. 119, no. August 2019, p. 105-113, 2020, doi: 10.1016/j.ijepes.2020.105853.

[129] B. Qiao and J. Liu, "Multi-objective dynamic economic emission dispatch based on electric vehicles and wind power integrated system using differential evolution algorithm," *Renew. Energy*, vol. 154, pp. 316–336, 2020, doi: 10.1016/j.renene.2020.03.012.

[130] V. L. Devi, P. B. Kumar, and P. Sujatha, "A Hybrid BAT-GA Optimisation of Security Constrained Unit Commitment Problem for 10-unit System," vol. 10, no. 5, pp. 823–830, 2017.

[131] Na Zhang, Weidong Li, Rao Liu, Quan Lv and Liang Sung, "A Three-Stage Birandom Program for Unit Commitment with Wind Power Uncertainty", Scientific World Journal, Volume 2014, pp. 1-12,2014, http://dx.doi.org/10.1155/2014/583157